SIMPLIFIED LOCAL-DENSITY MODELING OF PURE AND MULTI-COMPONENT GAS ADSORPTION ON DRY AND WET COALS

By

JING SHYAN CHEN

Bachelor of Science in Chemical Engineering
Oklahoma State University
Stillwater, Oklahoma
2005

Submitted to the Faculty of the
Graduate College of the
Oklahoma State University
in partial fulfillment of
the requirements for
the Degree of
MASTER OF SCIENCE
December, 2007

SIMPLIFIED LOCAL-DENSITY MODELING OF PURE AND MULTI-COMPONENT GAS ADSORPTION ON DRY AND WET COALS

Dissertation Approved:

Dr. Khaled A.M. Gasem

Thesis Adviser

Dr. Robert L. Robinson, Jr.

Dr. Karen A. High

Dr. A. Gordon Emslie

Dean of the Graduate College

PREFACE

Generalized correlations for the model parameters in the modified simplified local-density/Peng-Robinson (SLD-PR) model were develop to provide reliable predictions for the equilibrium adsorption of methane, nitrogen, CO_2 and their mixtures on dry and wet coals in the range of conditions encountered in coalbed methane (CBM) production and CO_2 sequestration. The adsorption of pure methane, nitrogen and CO_2 and their mixtures on Argonne premium coals and OSU coals were considered in this study. The coals used included five Argonne premium coals (Illinois #6, Beulah Zap, Wyodak, Upper Freeport, Pocahontas coal) and five OSU coals (Illinois #6, Fruitland OSU #1 and #2, Tiffany and Lower Basin Fruitland coal).

The SLD-PR model parameters (coal surface areas and solid-solid interaction energy) were regressed to obtain precise representation of pure-gas adsorption on each coal. The results obtained indicate that the SLD-PR model is able to represent the pure-gas adsorption on these coals within expected experimental uncertainties.

The regressed model parameters were correlated (generalized) in terms of the excess adsorption of adsorbates (methane or nitrogen or CO_2) at 400 psia and the coal characteristics, including the fixed carbon and the equilibrium moisture. The generalized parameters facilitate the SLD-PR model prediction of the pure-gas adsorption on these coals within twice the experimental uncertainties.

The generalized model parameters from the pure-gas adsorption were used to predict mixture adsorption of these gases on wet coals. Specifically, the mixed-gas adsorption on wet Illinois #6, Fruitland OSU #1 and wet Tiffany coal were modeled. With few exceptions, the model was able to predict the mixture adsorption within three times the experimental uncertainties.

Furthermore, inclusion of binary interaction parameters (BIPs) in the SLD-PR model improves the generalized prediction for mixture adsorption. Using generalized model parameters from the pure gases, the BIPs were regressed to obtain a better correlation for the mixture adsorption. When generalized in terms of coal characterization or gas properties, the BIPs resulted in predictions of the mixed-gas adsorption, on average, within twice of the experimental uncertainties.

ACKNOWLEDGMENTS

During the course of my graduate studies, there are many people for whom I would like to show my appreciation. I would like to offer my sincere gratitude to my advisor, Dr. Khaled A. M. Gasem, for giving me the opportunity to work on this project. His enthusiasm for the research showed me the significance of the project, and made my graduate studies very enlightening. Without his intelligence guidance, encouragement and endless support, I could have not completed this work successfully.

I am also grateful to Dr. Robert L. Robinson, Jr. for his guidance, valuable advice and encouragement during the course of my studies.

I would also like to thank my graduate advisory committee member, Dr. Karen High, for her valuable input and suggestions.

I am thankful to my colleagues, Dr. James E. Fitzgerald and Sayeed Mohammad, who have been great mentors to me. Their generous suggestions have helped me in completing the study.

Most of all, I would like to thank my family for their patience, understanding, and support during the course of my graduate program, especially my mother and father, Pek Yong Lim and Ah Chong Chen. Also, I also appreciate the encouragement of my brother (Foo Sen), sister-in-law (Miow Tieng) and sisters (Jing Voon and Jing Ting).

TABLE OF CONTENTS

Chapter Page

LIST OF TABLES

Table Page

Table Page

Table Page

LIST OF FIGURES

Figure Page

Figure Page

Figure Page

Figure Page

Figure Page

Figure Page

Figure Page

NOMENCLATURE

A	surface area
a	Peng-Robinson attractive parameter
a_{ads}	local Peng-Robinson attractive parameter for adsorbed phase
%AAD	average absolute deviation
b	Peng-Robinson covolume
Car	percentage carbon in basis of moisture and ash free
b_{ads}	modified Peng-Robinson covolume for adsorbed phase
C_{ij}	binary interaction parameter for species i and j
C_1-C_3	Mathias Copeman Expression constants
f	fugacity
F	Fahrenheit
FC	percentage fixed carbon
i	dummy index
k	Boltzmann constant
K	Kelvin
L	slit width; defined as the normal distance between the carbon planes
n	amount of adsorption

N_A	Avogadro's number
NC	number of component
n^{Ex}	amount of excess adsorption
NPTS	number of data points
P	pressure
psia	pounds per square inch absolute
Q	objective function for equilibrium criterion
R	universal gas constant
RMSE	root mean square error
T	temperature
V_{void}	void volume
W	objective function for mass balance
WAAD	weighted average absolute deviation
WRMS	weighted root mean square
x_i	composition of species i in the adsorbed phase
Y	coal or adsorbing fluid property
y_i	composition of species i in the bulk phase
Z	compressibility factor
z_i	composition of species i in the feed gas
z	normal position between carbon planes
z'	dummy position variable: $z' = z + 3\sigma_{ff}/8$

Subscripts and Superscripts

CH_4@400	Methane at 400 psia
N_2@400	Nitrogen at 400 psia
CO_2@400	CO_2 at 400 psia
ads	adsorbed-phase property
bulk	bulk phase
C	critical condition
calc	calculated
Ex	excess
ff	fluid-fluid interaction
fs	fluid-solid interaction
gas	gas phase
Gibbs	Gibbsian adsorption quantity
He	Helium
i	component “i”
k	Iteration number in Newton-Raphson method
LCL	local
reg	regressed
ss	solid-solid interaction
tot	total
0	reference state

Greek

$\alpha(T)$	temperature dependent function for Peng-Robinson EOS
Δ	difference
ε	interaction parameter
Λ_b	Peng-Robinson EOS covolume "b" correction
μ	chemical potential
ρ	density
$<\rho>$	average adsorbed-phase density
ρ_{atoms}	carbon density
σ	molecular diameter
σ_{exp}	expected experimental uncertainty
η	number of regions divided in the slit interval
Ψ	fluid-solid potential function
$<x_i>$	total adsorbed mole fraction of component "i"
χ_C	carbon weight fraction (%carbon / 100) in basis of moisture and ash free
λ_M	equilibrium moisture weight fraction
φ_{FC}	fixed carbon weight fraction
θ_{Vol}	volatile matter weight fraction

Abbreviation

FR	Fruitland coal
LB FR	Lower Basin Fruitland

CHAPTER 1

INTRODUCTION

A reliable energy supply is essential for our modern lifestyle. The current energy supply relies to varying degrees on fossil fuels (oil, natural gas and coal), nuclear, bio-fuels, hydropower, solar, and wind energy. Among these sources, the fossil fuels provide more than 85% of all the energy consumed in the United States, including two-thirds of the electricity and all of the transportation needs [1].

In the year 2000, natural gas provided 24% of the energy consumed in the United States [2]. As such, it is a vital component of the Nation's energy portfolio. Natural gas, primarily composed of methane, is a cleaner fuel than coal and oil. Unlike coal and oil, natural gas produces very small amounts of greenhouse gases (nitrogen oxides, sulfur dioxide and others) during combustion. In contrast, the combustion products of coal and oil consist of significant amounts of methane, nitrogen oxides and sulfur dioxide. These are harmful products that are emitted into the atmosphere [3]. Hence, natural gas represents a relatively clean supply of energy.

The current estimate of natural gas reserves in the United States is 1,279 Tcf (trillion cubic feet) according to the Energy Information Administration (EIA), 1,451 Tcf according to the National Petroleum Council (NPC) and 1,127 Tcf according to the Potential Gas Committee (PGC). This estimated amount can last over 75 years based on the current consumption rate [4].

Coalbed methane (CBM) is one of the unconventional forms of natural gas. It represents a source for a large amount of methane that resides in coal seams as an adsorbed gas on the surface of the coal. A good portion of this CBM gas can be recovered and used for power generation and other applications. According to the United States Geological Survey [5], the proven reserves of CBM are more than 700 Tcf, and over 100 Tcf of this gas is economically recovered. This corresponds to 7.5% of the U.S. natural gas production [5].

The primary approach to recover methane from coal seams is to depressurize the coalbed by pumping the water out of the reservoirs. In the coalbed, methane resides on the surface of the coal surrounded by water. Pumping water out of the reservoir decreases the pressure within the coalbed; hence, methane is released from the coalbed and is transported to processing facilities through pipelines. However, some solid residues are also produced when water is pumped out of the coal; this raises environmental issues concerning the disposal of water [5].

Further, to improve the recovery rates of this valuable resource, enhanced coalbed methane (ECBM) recovery methods have been developed. These methods rely mainly on nitrogen (N_2), carbon dioxide (CO_2) and/or their mixtures injected into coal seams. Upon injection, the CO_2 replaces the adsorbed methane on the coal matrix, and methane is released. Two to three molecules of CO_2 are adsorbed for each molecule of methane released [6, 7].

Alternatively, methane can also be released by injecting the nitrogen into the coal. Injected nitrogen is not highly adsorbed by the coal, which results in rapid breakthrough

of nitrogen in the recovered natural gas. This requires a separation process after recovery, which increases the cost of production of coalbed methane [8].

Beyond the energy benefits derived from injecting CO_2 in coals, such injections may have a potential environmental benefit. CO_2 is one the greenhouse gases that may contribute to global warming. In 2005, the CO_2 emissions in the United States were 6,008 million metric ton, which represents 84% of the total greenhouse gas emissions [9]. The Energy Information Administration reports that 98% of the CO_2 emissions originated from the combustion of fossil fuels [9]. Many researchers in the field have determined that the presence of such a large quantity of CO_2 in the atmosphere is a major contributor to the rise of the global surface temperature. As such, sequestrating CO_2 in coal seams represents a promising strategy for reducing CO_2 emissions, and thus, reducing its effect on the climate.

To realize the full potential of CBM gas production and CO_2 sequestration, reliable equilibrium adsorption models are required to develop effective processes. Such models should be capable of:

1. Representing precisely high-pressure pure-gas adsorption
2. Facilitating generalized predictions of pure-gas adsorption based on accessible adsorbent and adsorbate characterization
3. Predicting mixed-gas adsorption based on pure-gas isotherms
4. Accounting for the presence of moisture in the coal, since the coalbed usually contains water

Different models with various theoretical underpinnings have been applied to describe the adsorption behaviors of CBM gases. These include the Langmuir equation

[10], Brunauer-Emmett-Teller (BET) model [11], Ideal Adsorbed Solution (IAS) theory [12], Two-Dimensional equation of states (2-D EOS) [13, 14], the Ono-Kondo Lattice model [15-17] and Simplified Local-Density model [18-22]. Most of these adsorption models work well for low pressures systems; however, fewer are capable of describing high-pressure adsorption adequately.

The Langmuir model was developed in 1918. This model describes the dynamic equilibrium between the rates of adsorption and desorption of a gas on a solid adsorbent [10]. Although this model is restricted to monolayer coverage, it is still applied widely because of its simplicity and ability to represent low-pressure adsorption behavior. The BET model, developed in 1938, is an extension of the Langmuir model which accounts for multilayer adsorption [11]. The Ideal Adsorbed Solution (IAS) model is an adsorption equilibrium analog to Raoult's law, and it is applied to determine multi-component adsorption equilibria based on pure-component adsorption data [12].

Recently at Oklahoma State University (OSU), the 2-D EOS, the Ono-Kondo lattice and the simplified local-density models have been developed further to represent and predict the adsorption of CBM gases. The 2-D EOS is an analog to 3-D EOS, which has been implemented successfully for supercritical fluid adsorption on various matrices [13]. More recently, Pan and coworkers [14] developed temperature relations for the 2-D Peng-Robinson (PR) EOS to facilitate precise representation and predictions of high pressure, supercritical pure-gas adsorption.

The Ono-Kondo lattice theory was developed in 1960 [15]. This model is based on the lattice theory, which aims to describe the monolayer and multilayer adsorption. Sudibandriyo [16] further developed the Ono-Kondo (OK) for high-pressure gas

adsorption and presented a strategy for generalizing the OK model parameters as they apply to CBM systems. More recently, Arumugam [16, 17] implemented and further refined these model generalizations for CBM gas adsorption on dry Argonne premium coals.

The simplified local-density (SLD) model describes adsorption behavior using fluid-fluid and fluid-solid interactions. The model delineates the adsorbent structural properties with an assumed physical geometry of the adsorbent. It was first developed by Rangarajan [18], who used the van der Waals EOS to provide the fluid-fluid interaction information. Nevertheless, the SLD model can be applied with various EOSs capable of describing the fluid-fluid interactions. Over the years, researchers have used different equations, including the Peng-Robinson, Bender and Elliot-Suresh-Donohue EOSs to provide fluid-fluid interaction information [19-22].

Recently, Fitzgerald [23] applied the SLD model with a modified PR EOS to represent precisely the high-pressure adsorption of CO_2, nitrogen, methane, and ethane and their mixtures on dry and wet coals and activated carbons. Careful evaluations of the model revealed several distinct advantages, including the ability to:

1. Correlate pure-gas adsorption on dry and wet coals within the expected experimental uncertainties
2. Extend pure-gas adsorption to multi-component gas prediction using appropriate mixing rules
3. Facilitate viable model parameter generalizations based on adsorbent characteristics and gas properties

As such, the SLD-PR model provides a suitable framework for developing generalized models for the prediction of CBM gas adsorption on wet coals.

Objectives

The purpose of this study is to develop the generalized correlations for the modified SLD-PR model parameters. The goal is to render the SLD framework capable of providing reliable predictions for the equilibrium adsorption of CO_2, methane, nitrogen and their mixtures on dry and wet coals in the range of conditions encountered in CBM production and CO_2 sequestration. The specific objectives of this study are to:

- Correlate precisely the CO_2, methane and nitrogen adsorption on dry and wet coals using the modified SLD-PR model
- Evaluate the quality of the representations of the modified SLD-PR model for pure-gas adsorption
- Generalize the modified model parameters in terms of accessible coal characterizations and fluid properties
- Extend the model generalization to binary and ternary gas adsorption on wet coals based on pure-gas adsorption generalizations and, when needed, generalized the binary interaction parameters

Organization

In this thesis, Chapter 2 provides an overview of the modified SLD-PR model. In Chapter 3, the modified SLD-PR model representations of pure-gas adsorption are evaluated. Chapter 4 presents the SLD-PR parameter generalization for pure-gas

adsorption and assesses the quality of pure-gas adsorption predictions. Chapter 5 describes methods used to extend the SLD-PR generalizations to mixed-gas adsorption and examines the predictive capability of the generalized model for binary and ternary mixtures. Chapter 6 presents the conclusions and recommendations of this study.

CHAPTER 2

SIMPLIFIED LOCAL-DENSITY MODEL

The Simplified local-density (SLD) model has been found capable of describing the adsorption behavior of gases encountered in CBM production and CO_2 sequestration. This model superimposes the fluid-solid potential on a fluid equation of state to predict the adsorption of supercritical fluids on a flat wall [18, 24].

For the slit geometry, the SLD model assumes the adsorbate molecules reside between two-surface slit, as shown in Figure 2.1 [22]. The distance between surfaces is L, and the position of a molecule within the slit is z. The position, z, is orthogonal to surface of solid which is formed by carbon atoms. Within the slit, the adsorbate molecule interacts with both the slit surfaces and the fluid molecules in the bulk gas.

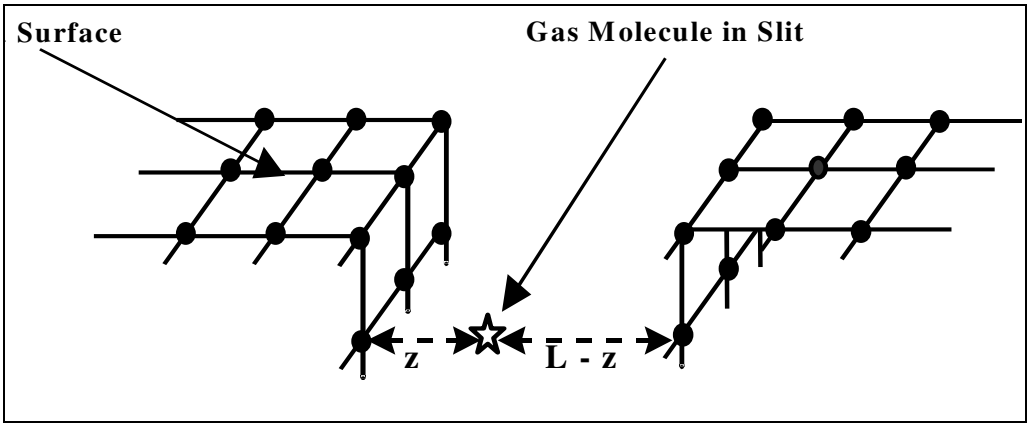

Figure 2.1 – SLD Model Slit Geometry

A number of assumptions have been made in developing the SLD model [18]:

1. The chemical potential at any point near the adsorbent surface is equal to the bulk phase chemical potential.
2. The chemical potential at any point above the surface is the sum of the fluid-fluid and fluid-solid interactions.
3. The attractive potential between fluid and solid is independent of the number of molecules at and around the point.

Hence, at equilibrium, the chemical potential of the fluid, μ, is expressed as the sum of the fluid-fluid and fluid-solid potentials as follows:

$$\mu(z) = \mu_{ff}(z) + \mu_{fs}(z) = \mu_{bulk} \tag{2-1}$$

where subscript "bulk" refers to bulk fluid, "ff" refers to fluid-fluid interactions, and "fs" signify fluid-solid interaction.

The chemical potential of the bulk fluid is typically expressed in terms of fugacity as:

$$\mu_{bulk} = \mu_0(T) + RT\ln\left(f_{bulk}/f_0\right) \tag{2-2}$$

where subscript "0" designates the reference state and "f" refers to fugacity. Similarly, the chemical potential from fluid-fluid interactions is:

$$\mu_{ff}(z) = \mu_0(T) + RT\ln\left(f_{ff}(z)/f_0\right) \tag{2-3}$$

where "$f_{ff}(z)$" is fluid fugacity at a position z.

The fluid-solid interactions are accounted for through the potential energy function. As such, the fluid-solid chemical potential is given as:

$$\mu_{fs}(z) = N_A\left[\Psi^{fs}(z) + \Psi^{fs}(L - z)\right] \tag{2-4}$$

where "N_A" is Avogadro's number, "$\Psi(z)$" and "$\Psi(L-z)$" are the fluid-solid interactions for two-surface slits with the distance L.

Substituting Equations (2-2), (2-3) and (2-4) into Equation (2-1), one gets the equilibrium relationship adsorption within the slit:

$$f_{ff}(z) = f_{bulk}\exp\left(-\frac{\Psi^{fs}(z) + \Psi^{fs}(L - z)}{kT}\right) \tag{2-5}$$

Typically, a van der Waals-type equation of state such as the Peng-Robinson [25] equation and an integrated potential function (e.g., 10-4 Lennard-Jones model) are used to determine the fluid-fluid and fluid-solid chemical contributions.

The SLD model is a simplification of local-density theory. According to this theory, the density profile is obtained by minimizing the total energy functional, which depends on all point densities and their spatial derivatives [26]. The term "local" refers to the thermodynamics properties of a fluid at any local point z, where an average single density value is calculated, $\rho(z)$ [18]. In addition, the SLD model assumes a mean-field theory in calculating the chemical potential. The mean-field theory replaces all interactions with an effective or average interaction so that no fluctuations are considered within the slit. Hence, the chemical potential of the fluid at each point is corrected for the proximity of the fluid molecule to the molecular wall of the adsorbents [23].

Applying the SLD model, the excess adsorption (n^{Ex}) is given as:

$$n^{Ex} = \frac{A}{2}\int_{\text{Left Side of Slit}}^{\text{Right Side of Slit}}(\rho(z) - \rho_{bulk})dz \tag{2-6}$$

Here, n^{Ex} is the excess adsorption of adsorbate in number of moles per unit mass of

adsorbent, and "A" is the surface area of the adsorbate on particular solid. The lower limit in Equation (2-6) is $3\sigma_{ff}/8$, which is 3/8 of an adsorbed molecule touching the left plane surface. The upper limit is $L-3\sigma_{ff}/8$, the location of an adsorbed molecule touching right plane surface. The local density is assumed to be zero for the distance less than $3\sigma_{ff}/8$ away from the wall. The value $3\sigma_{ff}/8$ is chosen to account for most of the adsorbed gas; details are given elsewhere by Fitzgerald [6]. The left and right sides of the slit each comprise half of the total surface area, A/2.

Following previous studies at OSU [23], the Peng-Robinson equation of state (PR EOS) is used to provide the bulk fluid fugacity and the fluid fugacity. The compressibility factor, expressed in terms of density, is given as:

$$\frac{P}{\rho RT} = \frac{1}{(1-\rho b)} - \frac{a(T)\rho}{RT\left[1+\left(1-\sqrt{2}\right)\rho b\right]\left[1+\left(1+\sqrt{2}\right)\rho b\right]} \tag{2-7}$$

where

$$a(T) = \frac{0.457535\,\alpha(T)R^2T_C^2}{P_C} \tag{2-8}$$

$$b = \frac{0.077796\,RT_C}{P_C} \tag{2-9}$$

The term, $\alpha(T)$ in Equation (2-8) is calculated using the Mathias-Copeman expression.

$$\alpha(T) = \left[1 + C_1\left(1-\sqrt{\frac{T}{T_C}}\right) + C_2\left(1-\sqrt{\frac{T}{T_C}}\right)^2 + C_3\left(1-\sqrt{\frac{T}{T_C}}\right)^3\right]^2 \tag{2-10}$$

The regressed coefficients, C_1-C_3 [27] along with the gas physical properties, are given in the Table 2.1.

Table 2.1 – Fluid Physical Properties [27, 28]

	Nitrogen	**Methane**	**CO_2**
T_C (K)	126.19	190.56	304.13
P_C (MPa)	3.396	4.599	7.377
σ_{ff} (nm)	0.3798	0.3758	0.3941
ε_{ff}/k (K)	71.4	148.6	195.2
C_1	0.43694	0.41108	0.71369
C_2	-0.07912	-0.14020	-0.44764
C_3	0.32185	0.27998	2.43752

The fugacity of a bulk fluid calculated using PR EOS, where:

$$\ln\frac{f_{bulk}}{P} = \frac{b\rho}{1-b\rho} - \frac{a(T)\rho}{RT\left(1+2b\rho - b^2\rho^2\right)}$$

$$-\ln\left[\frac{P}{RT\rho} - \frac{Pb}{RT}\right] - \frac{a(T)}{2\sqrt{2}bRT}\ln\left[\frac{1+(1+\sqrt{2})\rho b}{1+(1-\sqrt{2})\rho b}\right] \qquad (2\text{-}11)$$

For adsorbing fluid, the fugacity for fluid-fluid interactions is as follows:

$$\ln\frac{f_{ff}(z)}{P} = \frac{b\rho(z)}{1-b\rho(z)} - \frac{a_{ads}(z)\rho(z)}{RT\left(1+2b\rho(z) - b^2\rho^2(z)\right)}$$

$$-\ln\left[\frac{P}{RT\rho(z)} - \frac{Pb}{RT}\right] - \frac{a_{ads}(z)}{2\sqrt{2}bRT}\ln\left[\frac{1+(1+\sqrt{2})\rho(z)b}{1+(1-\sqrt{2})\rho(z)b}\right] \qquad (2\text{-}12)$$

The parameter "$a_{ads}(z)$" in Equation (2-12) varies with the position within the slit. Chen *et al.* [22] provided the equations for "$a_{ads}(z)$" which depend on the ratio of slit width L to the molecular diameter σ_{ff}. Further details on these equations are given by Fitzgerald [23].

Rearranging the equilibrium relationship given in Equation (2-6) yields the working equation accounting for bulk, fluid-fluid and fluid-solid interactions:

$$\ln\left(\frac{f_{ff}[a_{ads}(z),\rho(z)]}{f_{bulk}}\right)=-\left(\frac{\Psi^{fs}(z)+\Psi^{fs}(L-z)}{kT}\right) \tag{2-13}$$

In the previous studies [23, 29], Fitzgerald adjusted the covolume "b" in the PR EOS to improve the predictive capability for adsorption of pure gases on activated carbon and coals. The covolume has significant effect on the local density of the adsorbed fluid, especially near the surface. In addition, the covolume is important in determining the density profile at high pressures. Thus, a simple empirical correction was used to account for the repulsive interactions of adsorbed fluid at high pressures. The covolume is corrected by an adjustable parameter, Λ_b:

$$b_{ads}=b(1+\Lambda_b) \tag{2-14}$$

Equation (2-12) then becomes:

$$\ln\frac{f_{ff}(z)}{P}=\frac{b_{ads}\rho(z)}{1-b_{ads}\rho(z)}-\frac{a_{ads}(z)\,\rho(z)}{RT[1+2b_{ads}\rho(z)-b_{ads}^2\rho(z)^2]}$$

$$-\ln\left[\frac{1-b_{ads}\rho(z)}{RT\rho(z)}\right]-\frac{a_{ads}(z)}{2\sqrt{2}b_{ads}RT}\ln\left[\frac{1+(1+\sqrt{2})\rho(z)b_{ads}}{1+(1-\sqrt{2})\rho(z)b_{ads}}\right] \tag{2-15}$$

The fluid-solid interaction, $\Psi^{fs}(z)$, is represented by Lee's partially-integrated Lennard-Jones 10-4 potential [30], the equation is shown below:

$$\Psi^{fs}(z)=4\pi\rho_{atoms}\varepsilon_{fs}\sigma_{fs}^2\left(\frac{\sigma_{fs}^{10}}{5(z')^{10}}-\frac{1}{2}\sum_{i=1}^{4}\frac{\sigma_{fs}^4}{(z'+(i-1)\cdot\sigma_{ss})^4}\right) \tag{2-16}$$

$$\varepsilon_{fs}=\sqrt{\varepsilon_{ff}\times\varepsilon_{ss}} \tag{2-17}$$

where ε_{fs} is the fluid-solid interaction energy parameter, and the ρ_{atoms} = 0.382 atoms/Å^2.

The parameters σ_{ff} and σ_{ss} signify, respectively, the molecular diameter of the adsorbate and the carbon interplaner distances. The value of carbon interplaner is taken to be the value of graphite, 0.335 nm [24], and values of σ_{ff} and ε_{ff} are taken from Reid [28]. The fluid-solid molecular diameter, σ_{fs} and dummy coordinate z' are defined as:

$$\sigma_{fs} = \frac{\sigma_{ff} + \sigma_{ss}}{2} \tag{2-18}$$

$$z' = z + \frac{\sigma_{ss}}{2} \tag{2-19}$$

In the bulk phase, the bulk fluid fugacity is calculated from the pressure and temperature. For the adsorbed phase, the slit is divided into two halfs and each is subdivided into 50 intervals. The local density is then calculated by solving the adsorbed phase fugacity and equilibrium criterion (Equations (2-15) and (2-13), respectively) simultaneously for each interval. Once the local density is determined across the slit, the excess adsorption is calculated by integrating Equation (2-6) numerically using Simpson's Rule. The details of the calculation are discussed in Appendix A.

CHAPTER 3

REPRESENTATION OF PURE-GAS ADSORPTION

In previous studies at OSU, the Simplified Local-Density/Peng-Robinson (SLD-PR) model with an adjusted PR covolume "b" was tested for its ability to correlate the adsorption behavior on coals of interest. The model was found capable of correlating adsorption data within the expected experimental uncertainties [23].

To correlate and predict the adsorption behavior on coals, the model requires physical parameters which can characterize both the adsorbent and adsorbate. In the modified SLD-PR model, all the adsorbates on a given adsorbent were analyzed simultaneously; hence, a set of parameters for that adsorbent were regressed to correlate to the respective adsorption data. These parameters are:

- A single value of surface area "A" for a given adsorbent applied to <u>all</u> adsorbates
- A single value of slit length "L" for a given adsorbent to <u>all</u> adsorbates
- Fluid-solid interaction energy parameters "ε_{fs}/k" for <u>each</u> adsorbate on a given adsorbent
- Covolume correction "Λ_b" for <u>each</u> adsorbate

These parameters depend on either adsorbent or adsorbate; thus, attempts to generalize the SLD-PR model parameters must account for adsorbent and adsorbate characteristics.

Model Development

The current study differs from the study described previously in that the surface area and the fluid-solid interaction energy parameter are adjusted to obtain precise representation of pure-gas adsorption. In the previous work, each adsorbent has a specific value for the surface area (independent of the adsorbate) [23]. However, this adsorbent-based surface area was not able to precisely quantify or differentiate the amount of adsorption for each adsorbate. Therefore, in this study, each adsorbate is allowed to have its own "accessible" surface area on a given adsorbent; thus, the adsorption model is capable of providing a more precise correlation of the adsorption data.

In addition, the solid-solid interaction energy parameter, ε_{ss}/k, is regressed instead of the fluid-solid interaction energy parameter, ε_{fs}/k. The regressed fluid-solid interaction energy for CO_2 was found to be twice as large as those for methane and nitrogen [31, 32]. However, for some adsorbents used in this study, the regressed fluid-solid interaction energy parameter for CO_2 was more than three times larger than those for methane and nitrogen and also greater than the value for CO_2 on activated carbon. This discrepancy in parameter values indicated that regressing directly the fluid-solid interaction energy parameter is unreliable and a modification is required. In fact, beyond the empirical evidence, separating the solid-solid and fluid-fluid interactions is advisable, since they express two different types of interactions, of which the fluid-fluid interaction data are available and the solid-solid interactions can be obtained by regression. The fluid-solid interaction energy parameter is then described in the model as the geometric mean of the

fluid-fluid and solid-solid interaction energy parameter (ε_{ff}/k and ε_{ss}/k), as expressed in Equation (2-17) [19, 32].

In this study, the fluid-fluid interaction parameter values are obtained from Reid *et al*. [28], and the solid-solid interaction energy parameter is regressed from the adsorption data to facilitate the development of generalized model(s) in terms of adsorbent properties. As such, the solid-solid interaction energy parameter provides specific information about the particular coal, independent of the type of adsorbate involved.

For each adsorbent, the adsorption isotherms for different adsorbate gases are correlated simultaneously to obtain single regressed values for the slit length and the solid-solid interaction energy parameter. Therefore, the parameters regressed for each adsorbent are:

- A separate surface area for each adsorbate
- Slit length
- Solid-solid interaction energy parameter "ε_{ss}/k"
- A covolume correction "Λ_b" for each adsorbate

As such, for each adsorbent, there are a total of (2N +2) parameters, where N is the number of adsorbates.

During the model parameter regressions, three different scenarios examining the effect of the covolume correction and the slit length were investigated:

Scenario 1: All model parameters were regressed (2N + 2 parameters)

Scenario 2: Surface areas of all adsorbates, the solid-solid interaction energy parameter and the slit length were regressed after fixing the covolume correction "Λ_b" at a value of -0.20 (N + 3 parameters)

Scenario 3: In addition to Scenario 2, the slit length is fixed at 1.15 nm, and the surface area for each adsorbate and the solid-solid interaction energy parameters were regressed (N + 2 parameters)

The -0.20 value of the covolume correction used in Scenarios 2 and 3 was established based on the results obtained in Scenario 1. This correction produced a precise correlation for the experimental data considered. The slit length of 1.15 nm used in Scenario 3 was the average value of the regressed slit lengths obtained in Scenario 2.

Database Employed in this Study

Experimental measurements were conducted at Oklahoma State University on ten solid matrices, which include the following [17, 23]:

a) Pure methane, nitrogen and CO_2 adsorption on dry Illinois #6, dry Beulah Zap, dry Wyodak, dry Upper Freeport and dry Pocahontas coals

b) Pure methane, nitrogen and CO_2 adsorption on the wet Illinois #6, wet Fruitland OSU #1, wet Fruitland OSU #2, wet Lower Basin Fruitland, Wet Tiffany coals

Coals listed in (a) were prepared by Argonne National Laboratory (Argonne premium coals) and the respective isotherms were measured at 328.15K (131°F) and pressures to 13.7 MPa (2000 psia). The measurements on the Fruitland OSU #1 and #2, Lower Basin Fruitland and Ilinois #6 coals in category (b) were at 319.3K (115°F) and

pressures to 12.4 MPa (1800 psia) while the experiments on the Tiffany coal were measured at 328.15K (131°F) and pressures to 12.4 MPa (2000 psia). These five coals were classified as OSU coals to differentiate them from coals prepared by Argonne National Laboratory.

The pure-gas adsorption database on dry Argonne premium coals and wet OSU coals are presented in Tables 3.1 and 3.2, respectively. In the tables, the system number, adsorbent, adsorbate, number of data points (NTPS), temperature and pressure ranges are given.

Table 3.1 – Pure-Gas Adsorption Database Used in this Study: Argonne Premium Coals

System No.	Adsorbent	Adsorbate	NPTS	Temp (K)	Pressure Range (MPa)
1	Dry Illinois #6	N_2	16	328	0.7 – 13.7
2	Dry Illinois #6	CH_4	15	328	0.7 – 13.7
3	Dry Illinois #6	CO_2	22	328	0.7 – 13.7
4	Dry Beulah Zap	N_2	15	328	0.7 – 13.7
5	Dry Beulah Zap	CH_4	14	328	0.7 – 13.7
6	Dry Beulah Zap	CO_2	33	328	0.7 – 13.7
7	Dry Wyodak	N_2	14	328	0.7 – 13.7
8	Dry Wyodak	CH_4	14	328	0.7 – 13.7
9	Dry Wyodak	CO_2	22	328	0.7 – 13.7
10	Dry Upper Freeport	N_2	14	328	0.7 – 13.7
11	Dry Upper Freeport	CH_4	14	328	0.7 – 13.7
12	Dry Upper Freeport	CO_2	22	328	0.7 – 13.7
13	Dry Pocahontas	N_2	14	328	0.7 – 13.7
14	Dry Pocahontas	CH_4	14	328	0.7 – 13.7
15	Dry Pocahontas	CO_2	22	328	0.7 – 13.7

Table 3.2 – Pure-Gas Adsorption Database Used in this Study: OSU Coals

System No.	Adsorbent	Adsorbate	NPTS	Temp (K)	Pressure Range (MPa)
16	Wet Illinois #6	N_2	20	319	0.7 – 12.4
17	Wet Illinois #6	CH_4	20	319	0.7 – 12.4
18	Wet Illinois #6	CO_2	30	319	0.7 – 12.4
19	Wet Fruitland OSU #1	N_2	20	319	0.7 – 12.4
20	Wet Fruitland OSU #1	CH_4	20	319	0.7 – 12.4
21	Wet Fruitland OSU #1	CO_2	14	319	0.7 – 12.4
22	Wet Fruitland OSU #2	N_2	37	319	0.7 – 12.4
23	Wet Fruitland OSU #2	CH_4	20	319	0.7 – 12.4
24	Wet Fruitland OSU #2	CO_2	38	319	0.7 – 12.4
25	Wet Tiffany	N_2	21	328	0.7 – 13.7
26	Wet Tiffany	CH_4	34	328	0.7 – 13.7
27	Wet Tiffany	CO_2	16	328	0.7 – 13.7
28	Wet LB Fruitland	N_2	17	319	0.7 – 12.4
29	Wet LB Fruitland	CH_4	16	319	0.7 – 12.4
30	Wet LB Fruitland	CO_2	48	319	0.7 – 12.4

Tables 3.3 and 3.4 give the compositional analyses of the OSU and Argonne premium coals, respectively [23]. For the OSU coals, Illinois #6 is a highly volatile bituminous coal. The Fruitland OSU #1 and #2 have different compositions; they are both medium volatile bituminous coals from the San Juan Basin. The Lower Basin Fruitland (#3a and #3b) is from the same coal seam as Fruitland OSU #1 and #2, but it was taken from a different location. The Tiffany is the BP Amoco Tiffany Well #1 and #10. These coals are moistened with water from 4 to 15% by weight, which is above the equilibrium moisture content of all these coals [23]. From Table 3.3, the increasing order in the percent carbon on a moisture and ash-free basis is as follows for these coals: Lower Basin Fruitland, Tiffany, Fruitland OSU #2, Fruitland OSU #1, and Illinois #6. The increasing order in percent fixed carbon for these coals is: Lower Basin Fruitland, Tiffany, Illinois #6, Fruitland OSU #2 and Fruitland OSU #1.

Table 3.3 – Compositional Analysis of OSU Coals Used in this Study

Analysis*	Fruitland OSU #1	Fruitland OSU #2	Illinois #6	Lower Basin Fruitland OSU #3a	Lower Basin Fruitland OSU #3b	Tiffany Well #1	Tiffany Well #10
Ultimate							
Carbon %	68.63	66.58	71.47	38.92	40.20	47.78	56.75
Hydrogen %	4.27	4.23	5.13	3.08	3.10	2.62	2.77
Oxygen %	0.89	5.08	9.85	3.75	2.87	6.19	5.16
Nitrogen %	1.57	1.47	1.46	0.87	0.89	0.92	1.02
Sulfur %	4.19	0.72	1.27	1.73	2.14	0.57	0.52
Ash %	20.45	21.92	10.81	51.66	50.81	49.71	47.74
Proximate							
Vol. Matter %	20.20	20.33	30.61	20.01	14.00	15.48	15.35
Fixed Carbon %	59.35	57.75	55.90	28.33	35.19	34.82	36.91
Moisture %	2.20	2.20	3.90	4.00	4.00	3.80	3.70

* Huffman Laboratories, Inc., Golden, Colorado.

The percent carbon and percent fixed carbon of these coals range from 38.0 to 69.0% and 28.0 to 60.0%, respectively. The percentage volatile matter of these coals ranges from 14.0 to 30.0%. The largest percent volatile matter is observed for the Illinois #6 coal, followed by Fruitland OSU #2 and #1 coals. The Tiffany and Lower Basin Fruitland coals have the smaller percentage of volatile matter. Regarding the equilibrium moisture content, the Lower Basin Fruitland has the largest percentage of 4.0%, followed by Illinois #6 and Tiffany coals, which have 3.9% and 3.75%, respectively. The Fruitland OSU #1 and #2 coals have the lowest equilibrium moisture content of 2.2%.

Table 3.4 - Compositional Analysis of Argonne Premium Coals Used in this Study

Analysis*	Beulah Zap	Wyodak	Illinois #6	Upper Freeport	Pocahontas
Ultimate					
Carbon %	72.9	75.00	77.70	85.50	91.10
Hydrogen %	4.83	5.35	5.00	4.70	4.44
Oxygen %	20.30	18.00	13.50	7.50	2.50
Sulfur %	0.80	0.63	4.83	2.32	0.66
Ash %	9.70	8.80	15.50	13.20	4.80
Proximate					
Moisture %	32.20	28.10	8.00	1.10	0.70
Vol. Matter %	30.50	32.20	36.90	27.10	18.50
Fixed Carbon %	30.70	33.00	40.90	58.70	76.10
Ash %	6.60	6.30	14.30	13.00	4.70

* Argonne National Laboratory

Among the Argonne premium coals, Beulah Zap is a lignite coal while Wyodak is a sub-bituminous coal. The Illinois #6, Upper Freeport and Pocahontas are high, medium and low volatile bituminous coals, respectively. As mentioned previously, these coals are prepared by Argonne National Laboratory, and the compositional ultimate and proximate analyses are also provided from this laboratory. The increasing order of percent carbon

(moisture and ash free) and fixed carbon of the Argonne premium coals is: Beulah Zap, Wyodak, Illinois #6, Upper Freeport and Pocahontas. The range of the percent carbon and fixed carbon is from 72.9% to 91.1% and 30.7% to 76.1%. The increasing order of equilibrium moisture content of these coals is opposite to the order of percent carbon and fixed carbon. The percentage for equilibrium moisture ranged from 0.7% to 32.2%. The largest percent volatile matter was 36.9% for Illinois #6, which was followed by Wyodak, Beulah Zap, Upper Freeport and Pocahontas at 32.2, 30.5, 27.1 and 18.5% [17]. The dry samples for pure-gas adsorption were dried under vacuum at 80℃ for 80 hours. The wet samples for pure CO_2 adsorption are "as-received" coals; which means the moisture content for adsorption is the equilibrium moisture content.

The adsorption isotherms of pure methane, nitrogen and CO_2 on the dry Argonne premium and the wet OSU coals were used to evaluate the correlative abilities of the modified SLD-PR model, and the model parameters were then generalized in terms of gas and adsorbent characteristics.

Statistical Quantities Used in Data Reduction

The objective function used in the parameter regressions was the sum of the squared weighted deviation (or the weighted root mean square deviation, WRMS):

$$\mathrm{WRMS} = \frac{\sqrt{\sum_{i=1}^{\mathrm{NPTS}} \left(\frac{n_{calc} - n_{exp}}{\sigma_{exp}} \right)_i^2}}{\mathrm{NPTS}} \qquad (3\text{-}1)$$

Here, NPTS is the number of data points, n_{exp} is the experimental excess adsorption, n_{calc} is the calculated excess adsorption and σ_{exp} is the expected experimental uncertainty. In addition, the weighted average absolute deviation (WAAD), the average absolute

percentage deviation (%AAD) and the root mean square error (RMSE) were calculated to assess the quality of the representations of the adsorption model, and are expressed as:

$$\text{WAAD} = \frac{\sum_{i=1}^{\text{NPTS}} \text{abs}\left(\frac{n_{\text{calc}} - n_{\text{exp}}}{\sigma_{\text{exp}}}\right)_i}{\text{NPTS}} \tag{3-2}$$

$$\%\text{AAD} = \frac{\sum_{i=1}^{\text{NPTS}} \text{abs}\left(\frac{n_{\text{calc}} - n_{\text{exp}}}{n_{\text{exp}}}\right)_i}{\text{NPTS}} \times 100\% \tag{3-3}$$

$$\text{RMSE} = \frac{\sqrt{\sum_{i=1}^{\text{NPTS}} \left(n_{\text{calc}} - n_{\text{exp}}\right)_i^2}}{\text{NPTS}} \tag{3-4}$$

Results and Discussions

The regression results for Scenarios 1, 2 and 3 are presented in Tables 3.5 to 3.7, respectively, for dry Argonne premium coals and wet OSU coals. The information given in the tables include the adsorbent, the adsorbate and the regressed parameters (surface area for each adsorbate, solid-solid interaction energy parameter, slit length and covolume correction of each adsorbate). The statistics described in Equations (3-1) through (3-4) are also provided.

As illustrated in Table 3.5, full regression of all the model parameters (Scenario 1) provides representation of the adsorption data within the expected experimental uncertainties. The overall %AAD is 3.2%, which also corresponds to an overall WAAD of 0.40, RMSE of 0.03 mmol/g, and WRMS of 0.55. The WRMS is less than the experimental uncertainty because the experimental uncertainties were taken to be twice the amount obtained from the raw data reduction procedure.

Table 3.5 – Scenario 1: Modified SLD-PR Model Representations of Pure-Gas Adsorption on Dry and Wet Coals

Coal	Adsorbate	Parameters				WAAD	%AAD	RMSE (mmol/g)	WRMS
		Area (m^2/g)	ε_{ss}/k (K)	L (nm)	Λ_b				
Dry Illinois #6	CH_4	74.8	29.8	1.88	0.00	0.36	2.5	0.02	0.45
	N_2	52.8			0.01				
	CO_2	119.2			0.13				
Dry Beulah Zap	CH_4	48.8	52.2	1.62	-0.11	0.43	2.9	0.04	0.54
	N_2	33.0			-0.09				
	CO_2	113.8			0.06				
Dry Wyodak	CH_4	50.2	47.5	1.74	-0.16	0.68	3.1	0.05	0.96
	N_2	32.2			-0.30				
	CO_2	109.3			0.02				
Dry Upper Freeport	CH_4	54.6	38.2	1.29	-0.07	0.30	1.5	0.01	0.42
	N_2	37.1			-0.15				
	CO_2	66.5			-0.02				
Dry Pocahontas	CH_4	73.8	36.7	1.22	-0.07	0.40	1.8	0.02	0.59
	N_2	51.6			-0.12				
	CO_2	83.8			-0.05				
Statistic for Dry Coals						0.43	2.4	0.03	0.59

Table 3.5 – Scenario 1: Modified SLD-PR Model Representations of Pure-Gas Adsorption on Dry and Wet Coals (Continued)

Coal	Adsorbate	Parameters				WAAD	%AAD	RMSE (mmol/g)	WRMS
		Area (m^2/g)	ε_{ss}/k (K)	L (nm)	Λ_b				
Wet Illinois #6	CH_4	31.4	20.9	1.36	-0.23	0.26	3.9	0.04	0.39
	N_2	17.4			-0.34				
	CO_2	52.0			-0.12				
Wet Fruitland OSU #1	CH_4	66.3	22.2	1.11	-0.16	0.28	1.9	0.03	0.41
	N_2	49.4			-0.21				
	CO_2	70.6			-0.22				
Wet Fruitland OSU #2	CH_4	68.7	20.8	1.11	-0.15	0.47	4.8	0.06	0.66
	N_2	43.1			-0.18				
	CO_2	66.1			-0.22				
Wet Tiffany	CH_4	37.5	19.6	1.11	-0.12	0.51	5.0	0.02	0.44
	N_2	24.3			-0.10				
	CO_2	55.7			0.01				
Wet Lower Basin Fruitland	CH_4	15.0	30.1	1.20	-0.42	0.34	4.7	0.02	0.66
	N_2	10.0			-0.43				
	CO_2	29.1			-0.13				
Statistics for Wet Coals						0.37	4.1	0.03	0.51
Overall Statistics for Coals						**0.40**	**3.2**	**0.03**	**0.55**

The largest %AAD (5.0%) and largest RMSE (0.06 mmol/g) are observed for pure-gas adsorption on wet Tiffany and wet Fruitland OSU #2, respectively. The largest WAAD (0.68) and WRMS (0.96) are observed for the pure-gas adsorption on dry Wyodak coal. The results indicate that regressing separate surface areas for each adsorbate along with the solid-solid interaction energy parameter produces adsorption data representations for both dry Argonne premium coals and wet OSU coals within the expected experimental uncertainties.

As expected, the amount of CO_2 adsorbed is higher than the amount of methane and nitrogen adsorbed on all coals. Hence, the regressed surface area of CO_2 is greater than that of methane and that of nitrogen and the average surface area ratio of methane to CO_2 and nitrogen to CO_2 is 0.66 and 0.47, respectively.

The average %AAD of the representations for wet OSU coals (4.1%) is larger than that for dry Argonne coals (2.4%); however, larger experimental uncertainties are estimated for the wet OSU coals than for the dry Argonne coals resulting in more precise representation of pure-gas adsorption for the wet OSU coals compared to those for dry Argonne coals. The respective WAAD is 0.37 and 0.41 for the OSU and Argonne coals, respectively. The slit length of the dry Argonne coals is larger than that of the wet OSU coals, and the new model parameter, ε_{ss}/k, of the dry Argonne coals is larger than that of wet OSU coals. The regressed covolume corrections for the dry Argonne coals are small numbers that have a minor effect on the adsorbed-phase density.

Appendix B.1 presents the regression results for the SLD-PR model representation when no covolume corrections are applied ($\Lambda_b = 0$) to the dry coals. In comparison with the results given above that involved a covolume correction, a

significant difference in the results is not observed, which indicates that covolume correction is not required for the dry Argonne coals. In contrast, the regressed covolume corrections for the wet OSU coal are relatively large numbers, which have a significant effect on the adsorbed-phase densities. Further, they affect the quality of the representations. Therefore, the covolume corrections are required for modeling the adsorption on wet OSU coals.

Table 3.6 documents the regression results for Scenario 2. The overall error for the combined dry Argonne and wet OSU coals is 3.9 %AAD, with a WAAD of 0.50, RMSE of 0.04 mmol/g and WRMS of 0.70. The largest average %AAD (5.6%) and RMSE (0.06 mmol/g) are observed for the pure-gas adsorption on wet Lower Basin Fruitland and wet Fruitland OSU #2 coals, respectively.

Pure-gas adsorption on the Wyodak coal has the largest WAAD and WRMS, 0.80 and 1.25, respectively. As shown in Table 3.6, the deviations for the dry coals have increased significantly compared to that for Scenario 1. This is due to the value of -0.20 for the covolume corrections is too big for the dry coals (see individual Λ_b values in Table 3.5). For wet coals, there is no significant increase in the deviations because the correction value of -0.20, chosen based on the results of Scenario 1, is closer to the average of the regressed values. Nevertheless, on average, the modified SLD-PR model can represent the adsorption data within experimental uncertainties for the regression including the fixed covolume correction of -0.20.

Table 3.6 – Scenario 2: Modified SLD-PR Model Representations of Pure-Gas Adsorption on Dry and Wet Coals

Coal	Adsorbate	Parameters				WAAD	%AAD	RMSE (mmol/g)	WRMS
		Area (m^2/g)	ε_{ss}/k (K)	L (nm)	Λ_b (fixed)				
Dry Illinois #6	CH_4	61.5	30.4	1.34	-0.2	0.67	4.6	0.06	0.92
	N_2	45.5							
	CO_2	77.5							
Dry Beulah Zap	CH_4	50.4	37.7	1.30	-0.2	0.63	3.9	0.04	0.83
	N_2	35.7							
	CO_2	92.8							
Dry Wyodak	CH_4	57.9	31.6	1.32	-0.2	0.80	3.5	0.05	1.25
	N_2	45.2							
	CO_2	96.4							
Dry Upper Freeport	CH_4	47.6	37.5	1.18	-0.2	0.39	2.1	0.02	0.54
	N_2	36.0							
	CO_2	54.1							
Dry Pocahontas	CH_4	63.6	37.2	1.15	-0.2	0.46	2.2	0.03	0.68
	N_2	47.9							
	CO_2	69.4							
Statistic for Dry Coals						0.59	3.3	0.04	0.84

Table 3.6 – Scenario 2: Modified SLD-PR Model Representations of Pure-Gas Adsorption on Dry and Wet Coals (Continued)

Coal	Adsorbate	Parameters				WAAD	%AAD	RMSE (mmol/g)	WRMS
		Area (m^2/g)	ε_{ss}/k (K)	L (nm)	Λ_b (fixed)				
Wet Illinois #6	CH_4	34.2	19.4	1.27	-0.2	0.28	4.4	0.04	0.41
	N_2	20.6							
	CO_2	47.9							
Wet Fruitland OSU #1	CH_4	62.5	22.9	1.11	-0.2	0.30	2.1	0.03	0.42
	N_2	49.0							
	CO_2	72.0							
Wet Fruitland OSU #2	CH_4	62.3	22.1	1.13	-0.2	0.48	4.9	0.06	0.66
	N_2	40.7							
	CO_2	65.9							
Wet Tiffany	CH_4	39.5	16.7	0.91	-0.2	0.57	5.4	0.02	0.74
	N_2	25.7							
	CO_2	51.1							
Wet Lower Basin Fruitland	CH_4	26.9	19.1	1.08	-0.2	0.45	5.6	0.02	0.55
	N_2	16.7							
	CO_2	32.2							
Statistic for Wet Coals						0.42	4.5	0.03	0.56
Overall Statistics for Coals						**0.50**	**3.9**	**0.04**	**0.70**

For both the dry Argonne and the wet OSU coals, the regressed slit length is less than 1.5 nm, and the solid-solid interaction energy parameter is less than 40K, which is the reported value for activated carbon. Similar to Scenario 1, the %AAD of the representation for the wet OSU coals (4.5%) is larger than that for the dry Argonne coals (3.3%). However, the WAAD values are better for the wet OSU coals (0.42) than for the dry Argonne coals (0.59).

Table 3.7 presents the regression results for Scenario 3. With fixed values for the covolume correction (-0.20) and the slit length (1.15 nm), the overall statistics for the dry and the wet coals is 4.5 %AAD, which corresponds to a WAAD of 0.57, RMSE of 0.04 mmol/g and WRMS of 0.75. Among all the coals, the largest %AAD of 6.4% is observed for pure-gas adsorption on dry Illinois #6 coal, the largest RMSE of 0.06 mmol/g is observed for pure-gas adsorption on the wet Tiffany coal, and the largest WAAD and WRMS, 1.04 and 1.39, respectively, are observed for the dry Wyodak coal. For the dry coals, the regressed slit length of the dry Illinois #6, Beulah Zap and Wyodak coals were greater than 1.30 nm; thus, the slit length of 1.15 nm did not provide a good fit for the experimental data. Nevertheless, the deviations obtained were still within the experimental uncertainties. For the wet coals, Fruitland OSU #1 and #2 and Lower Basin have regressed slit lengths close to 1.15 nm, so results similar to those of Scenario 2 were obtained. The regressed slit lengths for the wet Illinois #6 and Tiffany coals were 1.29 and 0.91 nm, respectively. The deviations have increased, but the representations are still within the expected experimental uncertainties. Therefore, the modified SLD-PR with constant values for covolume correction and slit length are capable for accurate representation of the adsorption data.

Table 3.7 – Scenario 3: Modified SLD-PR Model Representations of Pure-Gas Adsorption on Dry and Wet Coals

Coal	Adsorbate	Parameters				WAAD	%AAD	RMSE (mmol/g)	WRMS
		Area (m^2/g)	ε_{ss}/k (K)	L (nm) (fixed)	Λ_b (fixed)				
Dry Illinois #6	CH_4	71.1	21.1	1.15	-0.2	0.84	6.4	0.05	1.08
	N_2	56.3							
	CO_2	97.5							
Dry Beulah Zap	CH_4	58.9	27.3	1.15	-0.2	0.72	5.3	0.05	0.91
	N_2	42.9							
	CO_2	111.3							
Dry Wyodak	CH_4	68.8	22.4	1.15	-0.2	1.04	5.6	0.06	1.39
	N_2	55.3							
	CO_2	118.6							
Dry Upper Freeport	CH_4	48.9	35.5	1.15	-0.2	0.39	2.2	0.02	0.55
	N_2	37.1							
	CO_2	56.0							
Dry Pocahontas	CH_4	63.4	37.5	1.15	-0.2	0.46	2.2	0.03	0.68
	N_2	47.7							
	CO_2	69.0							
Statistic for Dry Coals						0.69	4.3	0.04	0.92

Table 3.7 – Scenario 3: Modified SLD-PR Model Representations of Pure-Gas Adsorption on Dry and Wet Coals (Continued)

Coal	Adsorbate	Parameters				WAAD	%AAD	RMSE (mmol/g)	WRMS
		Area (m^2/g)	ε_{ss}/k (K)	L (nm) (fixed)	Λ_b (fixed)				
Wet Illinois #6	CH_4	36.9	17.4	1.15	-0.20	0.31	4.6	0.05	0.46
	N_2	22.2							
	CO_2	54.0							
Wet Fruitland OSU #1	CH_4	60.9	23.7	1.15	-0.20	0.35	2.2	0.03	0.45
	N_2	47.8							
	CO_2	69.0							
Wet Fruitland OSU #2	CH_4	61.3	22.7	1.15	-0.20	0.49	4.9	0.06	0.67
	N_2	40.0							
	CO_2	64.4							
Wet Tiffany	CH_4	30.5	24.4	1.15	-0.20	0.59	5.9	0.03	0.77
	N_2	19.6							
	CO_2	36.6							
Wet Lower Basin Fruitland	CH_4	24.8	22.0	1.15	-0.20	0.46	5.9	0.02	0.56
	N_2	15.3							
	CO_2	29.0							
Statistics for Wet Coals						0.44	4.7	0.04	0.58
Overall Statistics for Coals						**0.57**	**4.5**	**0.04**	**0.75**

Similar to Scenario 1 and 2, the surface area of CO_2 is greater than that of methane and nitrogen. The average surface area ratio of methane to CO_2 and nitrogen to CO_2 is 0.7 and 0.5, respectively. Comparing Scenario 2 and 3, coals with a regressed slit length larger than 1.15 nm have larger surface areas but smaller solid-solid interaction energy. The opposite result is observed for coals with regressed slit length less than 1.15 nm. When comparing the overall statistics of Scenario 3 to Scenario 2, the overall %AAD for the representation of pure-gas adsorption on both dry and wet coals is increased by 0.7 %AAD, which also corresponds to an increase in WAAD of 0.07, WRMS of 0.05 and RMSE of 0.001 mmo/g. These small increases in deviation indicate that the surface areas and solid-solid interaction energy can represent the pure-gas adsorption on both dry and wet coals with fixed slit length.

These three scenarios demonstrate that the modified SLD-PR model capable of correlating the adsorption data within the expected experimental uncertainties when using constant values for the slit length and covolume correction.

Figures 3.1-3.10 present the adsorption representations of Scenarios 1 and 3. The first five figures are for the dry Argonne coal, and the latter five figures are for the wet OSU coals. The plots for Scenario 2 are given in Appendix B since Scenario 3 produces representation results similar to Scenario 2.

As illustrated in Figures 3.1-3.10, Scenario 1 gives a better correlation of the adsorption data on both the dry Argonne and the wet OSU coals. Scenario 3 provides a less precise correlation of the adsorption behavior, especially for CO_2 adsorption on dry Illinois #6, dry Beulah Zap and dry Wyodak, as shown in Figures 3.1-3.3. Fixing the values of the covolume correction and the slit length results in overestimation of the CO_2

excess adsorption on these coals at low pressures (P < 1000 psia). On the other hand, for the wet Illinois #6 and Fruitland OSU #2 coals, full regression of the parameters underestimates the CO_2 adsorption at pressures above 1200 psia, as shown for several experimental runs in Figures 3.6 and 3.8, respectively. Figure 3.7 presents the adsorption on the wet Fruitland OSU #1 coal. The CO_2 excess adsorption at 1600 psia is considered as an outlier and was excluded in all scenarios. Furthermore, no significant difference is observed between Scenarios 1 and 3 for methane and nitrogen adsorption isotherms. This demonstrates that the covolume correction and the slit length have only minor effects on methane and nitrogen adsorption when other parameters are regressed.

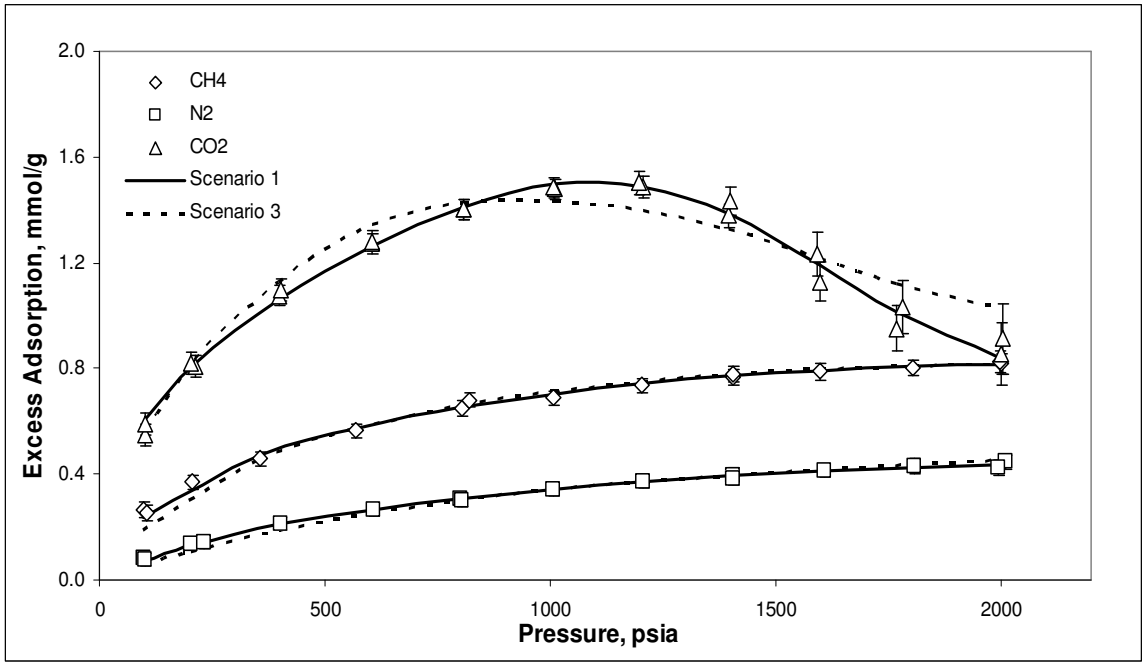

Figure 3.1 – Representation of Pure-Gas Adsorption on Dry Illinois #6 Coal at 131°F

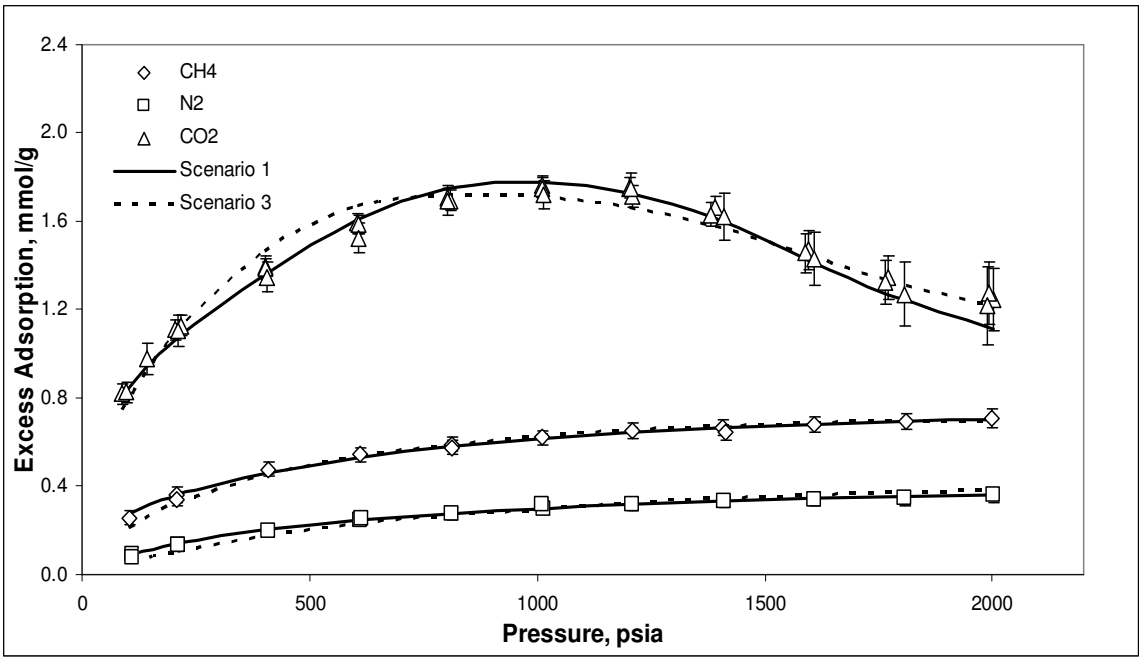

Figure 3.2 – Representation of Pure-Gas Adsorption on Dry Beulah Zap Coal at 131°F

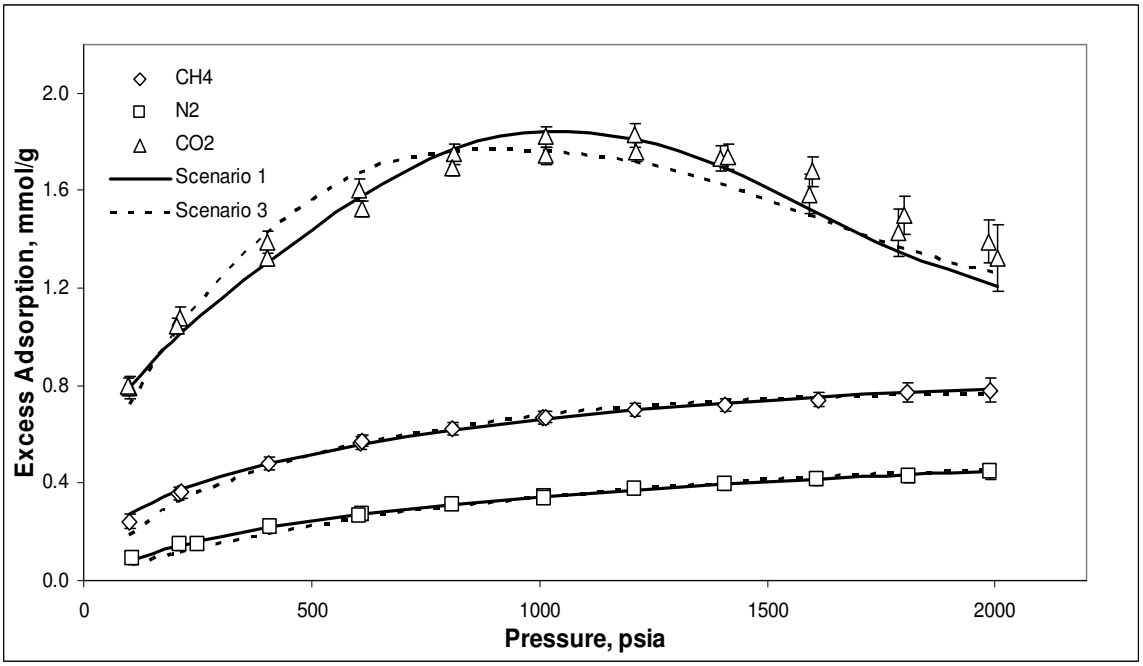

Figure 3.3 – Representation of Pure-Gas Adsorption on Dry Wyodak Coal at 131°F

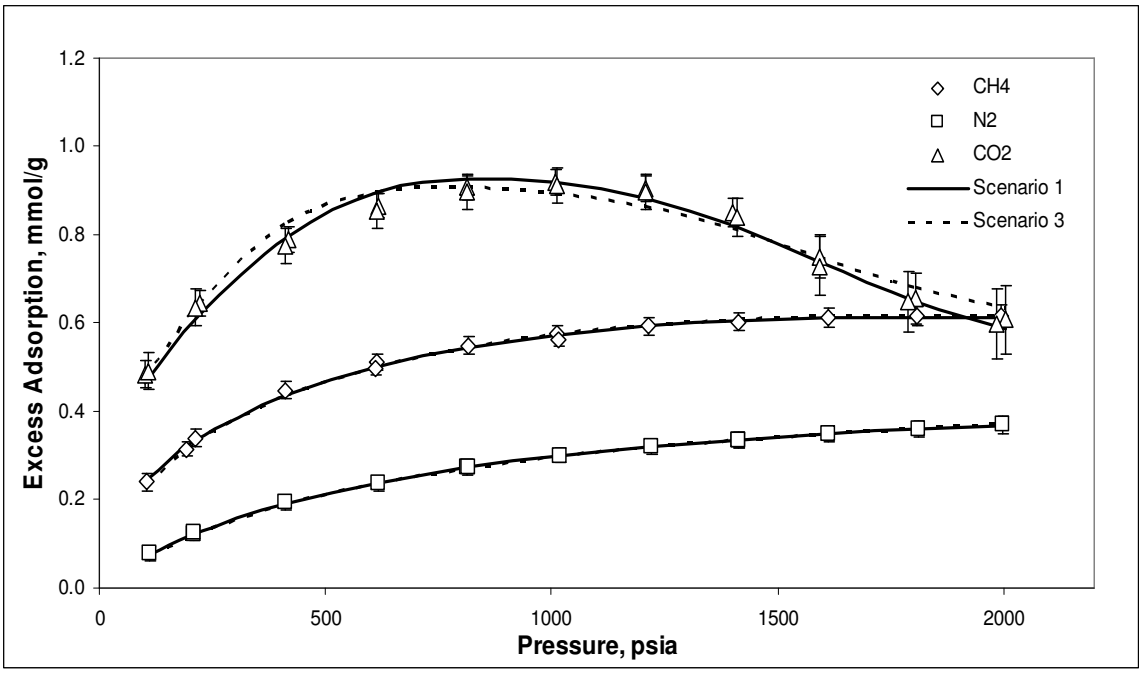

Figure 3.4 – Representation of Pure-Gas Adsorption on Dry Upper Freeport Coal at 131°F

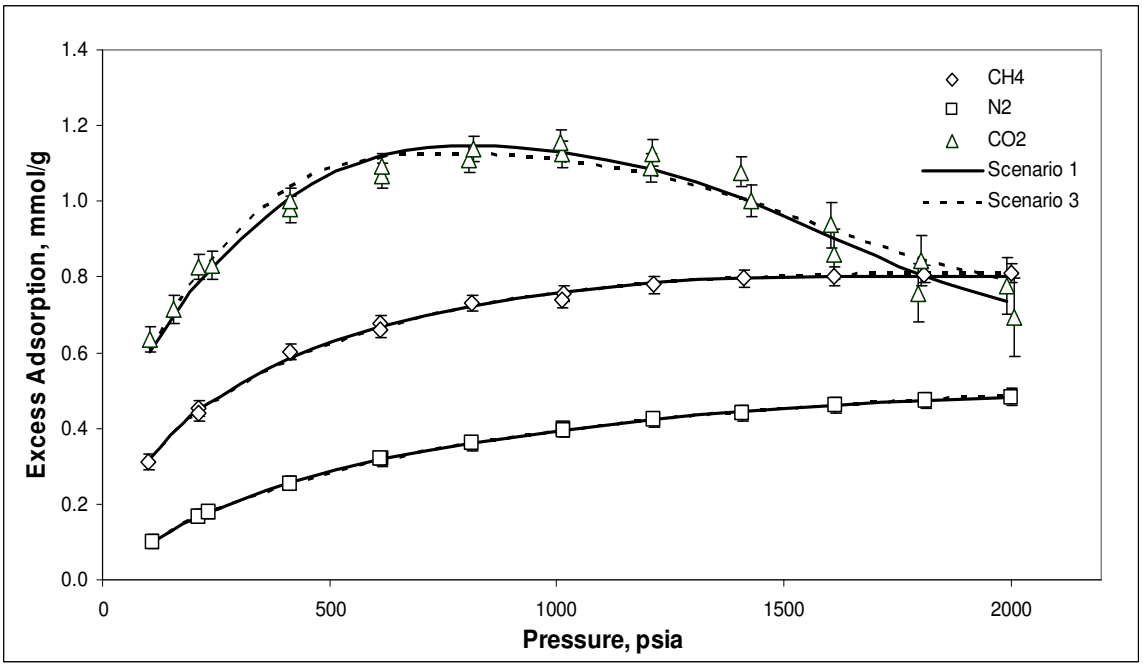

Figure 3.5 – Representation of Pure-Gas Adsorption on Dry Pocahontas Coal at 131°F

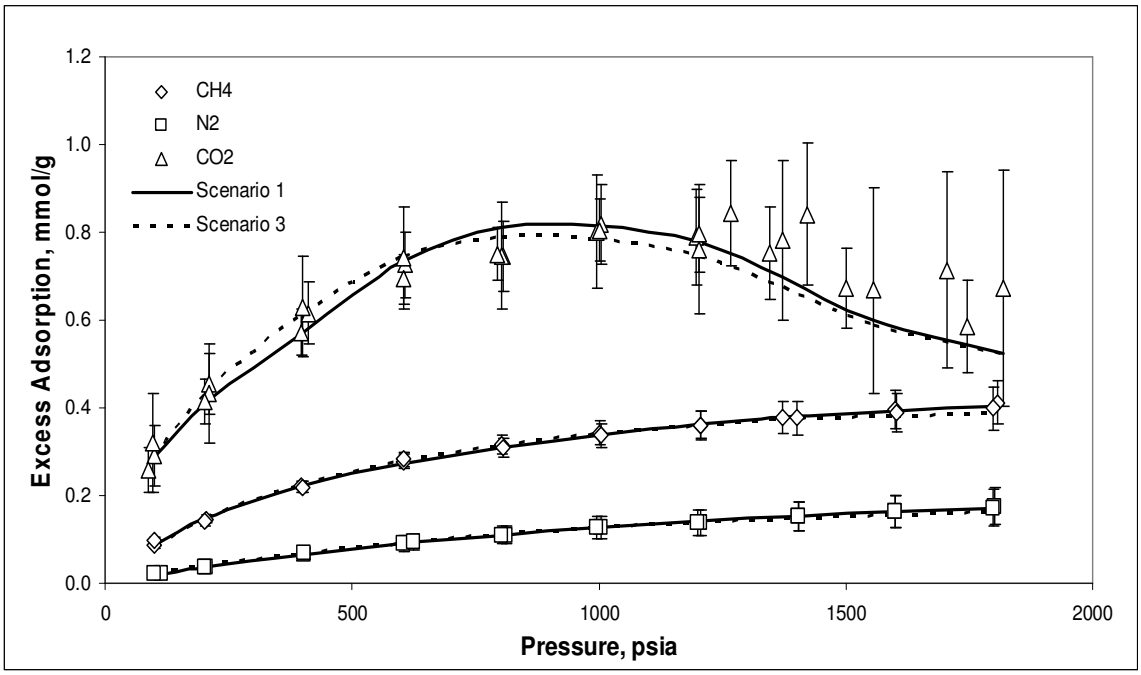

Figure 3.6 – Representation of Pure-Gas Adsorption on Wet Illinois #6 Coal at 115°F

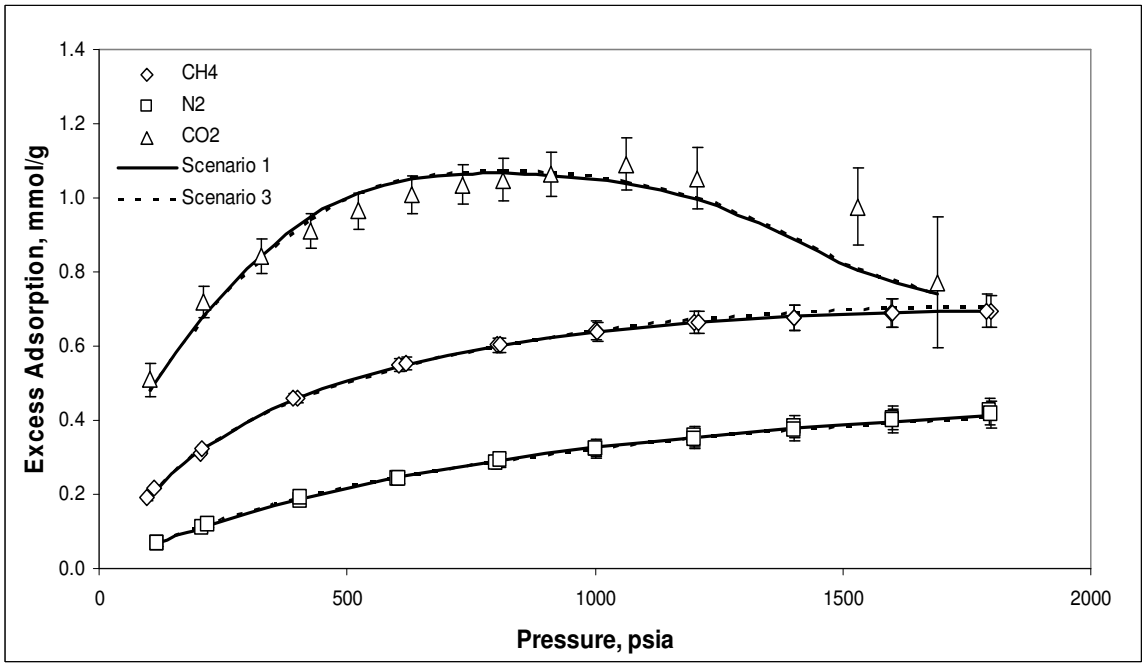

Figure 3.7 – Representation of Pure-Gas Adsorption on Wet Fruitland OSU #1 Coal at 115°F

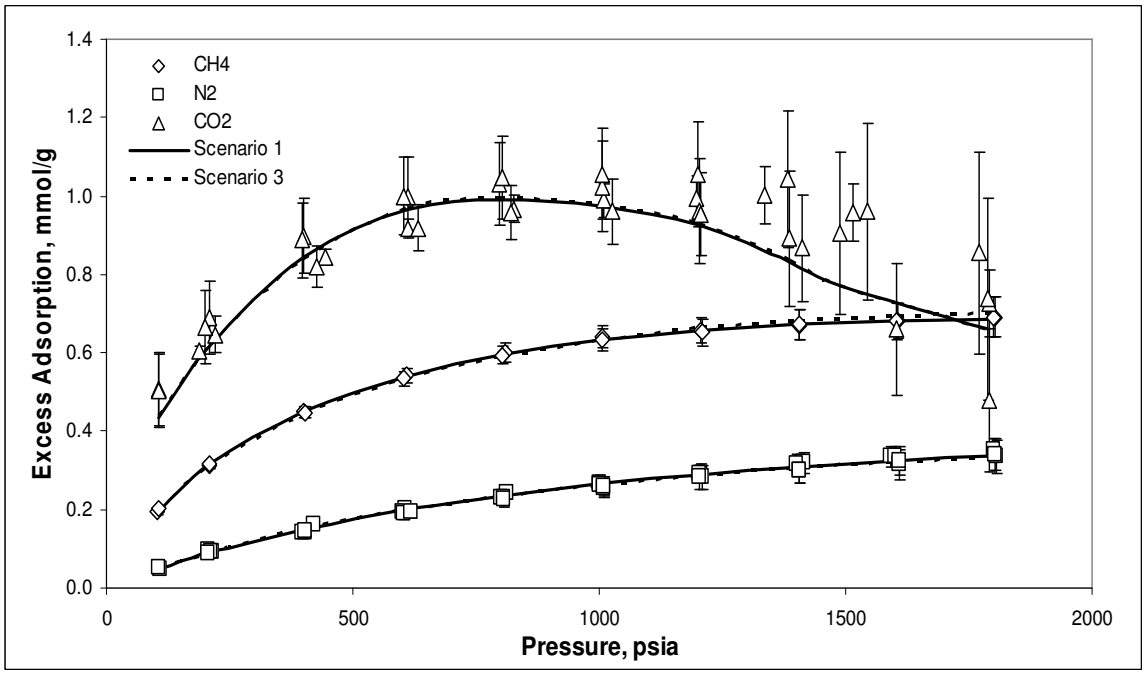

Figure 3.8 – Representation of Pure-Gas Adsorption on Wet Fruitland OSU #2 Coal at 115°F

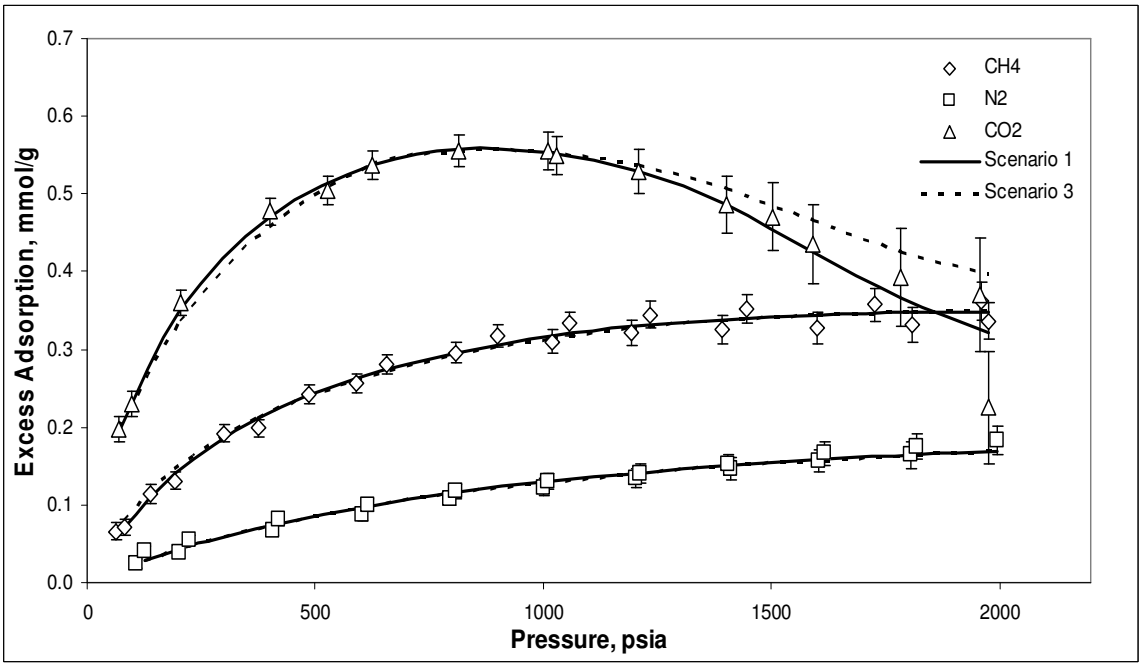

Figure 3.9 – Representation of Pure-Gas Adsorption on Wet Tiffany Coal at 130°F

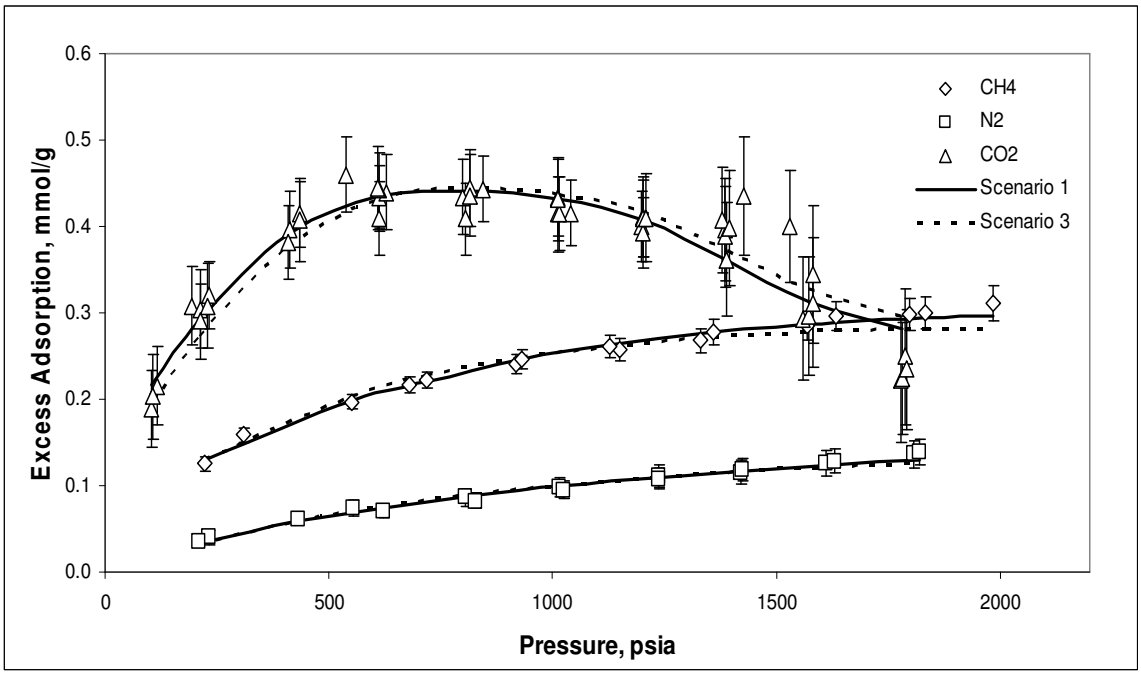

Figure 3.10 – Representation of Pure-Gas Adsorption on Wet Lower Basin Fruitland Coal at 115°F

Figure 3.11 shows the deviation plot for the SLD-PR model representation of the pure-gas adsorption on dry and wet coals. For all three scenarios, about 85% of the data can be represented by the model within expected experimental data. As shown in the figure, large deviation occurred mainly when the Gibbs excess adsorption values are small at relatively low to medium pressures.

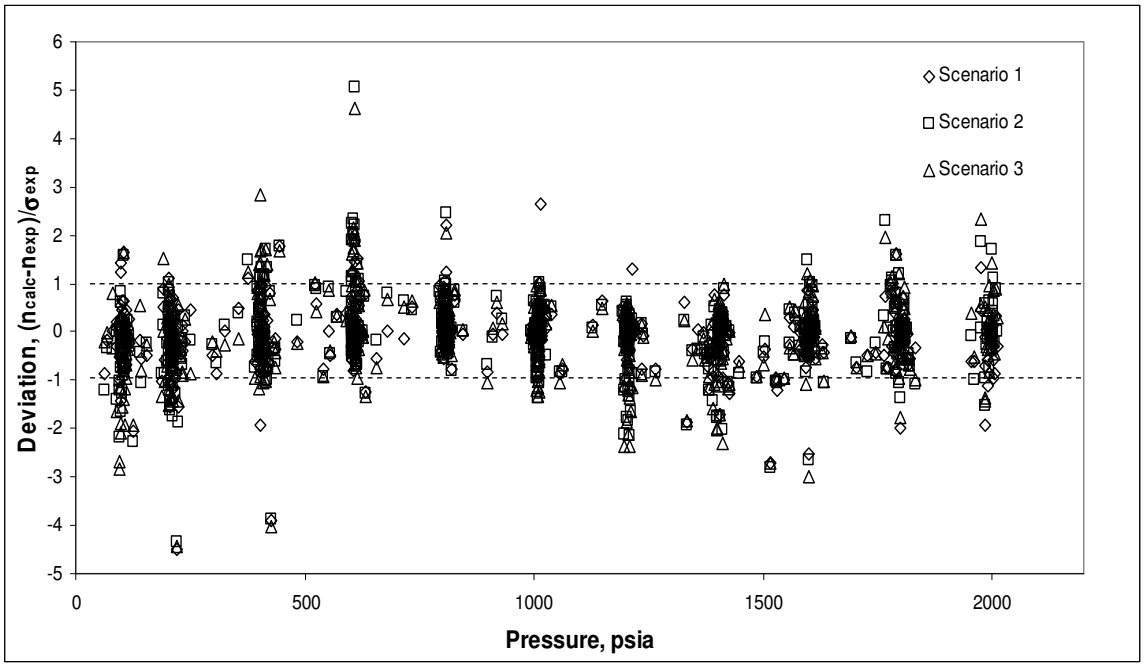

Figure 3.11 – Deviations Plot for SLD-PR Model Representation of Pure-Gas Adsorption on Dry and Wet Coals

Conclusions

Using a separate surface area for each adsorbate and a common solid-solid interaction energy parameter provides precise representations for the pure-gas adsorption on both the dry and wet coals. With fixed values for the covolume correction and the slit length, the SLD-PR model can represent the pure-gas adsorption on the coals considered within the expected experimental uncertainties. The results of Scenarios 2 and 3 indicate that the variation in the covolume and the slit length have no significant effect on the methane or nitrogen adsorption but are more significant in representing or predicting the CO_2 adsorption.

Fixing the values of the covolume correction and the slit length proved beneficial in reducing the number of regressed parameters in the SLD-PR model. Accordingly, Scenario 3 was selected for model generalization because the respective overall %AAD is

comparable in value to that of Scenario 1; thus, only four parameters (surface areas for methane, nitrogen and CO_2; and the solid-solid interaction energy parameter) were correlated in terms of coal or adsorbate properties.

CHAPTER 4

GENERALIZED MODEL FOR PURE-GAS ADSORPTION

To develop a generalized model for the prediction of pure-gas adsorption of CBM-type systems, the regressed model parameters (Chapter 3) of the SLD-PR model were correlated as mathematical relations in terms of accessible adsorbent or adsorbate physical properties. As expected, these relations do not provide exact representations of the model parameters; thus, the generalized predictions are less accurate than those made directly from the regressed parameters. Nevertheless, useful predictions can be made for cases where extensive data are not available.

To obtain the generalized model coefficients, the regressed parameters for each coal were expressed in terms of the respective coal characteristics (such as carbon, equilibrium moisture content), or adsorbate properties (such as fluid molecular diameter).

The pure methane, nitrogen and CO_2 adsorption isotherms that were used for evaluating the ability of the SLD-PR model to represent the data (Chapter 3) were used in the model generalizations. The adsorption information and the analyses of these coals are discussed in Chapter 2.

Generalized Correlations

Trends in the regressed SLD-PR model parameters were examined graphically. The coal fixed carbon, the carbon weight fraction, and the equilibrium moisture content showed reasonable correlation with the regressed parameters. In addition, as concluded by Fitzgerald [33], the coal surface area could not be correlated adequately in terms of coal physical properties. However, it was found to be proportional to methane excess adsorption at 400 psia. The use of a single experimental data point is valuable in that it can (at least partially) compensate for our lack of knowledge of the solid-gas interactions in the model. It does, however, render the model a "calibrated, generalized" model rather than a completely generalized one.

For this work, the regressed parameters (surface area for each adsorbate and the solid-solid interaction energy parameter) of Scenario 3 used in the representation of pure-gas adsorption (Chapter 3) were applied to develop the parameter generalizations as follows:

1. A generalized correlation was obtained for the solid-solid interaction energy parameter based on the observed graphical trends.
2. Using the solid-solid interaction energy parameters obtained from the above correlation, the surface area for *each adsorbed gas on each coal* was re-regressed. This was done to obtain the surface areas which can correlate precisely the adsorption data using the predicted solid-solid interaction energy.

3. A generalized correlation for each surface area (from 2, above) was developed in terms of a single-point adsorbate excess adsorption, coal characteristics or gas properties.
4. The generalized correlations for each model parameter were then incorporated into the SLD-PR model, and the coefficients in the generalized correlations were re-regressed *simultaneously*, using the entire data set. The objective function (WRMS) expressed by Equation (3-1) was minimized. For details, an outline for the generalization steps in the FORTRAN program is given in Appendix C.1.

As stated earlier, the generalization results for the coals considered indicated that surface areas were proportional to methane excess adsorption at 400 psia. As such, the resultant generalization is restricted because it can be only applied when this information on methane adsorption at 400 psia is available. Therefore, analogous correlations were developed to predict the adsorbate surface areas in terms of the nitrogen and the CO_2 excess adsorption at 400 psia. This means a set of generalized correlations can be applied to perform adsorption predictions for the coal of interest based on the available adsorption information at this pressure on any of the three gases.

To evaluate the efficacy of the proposed correlations, three case studies were conducted addressing the surface area predictions:

Case 1 – The surface areas of methane, nitrogen and CO_2 are correlated in terms of methane excess adsorption at 400 psia.

Case 2 – The surface areas of methane, nitrogen and CO_2 are correlated in terms of nitrogen excess adsorption at 400 psia

Case 3 – The surface areas of methane, nitrogen and CO_2 are correlated in terms of CO_2 excess adsorption at 400 psia

Values of the excess adsorption of these gases at 400 psia are listed in Table 4.1.

A generalized correlation for the solid-solid interaction energy parameter is included in all the cases above; thus, a total of four correlations were developed for each case.

Table 4.1 – Excess Adsorption of Adsorbates at 400 psia

Coal	Excess Adsorption at 400 psia, mmol/g dry coal		
	CH_4	N_2	CO_2
Dry Illinois #6	0.51	0.22	1.11
Dry Beulah Zap	0.48	0.20	1.42
Dry Wyodak	0.49	0.22	1.40
Dry Upper Freeport	0.45	0.19	0.78
Dry Pocahontas	0.60	0.25	0.99
Wet Illinois #6	0.23	0.07	0.61
Wet Fruitland OSU#1	0.46	0.19	0.90
Wet Fruitland OSU#2	0.45	0.15	0.85
Wet Tiffany	0.22	0.07	0.47
Wet Lower Basin Fruitland	0.18	0.06	0.39

The adsorption on Tiffany coal samples from wells #1 and #10 are combined and generalized as mixed Tiffany coal. Similarly, the adsorption on Lower Basin Fruitland #3a and #3b coals are combined. For the mixed Tiffany and mixed Lower Basin Fruitland coals, the characterization is the average value of the combined coals, e.g., $FC_{\text{mixed Tiffany}} = 0.5(FC_{\text{Tiffany well \#1}} + FC_{\text{Tiffany Well \#10}})$. The characterization for these two coals is listed in Table 4.2.

Table 4.2 – Combined Compositional Analysis of Lower Basin Fruitland and Tiffany Coal Used in This Study

Analysis*	Mixed Lower Basin Fruitland	Mixed Tiffany
Ultimate		
Carbon %	38.92	52.27
Hydrogen %	3.08	2.70
Oxygen %	3.75	5.68
Nitrogen %	0.87	0.97
Sulfur %	1.73	0.55
Ash %	51.66	48.73
Proximate		
Vol. Matter %	20.01	15.42
Fixed Carbon %	28.33	25.87
Moisture %	4.00	3.80

For all the developed correlations, unless otherwise stated, the coal properties applied are weight fractions. For example, fixed carbon refers to fixed carbon weight fraction.

Results and Discussions

The summary results for the generalized predictions of pure-gas adsorption on all coals are represented in Tables 4.3-4.14 and Figures 4.1-4.33. A total of ten figures are shown for each case. The first five figures are for the pure-gas adsorption on dry coals, while the latter five figures are for the pure-gas adsorption on wet coals. Following are detailed discussions for each of the three cases considered.

Case 1: Methane-Based Generalizations

Table 4.3 presents the SLD-PR pure-fluid parameter generalizations of Case 1. The table shows the generalized correlations for the surface areas and the solid-solid interaction energy. In developing the methane-based generalization of this case, both the surface areas of methane and nitrogen are expressed as a function of methane excess adsorption at 400 psia only. However, the CO_2 surface areas for the dry coals are not correlated adequately by the methane calibration point. Hence, based on observed trends, both the methane excess adsorption and the product of the equilibrium moisture and carbon fraction are used.

Table 4.3 – Case 1: Generalized Correlations of the Surface Areas and the Solid-Solid Interaction Energy Parameter

$$A_{CH4} = 110.66\left(n^{Ex}_{CH4@400}\right) + 5.40$$

$$A_{N2} = 91.42\left(n^{Ex}_{CH4@400}\right) - 1.20$$

$$A_{CO2} = 117.82\left(n^{Ex}_{CH4@400}\right) + 125.69\left(\lambda_M \times \chi_C\right) - 6.76$$

$$\varepsilon_{ss}/k = \frac{1.505}{\lambda_M^{0.5}} + 12.16\left(\frac{\chi_C}{\varphi_{FC}}\right)$$

Table 4.4 gives the model parameters generated from the generalized correlations of Table 4.3. A comparison of the generalized and the regressed model parameters is provided in Figure 4.1, and Table 4.5 documents the %AAD of generalized parameters relative to the regressed model parameters. Additional details are given in Appendix C.2.

Table 4.4 – Case 1: Generalized SLD-PR Model Parameters

Coal	Surface Area (m^2/g)			Slit Length (nm)	ε_{ss}/k (K)
	CH_4	N_2	CO_2		
Dry Illinois #6	62.0	45.6	84.9	1.15	28.4
Dry Beulah Zap	58.5	42.7	110.7	1.15	31.5
Dry Wyodak	59.6	43.6	108.7	1.15	30.5
Dry Upper Freeport	55.1	39.9	58.4	1.15	32.1
Dry Pocahontas	71.5	53.4	73.6	1.15	32.6
Wet Illinois #6	30.3	19.3	40.7	1.15	23.2
Wet FR OSU #1	56.5	41.0	63.1	1.15	24.2
Wet FR OSU #2	55.4	40.1	61.7	1.15	24.2
Wet Tiffany	29.4	18.6	36.4	1.15	25.5
Wet LB FR	24.9	14.9	29.7	1.15	24.2

Table 4.5 – Case 1: Summary Results of the Generalized Parameters

Coal	%AAD			
	A_{CH4}	A_{N2}	A_{CO2}	ε_{ss}/k
Dry Illinois #6	16.3	19.1	12.9	9.0
Dry Beulah Zap	0.7	0.5	0.6	15.7
Dry Wyodak	13.4	21.2	8.4	0.0
Dry Upper Freeport	12.7	7.6	4.3	8.0
Dry Pocahontas	12.8	12.0	6.6	4.5
Wet Illinois #6	18.0	13.1	24.6	22.9
Wet FR OSU #1	7.3	14.2	8.5	1.7
Wet FR OSU #2	9.6	0.3	4.2	6.3
Wet Tiffany	3.8	5.2	0.7	5.5
Wet LB FR	0.5	2.3	2.5	0.0
Overall Total	9.5	9.5	7.3	7.4

As illustrated in Figure 4.1, the generalized surface areas of methane and nitrogen approximate the regressed values well. As shown in Table 4.5, the overall %AAD between generalized and regressed surface areas for these gases are both 9.5%. The methane surface areas of the dry Illinois #6, Wyodak, Upper Freeport, Pocahontas and wet Illinois #6 coals are different from the respective regressed values by at least 10%. It is observed that the ascending order of the methane surface area for these coals is: Pocahontas, Wyodak and Illinois, but the order of methane excess adsorption of these

coals is: Wyodak, Pocahontas and Illinois #6. Therefore, the methane surface areas are not predicted accurately, which is similar to the surface area predictions of nitrogen for dry Illinois #6, dry Wyodak and wet Fruitland OSU #1. This is because the regressed surface areas of these coals are not proportional to the respective methane excess adsorption.

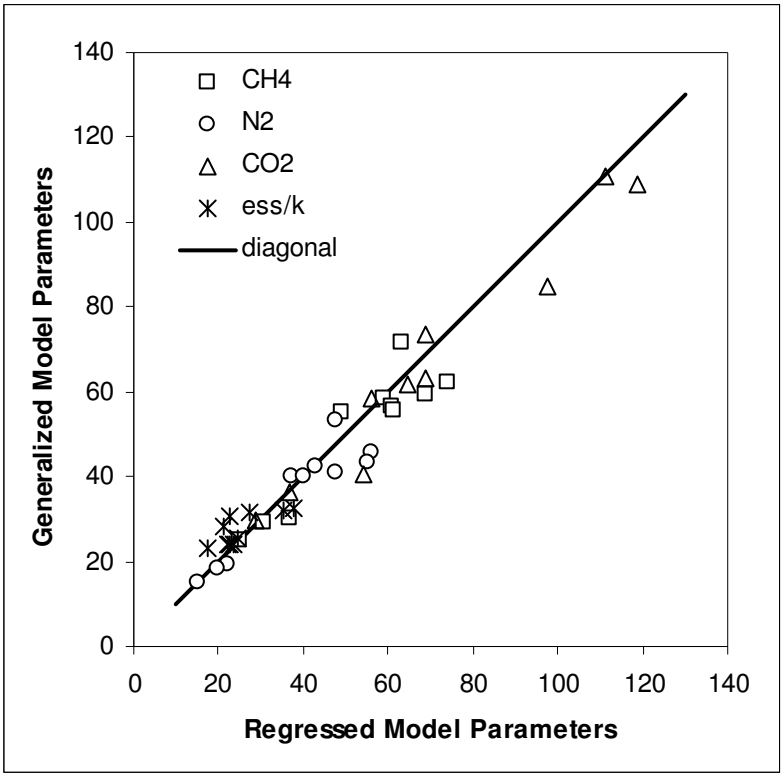

Figure 4.1 – Case 1: Comparison of the Regressed and Generalized SLD-PR Model Parameters

For CO_2, the generalized surface areas of all coals except for dry and wet Illinois #6 match the respective regressed values within 10%. The deviations for dry and wet Illinois #6 are 12.9% and 24.6%, respectively. This discrepancy occurs because the combination of the excess adsorption and the selected coal characteristic are not in order with the regressed surface areas. For the solid-solid interaction energy parameters, most

of the generalized values differ from the regressed values, as shown in Figure 4.1. The overall %AAD is 7.4% with the largest error contributions attributable to dry Beulah Zap and wet Illinois #6. The corresponding solid-solid interaction energy parameters differ by at least fifteen percent relative to the regressed parameters.

Summary results for the adsorption of all adsorbates on both dry and wet coals are given in Table 4.6. The respective generalized predictions for the pure-gas adsorption on these coals are given in Figures 4.2 through 4.11. As shown in Table 4.6, the overall WAAD is 1.05, the %AAD is 7.1%, RMSE is 0.05 mmol/g and WRMS is 1.22. The largest WAAD and WRMS, which are 2.30 and 2.67, respectively, are both observed for the CO_2 adsorption on dry Wyodak coal. Figure 4.4 indicates that the amount of CO_2 adsorbed by this coal is under predicted at intermediate pressures. The largest %AAD of 20.4% is observed for the CO_2 adsorption on wet Illinois #6 coal; however, the weighted deviations are less than two because of relatively large experimental uncertainties.

The CO_2 adsorption on dry Illinois #6 coal, as shown in Figure 4.2, is predicted poorly due to the use of a smaller of surface area value with a larger solid-solid interaction energy value. The statistics, WRMS, %AAD, RMSE and WAAD, for dry Illinois #6 are 2.54, 7.2%, 0.11 mmol/g and 1.87, respectively. The methane adsorption on the dry Upper Freeport and Pocahontas coals (Figures 4.5 and 4.6, respectively) are predicted within three times the experimental uncertainties; however, the pure-gas adsorption on the remaining coals is predicted within twice the experimental uncertainties.

Table 4.6 – Case 1: Summary Results for the Generalized SLD-PR Adsorption Predictions

Coal	WAAD			%AAD			RMSE			WRMS		
	CH_4	N_2	CO_2	CH_4	N_2	CO_2	CH_4	N_2	CO_2	CH_4	N_2	CO_2
Dry Illinois #6	1.30	0.72	1.87	6.5	8.0	7.2	0.05	0.02	0.11	1.48	0.75	2.54
Dry Beulah Zap	0.80	0.73	1.04	4.6	8.6	4.1	0.03	0.03	0.08	0.93	0.89	1.50
Dry Wyodak	0.39	0.95	2.30	2.0	8.8	7.8	0.02	0.02	0.13	0.55	0.97	2.67
Dry Upper Freeport	2.12	0.47	0.69	7.3	3.6	4.1	0.05	0.01	0.04	2.39	0.51	0.83
Dry Pocahontas	1.99	0.75	1.12	6.0	4.0	5.9	0.05	0.02	0.06	2.34	0.89	1.30
Wet Illinois #6	0.91	0.31	1.32	8.0	8.2	20.4	0.03	0.01	0.17	0.98	0.38	1.47
Wet FR OSU #1	1.74	1.74	1.25	6.0	13.2	9.7	0.03	0.04	0.10	1.91	1.78	1.35
Wet FR OSU #2	1.47	0.62	0.84	6.2	5.2	10.1	0.04	0.01	0.11	1.59	0.77	1.01
Wet Tiffany	0.72	0.66	0.60	4.5	7.1	8.2	0.01	0.01	0.05	0.87	0.82	0.79
Wet LB FR	1.07	0.42	0.52	5.4	4.8	8.4	0.01	0.01	0.03	1.22	0.56	0.63
Overall Statistics for Coals	**1.05**			**7.1**			**0.05**			**1.22**		

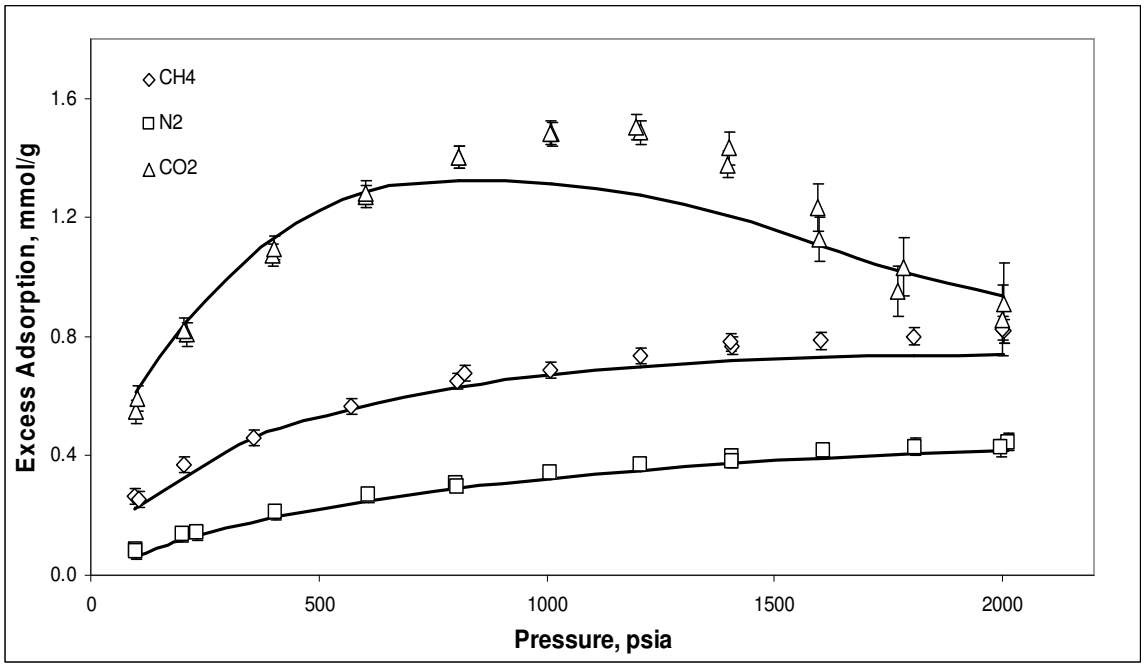

Figure 4.2 – Generalized Predictions of Pure-Gas Adsorption on Dry Illinois #6 Coal at 131°F Using Methane Excess Adsorption at 400 psia

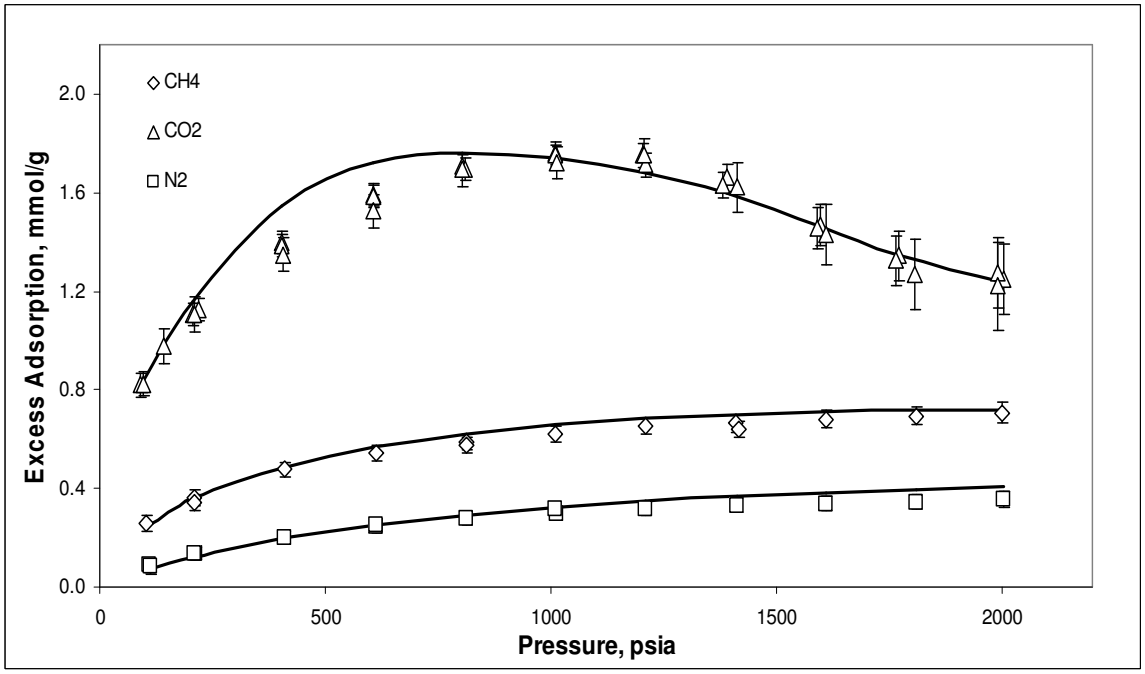

Figure 4.3 – Generalized Predictions of Pure-Gas Adsorption on Dry Beulah Zap Coal at 131°F Using Methane Excess Adsorption at 400 psia

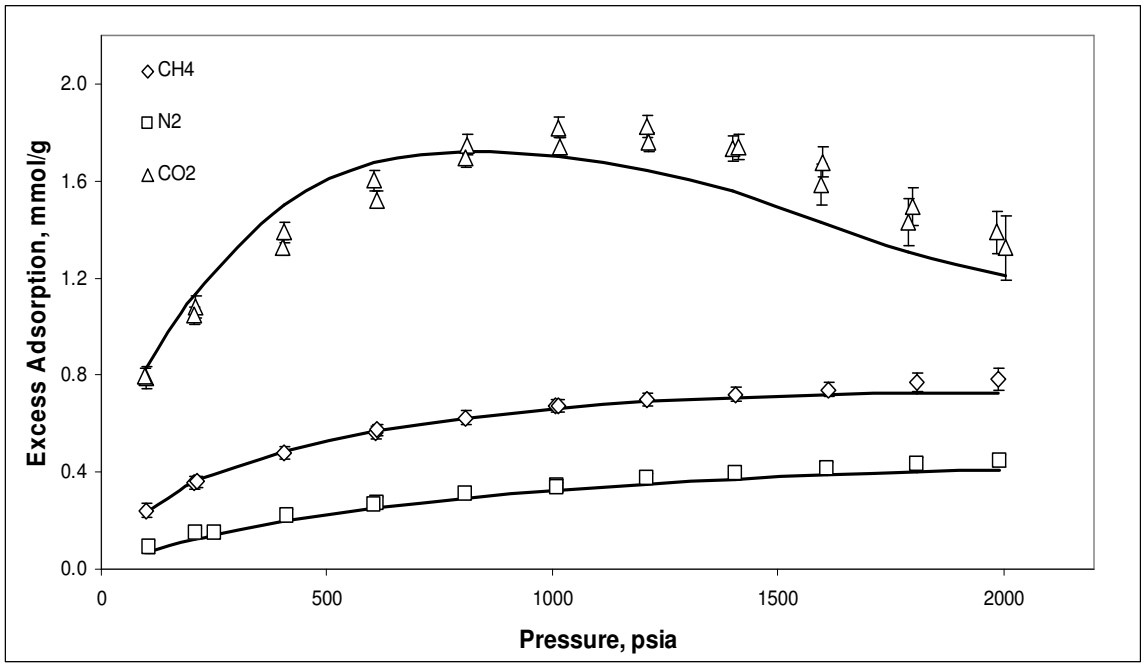

Figure 4.4 – Generalized Predictions of Pure-Gas Adsorption on Dry Wyodak Coal at 131°F Using Methane Excess Adsorption at 400 psia

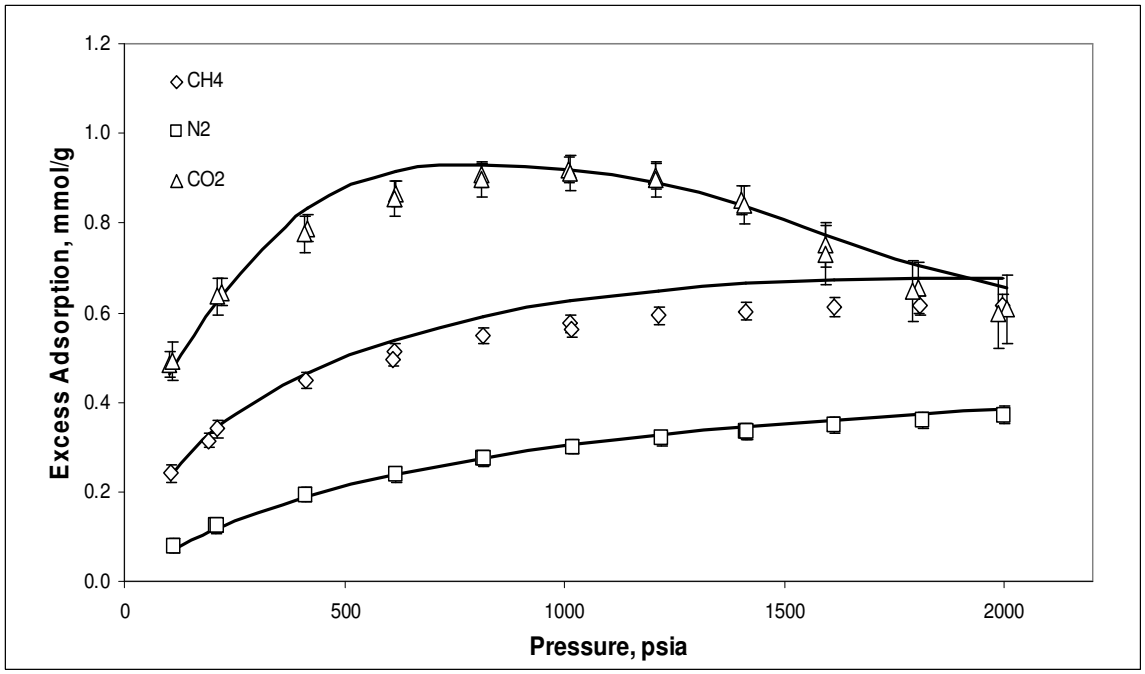

Figure 4.5 – Generalized Predictions of Pure-Gas Adsorption on Dry Upper Freeport Coal at 131°F Using Methane Excess Adsorption at 400 psia

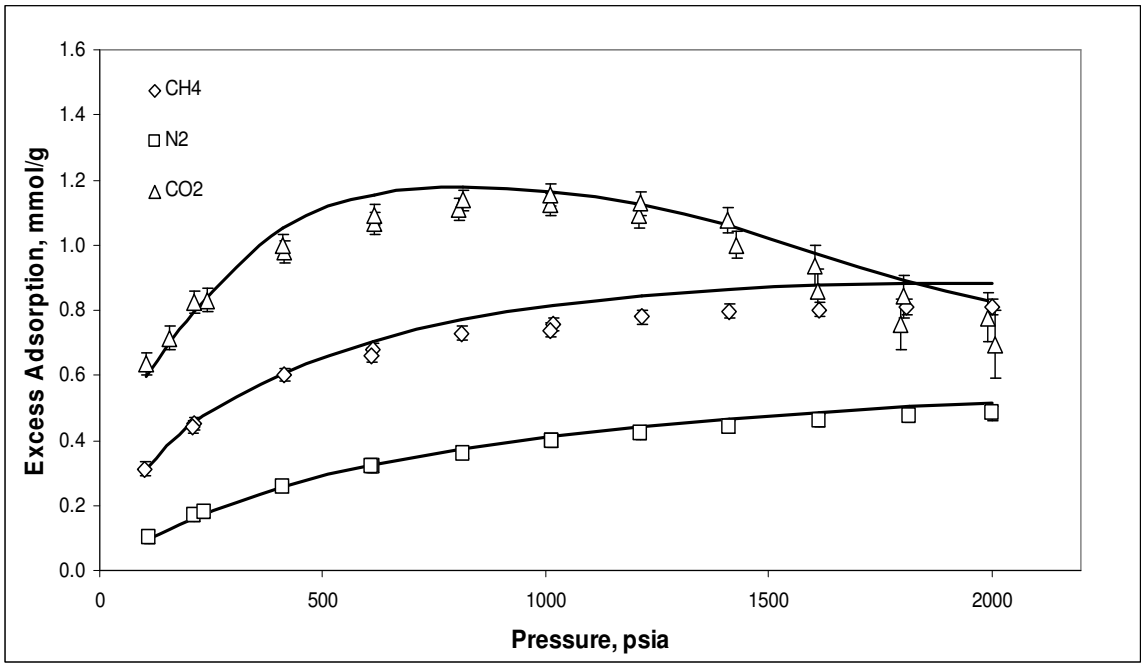

Figure 4.6 – Generalized Predictions of Pure-Gas Adsorption on Dry Pocahontas Coal at 131°F Using Methane Excess Adsorption at 400 psia

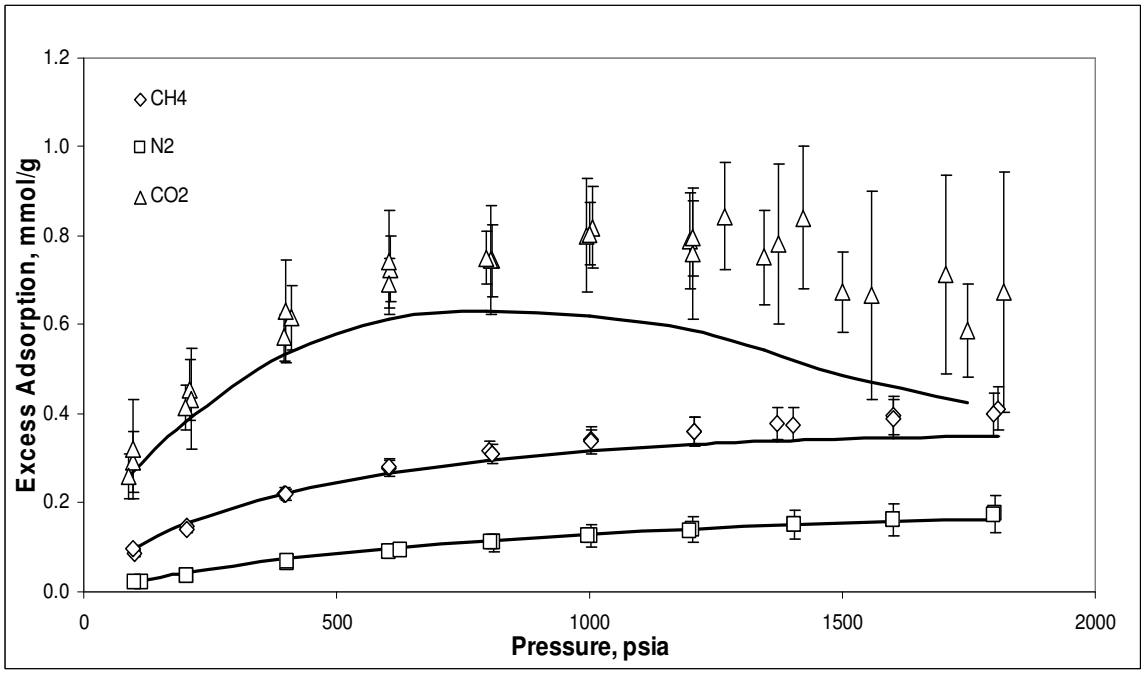

Figure 4.7 – Generalized Predictions of Pure-Gas Adsorption on Wet Illinois #6 Coal at 115°F Using Methane Excess Adsorption at 400 psia

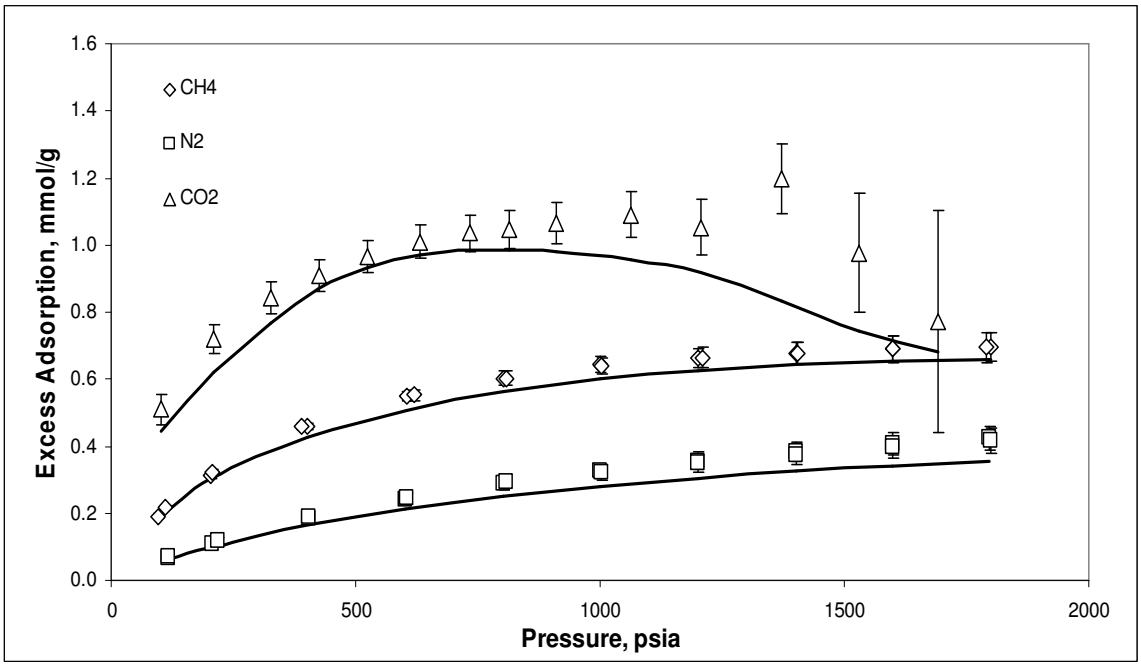

Figure 4.8 – Generalized Predictions of Pure-Gas Adsorption on Wet Fruitland OSU #1 Coal at 115°F Using Methane Excess Adsorption at 400 psia

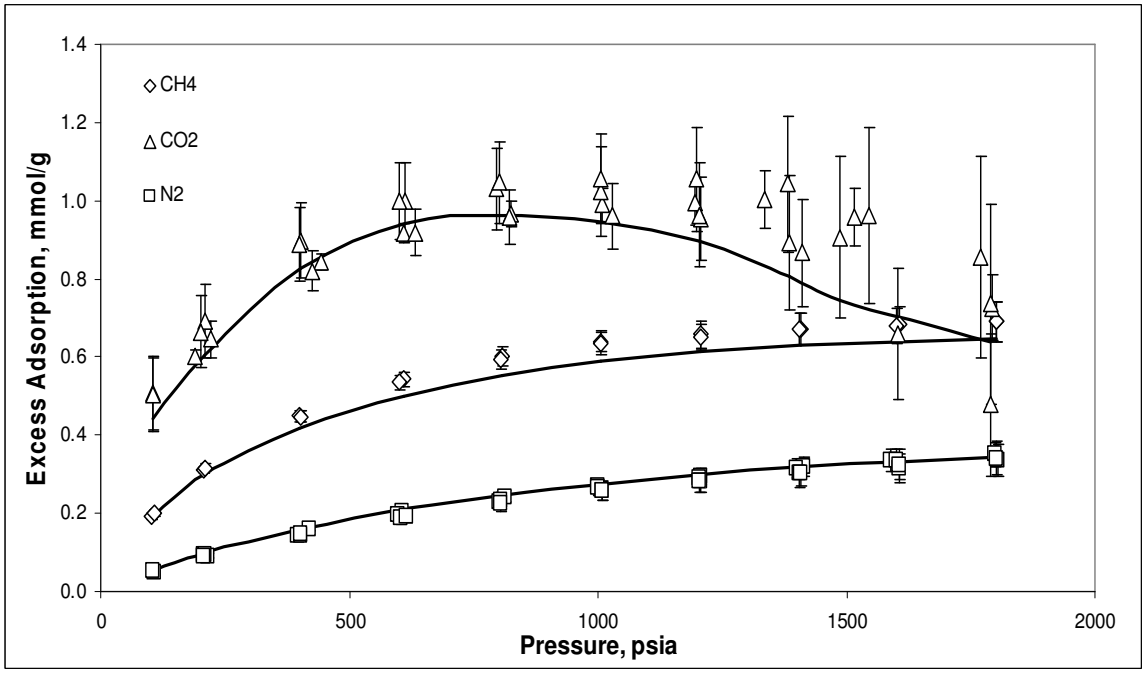

Figure 4.9 – Generalized Predictions of Pure-Gas Adsorption on Wet Fruitland OSU #2 Coal at 115°F Using Methane Excess Adsorption at 400 psia

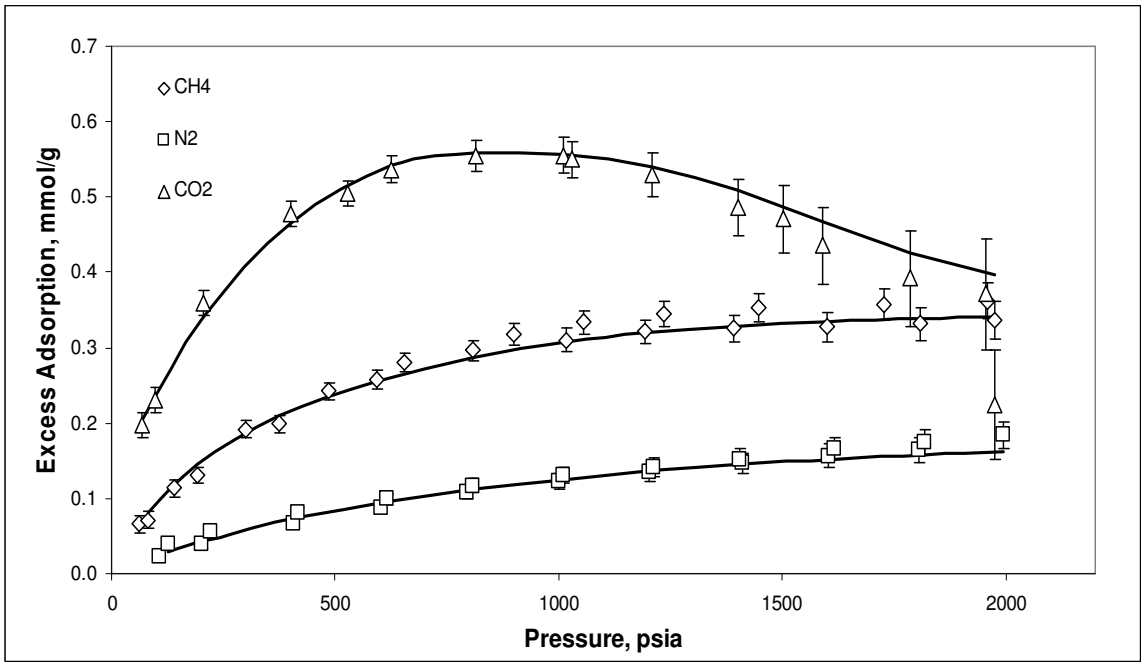

Figure 4.10 – Generalized Predictions of Pure-Gas Adsorption on Wet Tiffany Coal at 130°F Using Methane Excess Adsorption at 400 psia

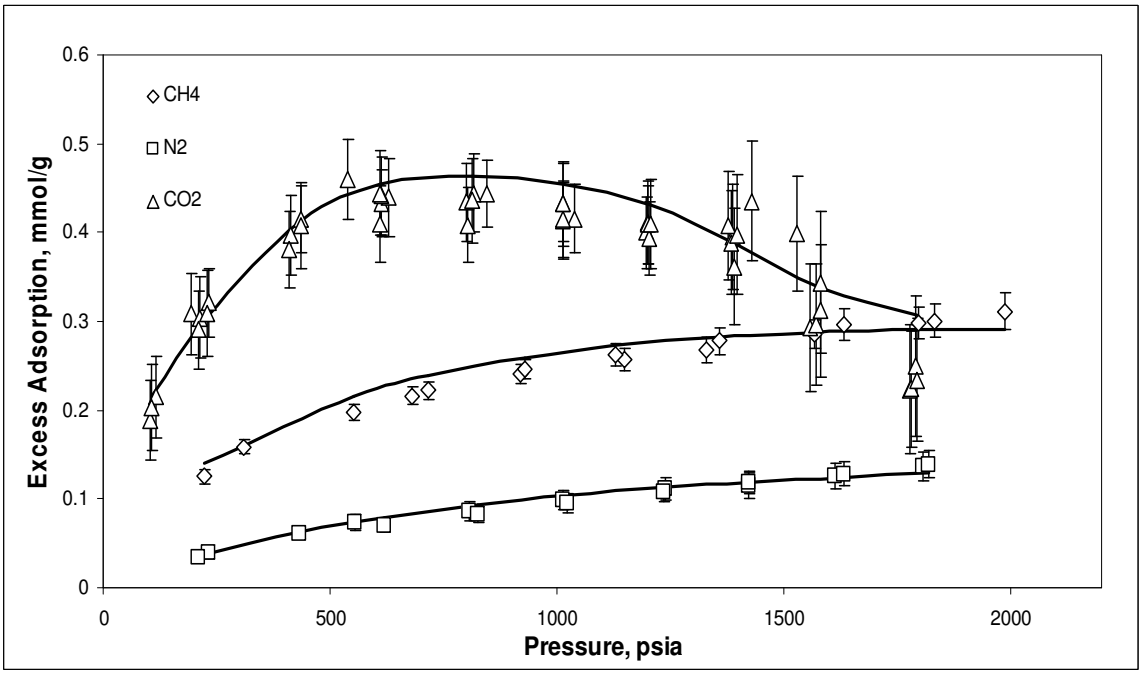

Figure 4.11 – Generalized Predictions of Pure-Gas Adsorption on Wet Lower Basin Fruitland Coal at 115°F Using Methane Excess Adsorption at 400 psia

The model parameters are not correlated precisely with the coal properties for dry and wet Illinois #6 and dry Wyodak, but for dry Beulah Zap, wet Fruitland OSU #2, wet Tiffany and wet Lower Basin Fruitland, the model parameters are correlated closely with coal properties. Nevertheless, the generalization using methane excess adsorption can predict the pure-gas adsorption within three times the uncertainties.

Case 2: Nitrogen-Based Generalizations

The regressed surface areas for methane, nitrogen and CO_2 are not correlated well with the nitrogen excess adsorption at 400 psia; hence, coal properties such as fixed carbon, volatile matter, and equilibrium moisture content are required to obtain improved generalizations for the model parameters. Table 4.7 presents the generalized correlations for both the surface areas using nitrogen excess adsorption at 400 psia and the solid-solid interaction energy parameter. Table 4.8 provides the generalized model parameters from these correlations.

Table 4.7 – Case 2: Generalized Correlations of the Surface Areas and the Solid-Solid Interaction Energy Parameter

$$A_{CH4} = 407.81\left(n^{Ex}_{N2@400}\right)\left(\theta_{Vol}\right)^{0.5} + 16.04$$

$$A_{N2} = 173.61\left(n^{Ex}_{N2@400}\right) + 51.04\left(\varphi_{FC} \times \lambda_{M}\right)^{0.5}$$

$$A_{CO2} = 195.84\left(n^{Ex}_{N2@400}\right) + 503.23\left(\lambda_{M}\right)^{0.5}\left(\varphi_{FC}\right) - 13.16$$

$$\varepsilon_{ss}/k = \frac{2.831}{\lambda_{M}^{0.5}} + 8.14\left(\frac{\chi_{C}}{\varphi_{FC}}\right)$$

Table 4.8 – Case 2: Generalized SLD-PR Model Parameters

Coal	Surface Area (m^2/g)			Slit Length (nm)	ε_{ss}/k (K)
	CH_4	N_2	CO_2		
Dry Illinois #6	69.2	46.5	87.1	1.15	25.5
Dry Beulah Zap	61.4	51.0	113.9	1.15	24.3
Dry Wyodak	67.3	54.0	118.3	1.15	23.8
Dry Upper Freeport	56.5	37.2	55.2	1.15	38.8
Dry Pocahontas	60.5	47.7	68.5	1.15	43.6
Wet Illinois #6	30.9	18.9	55.3	1.15	24.7
Wet FR OSU #1	50.1	38.1	67.5	1.15	28.5
Wet FR OSU #2	43.5	31.7	59.2	1.15	28.5
Wet Tiffany	27.8	18.7	36.4	1.15	26.4
Wet LB FR	26.5	15.4	26.6	1.15	25.3

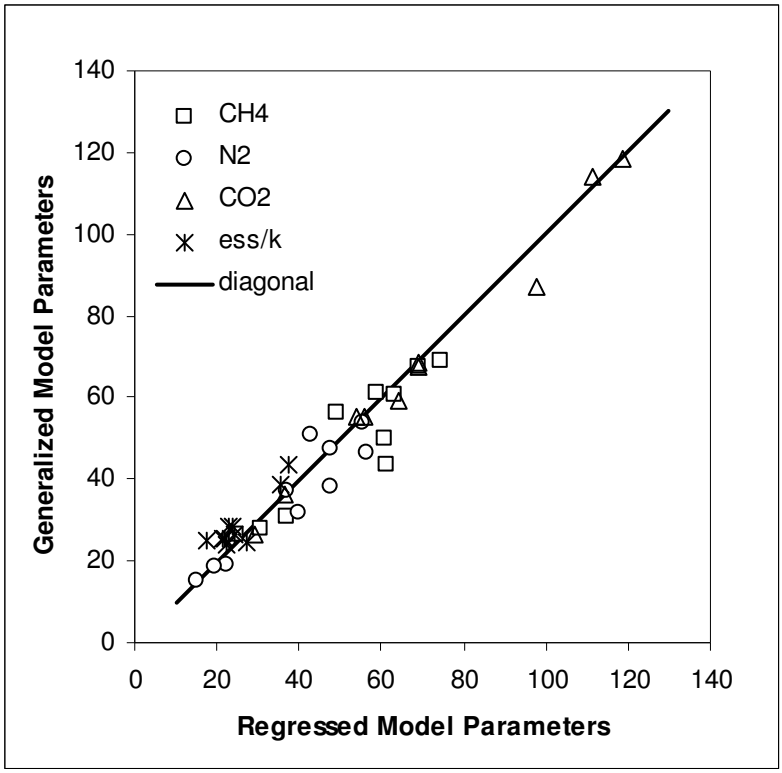

Figure 4.12 – Case 2: Comparison of the Regressed and Generalized SLD-PR Model Parameters

Table 4.9 – Case 2: Summary Results of the Generalized Parameters

Coal	%AAD			
	A_{CH4}	A_{N2}	A_{CO2}	ε_{ss}/k
Dry Illinois #6	6.6	17.4	10.7	20.4
Dry Beulah Zap	4.2	18.9	2.4	10.8
Dry Wyodak	2.1	2.4	0.3	6.2
Dry Upper Freeport	15.5	0.4	1.4	9.4
Dry Pocahontas	4.6	0.0	0.8	16.1
Wet Illinois #6	16.3	14.8	2.3	42.1
Wet FR OSU #1	17.8	20.3	2.1	20.2
Wet FR OSU #2	29.0	20.8	8.1	25.6
Wet Tiffany	9.1	4.9	0.7	8.0
Wet LB FR	7.0	0.9	8.3	15.0
Overall Total	11.2	10.1	3.7	17.4

Figure 4.12 shows the comparison between the generalized and regressed model parameters. Further, the quality of the parameter generalizations, as given by %AAD of the generalized parameters relative to regressed parameters, is examined in Table 4.9 (Additional details on this comparison are given in Appendix C.2). Figure 4.12 shows that the methane surface area is predicted less accurately than the nitrogen and CO_2 surface areas.

As shown in Table 4.9, the %AAD for the generalized methane surface areas is 11.2%. The main contributions to the overall error are from the wet Fruitland OSU #2 and #1 (29.0% and 17.8%, respectively), wet Illinois #6 (16.3%) and dry Upper Freeport (15.5%) coals. The methane surface areas for these coals are not predicted accurately. Comparable results are observed for the generalized nitrogen surface areas, which yielded %AAD of 10.1%. Among these coals, the generalized nitrogen surface areas of dry and Illinois #6, dry Beulah Zap and wet Fruitland OSU #1 and #2 have %AAD of 17.4, 18.9, 19.5 and 17.5%, respectively. In contrast, the generalized CO_2 surface areas are

comparable to the regressed values with a %AAD of 4.4%. The largest %AAD is observed for dry Illinois #6 coal.

Figure 4.12 indicates that most of the solid-solid interaction energy parameters are over predicted. As indicated in Table 4.9, only the solid-solid interaction energies of dry Wyodak, Upper Freeport and wet Tiffany are comparable to calculated values; the others have differences greater than 10%. These trends indicate that simultaneous regression of the model parameters has resulted in some trade offs among the parameters estimates. This is an expected outcome when the model parameters are not fully orthogonal.

Table 4.10 presents the summary results for the generalized SLD-PR model predictions of pure-gas adsorption on both dry and wet coals. As documented, the overall WAAD, %AAD, RMSE and WRMS are 1.05, 8.4%, 0.05 mmol/g and 1.47, respectively. The quality of the corresponding generalized predictions is exhibited in Figures 4.13 to 4.22.

As discussed previously, the predicted methane surface areas for many coals differ from the regressed values, and the solid-solid interaction energy parameters tend to be over predicted. This results in large deviations for methane adsorption relative to the expected experimental uncertainties. Specifically, the WRMS and WAAD of methane adsorption on dry Upper Freeport and wet Fruitland OSU #2 are above 4.0. Methane adsorption on dry Upper Freeport, shown in Figure 4.16, is more than five times the experimental error due to the overestimation of the surface area from the parameter generalization. The respective RMSE and %AAD are 0.10 mmol/g and 19.3%.

Table 4.10 – Case 2: Summary Results for the Generalized SLD-PR Adsorption Predictions

Coal	WAAD			%AAD			RMSE			WRMS		
	CH_4	N_2	CO_2	CH_4	N_2	CO_2	CH_4	N_2	CO_2	CH_4	N_2	CO_2
Dry Illinois #6	0.60	1.17	1.61	3.8	12.6	6.0	0.02	0.03	0.11	0.74	1.20	2.33
Dry Beulah Zap	0.64	1.15	0.83	5.3	13.8	3.7	0.03	0.04	0.06	0.87	1.39	1.06
Dry Wyodak	0.52	0.54	1.66	3.4	6.4	5.4	0.02	0.01	0.09	0.64	0.62	2.06
Dry Upper Freeport	5.18	0.80	0.70	19.3	5.2	3.5	0.10	0.01	0.03	5.34	0.84	0.86
Dry Pocahontas	0.46	1.51	1.01	1.9	9.3	4.9	0.01	0.03	0.05	0.59	1.52	1.27
Wet Illinois #6	0.91	0.38	1.01	7.3	10.2	14.8	0.02	0.01	0.10	1.22	0.48	1.33
Wet FR OSU #1	2.63	1.38	0.79	9.9	10.3	5.5	0.07	0.04	0.07	2.85	1.51	0.94
Wet FR OSU #2	4.64	1.01	0.87	20.2	8.3	10.2	0.13	0.03	0.11	4.86	1.20	1.08
Wet Tiffany	1.16	0.60	0.66	6.6	6.7	8.6	0.02	0.01	0.05	1.35	0.76	0.83
Wet LB FR	2.44	0.79	0.53	12.2	9.2	8.0	0.03	0.01	0.03	2.76	0.95	0.63
Overall Statistics for Coals	**1.05**			**8.4**			**0.05**			**1.47**		

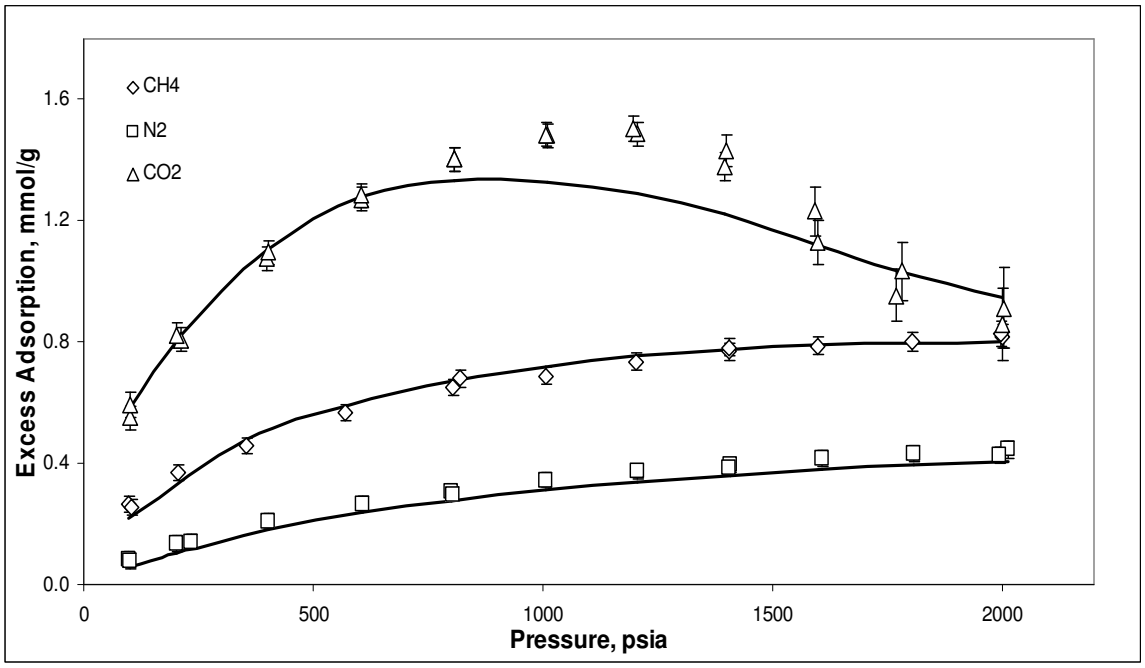

Figure 4.13 – Generalized Predictions of Pure-Gas Adsorption on Dry Illinois #6 Coal at 131°F Using Nitrogen Excess Adsorption at 400 psia

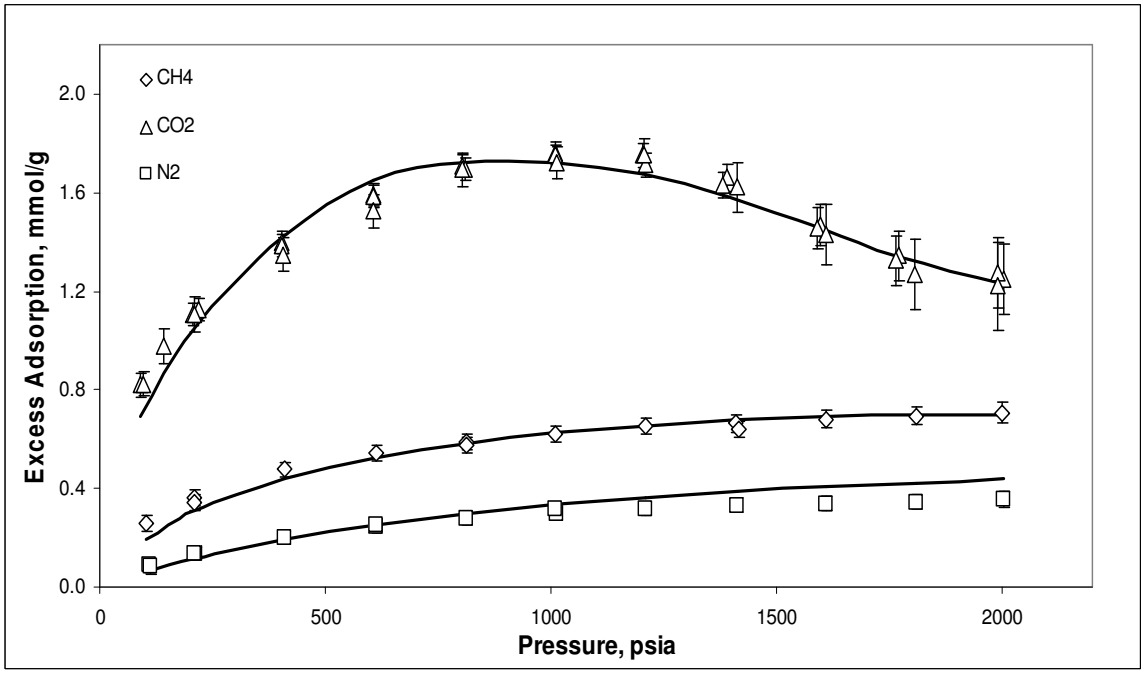

Figure 4.14 – Generalized Predictions of Pure-Gas Adsorption on Dry Beulah Zap Coal at 131°F Using Nitrogen Excess Adsorption at 400 psia

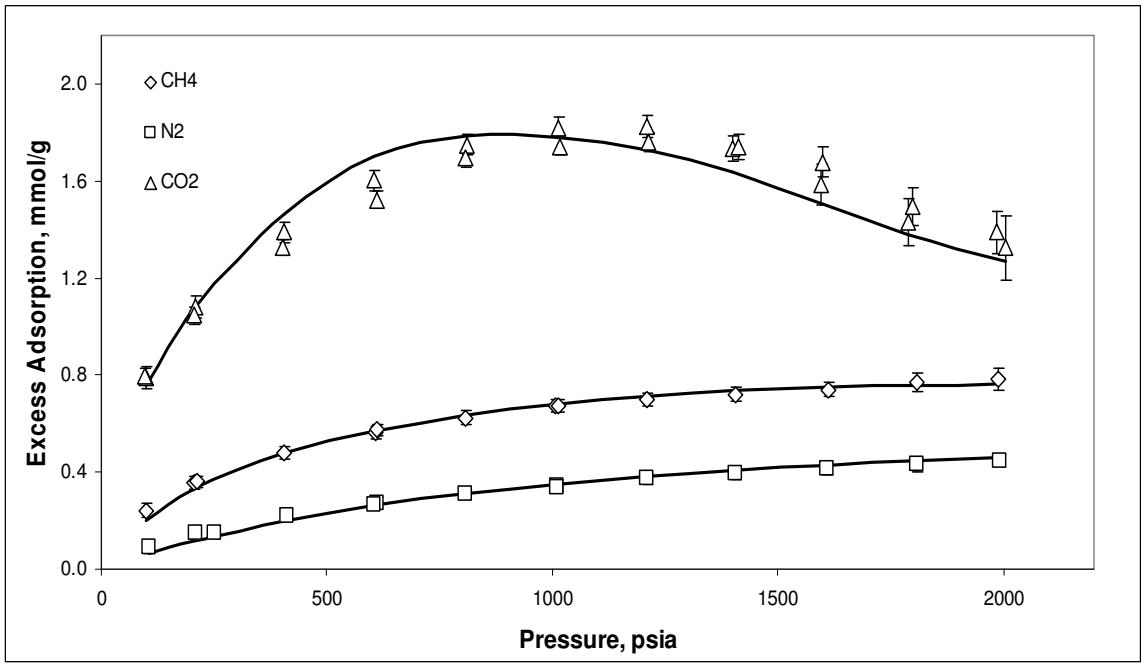

Figure 4.15 – Generalized Predictions of Pure-Gas Adsorption on Dry Wyodak Coal at 131°F Using Nitrogen Excess Adsorption at 400 psia

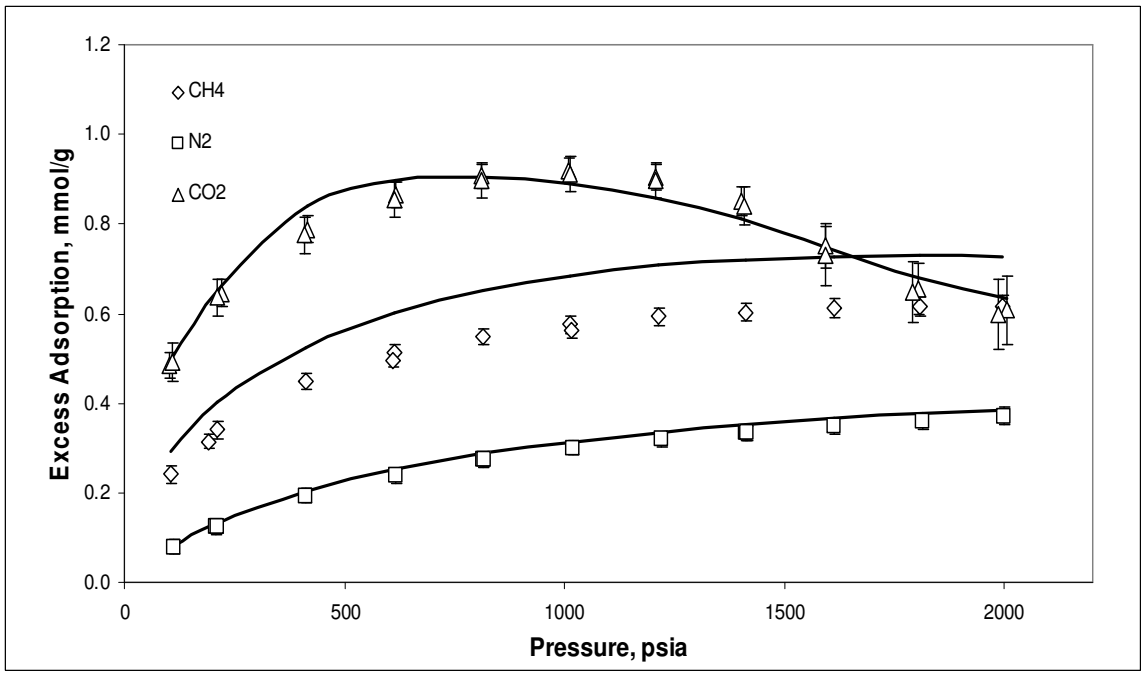

Figure 4.16 – Generalized Predictions of Pure-Gas Adsorption on Dry Upper Freeport Coal at 131°F Using Nitrogen Excess Adsorption at 400 psia

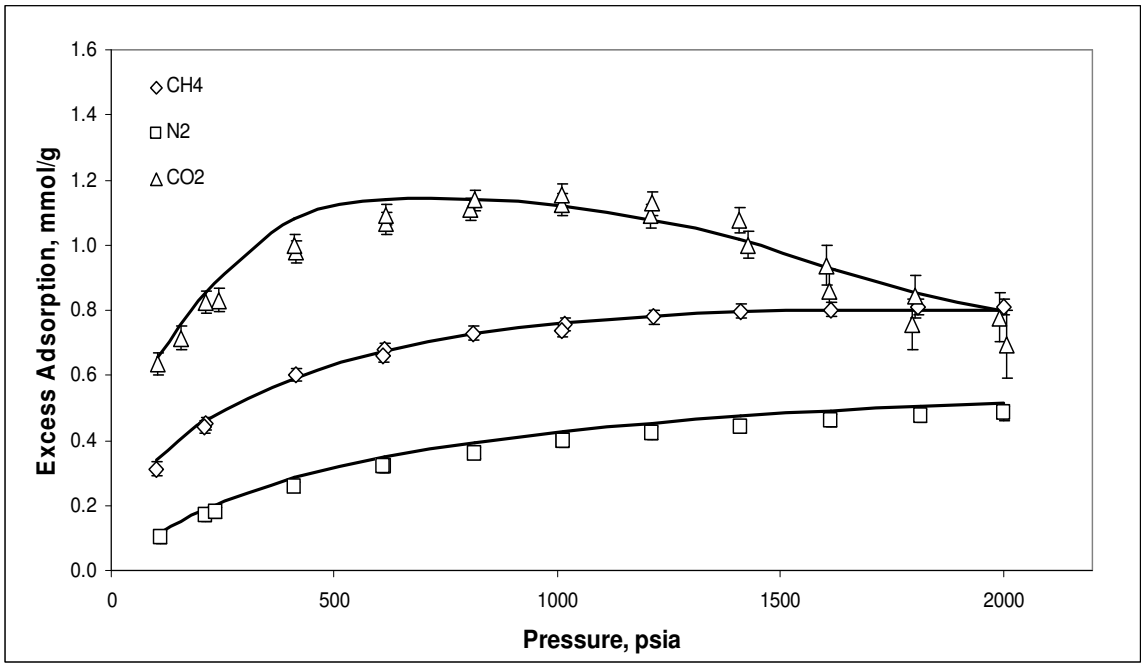

Figure 4.17 – Generalized Predictions of Pure-Gas Adsorption on Dry Pocahontas Coal at 131°F Using Nitrogen Excess Adsorption at 400 psia

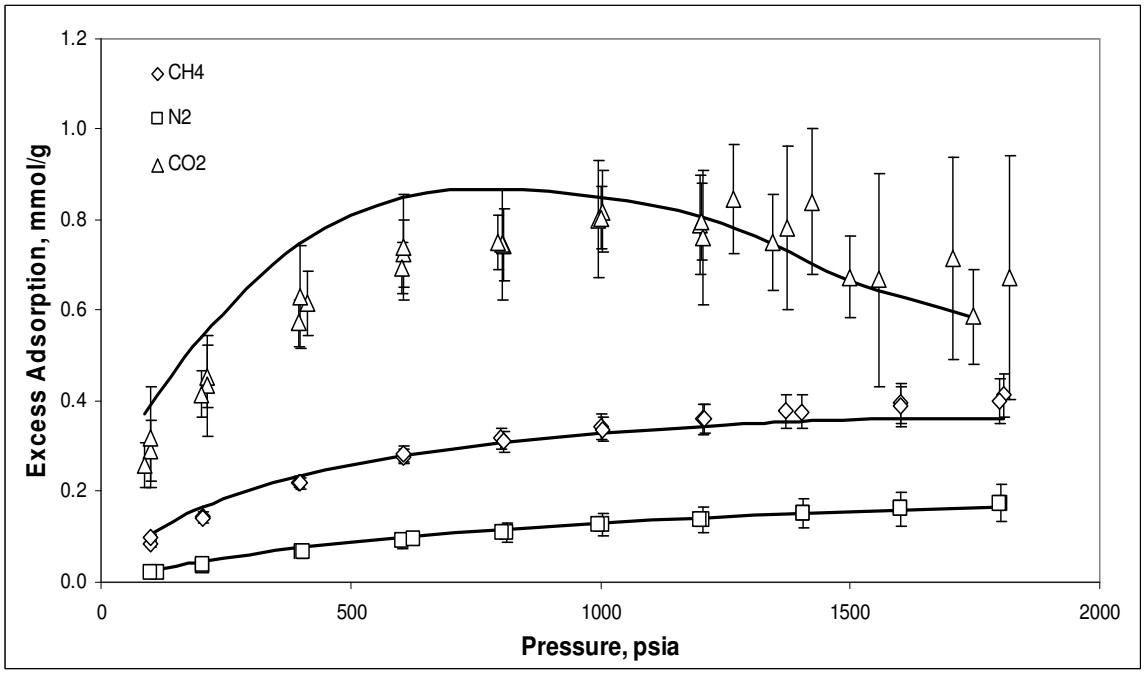

Figure 4.18 – Generalized Predictions of Pure-Gas Adsorption on Wet Illinois #6 Coal at 115°F Using Nitrogen Excess Adsorption at 400 psia

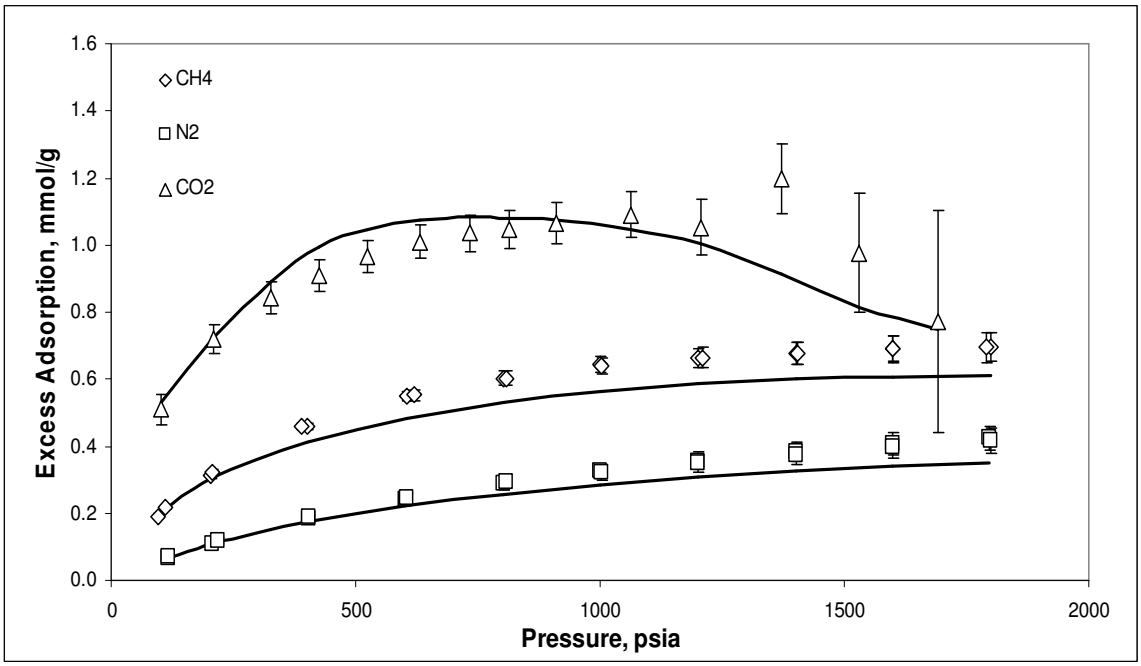

Figure 4.19 – Generalized Predictions of Pure-Gas Adsorption on Wet Fruitland OSU #1 Coal at 115°F Using Nitrogen Excess Adsorption at 400 psia

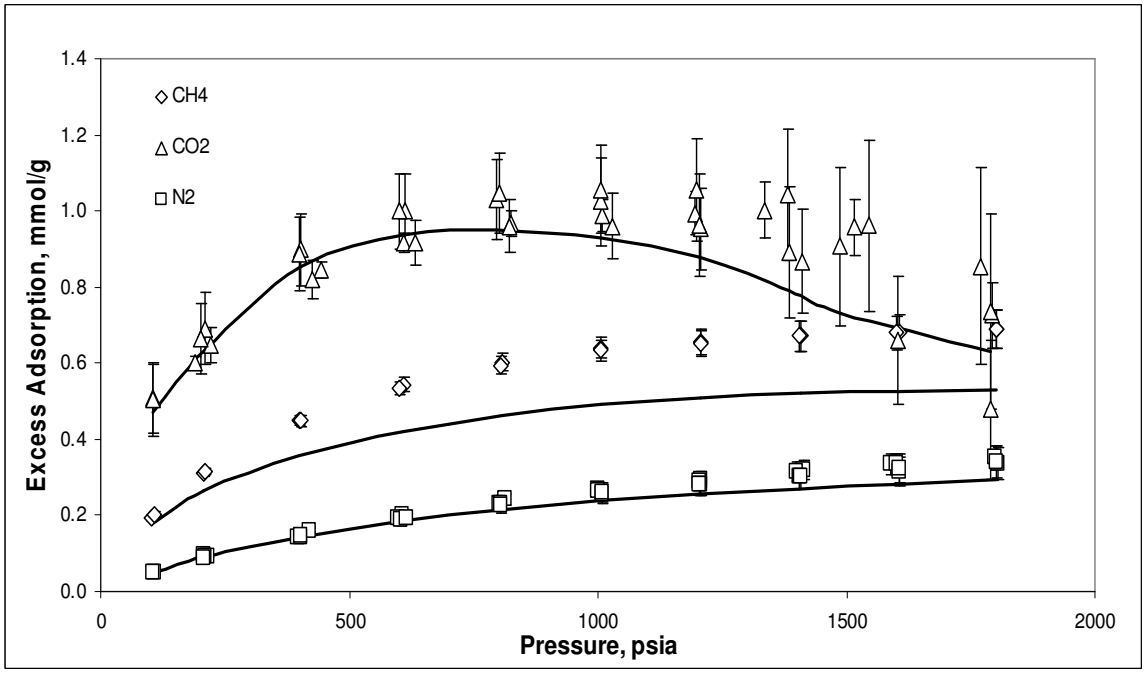

Figure 4.20 – Generalized Predictions of Pure-Gas Adsorption on Wet Fruitland OSU #2 Coal at 115°F Using Nitrogen Excess Adsorption at 400 psia

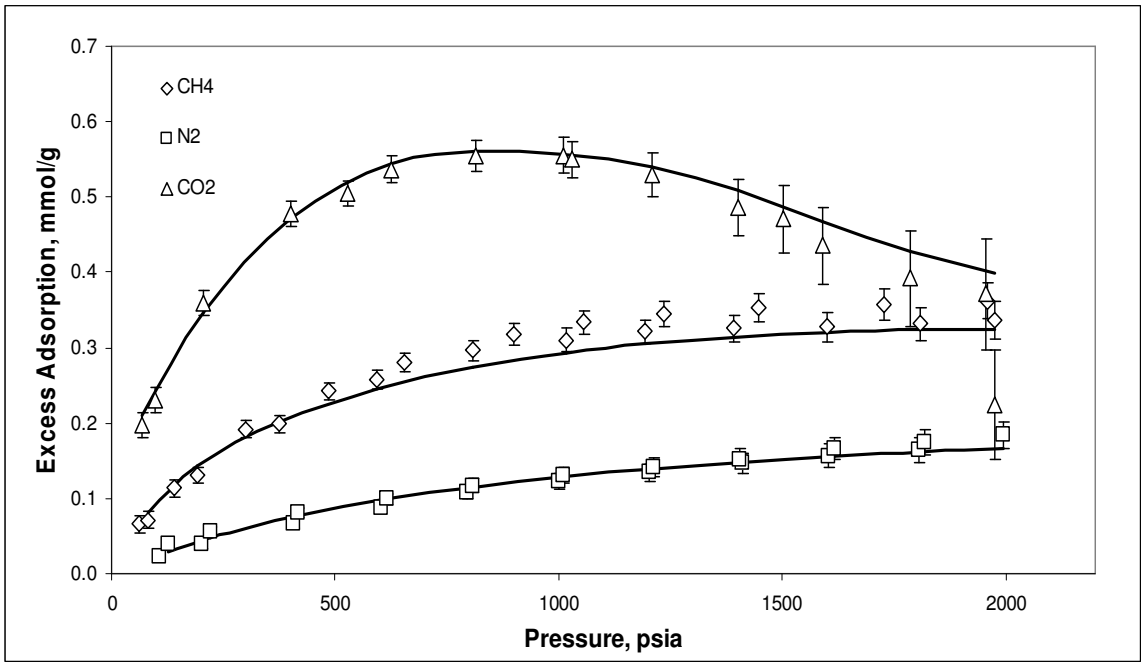

Figure 4.21 – Generalized Predictions of Pure-Gas Adsorption on Wet Tiffany Coal at 130°F Using Nitrogen Excess Adsorption at 400 psia

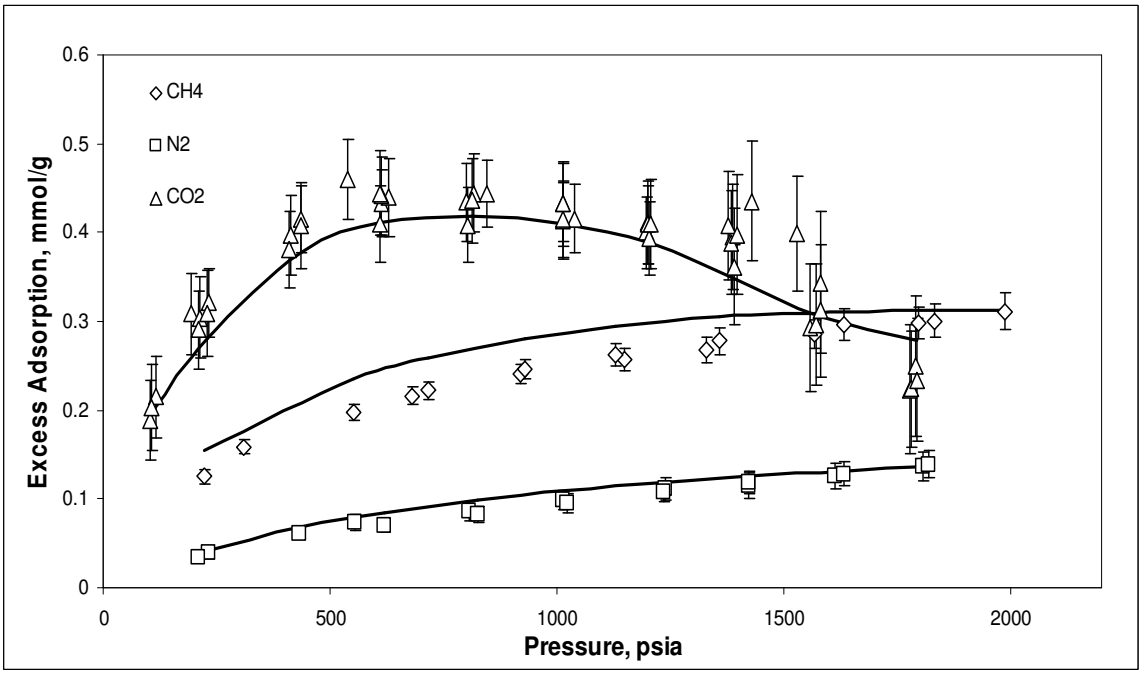

Figure 4.22 – Generalized Predictions of Pure-Gas Adsorption on Wet Lower Basin Fruitland Coal at 115°F Using Nitrogen Excess Adsorption at 400 psia

The methane adsorption on wet Fruitland OSU #2 (Figure 4.20) is predicted poorly because of surface area underestimation. The predicted adsorption is 20% lower than the experimental data with a RMSE of 0.13 mmol/g. In comparison, methane adsorption on wet Fruitland OSU #1 (Figure 4.19) and wet Lower Basin (Figure 4.22) are predicted within three times the experimental uncertainties.

Compared to methane adsorption, both the nitrogen and CO_2 adsorption are predicted within twice the experimental uncertainty. For nitrogen adsorption, the largest WAAD of 1.51 is observed for wet Fruitland OSU #1 and this value is followed by 1.39 for dry Beulah Zap. The %AAD values for these coals are 10.3% and 13.8% for the wet Fruitland OSU #1 and dry Beulah Zap, respectively, and RMSE of 0.04 mmol/g for both coals. For CO_2 adsorption, both the dry Illinois #6 and dry Wyodak coals show relatively larger WAAD values of 1.61 and 1.66, respectively.

Overall, the generalizations using nitrogen excess adsorption at 400 psia are able to predict most of the pure-gas adsorption isotherms within two times the experimental uncertainties, with the exception of the methane adsorption on the wet Fruitland OSU #2 and dry Upper Freeport coals.

Case 3: CO_2-Based Generalizations

In this case, the surface areas of all coals are correlated as a function of the CO_2 excess adsorption at 400 psia. Similar to Case 2, the methane, nitrogen and CO_2 surface areas of all coals are not correlated well with the CO_2 excess adsorption. Thus, additional coal properties are incorporated to achieve a better correlation with the surface area, as shown in Table 4.11.

Table 4.11 presents the generalized correlations for the surface areas using CO_2 excess adsorption at 400 psia and for the solid-solid interaction energy. The generalized parameters are shown in Table 4.12, and the plots of comparison between generalized parameters and regressed parameters are depicted in Figure 4.23. Also, an assessment of the quality of the parameter generalization is provided in Table 4.13 in terms %AAD values obtained for the predicted parameters relative to the regressed parameters. (The details are in Appendix C.2).

Table 4.11 – Case 3: Generalized Correlations of the Surface Areas and the Solid-Solid Interaction Energy Parameter

$$A_{CH4} = 72.482\left(n^{Ex}_{CO2@400}\right)\left(\frac{\varphi_{FC}}{\chi_C}\right)^{0.5} + 1.46$$

$$A_{N2} = 61.019\left(n^{Ex}_{CO2@400}\right) - 149.57\left(\lambda_M\right)^{0.5}\left(\varphi_{FC}\right)$$

$$A_{CO2} = 72.82\left(n^{Ex}_{CO2@400}\right) - 43.95\left(\lambda_M \times \chi_C\right)^{0.5} - 3.52$$

$$\varepsilon_{ss}/k = \frac{2.143}{\lambda_M^{0.5}} + 7.80\left(\frac{\chi_C}{\varphi_{FC}}\right)$$

Table 4.12 – Case 3: Generalized SLD-PR Model Parameters

Coal	Surface Area (m^2/g)			Slit Length (nm)	ε_{ss}/k (K)
	CH_4	N_2	CO_2		
Dry Illinois #6	60.0	50.7	88.5	1.15	22.7
Dry Beulah Zap	68.0	60.4	120.9	1.15	22.7
Dry Wyodak	68.6	59.2	118.3	1.15	22.1
Dry Upper Freeport	48.5	38.7	57.8	1.15	32.0
Dry Pocahontas	66.9	50.8	71.9	1.15	35.1
Wet Illinois #6	40.3	20.5	48.0	1.15	21.0
Wet FR OSU #1	62.3	42.0	67.6	1.15	23.7
Wet FR OSU #2	58.9	39.1	63.7	1.15	23.6
Wet Tiffany	29.8	18.5	37.0	1.15	22.7
Wet LB FR	25.3	15.1	30.1	1.15	21.7

Table 4.13 – Case 3: Summary Results of the Generalized Parameters

Coal	%AAD			
	A_{CH4}	A_{N2}	A_{CO2}	ε_{ss}/k
Dry Illinois #6	19.1	10.0	9.3	7.4
Dry Beulah Zap	15.6	41.0	8.6	16.8
Dry Wyodak	0.3	6.9	0.2	1.4
Dry Upper Freeport	0.8	4.4	3.3	9.8
Dry Pocahontas	5.6	6.6	4.2	6.4
Wet Illinois #6	9.3	7.6	11.2	20.8
Wet FR OSU #1	2.2	12.2	2.0	0.2
Wet FR OSU #2	3.9	2.1	1.1	4.3
Wet Tiffany	2.4	6.0	1.1	7.1
Wet LB FR	2.3	0.9	3.8	1.7
Overall Total	6.2	9.8	4.5	7.6

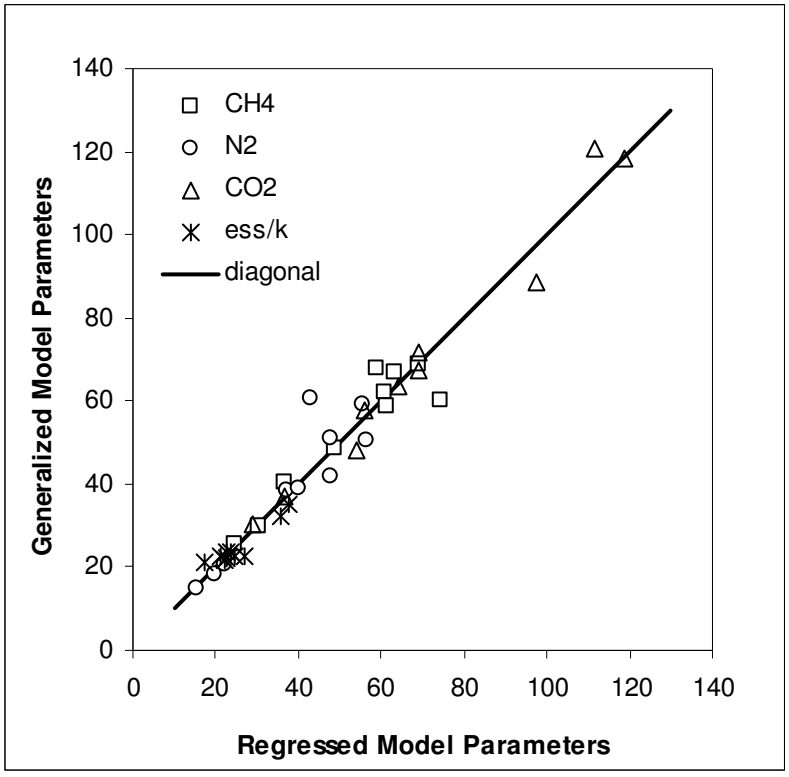

Figure 4.23 – Case 3: Comparison of the Regressed and Generalized SLD-PR Model Parameters

As illustrated in Figure 4.23 and Table 4.13, the generalized methane surface areas are comparable to the regressed values with an average difference of 6.2%; however, large %AAD of 11.1 and 15.6% are observed for dry Illinois #6 and Beulah Zap, respectively. The generalized methane surface area for the dry Illinois #6 is overestimated while that for Beulah Zap is overestimated. However, the surface areas for the remaining coals differ by less than 8.0% from the regressed surface areas.

The surface areas of nitrogen are also comparable to the regressed values. The average difference is 9.8% with the largest %AAD (41.0%) observed for the dry Beulah Zap coal. From Figure 4.23, this large error is due to an overestimation of the nitrogen surface area due to a large CO_2 excess adsorption.

Most of the generalized CO_2 surface areas are predicted accurately compared to the regressed values, as shown in Figure 4.23 and Table 4.13. The average %AAD is 4.5% with the largest difference of 11.2% observed for the wet Illinois #6 coal. As shown in Figure 4.23, the generalized solid-solid interaction energy parameters compare favorably with the regressed values; %AAD of less than 7.6% is reported in Table 4.13.

Table 4.14 presents the summary results of generalization using CO_2 excess adsorption at 400 psia. The generalized predictions for the adsorption are depicted in Figures 4.24 through Figure 4.33. The overall WAAD, %AAD, RMSE and WRMS are 1.06, 7.70%, 0.04 mmol/g and 1.23, respectively. As mentioned previously, the methane surface area of dry Illinois #6 and the nitrogen surface area of dry Beulah Zap and wet Fruitland OSU #1 differ from the regressed values; thus, the respective adsorption are predicted poorly.

Table 4.14 – Case 3: Summary Results for the Generalized SLD-PR Adsorption Predictions

Coal	WAAD			%AAD			RMSE			WRMS		
	CH_4	N_2	CO_2	CH_4	N_2	CO_2	CH_4	N_2	CO_2	CH_4	N_2	CO_2
Dry Illinois #6	3.75	0.95	1.77	19.3	11.6	6.7	0.11	0.02	0.11	3.80	1.00	2.43
Dry Beulah Zap	1.46	2.20	1.16	9.2	22.3	5.3	0.05	0.08	0.08	1.59	2.70	1.43
Dry Wyodak	0.60	0.97	1.64	4.3	8.8	5.8	0.02	0.03	0.09	0.86	1.07	1.92
Dry Upper Freeport	1.40	0.31	0.66	5.8	3.2	3.9	0.03	0.01	0.03	1.47	0.40	0.74
Dry Pocahontas	0.93	0.54	0.97	2.8	2.8	5.1	0.03	0.01	0.06	1.13	0.64	1.15
Wet Illinois #6	2.74	0.26	0.62	20.2	6.7	10.6	0.06	0.01	0.10	3.08	0.32	0.76
Wet FR OSU #1	0.63	1.65	0.60	2.5	12.5	5.2	0.02	0.04	0.06	0.70	1.68	0.72
Wet FR OSU #2	0.42	0.38	0.76	1.7	3.1	8.9	0.01	0.01	0.09	0.53	0.46	0.95
Wet Tiffany	1.01	1.17	0.68	5.8	11.8	8.5	0.02	0.02	0.05	1.25	1.35	0.99
Wet LB FR	0.66	0.40	0.51	3.5	4.8	8.2	0.01	0.01	0.03	0.74	0.47	0.61
Overall Statistics for Coals	**1.06**			**7.7**			**0.04**			**1.23**		

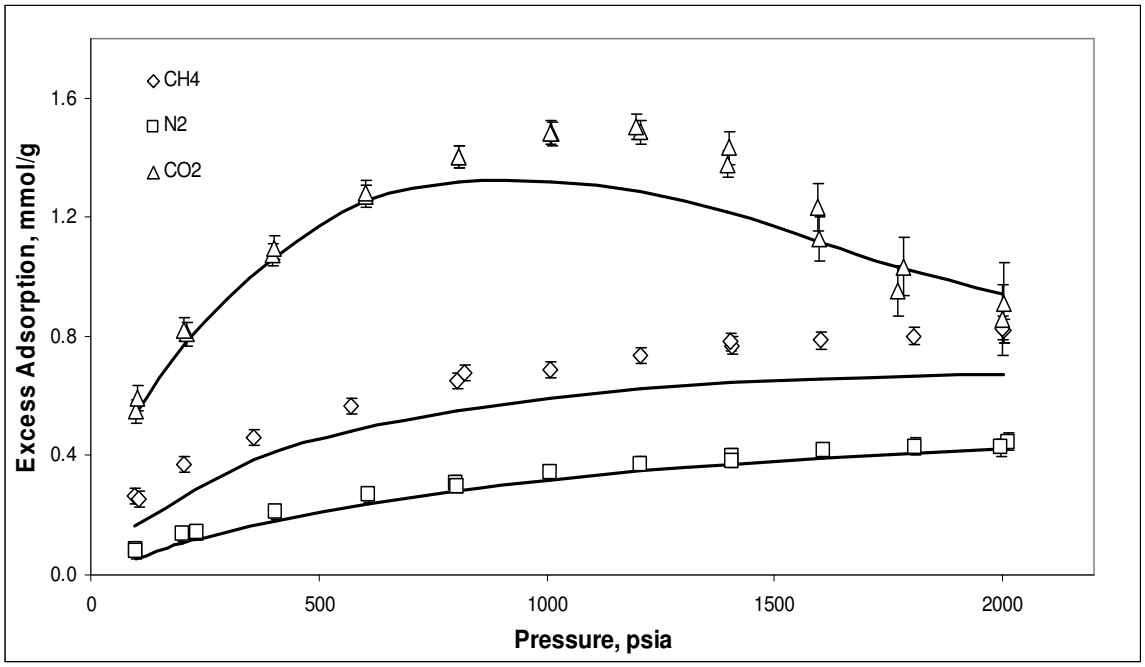

Figure 4.24 – Generalized Predictions of Pure-Gas Adsorption on Dry Illinois #6 Coal at 131°F Using CO_2 Excess Adsorption at 400 psia

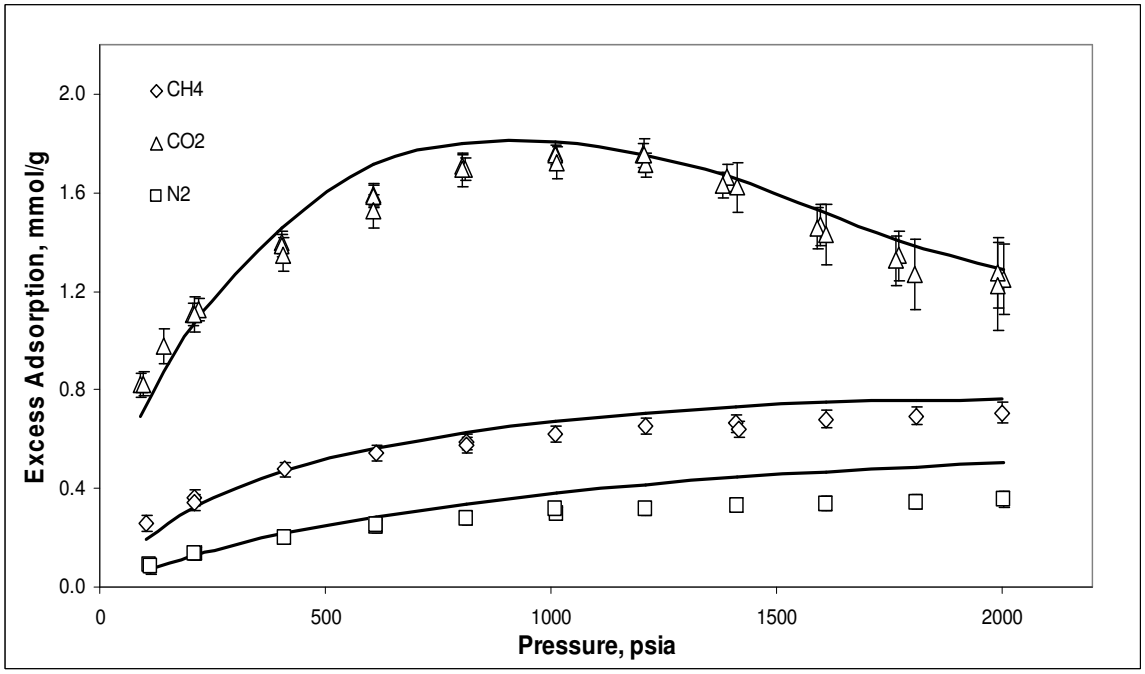

Figure 4.25 – Generalized Predictions of Pure-Gas Adsorption on Dry Beulah Zap Coal at 131°F Using CO_2 Excess Adsorption at 400 psia

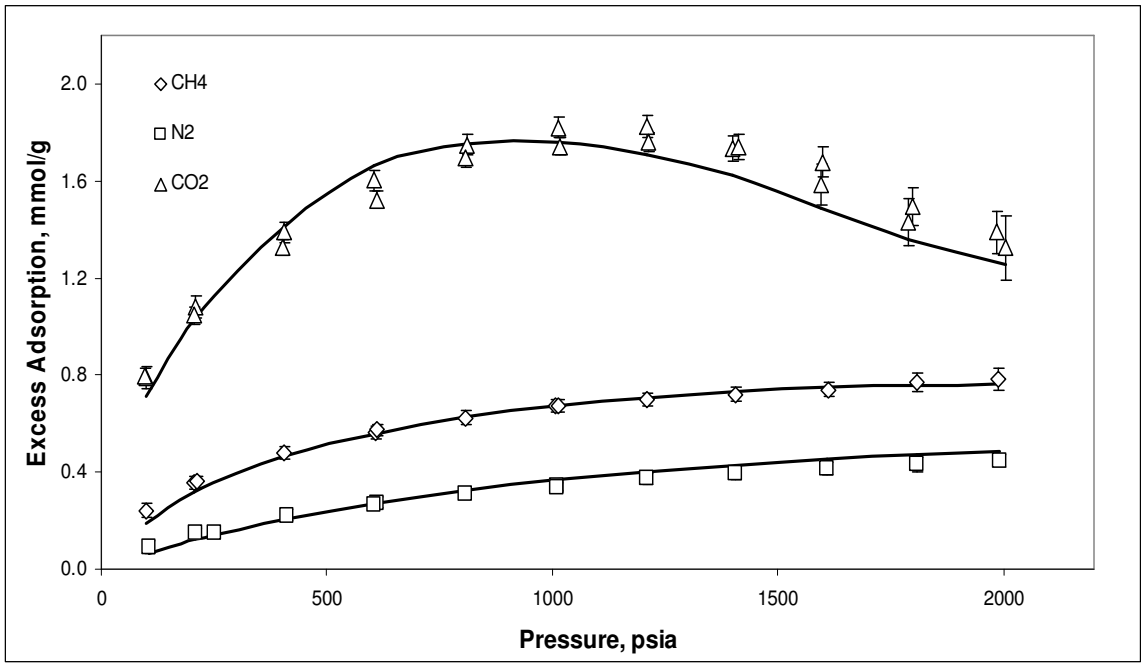

Figure 4.26 – Generalized Predictions of Pure-Gas Adsorption on Dry Wyodak Coal at 131°F Using CO_2 Excess Adsorption at 400 psia

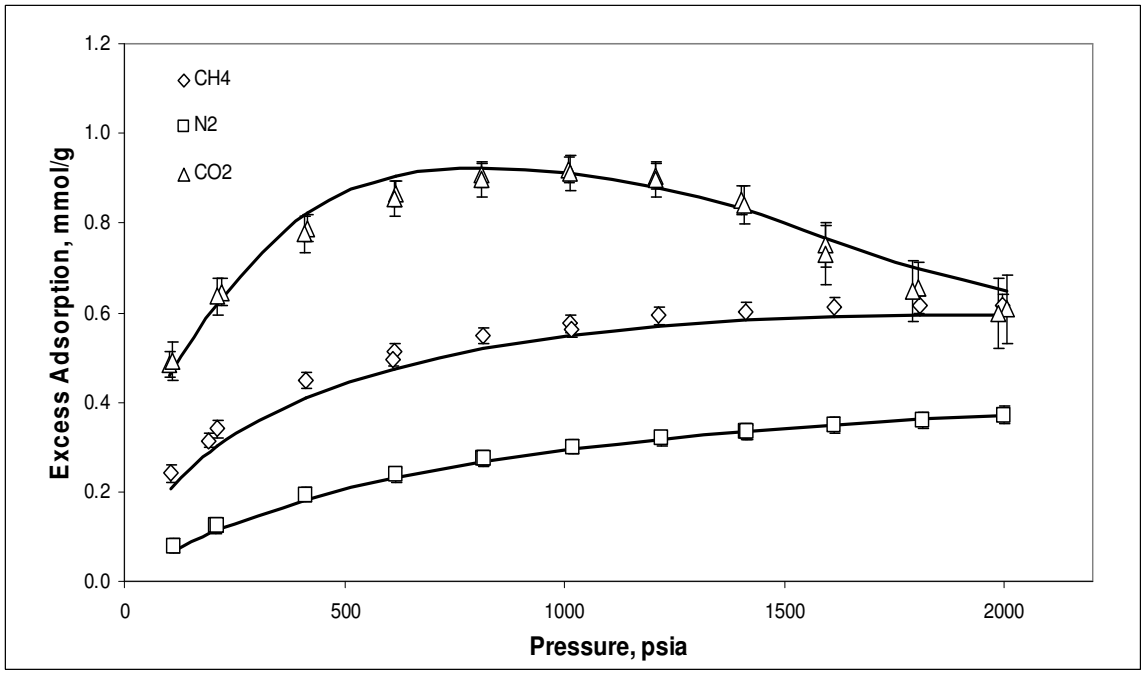

Figure 4.27 – Generalized Predictions of Pure-Gas Adsorption on Dry Upper Freeport Coal at 131°F Using CO_2 Excess Adsorption at 400 psia

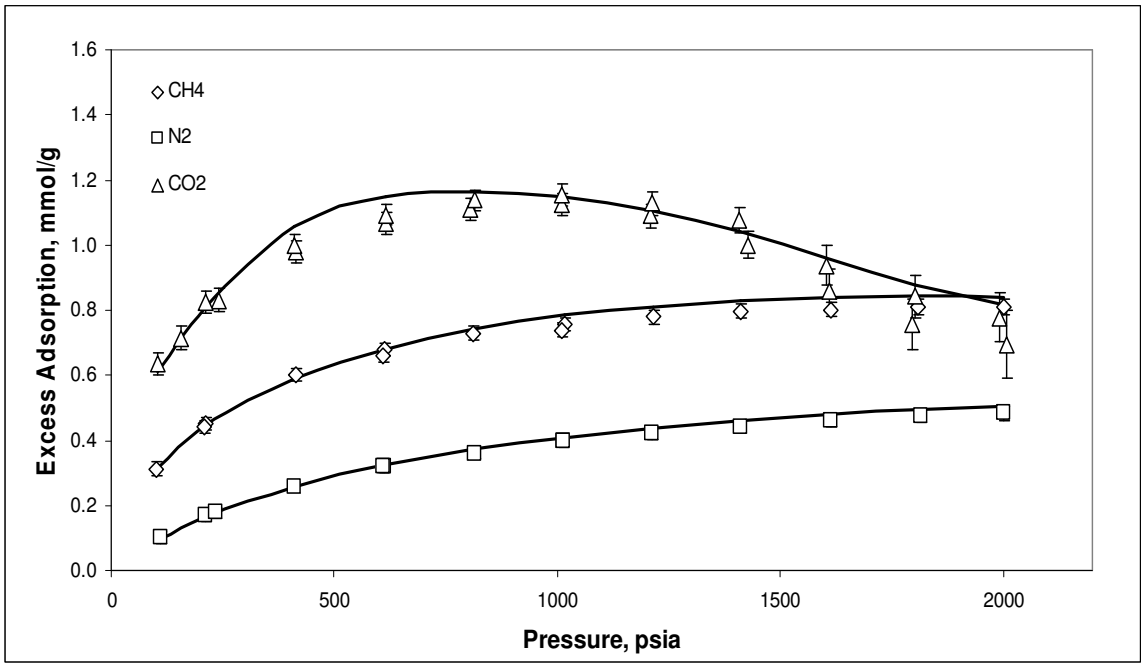

Figure 4.28 – Generalized Predictions of Pure-Gas Adsorption on Dry Pocahontas Coal at 131°F Using CO_2 Excess Adsorption at 400 psia

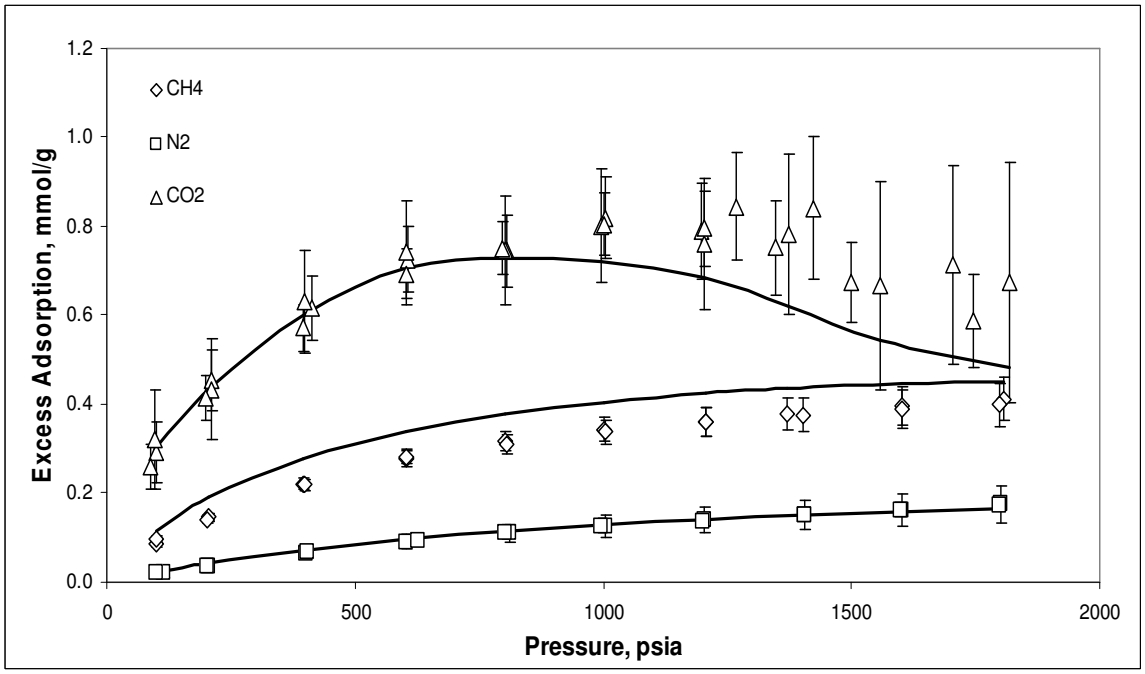

Figure 4.29 – Generalized Predictions of Pure-Gas Adsorption on Wet Illinois #6 Coal at 115°F Using CO_2 Excess Adsorption at 400 psia

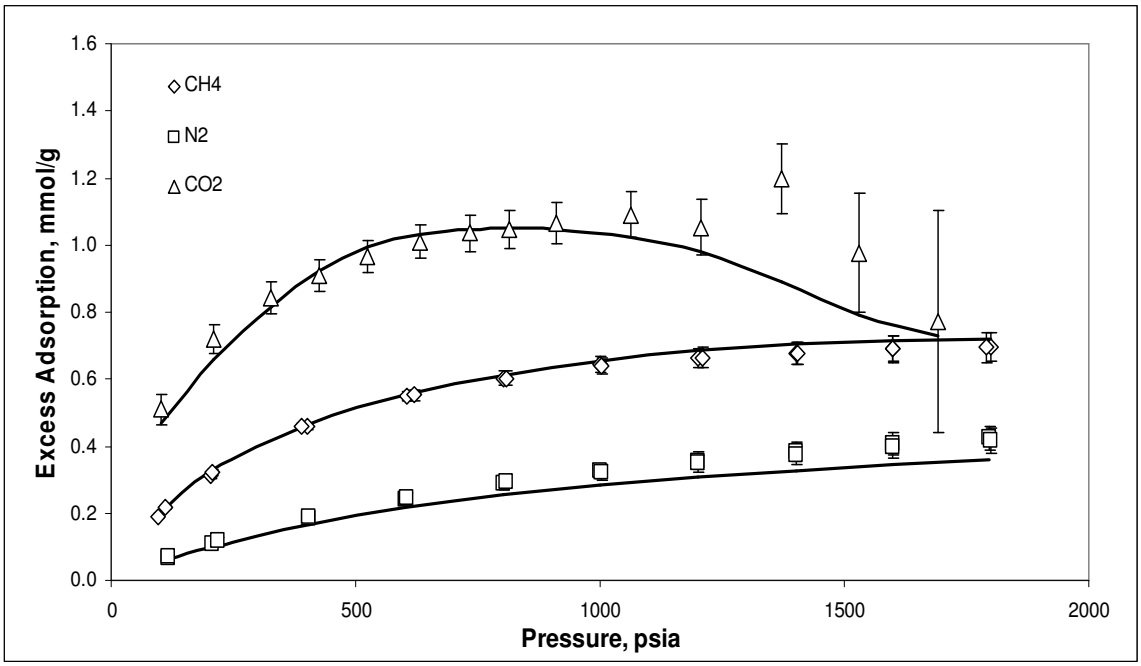

Figure 4.30 – Generalized Predictions of Pure-Gas Adsorption on Wet Fruitland OSU #1 at 115°F Using CO_2 Excess Adsorption at 400 psia

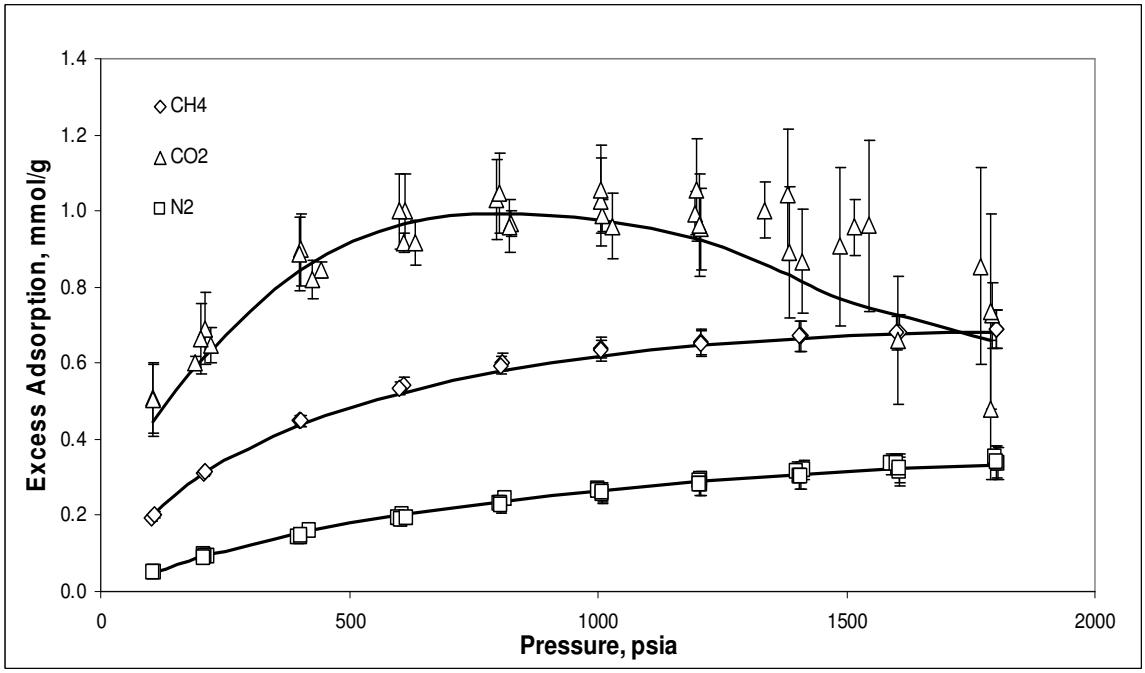

Figure 4.31 – Generalized Predictions of Pure-Gas Adsorption on Wet Fruitland OSU #2 Coal at 115°F Using CO_2 Excess Adsorption at 400 psia

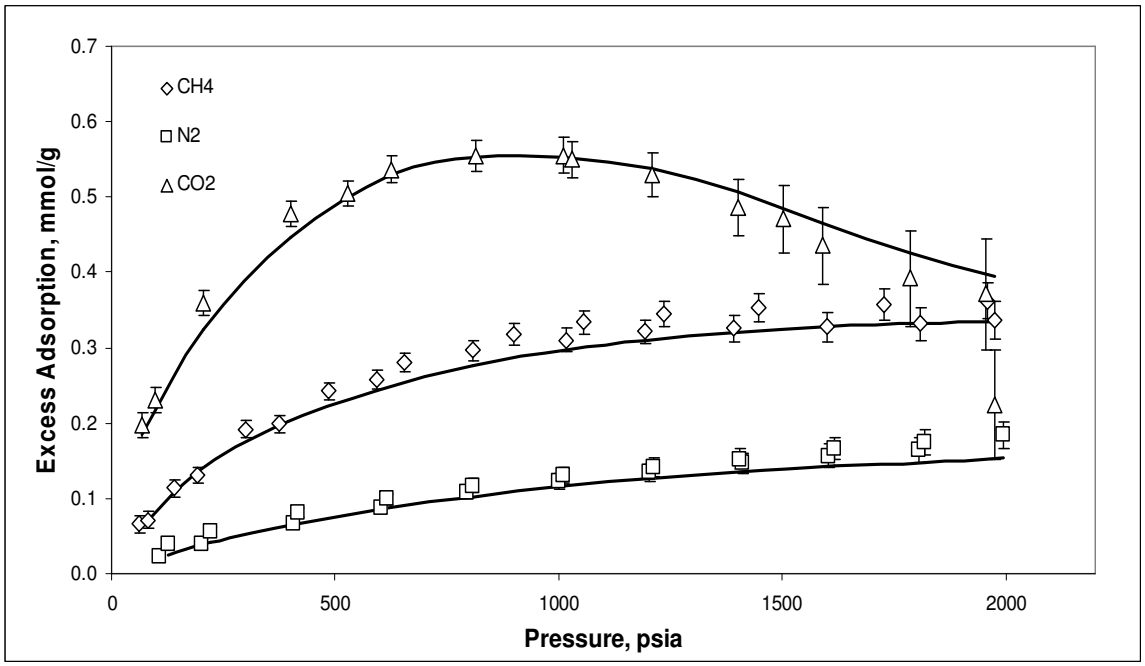

Figure 4.32 – Generalized Predictions of Pure-Gas Adsorption on Wet Tiffany Coal at 130°F Using CO_2 Excess Adsorption at 400 psia

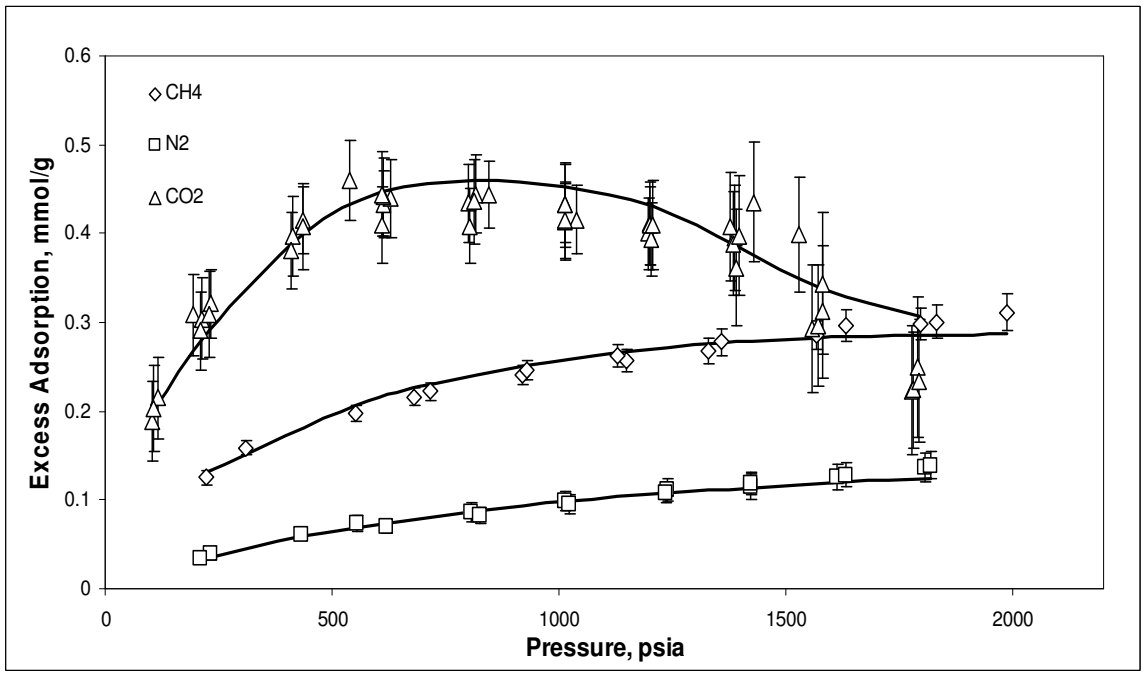

Figure 4.33 – Generalized Predictions of Pure-Gas Adsorption on Wet Lower Basin Fruitland Coal at 115°F Using CO_2 Excess Adsorption at 400 psia

The methane adsorption isotherm for dry Illinois #6, shown in Figure 4.24, is predicted less accurately for all pressures. For this coal, the WRMS, RMSE, %AAD and WAAD are 3.80, 0.11 mmol/g, 19.3% and 3.75, respectively. These deviations are large because of the low values obtained for the generalized methane surface areas and the relatively smaller experimental uncertainties. In comparison, the CO_2 surface area is slightly underestimated; nevertheless, the predictions produced relatively larger values for the WRMS (2.43) and RMSE (0.11 mmol/g). Also, the methane adsorption for the wet Illinois #6 coal is over predicted at lower pressures, as illustrated in Figure 4.29, because the methane surface area is also overestimated. For this coal the WRMS, RMSE, %AAD and WAAD are 3.08, 0.06 mmol/g, 20.2% and 2.74, respectively.

The nitrogen adsorption isotherm for dry Beulah Zap was not predicted accurately, as listed in Table 4.14, the WRMS, RMSE, %AAD WAAD is 2.70, 0.08 mmol/g, 22.3% and 2.20, respectively. For wet Fruitland OSU #1, as shown in Figure 4.30, the nitrogen adsorption was under predicted because the surface area is underestimated. For this coal the %AAD is 12.5% and RMSE is 0.04 mmol/g. In comparison, the nitrogen adsorption isotherms were predicted generally within twice the experimental uncertainties.

The results above for Case 3 indicate that the generalized parameters using CO_2 excess adsorption are, on average, are capable of predicting the pure-fluid adsorption on dry Wyodak, dry Upper Freeport, dry Pocahontas, wet Fruitland OSU #2, wet Tiffany and wet Lower Basin Fruitland within twice the experimental uncertainties. More importantly, the CO_2-based generalized predictions provided sufficiently accurate results for most CBM-type applications involving the coals considered.

Comparison of Generalized Predictions of Cases 1, 2 and 3

The results of the three cases demonstrate the generalized SLD-PR model is capable of predicting the pure-gas adsorption on the considered dry and wet coals with an overall WAAD of 1.10. This is comparable to the prediction results on activated carbon and coals using generalized Ono-Kondo lattice model [16, 17] and 2-D EOS model [14, 34] (both within twice the experimental uncertainties).

Specifically, the SLD-PR generalization based on methane excess adsorption predicts the pure-gas adsorption within three times the experimental uncertainties. In comparison, generalization using CO_2 excess adsorption provides pure-gas adsorption predictions also within three times the experimental uncertainties with the exception of the methane adsorption on dry Illinois #6 coal, which is predicted within four times the experimental uncertainty.

Similar to the CO_2 correlation, the generalization using nitrogen excess adsorption is also able to provide predictions for most of the pure-gas adsorption within three times the experimental uncertainties. However, the methane adsorption on dry Upper Freeport and wet Fruitland OSU #2 yield deviations larger than four times the experimental uncertainty. Figure 4.34 exemplifies the generalized predictions for pure-gas adsorption on dry Beulah Zap coal for the three cases. The figure demonstrates a common observation that the generalized SLD-PR model based on methane excess adsorption gives more accurate predictions for the pure-gas adsorption on dry and wet coals.

Nonetheless, these generalizations (including nitrogen and CO_2 excess adsorption) account for the moisture effect on the adsorption based on one calibration point (methane, nitrogen or CO_2 excess adsorption at 400 psia). Moreover, in the current

data reduction procedure, a few assumptions are used for determining the measured amount of gas adsorption on wet coals, which may affect the qualities of both the model representation and generalization. These assumptions are: (1) the amount of gas adsorbed is adjusted to account for the gas soluble in the adsorbed water, which is taken to be the full amount of water injected; and (2) the bulk-phase densities are calculated assuming the absence of water in that phase.

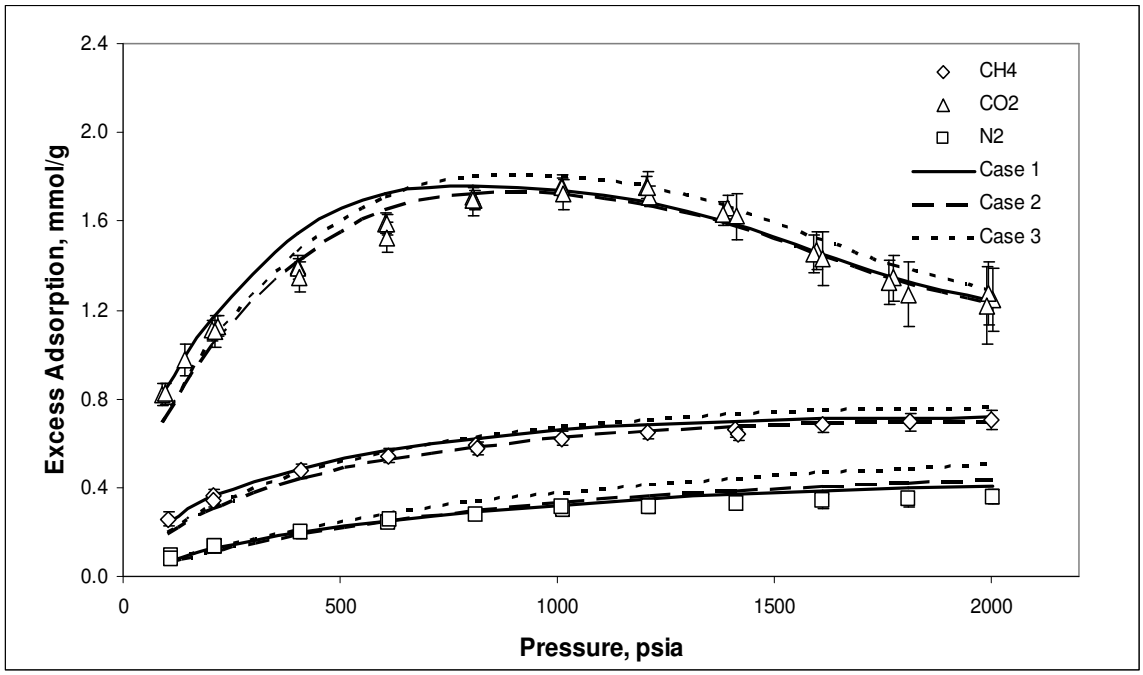

Figure 4.34 – Comparison among the SLD-PR Model Parameter Generalizations as Applied to Pure-Gas Adsorption on Dry Beulah Zap Coal at 131°F

Figure 4.35 presents the deviation plot for the SLD-PR model generalization of the pure-gas adsorption on dry and wet coals. The deviations of the model representations produced by Scenario 3 are compared to those of the generalized model predictions using methane excess adsorption (Case 1). From the figure, most of the data

are predicted by the methane-based generalization within three times the experimental uncertainties.

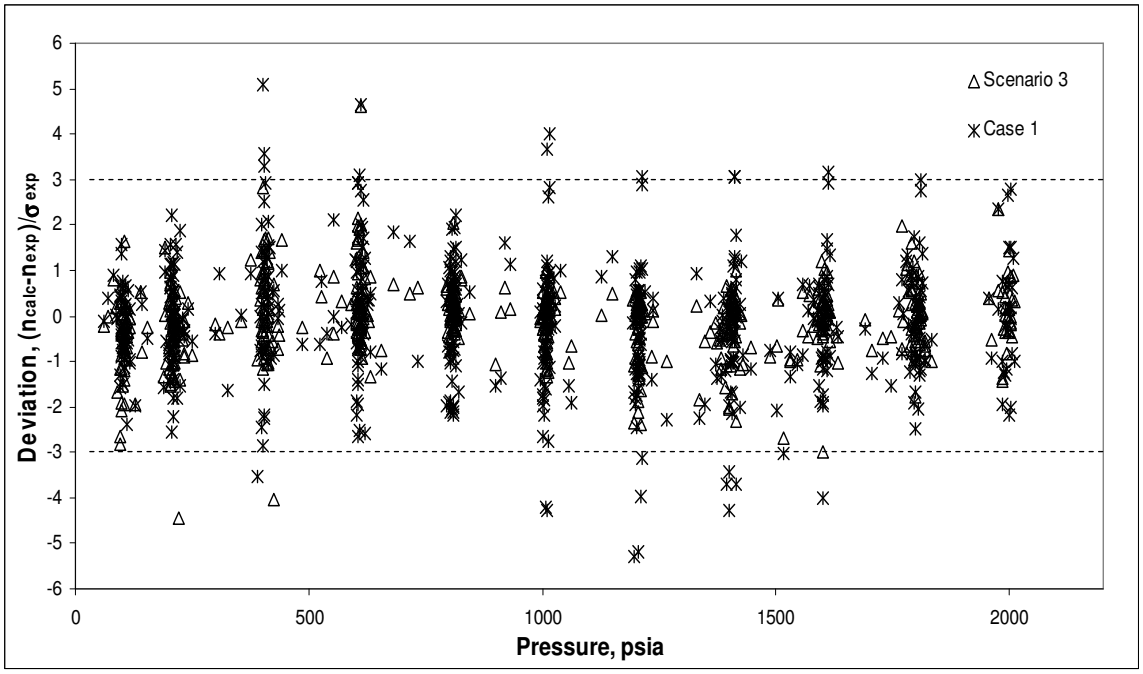

Figure 4.35 – Deviations Plot for SLD-PR Model Generalization of Pure-Gas Adsorption on Dry and Wet Coals

Conclusions

The SLD-PR model parameters are successfully generalized using the methane, nitrogen and CO_2 excess adsorption. On average, these generalized parameters are capable of predicting the pure-gas adsorption on dry Argonne premium coals and wet OSU coals within three times the experimental uncertainties.

Among generalized model parameters, the surface areas have a significant effect on the pure-gas adsorption predictions of all adsorbates. As indicated in Cases 1 and 2, most of the solid-solid interaction energy parameters do not match those obtained in Scenario 3; however, the resultant generalized surface areas produced predictions within the experimental uncertainties.

The results obtained for the three cases indicate that, only the pure-gas adsorption on dry Pocahontas and wet Tiffany coals are predicted within twice the experimental uncertainties, while the adsorption on the other coals is predicted within three times the experimental uncertainties.

In general, the generalized SLD-PR model parameters using methane excess adsorption give more accurate predictions for the pure-gas adsorption on the coals considered in this study.

Also, these generalizations use the one point calibration to account for the moisture effect. Thus, additional work is required to obtain more accurate generalizations that account more effectively for the effects of water on adsorption.

CHAPTER 5

MULTI-COMPONENT GAS ADSORPTION MODELING

In this chapter, the generalized-parameter SLD-PR model is used to describe mixed-gas adsorption on wet coals. Specifically, one-fluid mixing rules were applied within the SLD-PR model to extend it to mixture predictions. Then model evaluations were conducted to assess the efficacy of the pure-fluid parameter generalizations as well as the selected mixing rules in modeling multi-component gas adsorption of the CBM systems considered.

SLD-PR Model for Mixed-Gas Adsorption

The modified SLD-PR model, as presented by Fitzgerald and coworkers [23], is used in this study. Following previous studies [18, 23], the excess adsorption of a component "i" is:

$$n_i^{Ex} = \frac{A}{2}\int_{\frac{3}{8}\sigma_{ff,8}}^{L-\frac{3}{8}\sigma_{ff,i}} \left(\rho_{ads}(z)\, x_i(z) - \rho_{bulk}\, y_i\right) dz \qquad (5\text{-}1)$$

Here, the amount adsorbed of each component depends on the component mole fractions in the bulk and adsorbed phase for a mixture adsorption as well as the bulk-phase density and adsorbed-phase density.

The adsorbed-phase density and the adsorbed-phase mole fraction of a component at each position "z" can be obtained from the following equilibrium relationship:

$$\ln\left(\frac{\hat{f}_i^{ads}[\vec{x}(z),\rho_{ads}(z)]}{\hat{f}_i^{bulk}}\right) = -\left(\frac{\Psi_i^{fs}(z)+\Psi_i^{fs}(L-z)}{kT}\right) \qquad i = 1, NC \qquad (5\text{-}2)$$

Both the bulk-phase and the adsorbed-phase densities are determined using the PR EOS. Similarly, the component bulk fugacity at given temperature, pressure, density and composition is calculated using the PR EOS.

The bulk fugacity of component "i" as given by PR EOS, is:

$$\ln\left(\frac{\hat{f}_i^{bulk}}{y_i P}\right) = \frac{b_i}{b}(Z-1) - \ln\left(Z-\frac{pb}{RT}\right) + \frac{a}{2\sqrt{2}RTb}\left(\frac{b_i}{b}-\frac{2\sum_j y_j a_{ij}}{a}\right)\ln\left(\frac{\left(1+\rho b\left(1+\sqrt{2}\right)\right)}{\left(1+\rho b\left(1-\sqrt{2}\right)\right)}\right) \qquad (5\text{-}3)$$

In the bulk phase, the attractive constant "a" and covolume "b" of a mixture are calculated using the one-fluid mixing rules with linear quadratic combining rules, respectively. The expressions for "a" and "b" are:

$$a = \sum_i \sum_j y_i y_j (a_{bulk})_{ij} \qquad b = \sum_i y_i b_i \qquad (5\text{-}4)$$

The attractive constant "a" of a component "i" in PR EOS is calculated using the same method for pure component which is discussed in Chapter 2.

In the adsorbed phase, the fugacity of component "i" is a function of local composition, local density, temperature and pressure. The fugacity of component "i" in the adsorbed phase, as given by PR EOS, is as follows:

$$\ln\left(\frac{\hat{f}_i^{ads}(z)}{x_i(z)P}\right)=\frac{2\sum_j x_j(z)b_{ij}-b}{b}\left(\frac{P}{\rho_{ads}(z)RT}-1\right)-\ln\left(\frac{P}{\rho_{ads}(z)RT}-\frac{Pb}{RT}\right)+\frac{a(z)}{2\sqrt{2}RTb}\left(\frac{2\sum_j x_j(z)b_{ij}-b}{b}-\frac{2\sum_j x_j(z)a_{ij}(z)}{a(z)}\right)\ln\left(\frac{\left(1+\rho_{ads}(z)b\left(1+\sqrt{2}\right)\right)}{\left(1+\rho_{ads}(z)b\left(1-\sqrt{2}\right)\right)}\right) \quad (5\text{-}5)$$

The attractive constant "a" and covolume "b" in the adsorbed phase are calculated by one-fluid mixing rules. The respective expressions are:

$$a=\sum_i\sum_j y_i y_j (a_{ads})_{ij} \qquad b=\sum_i\sum_j y_i y_j (b_{ads})_{ij} \quad (5\text{-}6)$$

In calculating the adsorbed-phase fugacity, the $a_i(z)$ varies with position within the slit. Chen *et al.* [22] provided the required derivation for this functionality in terms of slit length, L, to molecular diameter, $\sigma_{ff,i}$ ratio. The details are given by Fitzgerald [23]. The cross coefficient $(a_{ads})_{ij}$ is obtained by the geometric mean combining rule. To obtain more precise representations for the mixture adsorption behavior, a binary interaction parameter (BIP), C_{ij} is applied to the adsorbed phase, as follows:

$$(a_{ads})_{ij}=\sqrt{(a_{ads})_i(a_{ads})_j}\left(1-C_{ij}\right) \quad (5\text{-}7)$$

As mentioned in Chapter 2, the covolume "b" of a pure component in the adsorbed phase is adjusted by a empirical parameter, $\Lambda_{b,i}$. Hence, when a linear combining rule is applied for the cross coefficient $(b_{ads})_{ij}$, one obtains:

$$(b_{ads})_{ij}=\left(\frac{b_i\left(1+\Lambda_{b,i}\right)+b_j\left(1+\Lambda_{b,j}\right)}{2}\right) \quad (5\text{-}8)$$

The fluid-solid potentials, $\Psi^{fs}{}_i(z)$ and $\Psi^{fs}{}_i(L\text{-}z)$, are functions of slit length and position. Similar to the pure-gas adsorption, Lee's partially-integrated 10-4 Lennard-

Jones is applied for the fluid-solid interactions for each component [22, 23]. The integrated 10-4 potential function is expressed as follows:

$$\Psi^{fs}{}_{i}(z) = 4\pi\rho_{atoms}\left(\varepsilon_{fs}\right)_i\left(\sigma_{fs}^2\right)_i\left(\frac{\left(\sigma_{fs}^{10}\right)_i}{5(z')^{10}} - \frac{1}{2}\sum_{i=1}^{4}\frac{\sigma_{fs,i}^4}{\left(z'+(i-1)\cdot\sigma_{ss}\right)^4}\right) \tag{5-9}$$

$$\left(\varepsilon_{fs}\right)_i = \sqrt{\varepsilon_{ff,i}\times\varepsilon_{ss}} \tag{5-10}$$

Here, $(\varepsilon_{fs})_i$ is the fluid-solid interaction energy parameter of component "i", which is the geometric mean of fluid-fluid and solid-solid interaction parameter, as shown in Equation (5-10). The ρ_{atoms} is equal to 0.382 atoms/Å^2; the $\sigma_{ff,i}$ and σ_{ss} are the molecular diameter of the adsorbate component "i" and the carbon interplaner distances. The value of carbon interplaner distance is taken to be the value of graphite, 0.335 nm [24], and the values of $\sigma_{ff,i}$ and $\varepsilon_{ff,i}$ are taken from Reid [28] and are listed in Table 2.1. The fluid-solid molecular diameter, $(\sigma_{fs})_i$ and dummy coordinate z' are defined as:

$$\left(\sigma_{fs}\right)_i = \frac{\sigma_{ff,i}+\sigma_{ss}}{2} \tag{5-11}$$

$$z' = z + \frac{\sigma_{ss}}{2} \tag{5-12}$$

Calculation Procedure

For mixture adsorption calculation, the temperature, pressure, feed (overall) mole fractions and void volume are needed to provide the experimental component excess adsorption and the bulk mole fractions for each component.

Similar to pure-gas adsorption, half of the slit width is subdivided into 50 intervals. Then the local density and adsorbed mole fractions in each interval are determined by solving the equilibrium criterion equations (Equations (5-2)), subject to

the mole fraction constraint, $\sum_i x_i = 1$. To complete this step, the adsorbed-phase densities are obtained from the solution of Equation (5-9). The adsorbed mole fractions are initialized as the feed mole fractions while the bulk mole fractions are the experimental bulk mole fractions. The Newton-Raphson method with numerical derivatives is used to solve the equilibrium criterion by changing the density and adsorbed mole fractions.

Once the adsorbed-phase density and mole fractions are obtained, trial excess adsorption of each component is calculated by solving Equation (5-1) using Simpson's rule for numerical integration. From the calculated excess adsorption, the component mass balances, expressed as follows, are then evaluated:

$$z_i = \frac{n_i^{Ex} + \rho_{bulk} V_{void} y_i}{n_{tot}^{Ex} + \rho_{bulk} V_{void}} \qquad i = 1, NC \qquad (5\text{-}13)$$

The bulk mole fractions are initialized as the experimental bulk mole fractions. The bulk mole fractions are key to this mixture calculation because they are used to calculate the component bulk fugacities which are applied in the equilibrium criterion. The Newton-Raphson method is also used to solve component mass balance (Equation (5-13)). When the component mass balances are not satisfied, a new set of bulk mole fractions are used to calculate the next trial excess adsorption. This procedure is repeated until the component mass balance (Equation (5-13)) and the equilibrium criterion (Equation (5-2)) are satisfied. The details of the calculation procedure are discussed in Appendix A.1.

To represent precisely the mixture adsorption, binary interaction parameters are regressed. In this study, three BIPs are used since there are three binary pairs (methane/nitrogen, methane/CO_2 and nitrogen/CO_2).

Statistical Quantities Used in Data Reduction

The weighted root-mean square (WRMS) error objective function is used in the parameters regressions:

$$WRMS = \frac{\sqrt{\sum_{i=1}^{NPTS} \left(\frac{n_{calc} - n_{exp}}{\sigma_{exp}} \right)_i^2}}{NPTS} \tag{5-14}$$

Here, NPTS is the number of data points, n_{exp} is the experimental excess adsorption, n_{calc} is the calculated excess adsorption, and σ_{exp} is the expected experimental uncertainty. In addition, the weighted average absolute deviation (WAAD) is calculated to access the quality of the model predictions. The WAAD is defined as:

$$WAAD = \frac{\sum_{i=1}^{NPTS} abs\left(\frac{n_{calc} - n_{exp}}{\sigma_{exp}} \right)}{NPTS} \tag{5-15}$$

Database Employed in this Study

Mixture adsorption experiments were conducted at Oklahoma State University involving methane, nitrogen and CO_2 on three wet OSU coals. Specifically, they are:

a) Three binary adsorption isotherms at 319.3 K (115°F), each with four different feed compositions, were measured on wet Illinois #6 and Fruitland

OSU #1 coals. These measurements were conducted at pressures to 12.4 MPa (1800 psia).

b) Three single-composition binary adsorption isotherms and a ternary isotherm (all at 328.15K (130°F)) were measured on wet Tiffany coal. These measurements were conducted at pressures to 12.4 MPa (1800 psia).

Table 5.1 presents the mixed-gas CBM adsorption database used in this study. In the table, the following information is included: OSU system number, adsorbent, adsorbate, number of data points (NTPS), temperature, and pressure range. The compositional analyses of these coals are discussed in Chapter 3.

Table 5.1 - Mixed-Gas Adsorption Database Used in this Study

System No.	Adsorbent	Adsorbates	NPTS	Temp (K)	Pressure Range (MPa)
31	Wet Illinois #6	$N_2 + CH_4$	40	319	0.7 – 12.4
32	Wet Illinois #6	$CH_4 + CO_2$	40	319	0.7 – 12.4
33	Wet Illinois #6	$N_2 + CO_2$	40	319	0.7 – 12.4
34	Wet Fruitland OSU #1	$N_2 + CH_4$	41	319	0.7 – 12.4
35	Wet Fruitland OSU #1	$CH_4 + CO_2$	40	319	0.7 – 12.4
36	Wet Fruitland OSU #1	$N_2 + CO_2$	40	319	0.7 – 12.4
37	Wet Tiffany	$N_2 + CH_4$	11	328	0.7 – 13.7
38	Wet Tiffany	$CH_4 + CO_2$	11	328	0.7 – 13.7
39	Wet Tiffany	$N_2 + CO_2$	11	328	0.7 – 13.7
40	Wet Tiffany	$N_2 + CH_4 + CO_2$	11	328	0.7 – 13.7

Note: The system number is continued from the pure-gas adsorption database

The SLD-PR Generalized Model Parameters

The ultimate goal of this study was to develop generalized correlations for the modified SLD-PR model parameters capable of providing reliable predictions for the equilibrium adsorption of methane, nitrogen, CO_2 and their mixtures on dry and wet coals

in the range of conditions encountered in CBM production and CO_2 sequestration. In Chapter 4, the SLD-PR model parameters were generalized in terms of accessible coal characterizations and fluid properties. The pure-gas adsorption isotherms of methane, nitrogen and CO_2 on both dry and wet coals were employed in developing the model parameter generalizations. Three cases of pure-fluid generalized parameter correlations were developed. Specifically, in addition to the solid-solid interaction energy parameter, the surface areas of each adsorbate were correlated in terms of methane, nitrogen or CO_2 excess adsorption at 400 psia. In general, the parameter generalizations proved capable of predicting the pure-gas adsorption within the experimental uncertainties.

In this chapter, the pure-fluid model generalizations are extended to binary and ternary mixture adsorption on wet coals. Three additional case studies were conducted to examine the representations and generalized predictions of the SLD-PR model. Two approaches are completed for each case in studying the mixed-gas adsorption:

Case 4 – Mixture adsorption predictions were performed using the pure-fluid *generalized parameters* and the selected mixing rules. This case provides *a priori* mixture predictions based solely on information obtained from pure-fluid adsorption data.

Case 5 – Mixture adsorption representations were obtained using the pure-fluid generalized parameters and regressed binary interaction parameters. This case assesses the quality of the mixture representations upon regression of the binary adsorption data.

Case 6 – Mixture adsorption predictions were performed using the pure-fluid *generalized parameters* and the *generalized binary interaction*

parameters. This case evaluates the generalized mixture predictions of the model.

In all cases, the mixture data considered were analyzed simultaneously. In Case 5, the BIPs were first regressed for the mixture adsorption on each coal using the generalized pure-fluid parameters. Then, in Case 6, the regressed BIPs were correlated in terms of the coal and adsorbate characteristics. The procedure used to obtain the generalized correlations for the BIPs follows that used in Chapter 4 for pure-gas model generalization.

Results and Discussion

In this study, the SLD-PR generalized parameters using methane, nitrogen and CO_2 correlations (Cases 1, 2 and 3, respectively) were tested for their ability to predict mixture adsorption. In Chapter 4, it was concluded that the pure-gas adsorption on dry Argonne coals and wet OSU coals were predicted more precisely using the methane-based correlations. Hence, the results of mixture adsorption from the methane correlations are discussed here, while the nitrogen- and CO_2-based correlations are presented in Appendix C.3 and C.4, respectively.

For Case 5 and 6, the generalized BIPs were comparable in value to the regressed ones; thus, both the cases are presented and discussed together. Finally, a comparison of the SLD-PR modeling predictions using the three pure-fluid generalizations is also given.

The weighted average absolute deviations (WAAD) of the pure and mixed-gas adsorption on wet coals are presented and the order of the presentation of the results is as follows: wet Illinois #6 coal, wet Fruitland OSU #1 coal and wet Tiffany coal. The

generalized predictions of all components adsorption in the mixed-gas isotherms are also plotted; a total of sixteen figures are presented. The first six figures are for the binary adsorption on the wet Illinois #6 coal; while the next six figures are for the binary adsorption on the wet Fruitland OSU #1 coal. Then, the last four figures present the binary and a ternary adsorption on the wet Tiffany coal. For the binary adsorption isotherms, component adsorption in the methane/nitrogen mixtures are first presented, followed by that in the methane/CO_2 mixtures and the nitrogen/CO_2 mixtures.

Case 4: Mixture Adsorption Prediction Using Pure-Fluid Methane-Based Generalized Parameters

Tables 5.2 through 5.4 (under "C_{ij} = 0.0") present the summary results for the SLD-PR generalized predictions for the pure-gas and mixture adsorption using the parameter generalization of Case 1, which are based on the methane calibration point. The generalized predictions (solid line) are shown Figures 5.1 through 5.16.

As documented in Tables 5.2 and 5.3, mixture adsorption on the wet Illinois #6 and Fruitland OSU #1 coals are predicted by the SLD-PR model within the experimental uncertainties, except for the methane adsorption in the methane/CO_2 mixture on Fruitland OSU #1 coal. An average WAAD of 1.27 is observed for the component adsorption isotherm of this binary mixture. Figure 5.9 depicts the methane adsorption of the methane/CO_2 mixture on Fruitland OSU #1 coal. The model under predicted the adsorption isotherms for all four compositions. This may be contributed to the low estimates of the methane surface area obtained for this Fruitland OSU #1 coal using methane-based generalization of Case 1.

Table 5.2 – Case 1: Summary Results for SLD-PR Modeling of Pure and Binary Mixture Adsorption on Wet Illinois #6 Coal at 115°F

	Weighted Average Absolute Deviation, WAAD			
Pure Gases				
Methane	0.91			
Nitrogen	0.31			
CO_2	1.32			
Feed Mixture	$C_{ij} = 0.0$		*Generalized* C_{ij}	
Methane/Nitrogen	*Methane*	*Nitrogen*	*Methane*	*Nitrogen*
20/80	0.27	0.59	0.23	0.47
40/60	0.37	0.71	0.41	0.22
60/40	0.31	0.63	0.31	0.26
80/20	0.24	0.41	0.23	0.44
All Feed	0.30	0.59	0.29	0.35
Methane/CO_2	*Methane*	*CO_2*	*Methane*	*CO_2*
20/80	0.21	0.76	0.23	0.75
40/60	0.55	0.69	0.57	0.67
60/40	0.96	1.16	0.92	1.15
80/20	0.63	0.59	0.62	0.61
All Feed	0.59	0.80	0.58	0.80
Nitrogen/CO_2	*Nitrogen*	*CO_2*	*Nitrogen*	*CO_2*
20/80	0.60	1.32	0.55	1.27
40/60	0.82	0.97	0.78	0.90
60/40	0.91	0.30	0.97	0.30
80/20	1.01	0.50	0.90	0.51
All Feed	0.83	0.77	0.80	0.75

Table 5.3 – Case 1: Summary Results for SLD-PR Modeling of Pure and Binary Mixture Adsorption on Wet Fruitland OSU #1 Coal at 115°F

	Weighted Average Absolute Deviation, WAAD			
Pure Gases				
Methane	1.74			
Nitrogen	1.74			
CO_2	1.25			
Feed Mixture	*C_{ij} = 0.0*		*Generalized C_{ij}*	
Methane/Nitrogen	*Methane*	*Nitrogen*	*Methane*	*Nitrogen*
20/80	1.05	0.62	0.86	0.73
40/60	0.84	0.74	0.81	1.16
60/40	0.65	0.82	0.70	0.18
80/20	0.50	0.87	0.55	0.32
All Feed	0.76	0.76	0.73	0.60
Methane/CO_2	*Methane*	*CO_2*	*Methane*	*CO_2*
20/80	1.14	0.90	0.38	1.00
40/60	1.33	0.44	0.64	0.47
60/40	1.16	0.34	0.66	0.34
80/20	1.45	0.31	1.37	0.54
All Feed	1.27	0.50	0.76	0.59
Nitrogen/CO_2	*Nitrogen*	*CO_2*	*Nitrogen*	*CO_2*
20/80	0.42	0.46	0.42	0.46
40/60	0.38	0.34	0.36	0.34
60/40	0.36	0.41	0.35	0.41
80/20	0.41	0.32	0.39	0.32
All Feed	0.39	0.38	0.38	0.38

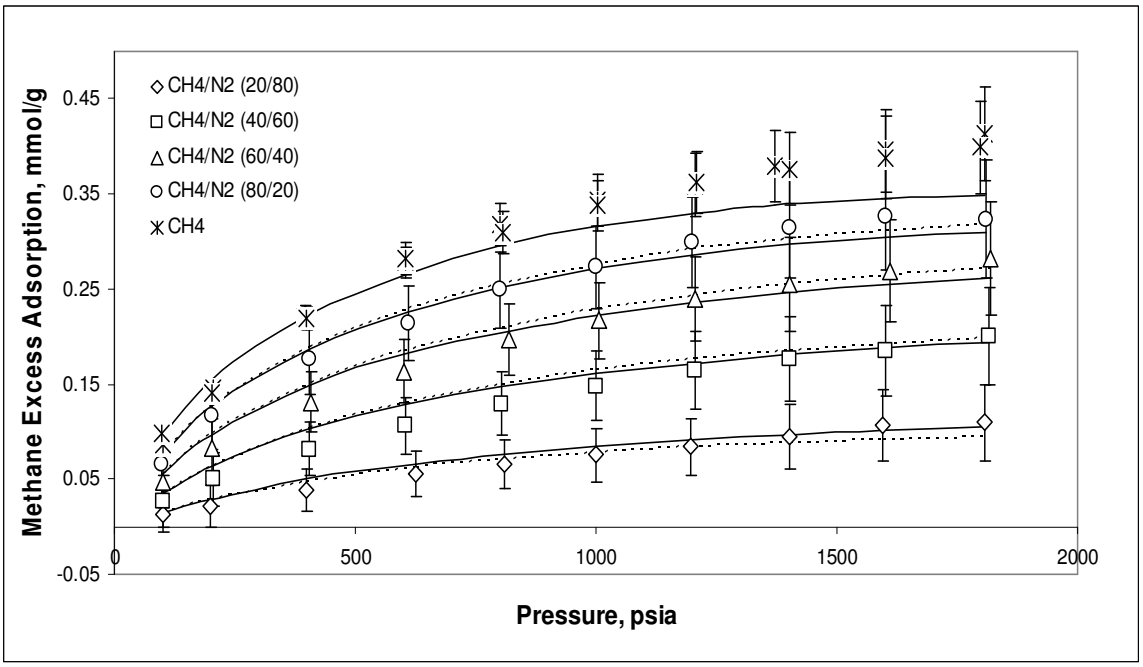

Figure 5.1 – Case 1
Methane Adsorption in Methane/Nitrogen Mixtures on Wet Illinois #6 Coal at 115°F (Solid Line – C_{ij} = 0.0, Dashed Line – Generalized C_{ij})

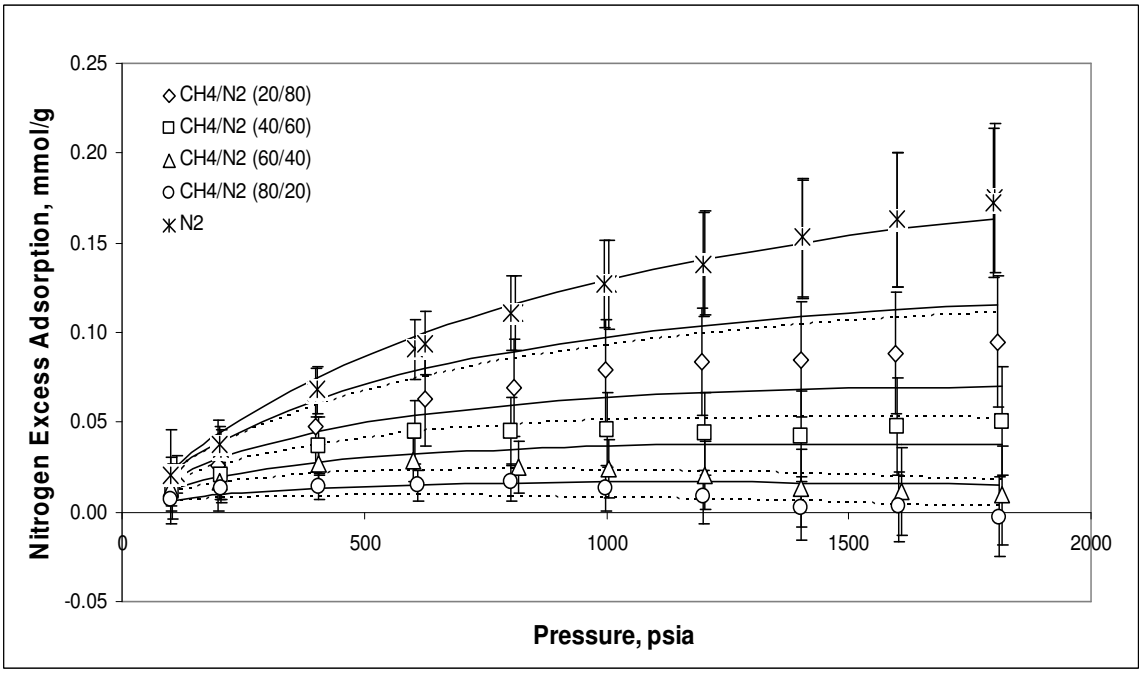

Figure 5.2 – Case 1
Nitrogen Adsorption in Methane/Nitrogen Mixtures on Wet Illinois #6 Coal at 115°F (Solid Line – C_{ij} = 0.0, Dashed Line – Generalized C_{ij})

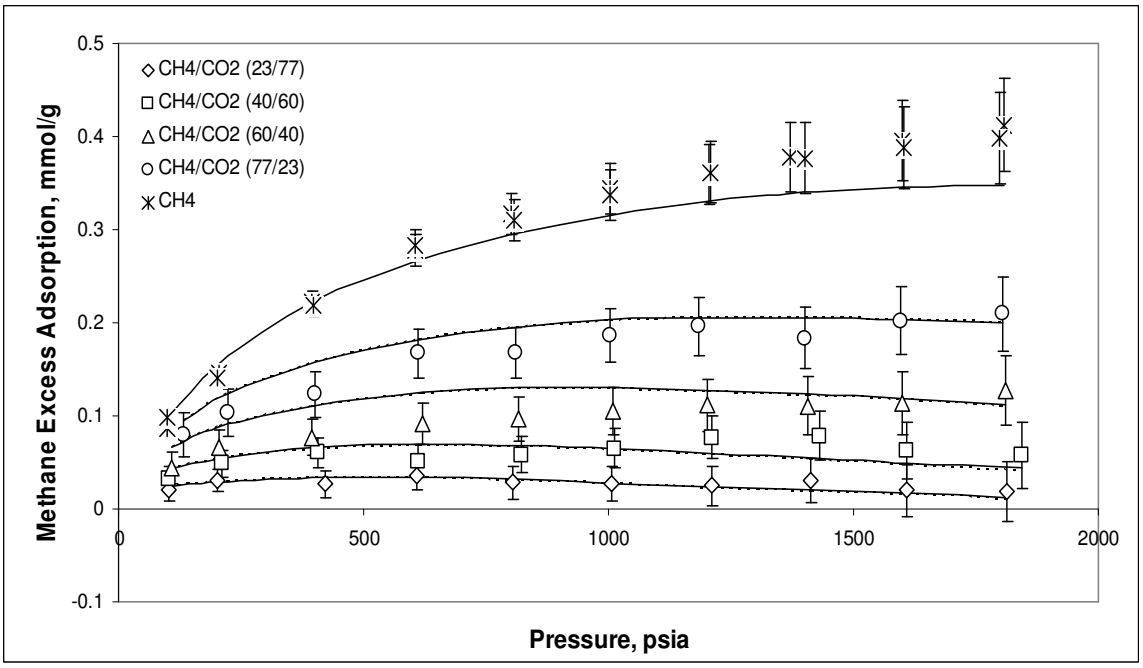

Figure 5.3 – Case 1
Methane Adsorption in Methane/CO_2 Mixtures on Wet Illinois #6 Coal at 115°F
(Solid Line – C_{ij} = 0.0, Dashed Line – Generalized C_{ij})

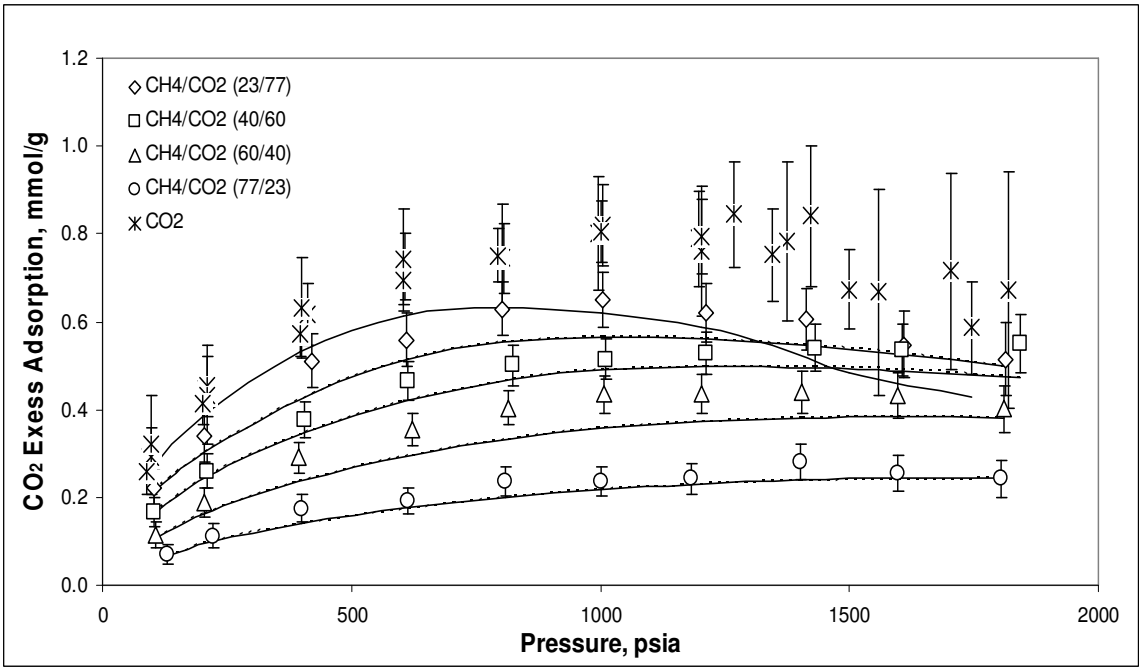

Figure 5.4 – Case 1
CO_2 Adsorption in Methane/CO_2 Mixtures on Wet Illinois #6 Coal at 115°F
(Solid Line – C_{ij} = 0.0, Dashed Line – Generalized C_{ij})

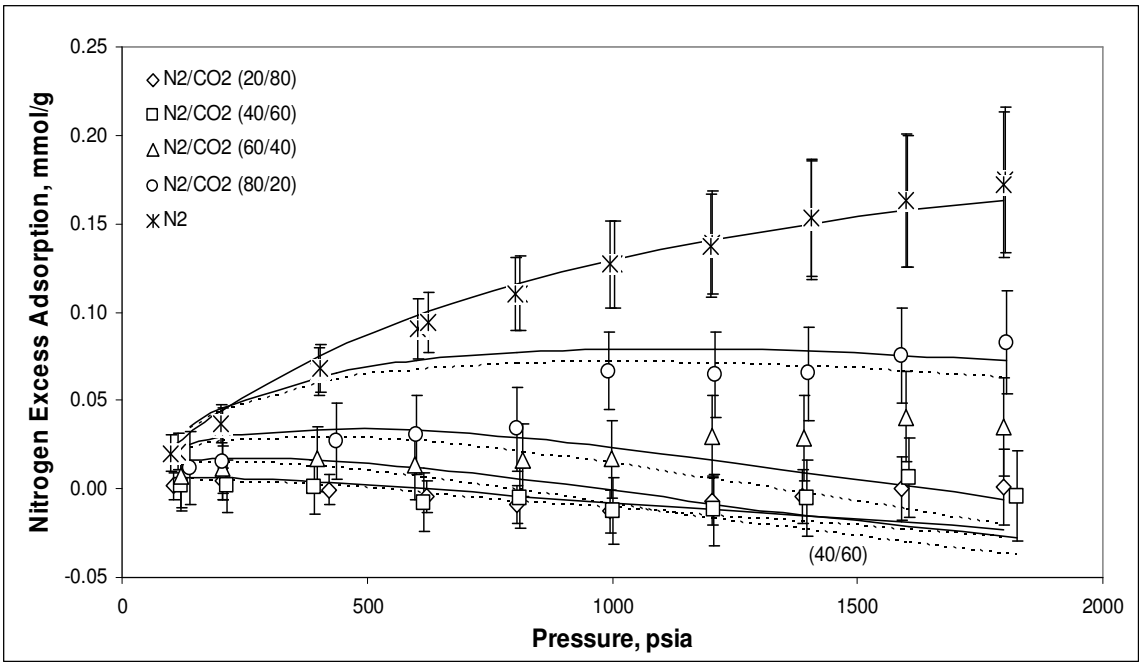

Figure 5.5 – Case 1
Nitrogen Adsorption in Nitrogen/CO_2 Mixtures on Wet Illinois #6 Coal at 115°F
(Solid Line – C_{ij} = 0.0, Dashed Line – Generalized C_{ij})

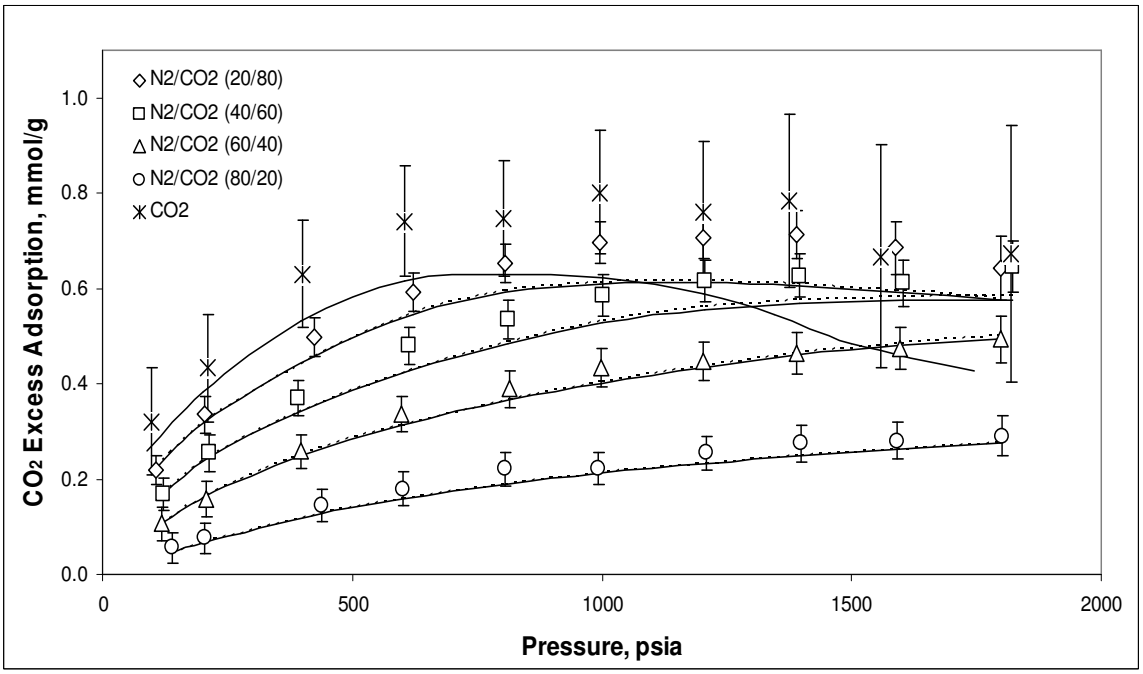

Figure 5.6 – Case 1
CO_2 Adsorption in Nitrogen/CO_2 Mixtures on Wet Illinois #6 Coal at 115°F
(Solid Line – C_{ij} = 0.0, Dashed Line – Generalized C_{ij})

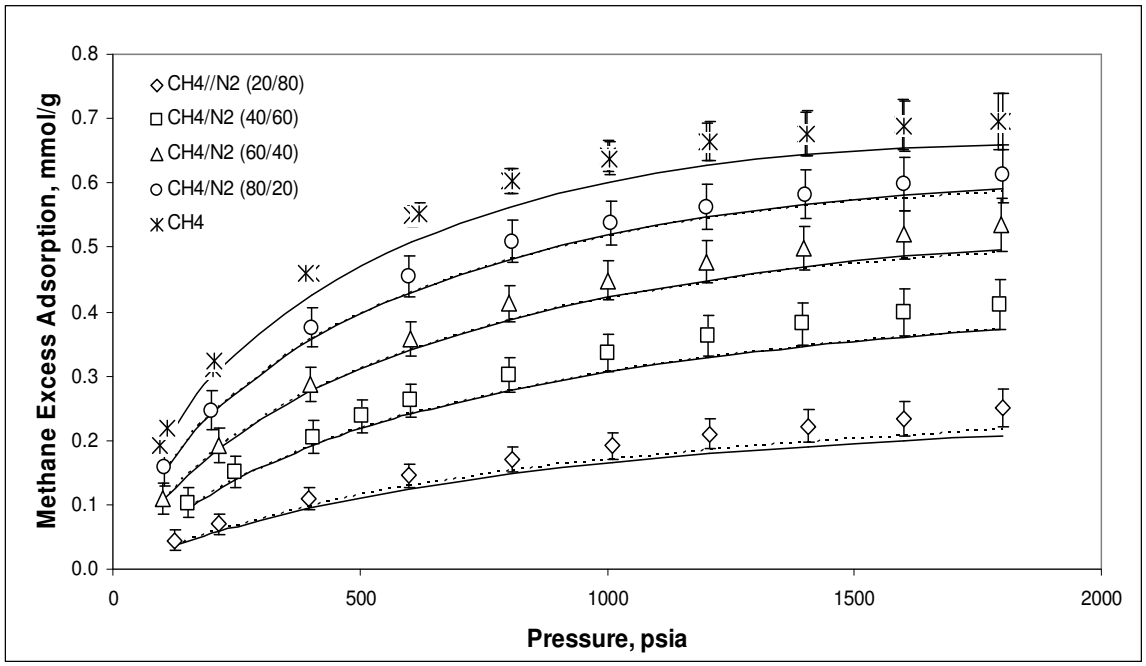

Figure 5.7 – Case 1
Methane Adsorption in Methane/Nitrogen Mixtures on Wet Fruitland OSU #1 Coal at 115°F (Solid Line – C_{ij} = 0.0, Dashed Line – Generalized C_{ij})

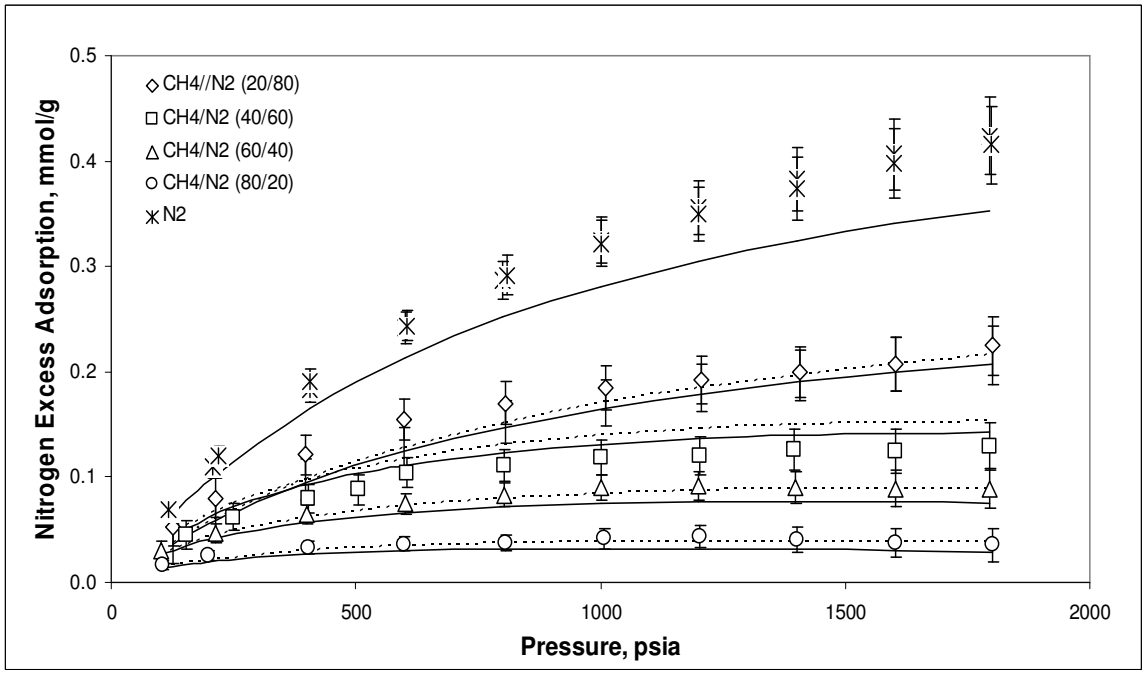

Figure 5.8 – Case 1
Nitrogen Adsorption in Methane/Nitrogen Mixtures on Wet Fruitland OSU #1 Coal at 115°F (Solid Line – C_{ij} = 0.0, Dashed Line – Generalized C_{ij})

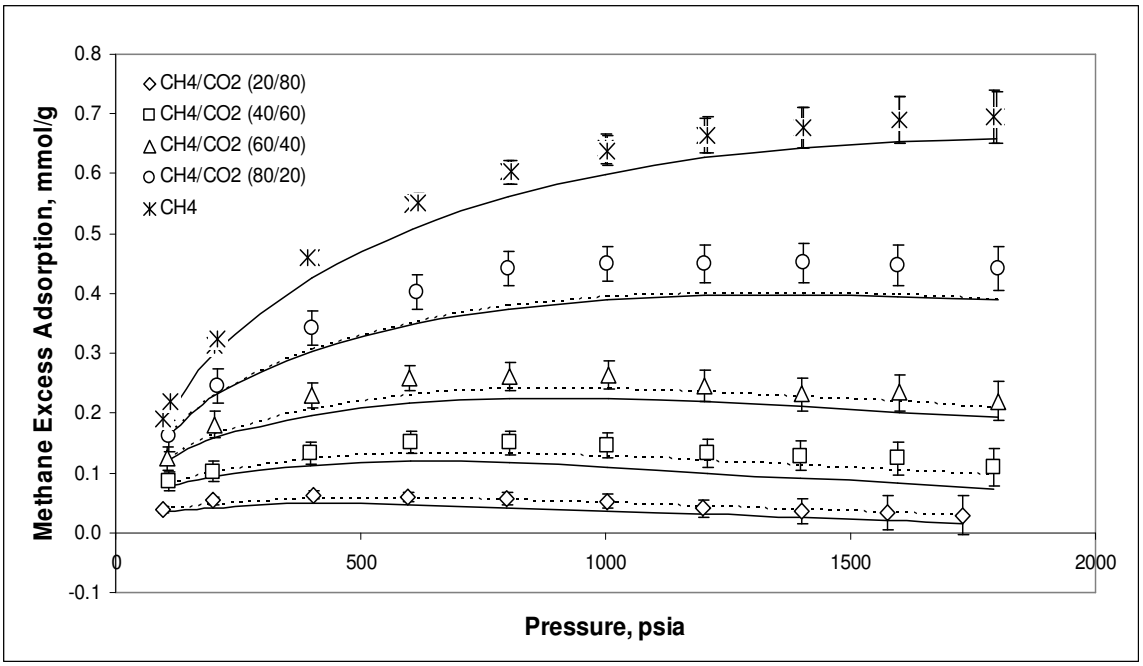

Figure 5.9 – Case 1
Methane Adsorption in Methane/CO_2 Mixtures on Wet Fruitland OSU #1 Coal at 115°F (Solid Line – C_{ij} = 0.0, Dashed Line – Generalized C_{ij})

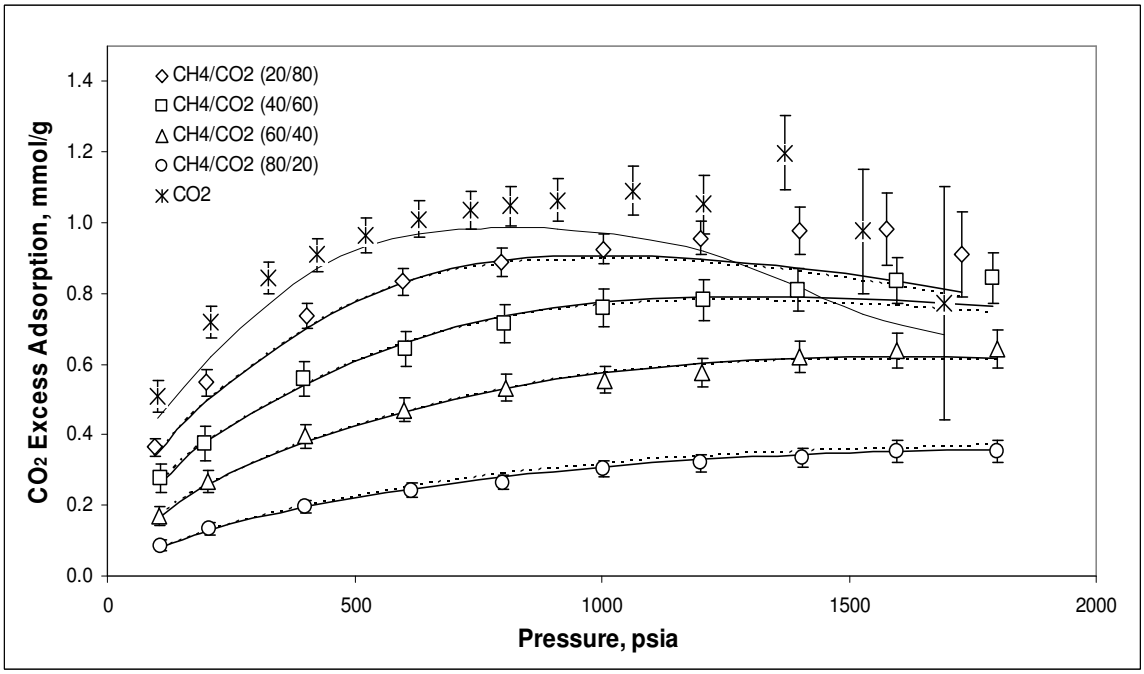

Figure 5.10 – Case 1
CO_2 Adsorption in Methane/CO_2 Mixtures on Wet Fruitland OSU #1 Coal at 115°F (Solid Line – C_{ij} = 0.0, Dashed Line – Generalized C_{ij})

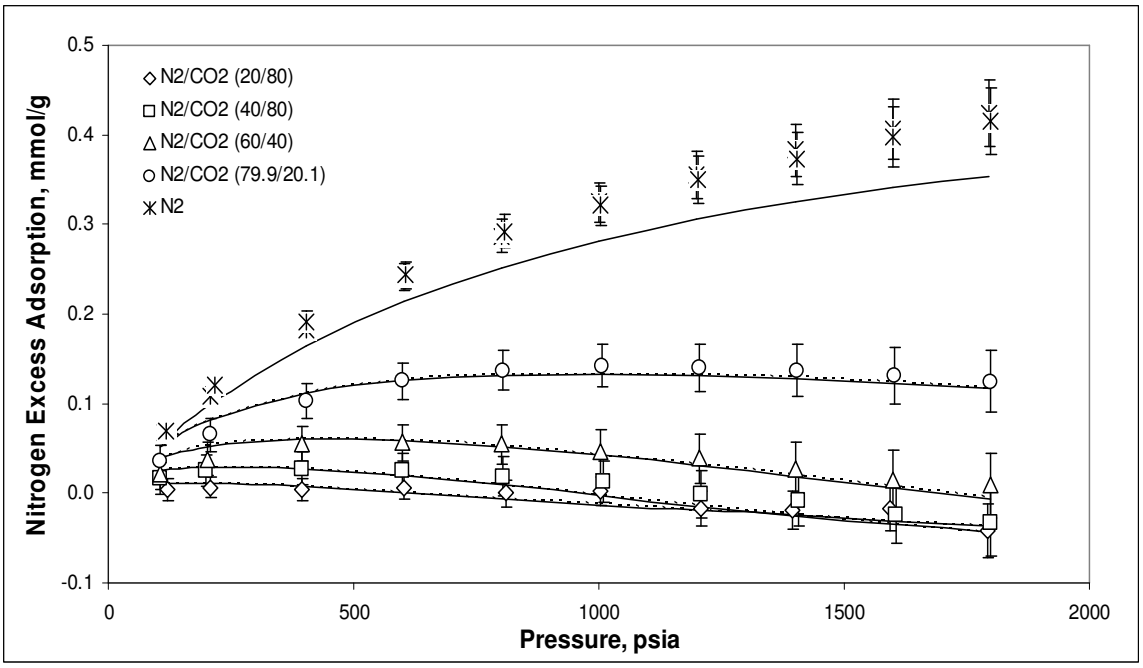

Figure 5.11 – Case 1
Nitrogen Adsorption in Nitrogen/CO_2 Mixtures on Wet Fruitland OSU #1 Coal at 115°F (Solid Line – C_{ij} = 0.0, Dashed Line – Generalized C_{ij})

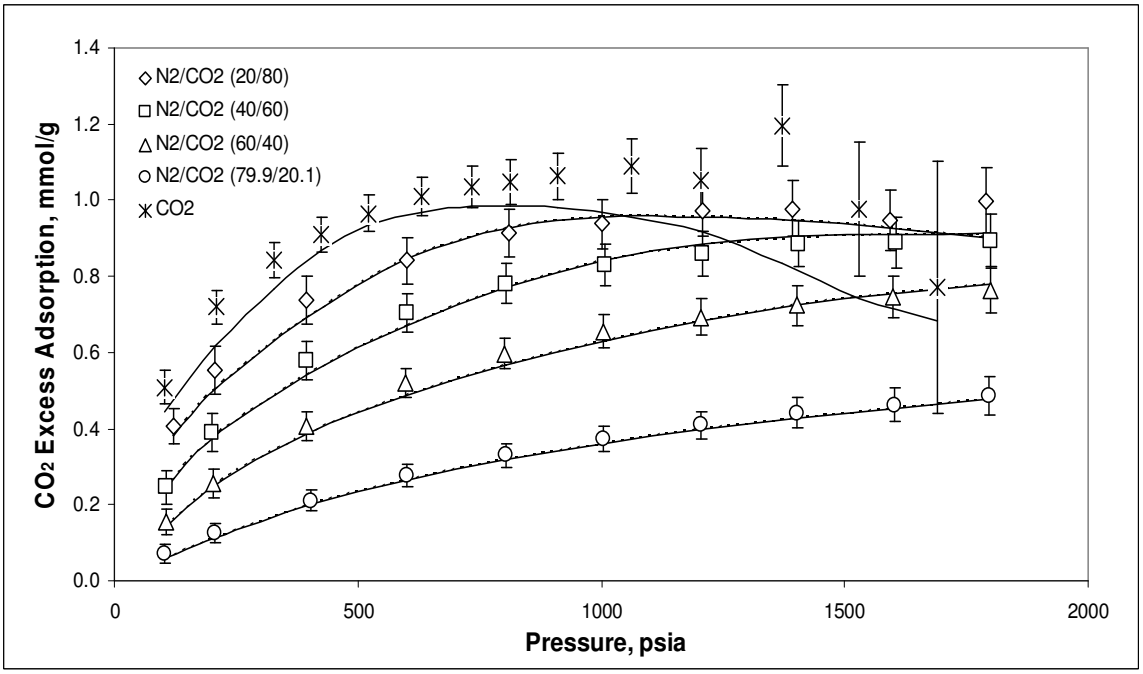

Figure 5.12 – Case 1
CO_2 Adsorption in Nitrogen/CO_2 Mixtures on Wet Fruitland OSU #1 Coal at 115°F (Solid Line – C_{ij} = 0.0, Dashed Line – Generalized C_{ij})

Table 5.4 – Case 1: Summary Results for SLD-PR Modeling of Pure and Mixture Adsorption on Wet Tiffany Coal at 130°F

	Weighted Average Absolute Deviation, WAAD					
Pure Gases						
Methane	0.72					
Nitrogen	0.66					
CO_2	0.52					
Feed Mixture	$C_{ij} = 0.0$			*Generalized* C_{ij}		
Methane/Nitrogen	*Methane*	*Nitrogen*		*Methane*	*Nitrogen*	
50/50	2.17	1.86		1.90	0.53	
Methane/CO_2	*Methane*	*CO_2*		*Methane*	*CO_2*	
41/59	4.09	1.63		0.84	0.80	
Nitrogen/CO_2	*Nitrogen*	*CO_2*		*Nitrogen*	*CO_2*	
20/80	1.80	0.96		0.57	0.64	
Methane/Nitrogen /CO_2	*Methane*	*Nitrogen*	*CO_2*	*Methane*	*Nitrogen*	*CO_2*
10/40/50	0.64	2.65	1.39	0.32	0.92	0.95

In contrast, the mixture adsorption on wet Tiffany is not well predicted, as shown in Table 5.4. The largest WAAD (4.09) is observed for the methane adsorption from the methane/CO_2 mixture. Also, the methane adsorption of both the methane/nitrogen and methane/CO_2 mixtures (Figure 5.13 and 5.14), and the nitrogen adsorption of the ternary mixtures (Figure 5.16) are predicted with more than twice the experimental uncertainties. The balance of the component adsorption isotherms are predicted within twice the experimental uncertainties.

Based on the above results, in general, the SLD-PR generalized parameters of Case 1 are effective in predicting the mixture adsorption on the wet coals considered. In fact, these results are quite adequate in light of the fact that the data reduction procedures

used to determine the experimental amount adsorbed do not account accurately for the moisture distribution between the gas phase and the adsorbed phase. Specifically, in the current data reductions, the amount of a gas adsorbed is adjusted to account for the gas soluble in the adsorbed water, which is taken to be the full amount of water injected.

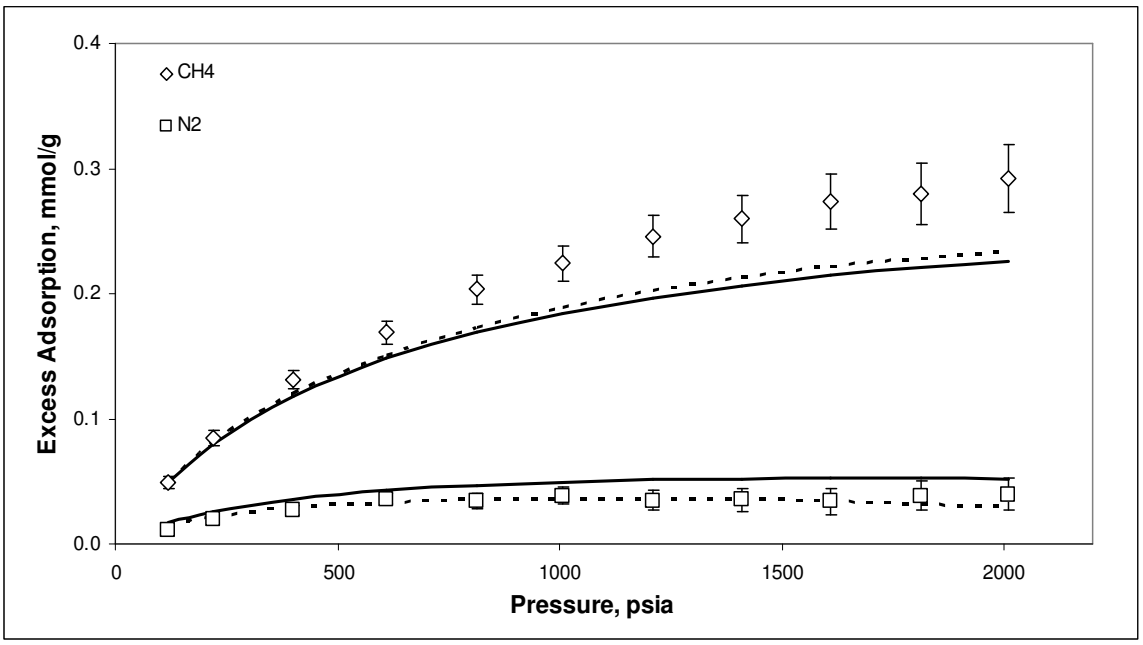

Figure 5.13 – Case 1
Methane/Nitrogen 50/50 Feed Gas Adsorption on Wet Tiffany Coal at 130°F
(Solid Line – C_{ij} = 0.0, Dashed Line – Generalized C_{ij})

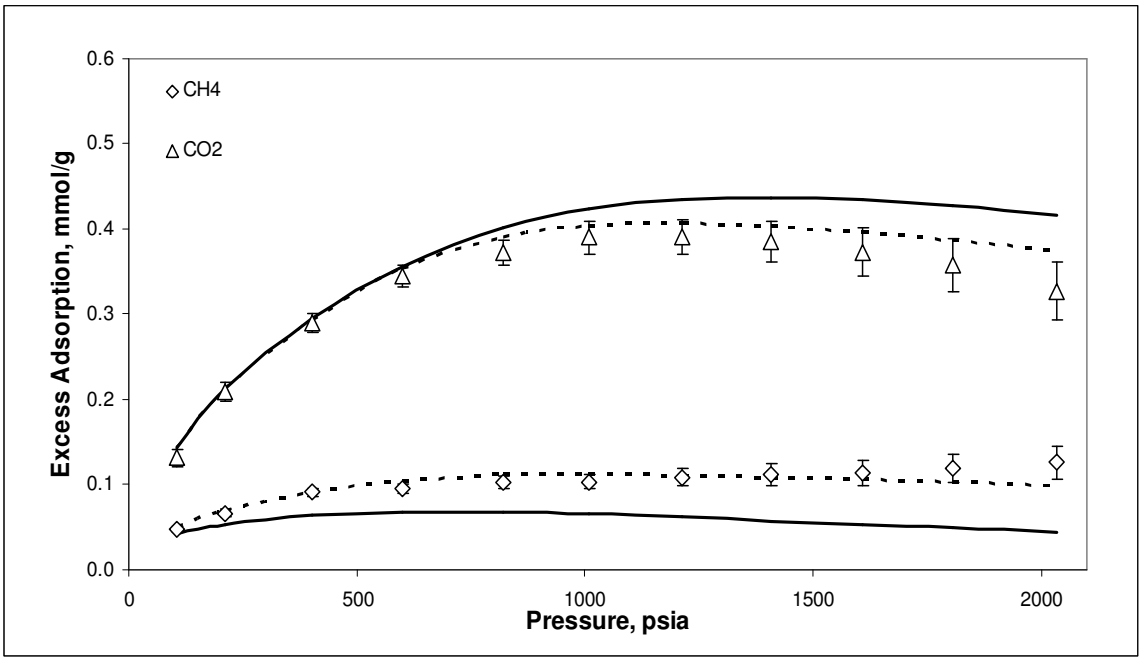

Figure 5.14 – Case 1
Methane/CO_2 41/59 Feed Gas Adsorption on Wet Tiffany Coal at 130°F
(Solid Line – C_{ij} = 0.0, Dashed Line – Generalized C_{ij})

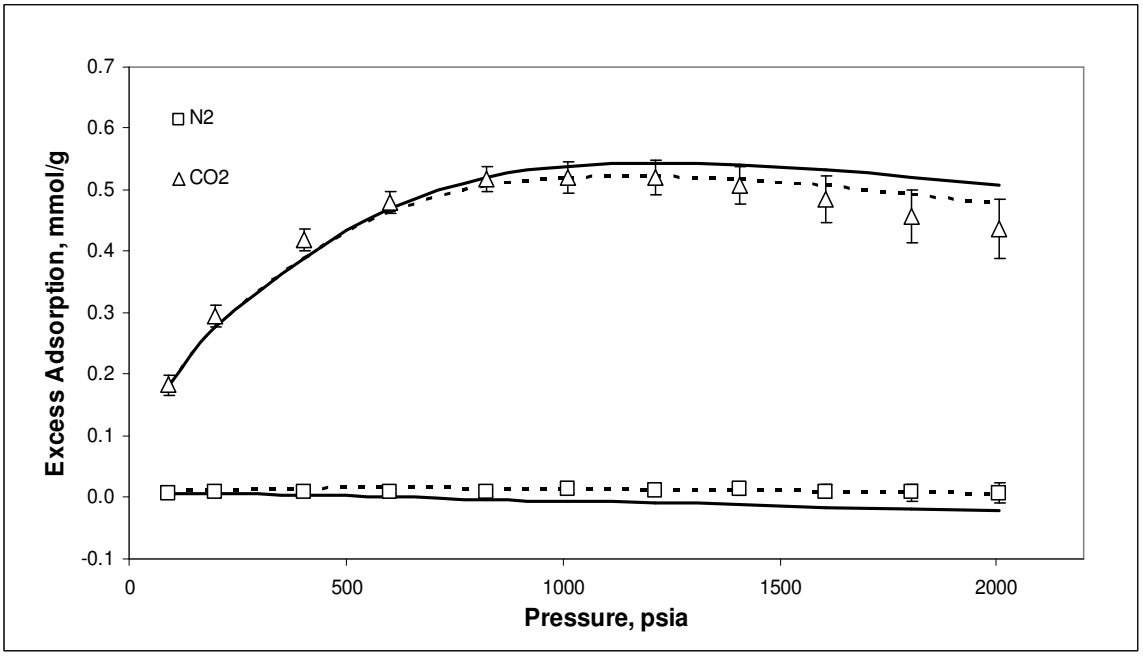

Figure 5.15 – Case 1
Nitrogen/CO_2 20/80 Feed Gas Adsorption on Wet Tiffany Coal at 130°F
(Solid Line – C_{ij} = 0.0, Dashed Line – Generalized C_{ij})

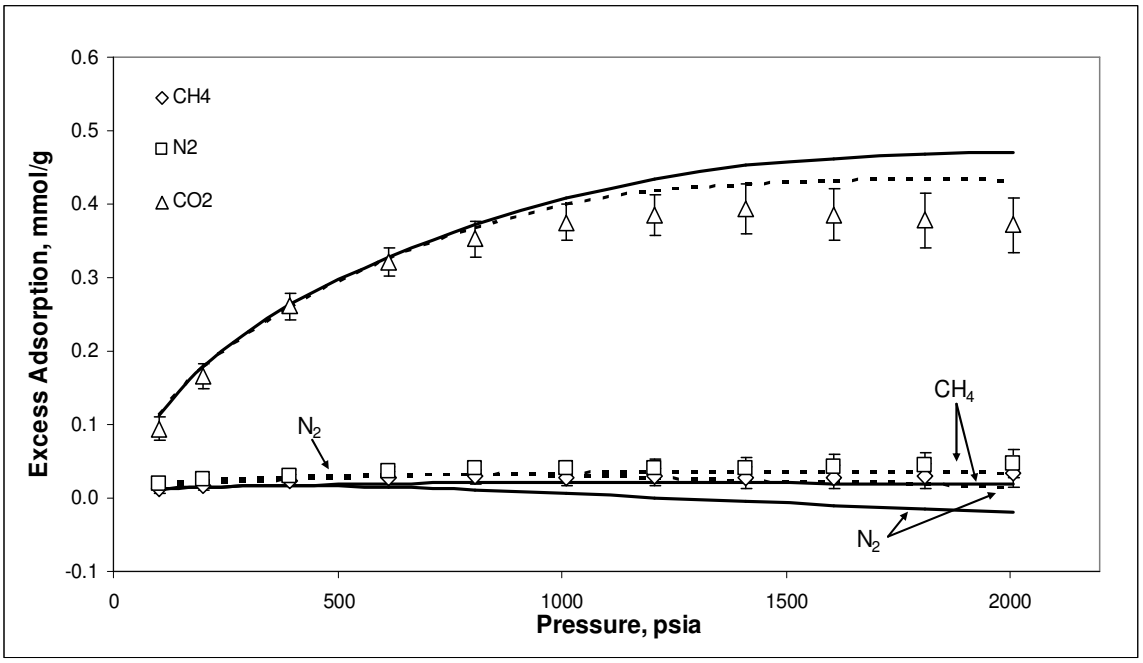

Figure 5.16 – Case 1
Methane/Nitrogen/CO_2 10/40/50 Feed Gas Adsorption on Wet Tiffany Coal at 130°F
(Solid Line – C_{ij} = 0.0, Dashed Line – Generalized C_{ij})

Cases 5 and 6: Mixture Adsorption Prediction Using Pure-Fluid Methane-Based Generalized Parameters and BIPs

Using the pure-fluid generalized parameters of Case 1, the BIPs were regressed for each coal. Tables 5.6 to 5.8 list the regressed BIPs (under "Regressed C_{ij}") and the pure-fluid generalized parameter for wet Illinois #6, Fruitland OSU #1 and Tiffany coal, respectively. As shown, for wet Illinois #6 and Tiffany coal, the BIPs for methane/nitrogen and nitrogen/CO_2 are greater than that for methane/CO_2. Further, the BIPs for the Fruitland OSU #1 coal are lower in value than those of the other two coals.

Table 5.5 presents the generalized equations for the BIPs. A study of trends generated by the BIPs with the adsorbent characteristic revealed that the methane/nitrogen BIP is inversely proportional to methane excess adsorption at 400 psia. The BIPs for methane/CO_2 and nitrogen/CO_2 are both proportional to the ratio of the

square of carbon to the solid-solid interaction energy since they have the same ascending order. The generalized BIPs are presented in Tables 5.6-5.8. As shown in the Tables 5.6-5.8 and in Figure 5.17, the generalized and regressed BIPs are comparable for all the coals considered.

Table 5.5 –- Generalized Correlations of the EOS BIPs Using Methane Excess Adsorption at 400 psia (Case 1)

$$C_{CH4-N2} = \frac{0.303}{n^{Ex}_{CH4@400}} - 0.844$$

$$C_{CH4-CO2} = 30.724 \left(\frac{\chi_C^2}{\varepsilon_{ss}/k} \right) - 0.665$$

$$C_{N2-CO2} = 84.693 \left(\frac{\chi_C^2}{\varepsilon_{ss}/k} \right) - 1.659$$

Table 5.6 – Case 1: Regressed and Generalized EOS BIPs for CBM Gas Adsorption on Wet Illinois #6 Coal

	CH_4	**N_2**	**CO_2**
Surface Area, m^2/g	30.3	19.3	40.7
ε_{ss}/k, K	23.2		
Λ_b	-0.20		
Slit Length, nm	1.15		
	Regressed C_{ij}	**Generalized C_{ij}**	
Methane-Nitrogen	0.50	0.51	
Methane-CO_2	0.09	0.01	
Nitrogen-CO_2	0.22	0.21	

Table 5.7 – Case 1: Regressed and Generalized EOS BIPs for CBM Gas Adsorption on Wet Fruitland OSU #1 Coal

	CH_4	**N_2**	**CO_2**
Surface Area, m^2/g	56.5	41.0	63.1
ε_{ss}/k, K	24.2		
Λ_b	-0.20		
Slit Length, nm	1.15		
	Regressed C_{ij}	**Generalized C_{ij}**	
Methane-Nitrogen	-0.19	-0.19	
Methane-CO_2	-0.09	-0.07	
Nitrogen-CO_2	-0.08	-0.01	

Table 5.8 – Case 1: Regressed and Generalized EOS BIPs for CBM Gas Adsorption on Wet Tiffany Coal

	CH_4	**N_2**	**CO_2**
Surface Area, m^2/g	29.4	18.6	36.4
ε_{ss}/k, K	25.4		
Λ_b	-0.20		
Slit Length, nm	1.15		
	Regressed C_{ij}	**Generalized C_{ij}**	
Methane-Nitrogen	0.55	0.56	
Methane-CO_2	-0.31	-0.33	
Nitrogen-CO_2	-0.63	-0.75	

Summary results for the mixture adsorption predictions using the pure-fluid generalized parameters and generalized BIPs are tabulated under "Regressed C_{ij}" in Tables 5.6-5.8. The respective generalized predictions are also depicted in Figures 5.1-5.16.

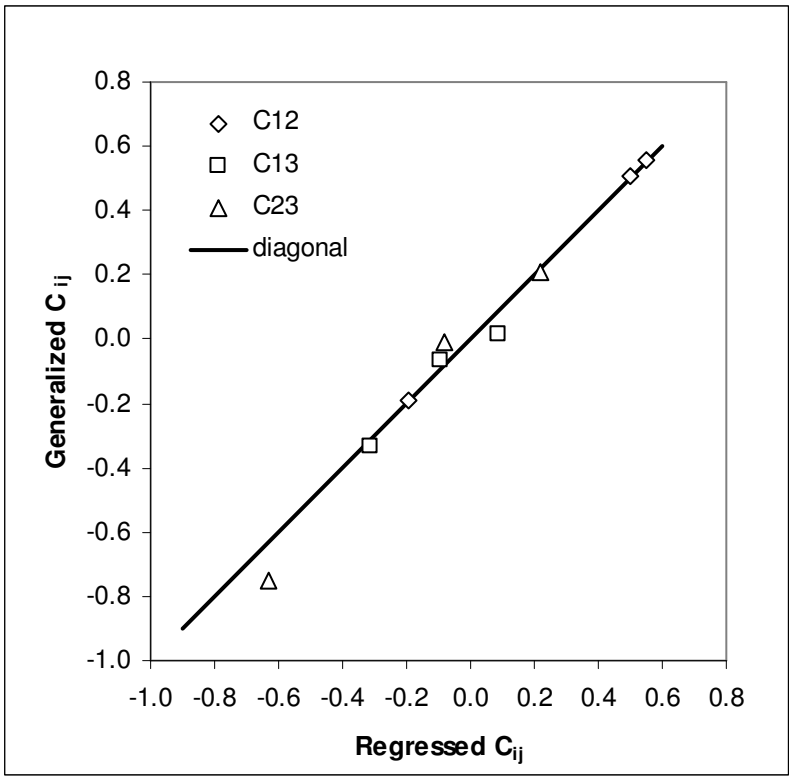

Figure 5.17 – Case 1: Comparison of the Regressed and Generalized SLD-PR Binary Interaction Parameters (1 – Methane, 2 – Nitrogen, 3 – CO_2)

As indicated by Tables 5.2 and 5.3, mixture adsorption on wet Illinois #6 and wet Fruitland OSU #1 coals are predicted within the experimental uncertainties using the generalized BIPs. No significant improvement is obtained beyond Case 4 (C_{ij} = 0.0) since similar results are obtained for the mixture adsorption without BIPs. Hence, the BIPs have a minor effect on these mixtures. Nonetheless, the methane adsorption of the methane/CO_2 mixtures on Fruitland OSU #1 coal are improved significantly when generalized BIPs are employed; specifically, the average WAAD for the component adsorption was reduced from 1.27 to 0.76. Further, among the four compositions, the methane predictions are within experimental uncertainties except for the 80/20 feed composition of the methane/CO_2 mixture.

For wet Tiffany, all the component adsorption on wet Tiffany is predicted within twice of the experimental uncertainties when generalized BIPs are incorporated. As illustrated in Figure 14, the predictions for methane adsorption from the methane/CO_2 mixture is improved significantly; the respective WAAD has reduced from 4.09 to 0.84. Also, the predictions for nitrogen adsorption from the ternary mixture, based on the binary adsorption, are greatly improved from WAAD of 2.65 to 0.92. However, these improvements required large BIPs value that modify the $(a_{ads})_{ij}$ by at least thirty percent. The methane component adsorption on methane/nitrogen mixture (Figure 5.13) did not improved significantly compared to that from the methane/CO_2 mixture.

Overall, the generalized SLD-PR model is capable of providing adsorption mixture predictions within twice the experimental uncertainties. The results obtained for the wet coals suggest that the pure-fluid parameter generalization of Case 1 combined with the one-fluid mixing rules are effective in modeling the adsorption behavior of CBM-type systems. Realistically, further improvement in the SLD-PR predictions may require accounting more accurately for the moisture effects in the raw data reduction procedures. This, in turn, would facilitate future modeling in which water is treated as an adsorbing component with full accounting of its interactions.

Comparison of Generalized Predictions Using Methane, Nitrogen and CO_2 Based Correlations

Tables 5.9 through 5.12 present comparison of the generalized mixture adsorption predictions for the wet Illinois #6, Fruitland OSU #1 and Tiffany coals, respectively, using pure-fluid parameter generalizations based on methane, nitrogen and CO_2 matrix calibrations of Cases 1-3.

As shown in the tables, the SLD-PR generalizations predict the mixture adsorption within three times the experimental uncertainties, on average. Comparable results were obtained from the generalized 2-D EOS model developed by Pan [14, 34].

For wet Illinois #6 and Fruitland OSU #1 coals, the mixture adsorption are predicted well using the methane correlation compared to similar predictions based on nitrogen and CO_2 correlations. For the wet Tiffany, the methane adsorption from the methane/nitrogen and methane/CO_2 mixtures, and the nitrogen adsorption from the ternary mixture are not predicted as well by the three correlations.

Nonetheless, as stated earlier, the SLD-PR model, using the methane pure-fluid parameter generalizations of Case 1 and the generalized BIPs, is capable of predicting the mixture adsorption within twice the experimental uncertainties.

Table 5.9 – Comparison for SLD-PR Modeling of Pure and Mixed-Gas Adsorption on Wet Illinois #6 Coal at 115°F

	Weighted Average Absolute Deviation, WAAD											
Pure Gases	**Case 1**				**Case 2**				**Case 3**			
Methane	0.91				0.91				2.74			
Nitrogen	0.31				0.38				0.26			
CO_2	1.32				1.01				0.62			
Mixture	*C_{ij} = 0.0*		*Generalized C_{ij}*		*C_{ij} = 0.0*		*Generalized C_{ij}*		*C_{ij} = 0.0*		*Generalized C_{ij}*	
Methane/Nitrogen	0.30	0.59	0.29	0.35	0.42	0.63	0.47	0.36	0.96	1.03	0.97	0.69
Methane/CO_2	0.59	0.80	0.58	0.80	1.58	1.31	1.32	1.41	1.30	0.42	1.10	0.50
Nitrogen/CO_2	0.83	0.77	0.80	0.75	1.30	2.14	1.31	2.14	1.02	0.34	1.03	0.34

Table 5.10 – Comparison for SLD-PR Modeling of Pure and Mixed-Gas Adsorption on Wet Fruitland #1 Coal at 115°F

	Weighted Average Absolute Deviation, WAAD											
Pure Gases	**Case 1**				**Case 2**				**Case 3**			
Methane	1.74				2.63				0.63			
Nitrogen	1.74				1.38				1.65			
CO_2	1.25				0.79				0.60			
Mixture	*C_{ij} = 0.0*		*Generalized C_{ij}*		*C_{ij} = 0.0*		*Generalized C_{ij}*		*C_{ij} = 0.0*		*Generalized C_{ij}*	
Methane/Nitrogen	0.76	0.76	0.73	0.60	0.89	0.80	0.88	0.53	0.47	0.79	0.46	0.77
Methane/CO_2	1.27	0.50	0.76	0.59	1.10	1.00	0.62	1.03	0.67	0.70	0.33	0.79
Nitrogen/CO_2	0.39	0.38	0.38	0.38	0.55	1.12	0.53	1.09	0.41	0.46	0.44	0.44

Table 5.11 – Comparison for SLD-PR Modeling of Pure-Gas and Binary Adsorption on Wet Tiffany Coal at 130°F

	Weighted Average Absolute Deviation, WAAD											
Pure Gases	**Case 1**				**Case 2**				**Case 3**			
Methane	0.72				1.16				1.01			
Nitrogen	0.66				0.60				1.17			
CO_2	0.52				0.66				0.68			
Mixture	*C_{ij} = 0.0*		*Generalized C_{ij}*		*C_{ij} = 0.0*		*Generalized C_{ij}*		*C_{ij} = 0.0*		*Generalized C_{ij}*	
Methane/Nitrogen	2.17	1.86	1.90	0.53	2.40	1.61	2.16	0.51	2.97	1.64	2.74	0.45
Methane/CO_2	4.09	1.63	0.84	0.80	4.15	1.72	0.93	0.77	4.08	1.29	0.66	0.70
Nitrogen/CO_2	1.80	0.96	0.57	0.64	1.82	0.94	0.60	0.60	1.73	1.26	0.60	1.08

Table 5.12 – Comparison for SLD-PR Modeling of Ternary Adsorption on Wet Tiffany Coal at 130°F

	Weighted Average Absolute Deviation, WAAD					
Mixture	*C_{ij} = 0.0*			*Generalized C_{ij}*		
Methane/Nitrogen/CO_2	Methane	Nitrogen	CO_2	Methane	Nitrogen	CO_2
Case 1	0.64	2.65	1.39	0.32	0.92	0.95
Case 2	0.64	2.67	1.55	0.44	0.97	1.05
Case 3	0.66	2.56	1.03	0.29	1.54	0.80

Figure 5.18 shows the deviation plot for the SLD-PR model generalizations (Cases 4 and 6) of the mixed-gas adsorption on wet OSU coals. As shown, most of the data were predicted within three times the experimental uncertainties using only the pure-fluid generalized parameters; while 90% of data were predicted within twice the experimental uncertainties using both the pure-fluid generalized parameters and generalized binary BIPs.

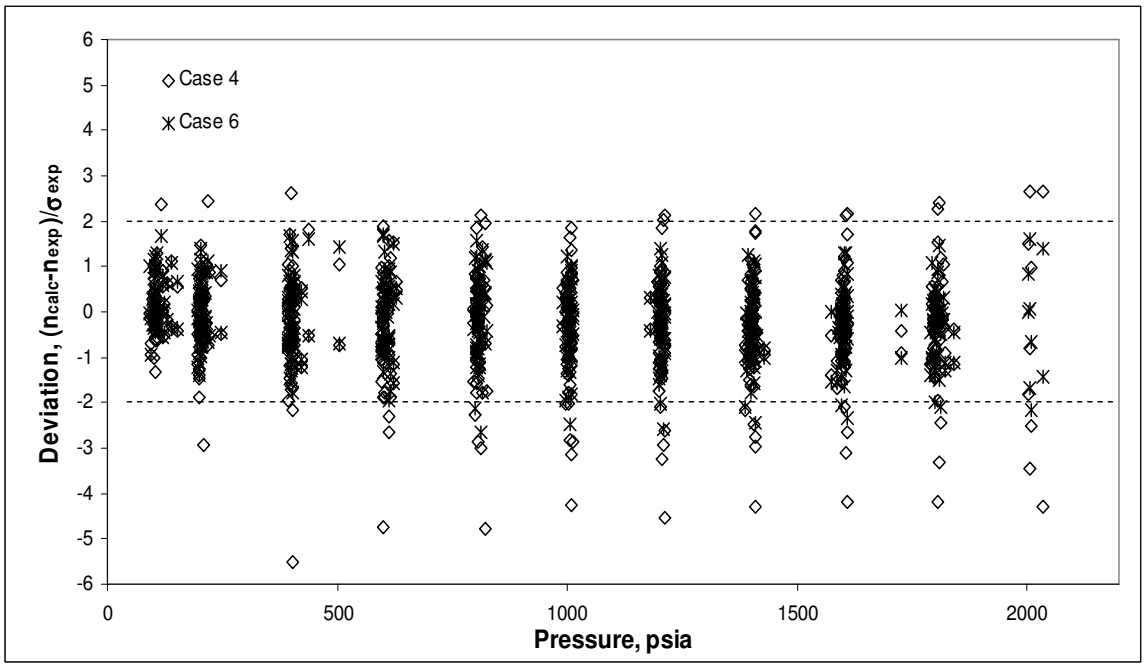

Figure 5.18 – Deviations Plot for SLD-PR Model Generalization of Mixed-Gas Adsorption on Wet OSU Coals

Conclusions

The pure-fluid generalized model parameters were used along with the one-fluid mixing rules to predict mixture adsorption on the wet OSU coals (Illinois #6, Fruitland OSU #1 and Tiffany). With few exceptions, the SLD-PR model can predict the mixture adsorption behavior without BIPs within three times the experimental uncertainties.

Using the generalized BIPs, the SLD-PR predictions for mixture adsorption are improved significantly to yield predictions within twice the experimental uncertainties, on average. Similar to pure-gas adsorption, the generalization based on one-point methane excess adsorption calibration produced the most accurate mixture predictions.

CHAPTER 6

CONCLUSIONS AND RECOMMENDANTIONS

The goal of this study was to develop generalized correlations for the modified SLD-PR model parameters that could provide reliable predictions for the equilibrium adsorption of methane, nitrogen and CO2 and their mixtures on dry and wet coals in the range of conditions encountered in CBM production and CO_2 sequestration. Following a thorough evaluation of the correlative abilities of the SLD-PR model, a generalized model was developed.

Conclusions

Following are the conclusions drawn from this study:

1. The SLD-PR model can represent simultaneously the pure methane, nitrogen and CO_2 adsorption on dry Argonne premium and wet OSU coals within their experimental uncertainties using parameters for *each gas* include a slit length, a solid-solid interaction energy parameter, a PR EOS covolume correction, and a surface area.

2. Using common values for the slit length (1.15 nm) and PR EOS covolume correction (Λ_b = -0.20) yields representations comparable in precision to those obtained from regressing all the model parameters described above. Therefore, these common approximations for the slit length and the covolume correction were applied in developing the generalized SLD-PR model.
3. Generalized correlations were developed for the SLD-PR model parameters in terms of the coal fixed carbon, carbon fraction, equilibrium moisture content, and a single excess adsorption datum at 400 psia. Specifically, a correlation for the solid-solid interaction energy parameter, and three correlations for estimating the surface areas of the three gases in terms of methane, nitrogen or CO_2 excess adsorption at 400 psia were developed.
4. The generalized SLD-PR model can predict pure-gas adsorption on both dry Argonne premium and wet OSU coals, on average, within twice the experimental uncertainties. Among the three generalization scenarios, the one based on methane excess adsorption at 400 psia gives the most accurate predictions.
5. The generalized model parameters were used, along with the selected mixing rules, to predict mixture adsorption on the wet OSU coals (Illinois #6, Fruitland OSU #1 and Tiffany). With few exceptions, the model can predict the mixture adsorption within three times the experimental uncertainties.
6. Using generalized BIPs, the predictions for the mixture adsorption are improved significantly to yield predictions within twice the experimental uncertainties, on average. Similar to pure-gas adsorption, the generalization

based on one-point methane excess adsorption calibration produces the best mixture predictions.

Recommendations

1. Expanded database involving CBM mixed-gas adsorption on dry and wet coals is needed. Mixture adsorption data on dry coals would be particularly useful, since such data are lacking in the current database.
2. The experimental data of pure and mixed-gas adsorption on wet coals should be revisited to account accurately for the effect of water in the raw data reduction procedures.
3. The current SLD-PR model generalizations should be further refined once the moisture effect is addressed properly in the raw data reduction procedures.

REFERENCE

1. U.S. Department of Energy: http://www.energy.gov/energysources/index.htm

2. U.S. Department of Energy: Annual Energy Outlook (2002)

3. Energy Information Administration: Natural Gas Issues and Trends (1998)

4. NaturalGas.Org: http://www.naturalgas.org

5. Rice, D. D.: Coalbed Methane - An Untapped Energy Resource and an Environmental Concern: U.S. Geological Survey Fact Sheet FS-019-97 (1997)

6. Arri, L. E., Yee, D.: Modeling Coalbed Methane Production with Binary Gas Sorption. SPE Rocky Mountain Regional Meeting, Casper, Wyoming (1992)

7. ARC: Reducing Greenhouse Gas Emission Using Coalbed Methane. Research & Development Magazine. Alberta Research Council (ARC), Canada (2001)

8. Stevenson, M. D., Pinczawski, W. V., Downey, R. A.: Economic Evaluation of Nitrogen Injection for Coalseam Gas Recovery. Gas Technology Symposium. Society of Petroleum Engineers (SPE), Canada (1993)

9. Energy Information Administration, U.S. Department of Energy: Emissions of Greenhouse Gases in the United States (2005)

10. Langmuir, I.: The Adsorption of Gases on Plane Glass, Mica and Platinum. American Chemical Society 40, 1361-1402 (1918)

11. Brunauer, S., Emmett, P. H., Teller, E.: Adsorption of Gases in Multimolecular Layers. American Chemical Society 60, 309-319 (1938)

12. Myers, A. L., Prausnitz, J. M.: Thermodynamics of Mixed-Gas Adsorption. AIChE Journal 11, 121-127 (1965)

13. Zhou, C., Hall, F. E., Gasem, K. A. M., Robinson, R. L. Jr.: Predicting Gas Adsorption Using Two-Dimensional Equations of State. Ind. Eng. Chem. Res. 33, 1280-1289 (1994)

14. Pan, Z.: Modeling of Gas Adsorption Using Two-Dimensional Equations of State. Ph.D. Thesis. Oklahoma State University, Stillwater, Oklahoma (2004)

15. Ono, S., Kondo, S.: Encyclopedia of Physics, Springer, Berlin (1960)

16. Sudibandriyo, M.: Generalized Ono-Kondo Lattice Model for High-Pressure Adsorption on Carbon Adsorbents. Ph.D. Thesis. Oklahoma State University, Stillwater, Oklahoma (2003)

17. Arumugam, A.: High-Pressure Adsorption of Pure Coalbed Methane Gases on Dry Coals. M.S. Thesis. Oklahoma State University, Stillwater, Oklahoma (2004)

18. Rangarajan, B., Lira, C. T., Subramanian, R.: Simplified Local Density Model for Adsorption over Large Pressure Ranges. AIChE Journal 41, 838-845 (1995)

19. Soule, A. D., Smith, C. A., Yang, X., Lira, C. T.: Adsorption Modeling with the ESD Equation of State. Langmuir 17, 2950-2957 (2001)

20. Puziy, A. M., Herbst, A., Poddubnaya, O. I., Germanus, J., Harting, P.: Modeling of High-Pressure Adsorption Using the Bender Equation of State. Langmuir 19, 314-320 (2003)

21. Yang, X., Lira, C. T.: Theoretical Study of Adsorption on Activated Carbon from a Supercritical Fluid by the SLD-ESD Approach. Journal of Supercritical Fluids 37, 191-200 (2006)

22. Chen, J. H., Wong, D. S. H., Tan, C. S., Subramanian, R., Lira, C. T., Orth, M.: Adsorption and Desorption of Carbon Dioxide onto and from Activated Carbon at High Pressures. Ind. Eng. Chem. Res. 36, 2808-2815 (1997)

23. Fitzgerald, J. E.: Adsorption of Pure and Multi-Component Gases of Importance to Enhanced CoalBed Methane Recovery: Measurements and Simplified Local Density Modeling. Ph.D. Thesis. Oklahoma State University, Stillwater, Oklahoma (2005)

24. Subramanian, R., Pyada, H., Lira, C. T.: An Engineering Model for Adsorption of Gases onto Flat Surfaces and Clustering in Supercritical Fluids. Ind. Eng. Chem. Res. 34, 3830-3837 (1995)

25. Peng, D. Y., Robinson, D. B.: A New Two-Constant Equation of State. Ind. Eng. Chem. Fund. 15, 59-64 (1976)

26. Henderson, D.: Fundamentals of Inhomogeneous Fluids, Marcel Dekker, Inc, New York (1992)

27. Hernandez-Garduza, O., Garcia-Sanchez, F., Apam-Martinez, D., Vazquez-Roman, R.: Vapor Pressures of Pure Compunds using the Peng-Robinson Equation of State with Three Different Attractive Terms. Fluid Phase Equilibria 198, 195-228 (2002)

28. Reid, R. C., Prausnitz, J. M., Poling, B. E.: The Properties of Gases and Liquids, McGraw-Hill, Inc, New York (1987)

29. Fitzgerald, J. E., Sudibandriyo, M., Pan, Z., Robinson, R. L. Jr., Gasem, K. A. M.: Modeling the Adsorption of Pure Gases on Coals with the SLD Model. Carbon 41, 2203-2216 (2003)

30. Lee, L. L.: Molecular Thermodynamics of Non-ideal Fluids, Butterworth, Stoneham, MA (1988)

31. Fitzgerald, J. E., Sudibandriyo, M., Pan, Z., Robinson, R. L. Jr., Gasem, K. A. M.: Modeling the Adsorption of Pure Gases on Coals with the SLD model. Carbon 41, 2203-2216 (2003)

32. Ustinov, E. A., Do, D. D.: High-Pressure Adsorption of Supercritical Gases on Activated Carbons: An Improved Approach Based on the Density Functional Theory and the Bender Equation of State. Langmuir 19, 8349-8357 (2003)

33. Fitzgerald, J. E., Mohammad, S., Chen, J. S., Gasem, K. A. M., Robinson, R. L. Jr.: Presentation: Adsorption Modeling Update at the Coal-Seq Forum (2006)

34. Gasem, K. A. M., Pan, Z., Mohammad, S., Robinson, R. L. Jr.: Two-Dimensional Equation-of-State Modeling of Adsorption of Coalbed Methane Gases, Stillwater, Oklahoma (2006)

APPENDIX A – THE WORKING EQUATIONS FOR THE SIMPLIFIED LOCAL-DENSITY/PENG-RONBINSON EOS MODEL

The appendix presents the working equations and procedures used in SLD-PR modeling of pure and mixed-gas adsorption on coals.

Mass Balance and Equilibrium Criterion

By definition, the component excess adsorption, n_i^{Ex} is given as:

$$n_i^{Ex} = z_i n^{total} - V_{Void}^{He} \rho_{gas} y_i \tag{A-1}$$

A mass balance equation may be written for each component as follows:

$$z_i = \frac{n_i^{Ex}\left[y_i, x_i, \rho_{gas}\right] + V_{Void}\rho_{gas} y_i}{n_{tot}^{Ex}\left[y_i, x_i, \rho_{gas}\right] + V_{Void}\rho_{gas}} \tag{A-2}$$

where

$$n_i^{Ex} = \frac{A}{2}\int_{\frac{3}{8}\sigma_{ff,i}}^{L-\frac{3}{8}\sigma_{ff,i}} \left(\rho(z)\, x_i(z) - \rho_{bulk}\, y_i\right) dz \tag{A-3}$$

To apply Equation (A-2), the bulk and adsorbed-phase density, the molar composition of the gas mixture and the excess adsorption are required. This, in turn, requires solving the equilibrium criterion:

$$\ln\left(\frac{\hat{f}_i^{ads}[\vec{x}(z), \rho_{ads}(z)]}{\hat{f}_i^{bulk}}\right) + \left(\frac{\Psi_i^{fs}(z) + \Psi_i^{fs}(L-z)}{kT}\right) = 0 \qquad i = 1, NC \tag{A-4}$$

where

$$\Psi^{fs}{}_i(z) = 4\pi\rho_{atoms}(\varepsilon_{fs})_i(\sigma^2_{fs})_i\left(\frac{(\sigma^{10}_{fs})_i}{5(z')^{10}} - \frac{1}{2}\sum_{i=1}^{4}\frac{\sigma^4_{fs,i}}{(z'+(i-1)\cdot\sigma_{ss})^4}\right)$$

$$\text{for } \frac{3}{8}\sigma_{ff,i} \geq z \geq L - \frac{3}{8}\sigma_{ff,i} \text{ and } \Psi_i(z) = \infty \quad \text{elsewhere}$$

and

$$(\varepsilon_{fs})_i = \sqrt{\varepsilon_{ff,i} \times \varepsilon_{ss}} \tag{A-5}$$

The expression for the adsorbed-phase fugacity using the PR EOS is given as:

$$\ln\left(\frac{\hat{f}_i^{ads}(z)}{x_i(z)P}\right) = \frac{2\sum_j x_j(z)b_{ij} - b}{b}\left(\frac{P}{\rho_{ads}(z)RT} - 1\right) - \ln\left(\frac{P}{\rho_{ads}(z)RT} - \frac{Pb}{RT}\right)$$
$$+ \frac{a(z)}{2\sqrt{2}RTb}\left(\frac{2\sum_j x_j(z)b_{ij} - b}{b} - \frac{2\sum_j x_j(z)a_{ij}(z)}{a(z)}\right)\ln\left(\frac{\left(1+\rho_{ads}(z)b\left(1+\sqrt{2}\right)\right)}{\left(1+\rho_{ads}(z)b\left(1-\sqrt{2}\right)\right)}\right)$$

(A-6)

where

$$a = \sum_i\sum_j y_i y_j (a_{ads})_{ij} \text{ and } b = \sum_i\sum_j y_i y_j (b_{ads})_{ij} \tag{A-7}$$

The following combining rules are used for $(a_{ads})_{ij}$ and $(b_{ads})_{ij}$:

$$(a_{ads})_{ij} = \sqrt{(a_{ads})_i (a_{ads})_j}(1 - C_{ij}) \tag{A-8}$$

$$(b_{ads})_{ij} = \left(\frac{b_i(1+\Lambda_{bi}) + b_j(1+\Lambda_{bj})}{2}\right) \tag{A-9}$$

The expression for the gas-phase fugacity using the PR EOS is:

$$\ln\left(\frac{\hat{f}_i^{bulk}}{y_i P}\right) = \frac{b_i}{b}(Z-1) - \ln\left(Z - \frac{pb}{RT}\right) + \frac{a}{2\sqrt{2}RTb}\left(\frac{b_i}{b} - \frac{2\sum_j y_j a_{ij}}{a}\right)\ln\left(\frac{\left(1+\rho b\left(1+\sqrt{2}\right)\right)}{\left(1+\rho b\left(1-\sqrt{2}\right)\right)}\right) \quad \text{(A-10)}$$

where

$$a = \sum_i \sum_j y_i y_j (a_{bulk})_{ij} \text{ and } \qquad b = \sum_i y_i b_i \quad \text{(A-11)}$$

$$(a_{bulk})_{ij} = \sqrt{(a_{bulk})_i (a_{bulk})_j} \quad \text{(A-12)}$$

The compressibility factor for each component in bulk phase using the PR EOS is:

$$\frac{P}{\rho RT} = \frac{1}{(1-\rho b)} - \frac{a(T)\rho}{RT\left[1+\left(1-\sqrt{2}\right)\rho b\right]\left[1+\left(1+\sqrt{2}\right)\rho b\right]} \quad \text{(A-13)}$$

where

$$a(T) = 0.47325\,\alpha(T)\frac{(RT_C)^2}{P_C} \quad \text{(A-14)}$$

$$\alpha(T) = \left[1 + C_1\left(1-\sqrt{\frac{T}{T_C}}\right) + C_2\left(1-\sqrt{\frac{T}{T_C}}\right)^2 + C_3\left(1-\sqrt{\frac{T}{T_C}}\right)^3\right]^2 \quad \text{(A-15)}$$

$$b = 0.077796\frac{RT_C}{P_C} \quad \text{(A-16)}$$

Equations (A-6) and (A-10) are used for the respective phases within Equation (A-4) to solve for x_i, ρ_{ads} and f_i^{ads}. Equation (A-13) provides the phase densities, when Equation (A-10) is used.

Calculation Procedure

To solve the mass balance for a component in a mixture, a constraint equation is imposed:

$$W_i = \frac{n_i^{Ex} + V_{void}\rho_{bulk}y_i}{n_{tot}^{Ex} + V_{void}\rho_{bulk}} - z_i \tag{A-17}$$

A Jacobian matrix is constructed to solve the nonlinear set of equations by the Newton-Raphson method. For a three-component mixture, the linear set of equations required is:

$$\begin{bmatrix} W_1 \\ W_2 \\ W_3 \end{bmatrix} = \begin{bmatrix} \frac{\partial W_1}{\partial y_1} & \frac{\partial W_1}{\partial y_2} & \frac{\partial W_1}{\partial y_3} \\ \frac{\partial W_2}{\partial y_1} & \frac{\partial W_2}{\partial y_2} & \frac{\partial W_2}{\partial y_3} \\ \frac{\partial W_3}{\partial y_1} & \frac{\partial W_3}{\partial y_2} & \frac{\partial W_3}{\partial y_3} \end{bmatrix} \begin{bmatrix} \Delta y_1 \\ \Delta y_2 \\ \Delta y_3 \end{bmatrix} \tag{A-18}$$

The next trial solution for the bulk mole fraction of component "i" becomes:

$$(y_i)^{k+1} = (y_i)^{k+1} + (\Delta y_i)^{k+1} \tag{A-19}$$

Note that in this study, all derivatives are computed numerically.

To determine the excess adsorption amounts in Equation (A-17), the equilibrium criterion given by Equation (A-20) is solved for 50 segments within half of the slit. This is accomplished by constructing a new Jacobian matrix, which is solved by the Newton-Raphson method. The objective function, Q_i, used for each component "i" is given as:

$$\ln\left(\frac{\hat{f}_i^{ads}[\rho_{LCL}, \vec{x}]}{\hat{f}_i^{Bulk}}\right) + \Psi_i^{fs} = Q_i \tag{A-20}$$

In addition, the sum of mole fractions for the gas mixture requires that:

$$Q_4 = 100 \times (x_1 + x_2 + x_3 - 1) \tag{A-21}$$

The resulting linear set of equations for three-component mixture is:

$$\begin{bmatrix} Q_1 \\ Q_2 \\ Q_3 \\ Q_4 \end{bmatrix} = \begin{bmatrix} \frac{\partial Q_1}{\partial \rho_{LCL}} & \frac{\partial Q_1}{\partial x_1} & \frac{\partial Q_1}{\partial x_2} & \frac{\partial Q_1}{\partial x_3} \\ \frac{\partial Q_2}{\partial \rho_{LCL}} & \frac{\partial Q_2}{\partial x_1} & \frac{\partial Q_2}{\partial x_2} & \frac{\partial Q_2}{\partial x_3} \\ \frac{\partial Q_3}{\partial \rho_{LCL}} & \frac{\partial Q_3}{\partial x_1} & \frac{\partial Q_3}{\partial x_2} & \frac{\partial Q_3}{\partial x_3} \\ 0 & 100 & 100 & 100 \end{bmatrix} \begin{bmatrix} \Delta\rho_{LCL} \\ \Delta x_1 \\ \Delta x_2 \\ \Delta x_3 \end{bmatrix} \tag{A-22}$$

Thus, the next trial solution becomes:

$$\begin{aligned} (\rho_{LCL})^{k+1} &= (\rho_{LCL})^k + (\Delta\rho_{LCL})^k \\ (x_1)^{k+1} &= (x_1)^k + (\Delta x_1)^k \\ (x_2)^{k+1} &= (x_2)^k + (\Delta x_2)^k \\ (x_3)^{k+1} &= (x_3)^k + (\Delta x_3)^k \end{aligned} \tag{A-23}$$

Again, the derivatives required for the Jacobian elements are calculated numerically.

The above Newton-Raphson iterations are continued until both the objective functions satisfy the set convergence tolerance. When convergence is achieved, the local compressibility factor and the adsorbed mole fractions are determined at that position in the slit. The procedure is then repeated for each position in the slit, and for each case the local compressibility factor and the local adsorbed mole fraction are calculated.

To calculate the Gibbs excess and the density-averaged component mole fraction of the adsorbed phase within the slit, the adsorbed-phase density and the mole fraction of the component "i" are needed. The Simpson's rule is used to evaluate the integrals for these quantities. The average adsorbed density is:

$$\langle \rho \rangle = \frac{2}{L - \sigma_{ff}} \int_{\eta=\frac{3}{8}\sigma_{ff,i}}^{\eta=\left(L+\frac{3}{8}\sigma_{ff,i}\right)/2} \rho[\eta] d\eta \tag{A-24}$$

The density-averaged mole fraction of component "i" in the adsorbed phase is:

$$\langle x_i \rangle = \frac{\langle x_i \rho \rangle}{\langle \rho \rangle} = \frac{2}{\langle \rho \rangle \left(L - \sigma_{ff,i} \right)} \int_{\eta = \frac{3}{8}\sigma_{ff,i}}^{\eta = \left(L + \frac{3}{8}\sigma_{ff,i} \right)/2} \rho[\eta_i] \cdot x_i[\eta] d\eta_i \tag{A-25}$$

In using the Simpson's rule, an odd number of function calls is needed, and hence the interval is subdivided evenly into "η" regions.

$$\Delta\eta_i = \frac{L - \frac{3}{8}\sigma_{ff,i}}{2n_{even}} \tag{A-26}$$

The integral required to calculate the density-averaged mole fraction of component "i" is approximated by Simpson's rule as follows:

$$\begin{aligned} \int_{\frac{3}{8}\sigma_{ff,i}}^{L/2 + \frac{3}{8}\sigma_{ff,i}/2} \rho[\eta_i] \cdot x_i[\eta_i] d\eta_i \approx \frac{2}{3}\Delta\eta \{ & x_i[\sigma_{fs,i}] \cdot \rho[\sigma_{fs,i}] + 4x_i[\sigma_{fs,i} + \Delta\eta_i] \cdot \rho[\sigma_{fs,i} + \Delta\eta_i] \\ & + 2x_i[\sigma_{fs,i} + 2\Delta\Delta_i] \cdot \rho[\sigma_{fs,i} + 2\Delta\Delta_i] + \ldots + 4x_i[(L + \sigma_{ss,i})/2 - \Delta\eta_i] \cdot \\ & \rho[(L + \sigma_{ss,i})/2 - \Delta\eta_i] + x_i[(L + \sigma_{ss,i})/2] \cdot \rho[(L + \sigma_{ss,i})/2] \} \end{aligned} \tag{A-27}$$

The component Gibbs excess is expressed as:

$$n_i^{Gibbs} = \frac{AL}{2}\left(\langle \rho x_i \rangle - \rho_{bulk} y_i \right), \tag{A-28}$$

and the total Gibbs excess becomes:

$$n_{total}^{Gibbs} = \frac{AL}{2}\left(\langle \rho \rangle - \rho_{bulk} \right) = \sum_i n_i^{Gibbs} \tag{A-29}$$

Once the component mass balance equations (Equation (A-17)) are satisfied through the equilibrium criterion, the molar composition, excess adsorption and densities are calculated as a final iterative step.

Optimization of Parameters

To solve the Jacobian matrices of mass balance and equilibrium criterion, the WRMS (weighted root mean square) objective function is used to correlate the excess adsorption of component "i" in the SLD-PR model. The function is expressed as follows:

$$WRMS = \frac{\sqrt{\sum_{i=1}^{NPTS} \left(\frac{n_{calc} - n_{exp}}{\sigma_{exp}} \right)_i^2}}{NPTS} \qquad \text{(A-30)}$$

A flowchart and an overview are provided for this procedure in Figures A.1 and A.2, respectively.

Figure A.1 – Flowchart for the SLD-PR Model

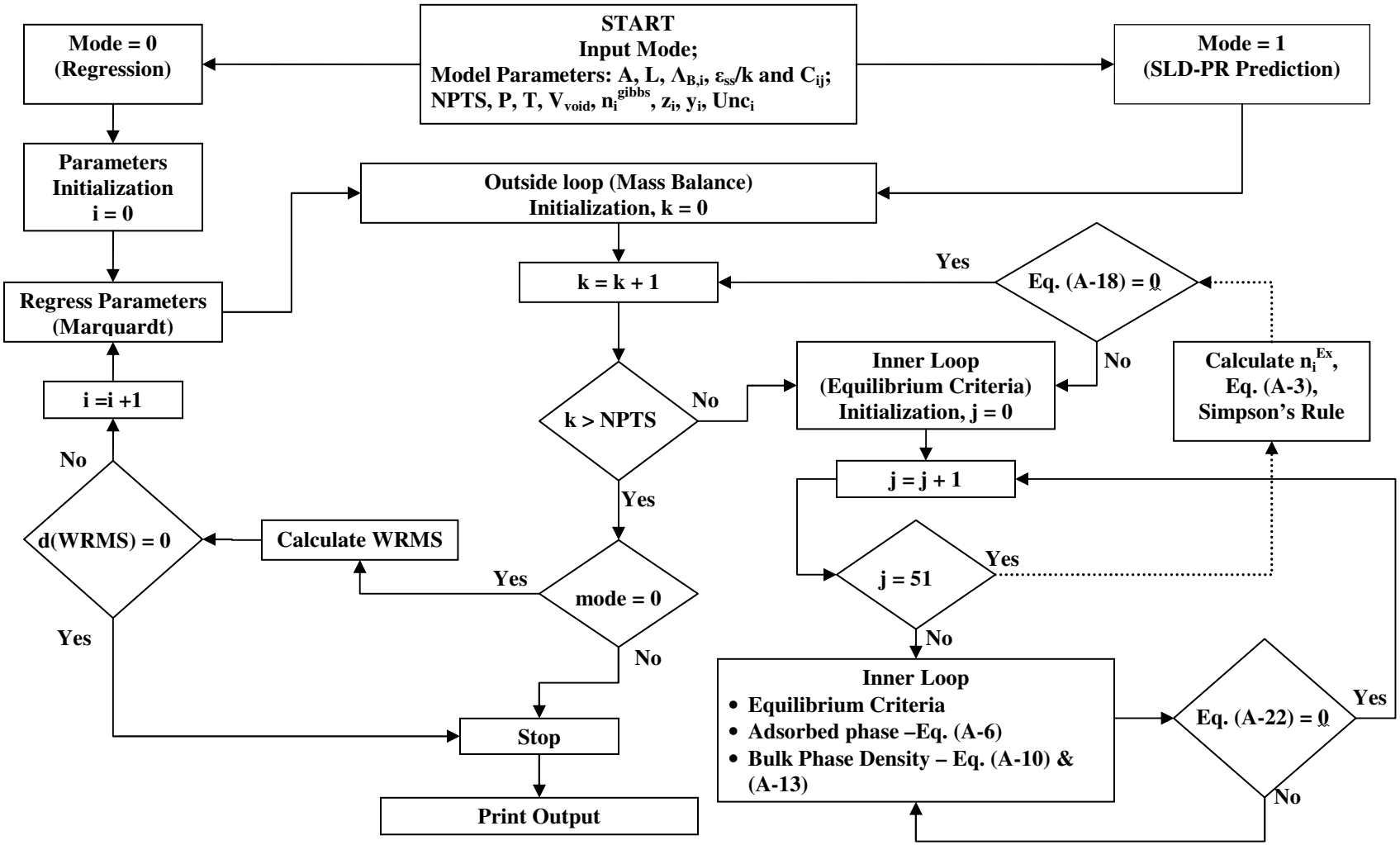

Figure A.2 – Overview of the SLD-PR Model

Model Parameters Input

A_1	Surface area for methane, m^2/g
$\Lambda_{b,1}$	Dimensionless covolume "b" correction for methane
A_2	Surface area for nitrogen, m^2/g
$\Lambda_{b,2}$	Dimensionless covolume "b" correction for nitrogen
A_3	Surface area for CO_2, m^2/g
$\Lambda_{b,3}$	Dimensionless covolume "b" correction for CO_2
L	Length of slit, nm
ε_{ss}/k	Solid-solid interaction energy parameter for the matrix, K
C_{12}:	Binary interaction parameter for methane-nitrogen
C_{13}:	Binary interaction parameter for methane - CO_2
C_{23}:	Binary interaction parameter for nitrogen - CO_2

Data Input

P	The bulk pressure, psia
T	The temperature, ºF
V_{void}	The Helium void volume per gram of adsorbent, cm^3/g
n_1	The Gibbs excess adsorption of methane, mmol/g
n_2	The Gibbs excess adsorption of nitrogen, mmol/g
n_3	The Gibbs excess adsorption of CO_2, mmol/g
z_1	The mole fraction of methane in feed
z_2	The mole fraction of nitrogen in feed
y_1	The mole fraction of methane in bulk phase
y_2	The mole fraction of nitrogen in bulk phase
Unc_1	The expected uncertainty of methane Gibbs adsorption
Unc_2	The expected uncertainty of nitrogen Gibbs adsorption
Unc_3	The expected uncertainty of CO_2 Gibbs adsorption
Mask	Enter 1 if the datum point is considered for regression Enter 0 if the datum point is "masked"

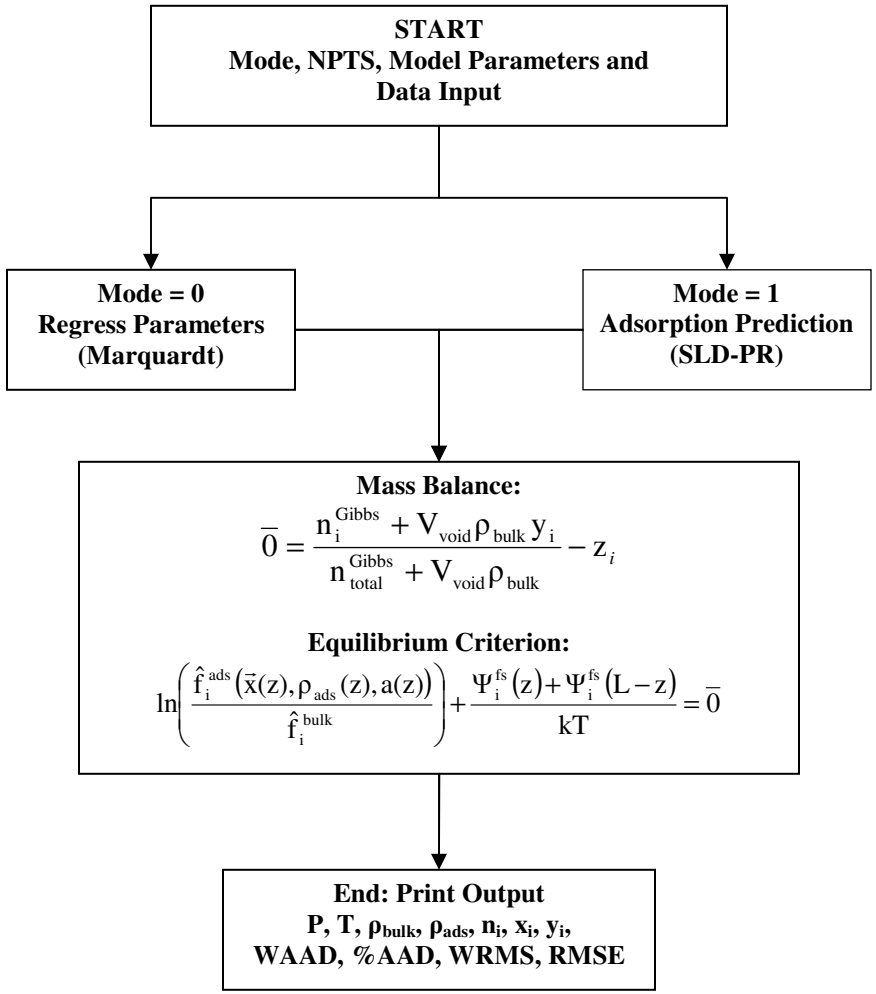

APPENDIX B – REPRESENTATION OF PURE-GAS ADSORPTION

Appendix B.1 – Representation of Modified SLD-PR Modeling on Dry Argonne Premium Coals without Covolume Correction ($\Lambda_b = 0.0$)

Table B.1 presents the regression results of pure-gas adsorption on dry Argonne premium coals without the covolume correction. As indicated in the table, the SLD-PR model can represent precisely the adsorption data within expected experimental uncertainties.

Table B.1 - Modified SLD-PR Model Representations of Pure-Gas Adsorption on Dry Argonne Premium Coals with $\Lambda_b = 0.0$

Coal	Adsorbate	Parameters			WAAD	%AAD	RMSE (mmol/g)	WRMS
		Area (m^2/g)	ε_{ss}/k (K)	L (nm)				
Dry Illinois #6	CH_4	80.4	27.2	1.49	0.46	3.2	0.03	0.59
	N_2	56.4						
	CO_2	107.0						
Dry Beulah Zap	CH_4	59.8	43.1	1.49	0.45	2.7	0.04	0.58
	N_2	39.3						
	CO_2	114.3						
Dry Wyodak	CH_4	67.8	35.7	1.59	0.76	3.6	0.06	1.03
	N_2	49.2						
	CO_2	118.3						
Dry Upper Freeport	CH_4	61.3	34.3	1.28	0.35	1.8	0.02	0.46
	N_2	44.4						
	CO_2	71.1						
Dry Pocahontas	CH_4	82.1	34.0	1.23	0.45	2.1	0.02	0.62
	N_2	59.3						
	CO_2	91.2						
Statistics for Dry Coals					0.49	2.7	0.03	0.65

Appendix B.2 – Representation Results for Scenario 2

The representation plots for pure-gas adsorption on dry Argonne premium and wet OSU coals are presented from Figures B.1 to B.10. The first five figures are the representation plots for dry Argonne coals (Illinois #6, Beulah Zap, Wyodak, Upper Freeport and Pocahontas). The last five figures are the plots for wet OSU coals (Illinois #6, Fruitland OSU #1, Fruitland OSU #2, Tiffany and Lower Basin Fruitland). In some figures, the experimental uncertainties of the adsorption are small in value that they are superimposed with the data symbol, so they cannot be seen.

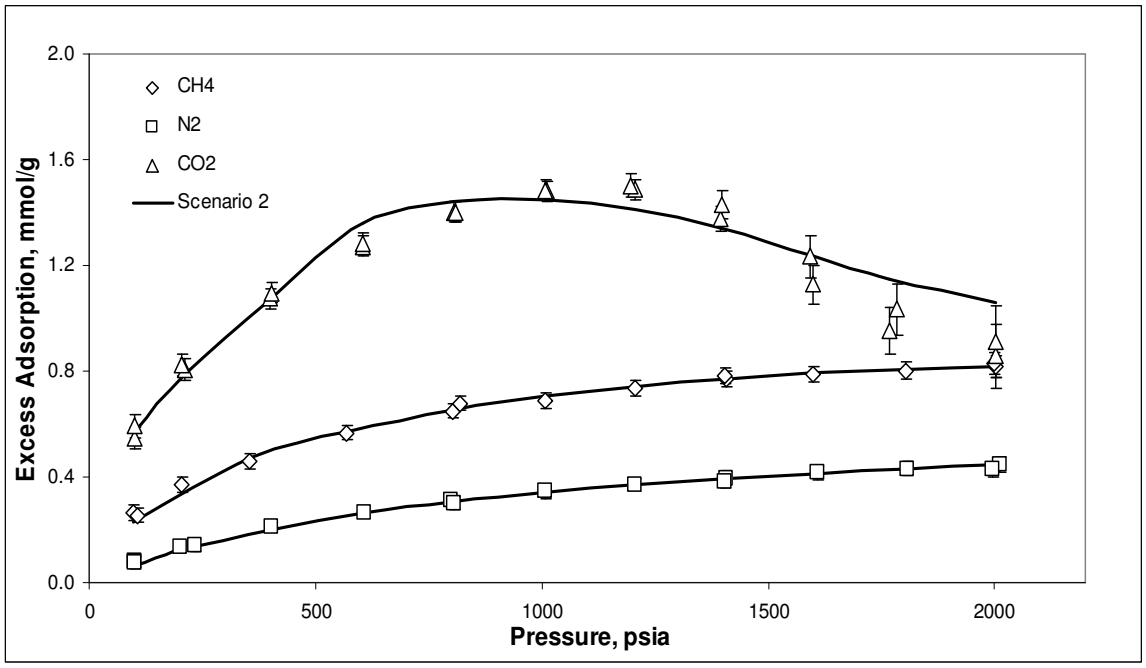

Figure B.1 – Scenario 2: Representation of Pure-Gas Adsorption on Dry Illinois #6 Coal at 131°F

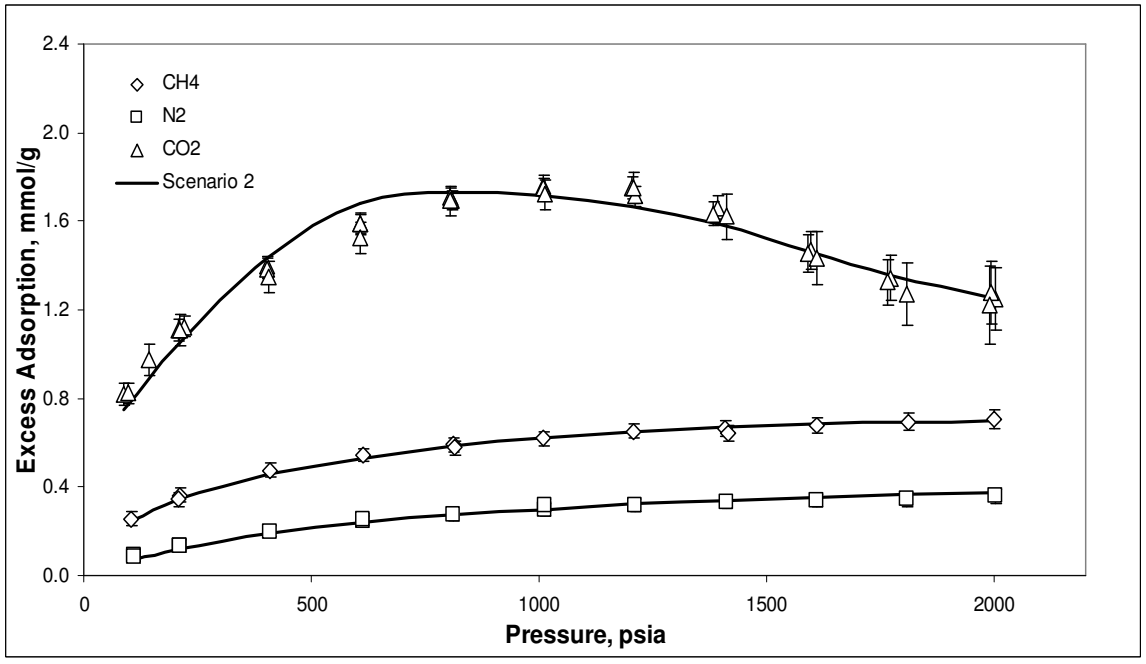

Figure B.2 – Scenario 2: Representation of Pure-Gas Adsorption on Dry Beulah Zap Coal at 131°F

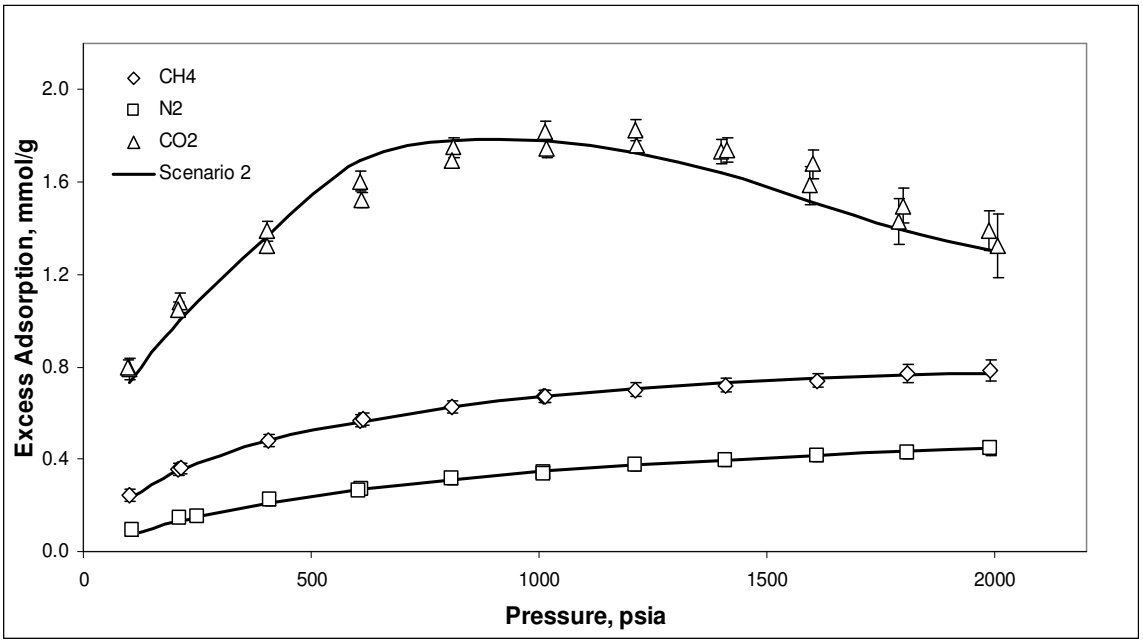

Figure B.3 – Scenario 2: Representation of Pure-Gas Adsorption on Dry Wyodak Coal at 131°F

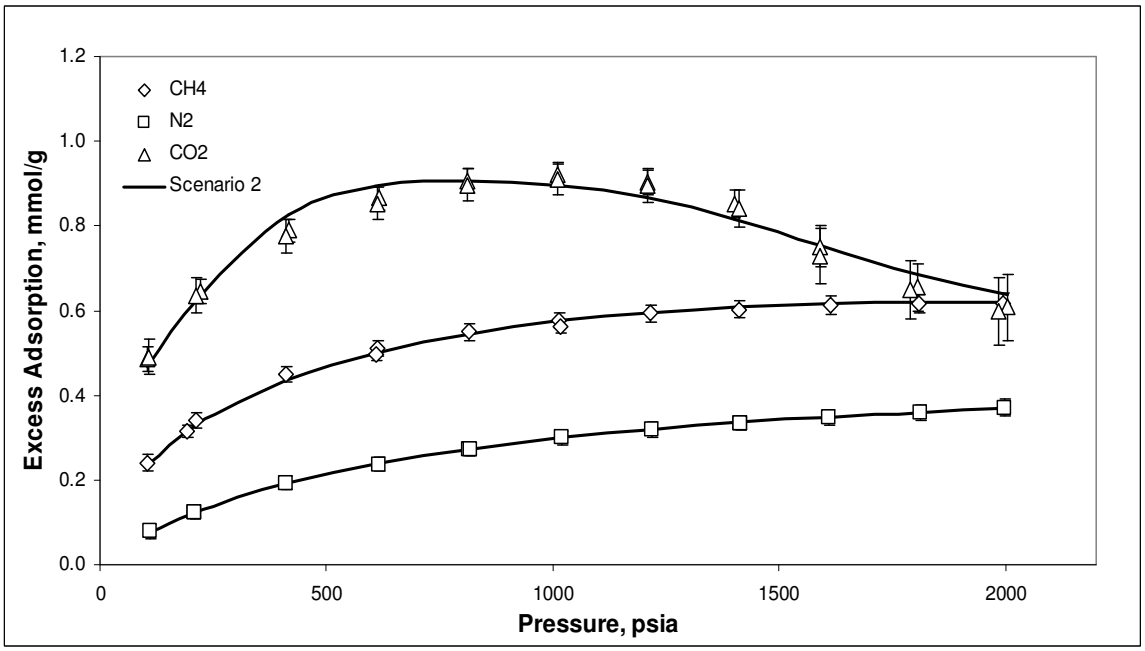

Figure B.4 – Scenario 2: Representation of Pure-Gas Adsorption on Dry Upper Freeport Coal at 131°F

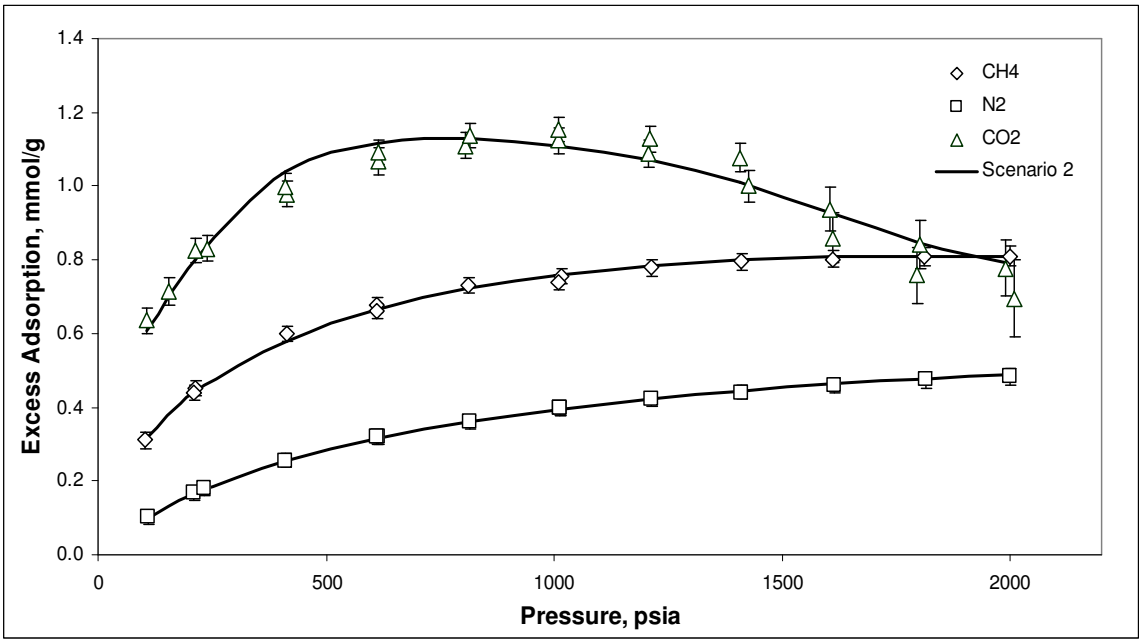

Figure B.5 – Scenario 2: Representation of Pure-Gas Adsorption on Dry Pocahontas Coal at 131°F

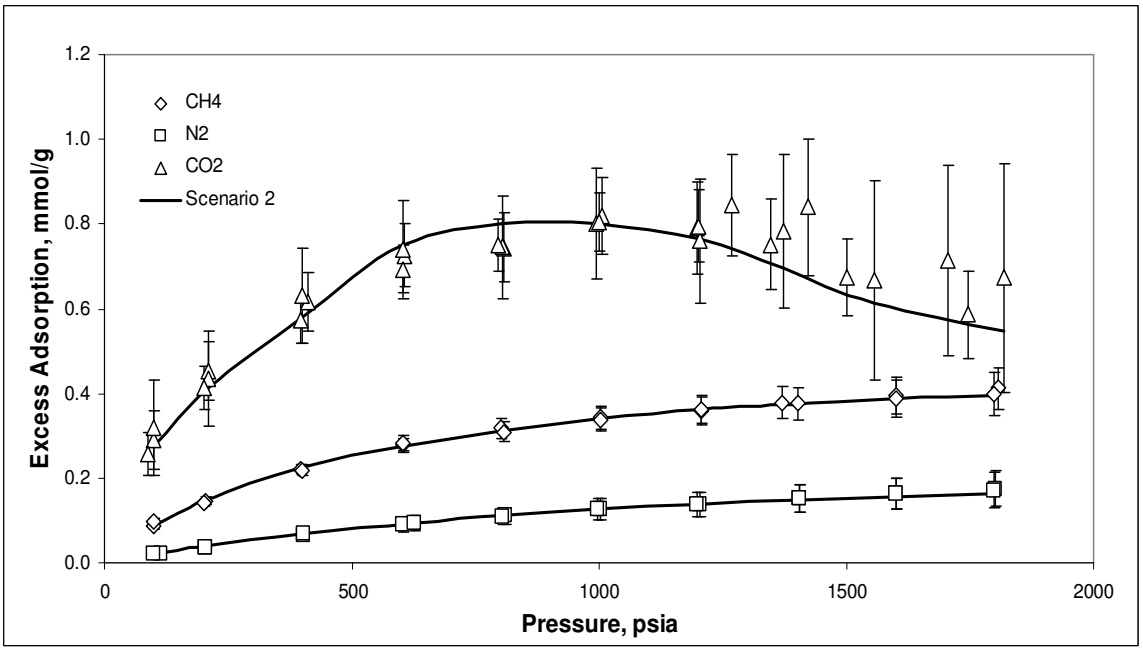

Figure B.6 – Scenario 2: Representation of Pure-Gas Adsorption on Wet Illinois #6 Coal at 115°F

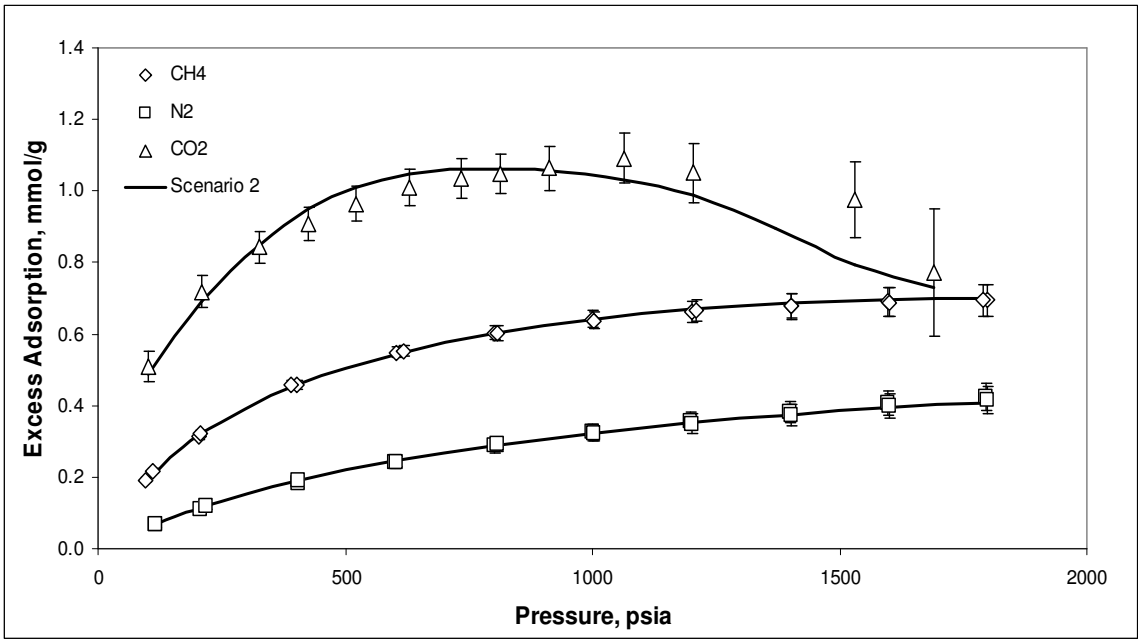

Figure B.7 – Scenario 2: Representation of Pure-Gas Adsorption on Wet Fruitland OSU #1 Coal at 115°F

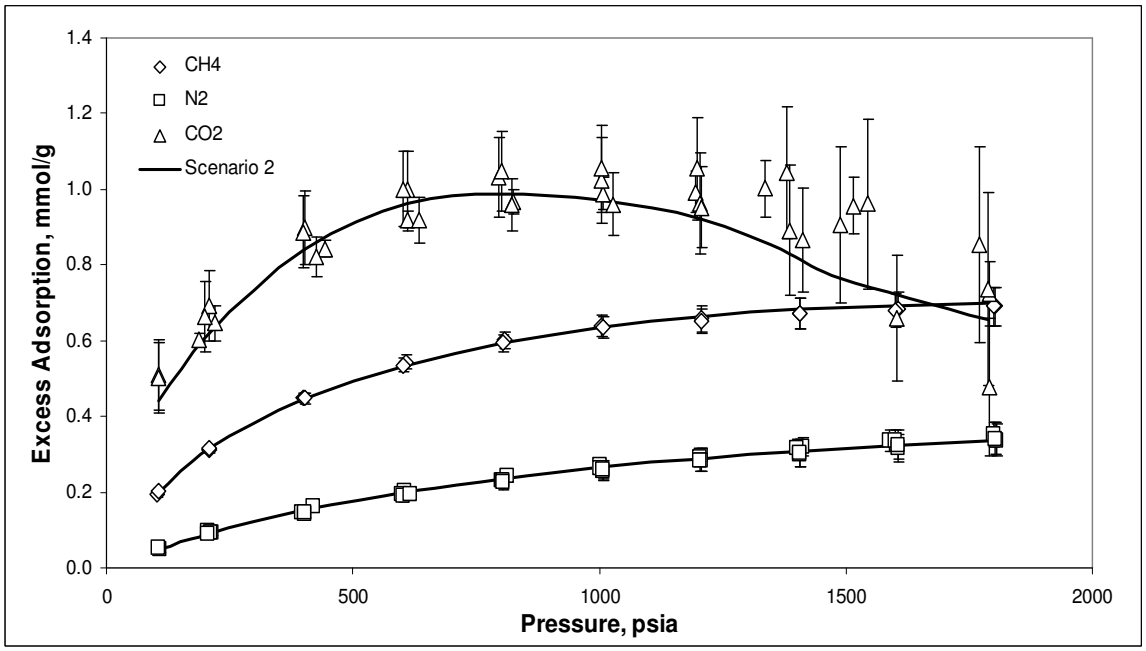

Figure B.8 – Scenario 2: Representation of Pure-Gas Adsorption on Wet Fruitland OSU #2 at 115°F

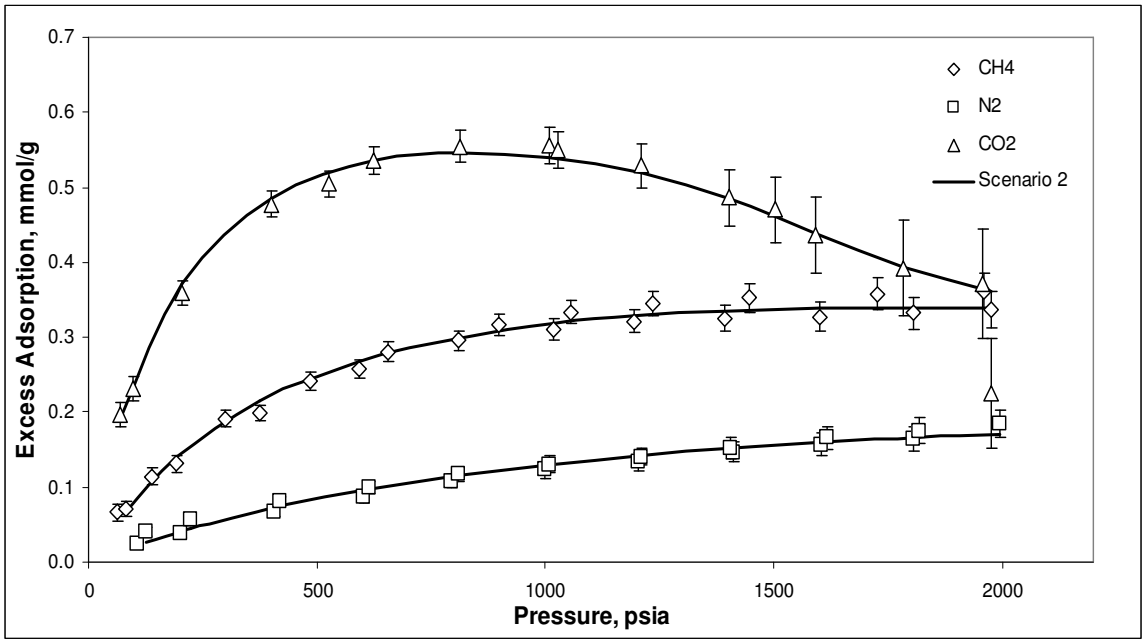

Figure B.9 – Scenario 2: Representation of Pure-Gas Adsorption on Wet Tiffany Coal at 130°F

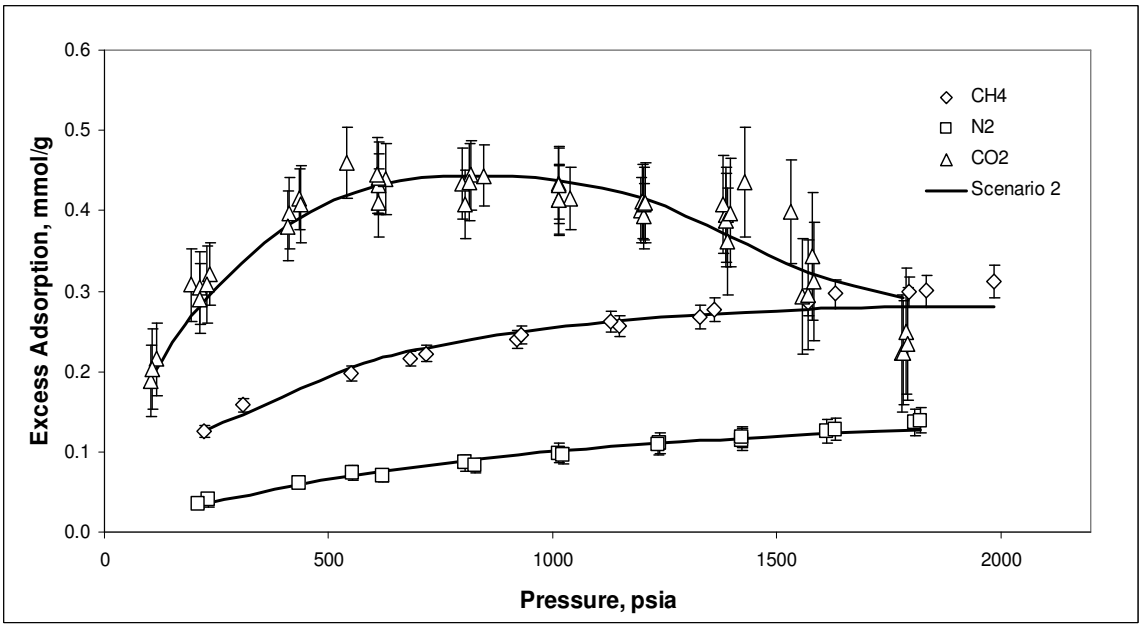

Figure B.10 – Scenario 2: Representation of Pure-Gas Adsorption on Wet Lower Basin Fruitland Coal at 115°F

APPENDIX C – MODEL PARAMETER GENERALIZATIONS

Appendix C.1 – Generalization in the OSU FORTRAN Program

Table C.1 – The Coal Numbers for the Argonne Premium and OSU Coals in Model Generalizations

Coal	Coal Number
Beulah Zap	1
Wyodak	2
Illinois #6	3
Upper Freeport	4
Pocahontas	5
Wet Illinois #6	11
Wet Fruitland OSU #1	12
Wet Fruitland OSU #2	13
Wet Tiffany	14
Wet Lower Basin Fruitland	15

Table C.2 – The System Numbers for the Argonne Premium and OSU Coals in Model Generalizations

System Number	NPTS	Coal
gen1-5	265	Pure-Gas Adsorption on Dry Argonne Premium Coals
gen6-10	60	Pure CO_2 Adsorption on Wet Argonne Premium Coals
gen11-15	359	Pure-Gas Adsorption on Wet OSU Coals
gen16-18	285	Mixed-Gas Adsorption on Wet Illinois #6, Fruitland OSU #1 and Tiffany Coals
gen19-28	624	Pure-Gas Adsorption on Dry Argonne Premium and Wet OSU Coals

Appendix C.2 – Comparison of Generalized and Regressed Model Results

Table C.3 – Case 1: Summary Results of the Generalized Parameters

(a) CH_4 Surface Area

Coal	Regressed A_{CH4}	Generalized A_{CH4}	%AAD
Dry Illinois #6	74.1	62.0	16.3
Dry Beulah Zap	58.9	58.5	0.7
Dry Wyodak	68.8	59.6	13.4
Dry Upper Freeport	48.9	55.1	12.7
Dry Pocahontas	63.4	71.5	12.8
Wet Illinois #6	36.9	30.3	18.0
Wet FR OSU #1	60.9	56.5	7.3
Wet FR OSU #2	61.3	55.4	9.6
Wet Tiffany	30.5	29.4	3.8
Wet LB FR	24.8	24.9	0.5
Overall Total			9.5

(b) N_2 Surface Area

Coal	Regressed A_{N2}	Generalized A_{N2}	%AAD
Dry Illinois #6	56.3	45.6	19.1
Dry Beulah Zap	42.9	42.7	0.5
Dry Wyodak	55.3	43.6	21.2
Dry Upper Freeport	37.1	39.9	7.6
Dry Pocahontas	47.7	53.4	12.0
Wet Illinois #6	22.2	19.3	13.1
Wet FR OSU #1	47.8	41.0	14.2
Wet FR OSU #2	40.0	40.1	0.3
Wet Tiffany	19.6	18.6	5.2
Wet LB FR	15.3	14.9	2.3
Overall Total			9.5

Table C.3 – Case 1: Summary Results of the Generalized Parameters (Continued)

(c) CO_2 Surface Area

Coal	Regressed A_{CO2}	Generalized A_{CO2}	%AAD
Dry Illinois #6	97.5	84.9	12.9
Dry Beulah Zap	111.3	110.7	0.6
Dry Wyodak	118.6	108.7	8.4
Dry Upper Freeport	56.0	58.4	4.3
Dry Pocahontas	69.0	73.6	6.6
Wet Illinois #6	54.0	40.7	24.6
Wet FR OSU #1	69.0	63.1	8.5
Wet FR OSU #2	64.4	61.7	4.2
Wet Tiffany	36.6	36.4	0.7
Wet LB FR	29.0	29.7	2.5
Overall Total			7.3

(d) Solid-Solid Interaction Energy Parameter, ε_{ss}/k

Coal	Regressed ε_{ss}/k	Generalized ε_{ss}/k	%AAD
Dry Illinois #6	21.1	23.1	9.0
Dry Beulah Zap	27.3	23.0	15.7
Dry Wyodak	22.4	22.4	0.0
Dry Upper Freeport	35.5	32.6	8.0
Dry Pocahontas	37.5	35.9	4.5
Wet Illinois #6	17.4	21.4	22.9
Wet FR OSU #1	23.7	24.1	1.7
Wet FR OSU #2	22.7	24.1	6.3
Wet Tiffany	24.4	23.1	5.5
Wet LB FR	22.0	22.0	0.0
Overall Total			7.4

Table C.4 – Case 2: Summary Results of the Generalized Parameters

(a) Methane Surface Area

Coal	Regressed A_{CH4}	Generalized A_{CH4}	%AAD
Dry Illinois #6	74.1	69.2	6.6
Dry Beulah Zap	58.9	61.4	4.2
Dry Wyodak	68.8	67.3	2.1
Dry Upper Freeport	48.9	56.5	15.5
Dry Pocahontas	63.4	60.5	4.6
Wet Illinois #6	36.9	30.9	16.3
Wet FR OSU #1	60.9	50.1	17.8
Wet FR OSU #2	61.3	43.5	29.0
Wet Tiffany	30.5	27.8	9.1
Wet LB FR	24.8	26.5	7.0
Overall Total			11.2

(b) Nitrogen Surface Area

Coal	Regressed A_{N2}	Generalized A_{N2}	%AAD
Dry Illinois #6	56.3	46.5	17.4
Dry Beulah Zap	42.9	51.0	18.9
Dry Wyodak	55.3	54.0	2.4
Dry Upper Freeport	37.1	37.2	0.4
Dry Pocahontas	47.7	47.7	0.0
Wet Illinois #6	22.2	18.9	14.8
Wet FR OSU #1	47.8	38.1	20.3
Wet FR OSU #2	40.0	31.7	20.8
Wet Tiffany	19.6	18.7	4.9
Wet LB FR	15.3	15.4	0.9
Overall Total			10.1

Table C.4 – Case 2: Summary Results of the Generalized Parameters (Continued)

(c) CO_2 Surface Area

Coal	Regressed A_{CO2}	Generalized A_{CO2}	%AAD
Dry Illinois #6	97.5	87.1	10.7
Dry Beulah Zap	111.3	113.9	2.4
Dry Wyodak	118.6	118.3	0.3
Dry Upper Freeport	56.0	55.2	1.4
Dry Pocahontas	69.0	68.5	0.8
Wet Illinois #6	54.0	55.3	2.3
Wet FR OSU #1	69.0	67.5	2.1
Wet FR OSU #2	64.4	59.2	8.1
Wet Tiffany	36.6	36.4	0.7
Wet LB FR	29.0	26.6	8.3
Overall Total			3.7

(d) Solid-Solid Interaction Energy Parameter, ε_{ss}/k

Coal	Regressed ε_{ss}/k	Generalized ε_{ss}/k	%AAD
Dry Illinois #6	21.1	25.5	20.4
Dry Beulah Zap	27.3	24.3	10.8
Dry Wyodak	22.4	23.8	6.2
Dry Upper Freeport	35.5	38.8	9.4
Dry Pocahontas	37.5	43.6	16.1
Wet Illinois #6	17.4	24.7	42.1
Wet FR OSU #1	23.7	28.5	20.2
Wet FR OSU #2	22.7	28.5	25.6
Wet Tiffany	24.4	26.4	8.0
Wet LB FR	22.0	25.3	15.0
Overall Total			17.4

Table C.5 – Case 3: Summary Results of the Generalized Parameters

(a) CH_4 Surface Area

Coal	Regressed A_{CH4}	Generalized A_{CH4}	%AAD
Dry Illinois #6	74.1	60.0	19.1
Dry Beulah Zap	58.9	68.0	15.6
Dry Wyodak	68.8	68.6	0.3
Dry Upper Freeport	48.9	48.5	0.8
Dry Pocahontas	63.4	66.9	5.6
Wet Illinois #6	36.9	40.3	9.3
Wet FR OSU #1	60.9	62.3	2.2
Wet FR OSU #2	61.3	58.9	3.9
Wet Tiffany	30.5	29.8	2.4
Wet LB FR	24.8	25.3	2.3
Overall Total			6.2

(b) N_2 Surface Area

Coal	Regressed A_{N2}	Generalized A_{N2}	%AAD
Dry Illinois #6	10.0	10.0	10.0
Dry Beulah Zap	41.0	41.0	41.0
Dry Wyodak	6.9	6.9	6.9
Dry Upper Freeport	4.4	4.4	4.4
Dry Pocahontas	6.6	6.6	6.6
Wet Illinois #6	7.6	7.6	7.6
Wet FR OSU #1	12.2	12.2	12.2
Wet FR OSU #2	2.1	2.1	2.1
Wet Tiffany	6.0	6.0	6.0
Wet LB FR	0.9	0.9	0.9
Overall Total			9.8

Table C.5 – Case 3: Summary Results of the Generalized Parameters (Continued)

(c) CO_2 Surface Area

Coal	Regressed A_{CO2}	Generalized A_{CO2}	%AAD
Dry Illinois #6	97.5	88.5	9.3
Dry Beulah Zap	111.3	120.9	8.6
Dry Wyodak	118.6	118.3	0.2
Dry Upper Freeport	56.0	57.8	3.3
Dry Pocahontas	69.0	71.9	4.2
Wet Illinois #6	54.0	48.0	11.2
Wet FR OSU #1	69.0	67.6	2.0
Wet FR OSU #2	64.4	63.7	1.1
Wet Tiffany	36.6	37.0	1.1
Wet LB FR	29.0	30.1	3.8
Overall Total			4.5

(d) Solid-Solid Interaction Energy Parameter, ε_{ss}/k

Coal	Regressed ε_{ss}/k	Generalized ε_{ss}/k	%AAD
Dry Illinois #6	21.1	22.7	7.4
Dry Beulah Zap	27.3	22.7	16.8
Dry Wyodak	22.4	22.1	1.4
Dry Upper Freeport	35.5	32.0	9.8
Dry Pocahontas	37.5	35.1	6.4
Wet Illinois #6	17.4	21.0	20.8
Wet FR OSU #1	23.7	23.7	0.2
Wet FR OSU #2	22.7	23.6	4.3
Wet Tiffany	24.4	22.7	7.1
Wet LB FR	22.0	21.7	1.7
Overall Total			7.6

Appendix C.3 – Generalization of Mixed-Gas Adsorption Using Nitrogen Excess Adsorption

This section presents the results of the mixture adsorption on wet coals using the SLD-PR generalized parameters from the nitrogen correlations (Case 2). The weighted average absolute deviations (WAAD) of the pure and mixed-gas adsorption on wet coals are listed and the generalized predictions of all components adsorption in the mixed-gas adsorption are also plotted. The tables and figures are arranged according to the arrangement for methane correlation.

Table C.6 – Case 2: Summary Results for SLD-PR Modeling of Pure and Binary Mixture Adsorption on Wet Illinois #6 Coal at 115°F

	Weighted Average Absolute Deviation, WAAD			
Pure Gases				
Methane	0.91			
Nitrogen	0.38			
CO_2	1.01			
Feed Mixture	*C_{ij} = 0.0*		*Generalized C_{ij}*	
Methane/Nitrogen	*Methane*	*Nitrogen*	*Methane*	*Nitrogen*
20/80	0.36	0.67	0.28	0.51
40/60	0.55	0.79	0.65	0.17
60/40	0.43	0.67	0.56	0.26
80/20	0.32	0.40	0.38	0.48
All Feed	0.42	0.63	0.47	0.36
Methane/CO_2	*Methane*	*CO_2*	*Methane*	*CO_2*
20/80	0.71	1.81	0.56	1.99
40/60	1.21	2.05	1.06	2.33
60/40	2.37	0.77	1.80	0.89
80/20	2.03	0.61	1.86	0.44
All Feed	1.58	1.31	1.32	1.41
Nitrogen/CO_2	*Nitrogen*	*CO_2*	*Nitrogen*	*CO_2*
20/80	0.83	2.93	0.84	2.93
40/60	1.15	2.60	1.16	2.59
60/40	1.26	2.37	1.26	2.37
80/20	1.97	0.67	1.98	0.67
All Feed	1.30	2.14	1.31	2.14

Table C.7 – Case 2: Summary Results for SLD-PR Modeling of Pure and Binary Mixture Adsorption on Wet Fruitland OSU #1 Coal at 115°F

	Weighted Average Absolute Deviation, WAAD			
Pure Gases				
Methane	2.63			
Nitrogen	1.38			
CO_2	0.79			
Feed Mixture	*C_{ij} = 0.0*		*Generalized C_{ij}*	
Methane/Nitrogen	*Methane*	*Nitrogen*	*Methane*	*Nitrogen*
20/80	0.83	0.40	0.55	0.57
40/60	0.80	0.32	0.79	1.00
60/40	0.97	1.26	1.08	0.24
80/20	0.98	1.20	1.08	0.31
All Feed	0.89	0.80	0.88	0.53
Methane/CO_2	*Methane*	*CO_2*	*Methane*	*CO_2*
20/80	0.92	1.23	0.25	1.17
40/60	1.11	1.06	0.48	0.99
60/40	0.92	0.93	0.38	0.85
80/20	1.45	0.79	1.36	1.12
All Feed	1.10	1.00	0.62	1.03
Nitrogen/CO_2	*Nitrogen*	*CO_2*	*Nitrogen*	*CO_2*
20/80	0.53	1.09	0.45	1.06
40/60	0.56	1.50	0.37	1.43
60/40	0.57	1.18	0.57	1.13
80/20	0.54	0.72	0.74	0.72
All Feed	0.55	1.12	0.53	1.09

Table C.8 – Case 2: Summary Results for SLD-PR Modeling of Pure and Mixture Adsorption on Wet Tiffany Coal at 130°F

	Weighted Average Absolute Deviation, WAAD					
Pure Gases						
Methane	1.16					
Nitrogen	0.60					
CO_2	0.66					
Feed Mixture	*C_{ij} = 0.0*			*Generalized C_{ij}*		
Methane/Nitrogen	*Methane*	*Nitrogen*		*Methane*	*Nitrogen*	
50/50	2.40	1.61		2.16	0.51	
Methane/CO_2	*Methane*	*CO_2*		*Methane*	*CO_2*	
41/59	4.15	1.72		0.93	0.77	
Nitrogen/CO_2	*Nitrogen*	*CO_2*		*Nitrogen*	*CO_2*	
20/80	1.82	0.94		0.60	0.60	
Methane/Nitrogen /CO_2	*Methane*	*Nitrogen*	*CO_2*	*Methane*	*Nitrogen*	*CO_2*
10/40/50	0.64	2.67	1.55	0.44	0.97	1.05

Table C.9 –- Generalized Correlations of the EOS BIPs Using Nitrogen Excess Adsorption at 400 psia (Case 2)

$$C_{CH4-N2} = \frac{0.096}{n^{Ex}_{N2@400}} - 0.818$$

$$C_{CH4-CO2} = 44.98 \left(\frac{\chi_C^{\,2}}{\varepsilon_{ss}/k} \right) - 0.818$$

$$C_{N2-CO2} = 3.104 \left(\chi_C\right)^2 - 1.593$$

Table C.10 – Case 2: Regressed and Generalized EOS BIPs for CBM Gas Adsorption on Wet Illinois #6 Coal

	CH_4	**N_2**	**CO_2**
Surface Area, m^2/g	30.9	18.9	55.3
ε_{ss}/k, K	24.7		
Λ_b	-0.20		
Slit Length, nm	1.15		
	Regressed C_{ij}	**Generalized C_{ij}**	
Methane-Nitrogen	0.48	0.64	
Methane-CO_2	0.11	0.11	
Nitrogen-CO_2	-0.04	-0.01	

Table C.11 – Case 2: Regressed and Generalized EOS BIPs for CBM Gas Adsorption on Wet Fruitland OSU #1 Coal

	CH_4	**N_2**	**CO_2**
Surface Area, m^2/g	50.0	38.1	67.5
ε_{ss}/k, K	28.5		
Λ_b	-0.20		
Slit Length, nm	1.15		
	Regressed C_{ij}	**Generalized C_{ij}**	
Methane-Nitrogen	-0.33	-0.30	
Methane-CO_2	-0.08	-0.07	
Nitrogen-CO_2	-0.14	-0.13	

Table C.12 – Case 2: Regressed and Generalized EOS BIPs for CBM Gas Adsorption on Wet Tiffany Coal

	CH_4	**N_2**	**CO_2**
Surface Area, m^2/g	27.8	18.7	36.4
ε_{ss}/k, K	26.4		
Λ_b	-0.20		
Slit Length, nm	1.15		
	Regressed C_{ij}	**Generalized C_{ij}**	
Methane-Nitrogen	0.49	0.49	
Methane-CO_2	-0.31	-0.32	
Nitrogen-CO_2	-0.66	-0.75	

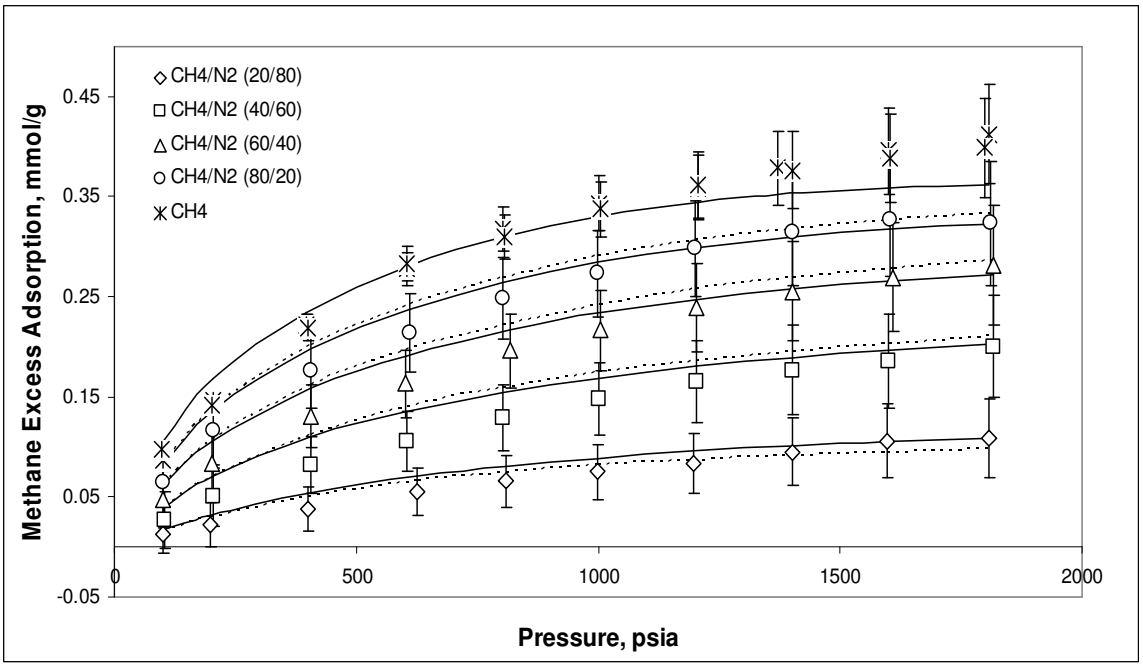

Figure C.1 – Case 2
Methane Adsorption in Methane/Nitrogen Mixtures on Wet Illinois #6 Coal at 115°F (Solid Line – C_{ij} = 0.0, Dashed Line – Generalized C_{ij})

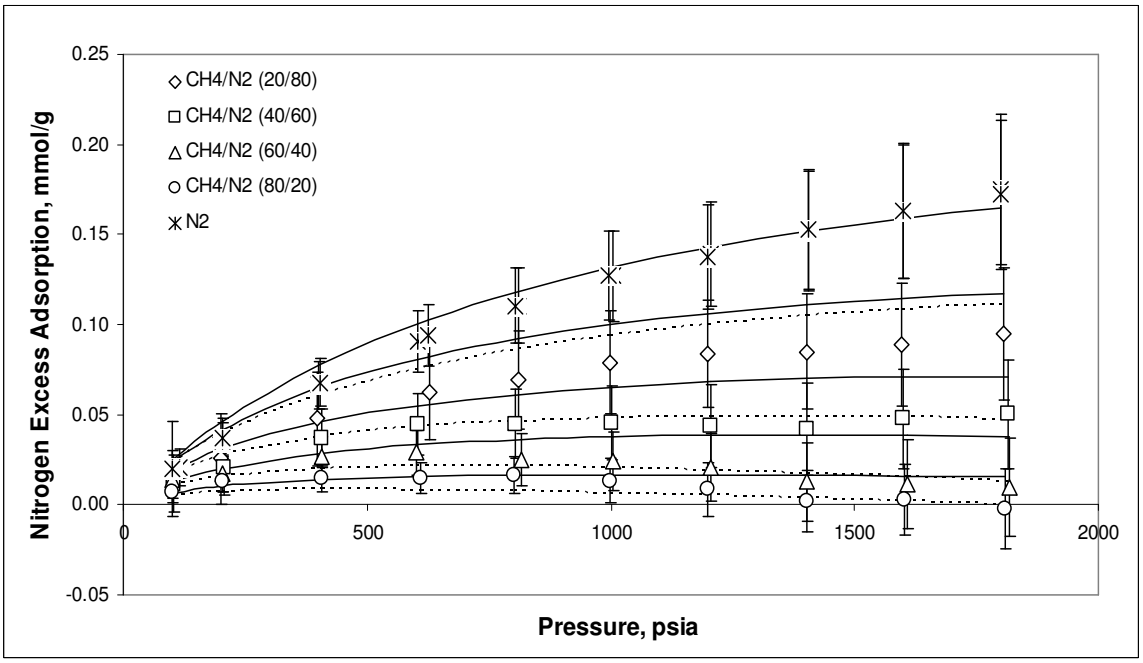

Figure C.2 – Case 2
Nitrogen Adsorption in Methane/Nitrogen Mixtures on Wet Illinois #6 Coal at 115°F (Solid Line – C_{ij} = 0.0, Dashed Line – Generalized C_{ij})

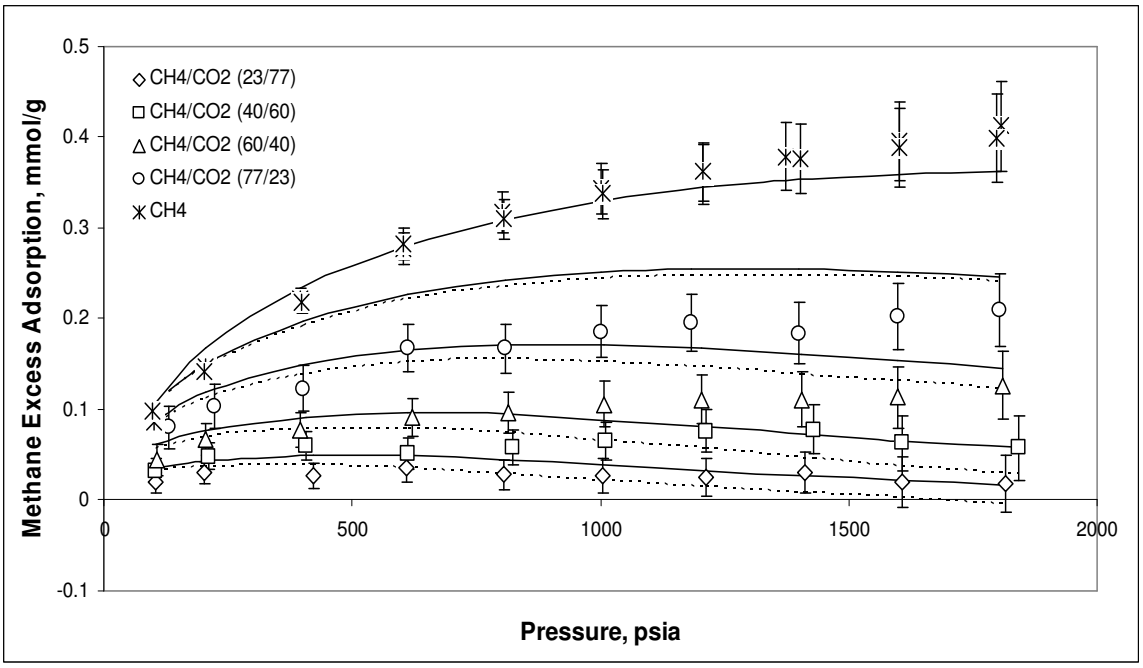

Figure C.3 – Case 2
Methane Adsorption in Methane/CO_2 Mixtures on Wet Illinois #6 Coal at 115°F
(Solid Line – C_{ij} = 0.0, Dashed Line – Generalized C_{ij})

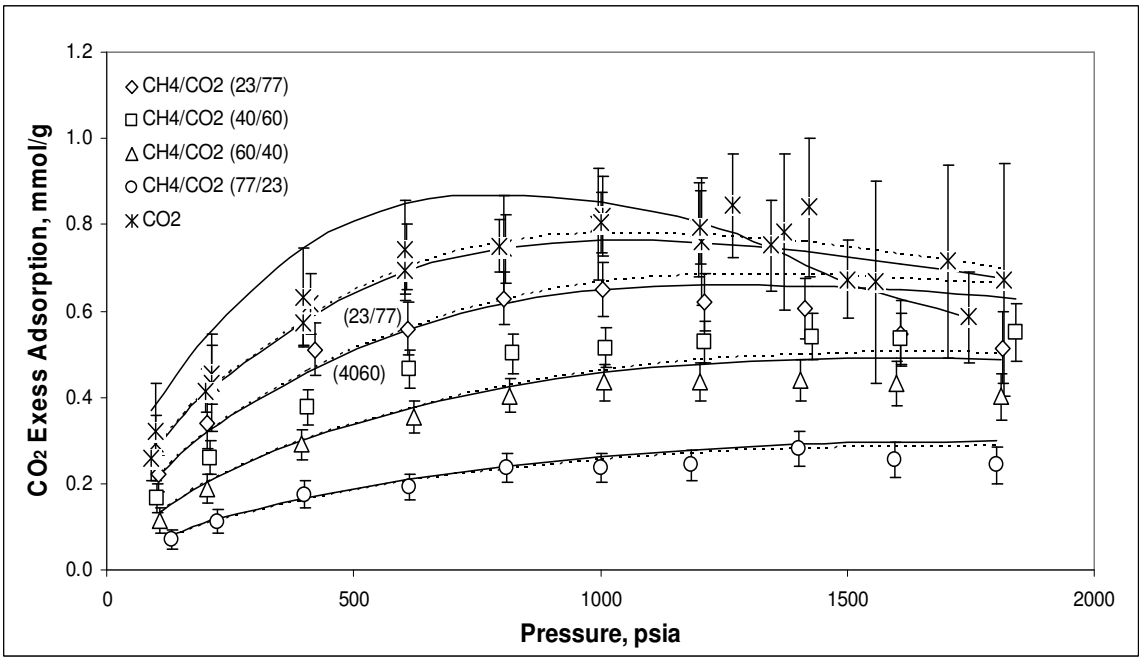

Figure C.4 – Case 2
CO_2 Adsorption in Methane/CO_2 Mixtures on Wet Illinois #6 Coal at 115°F
(Solid Line – C_{ij} = 0.0, Dashed Line – Generalized C_{ij})

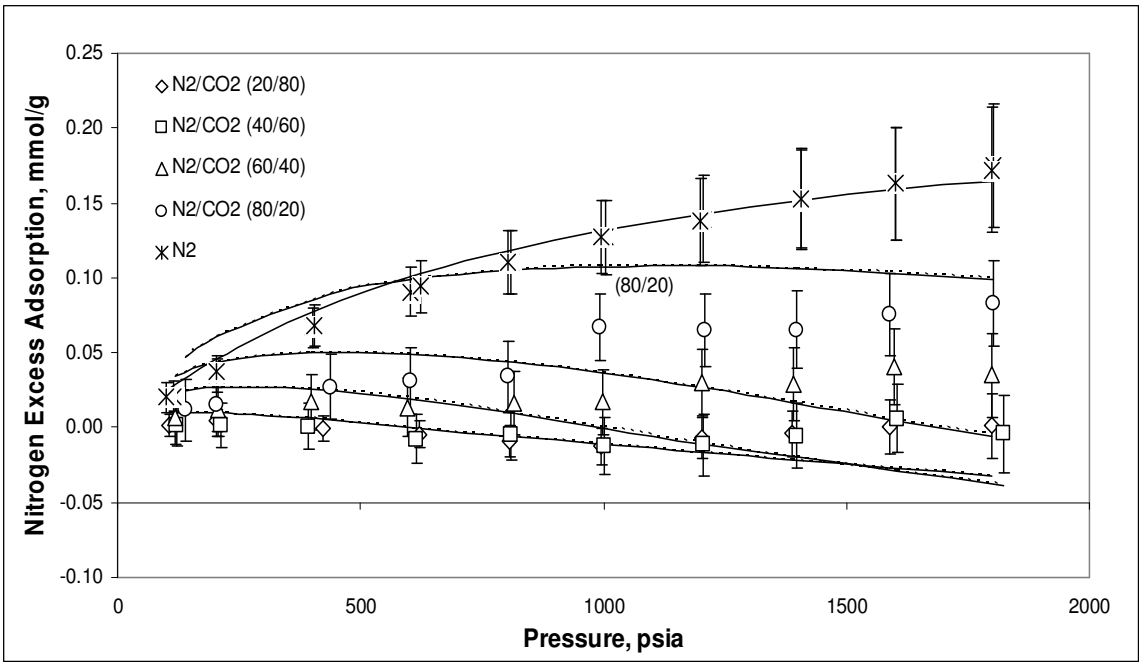

Figure C.5 – Case 2
Nitrogen Adsorption in Nitrogen/CO_2 Mixtures on Wet Illinois #6 Coal at 115°F
(Solid Line – C_{ij} = 0.0, Dashed Line – Generalized C_{ij})

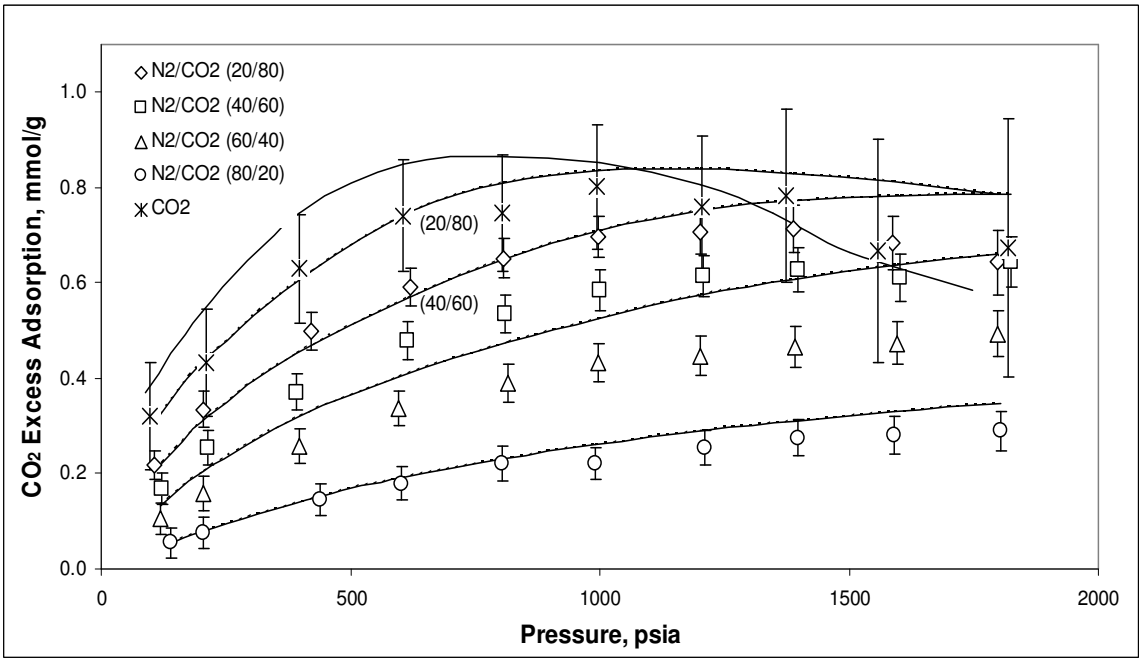

Figure C.6 – Case 2
CO_2 Adsorption in Nitrogen/CO_2 Mixtures on Wet Illinois #6 Coal at 115°F
(Solid Line – C_{ij} = 0.0, Dashed Line – Generalized C_{ij})

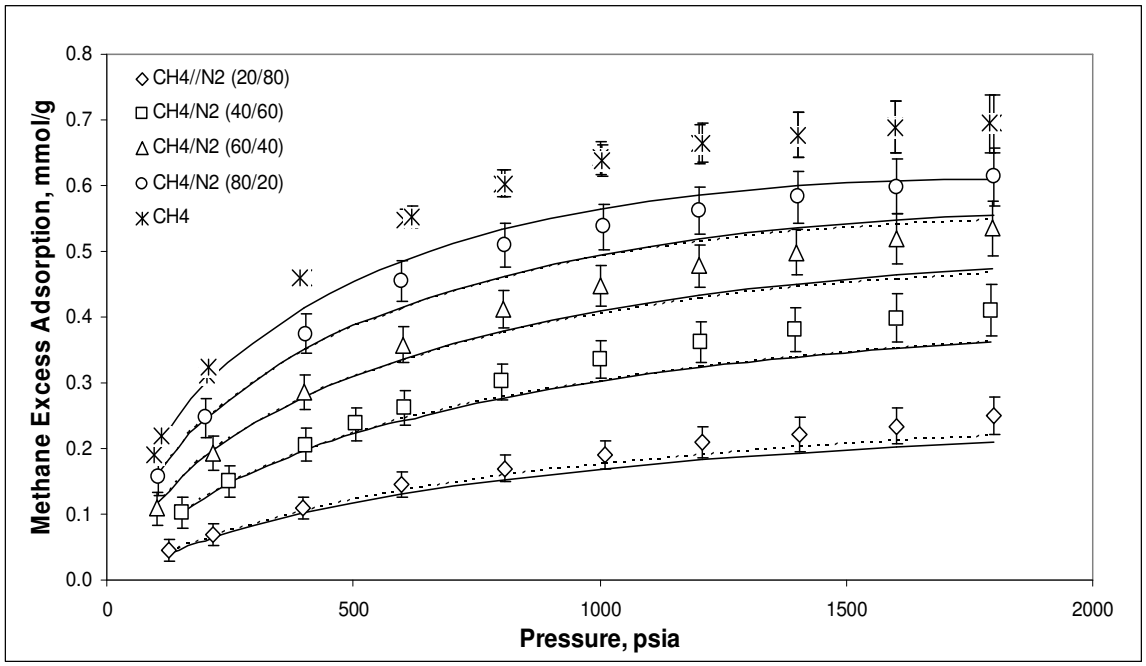

Figure C.7 – Case 2
Methane Adsorption in Methane/Nitrogen Mixtures on Wet Fruitland OSU #1 Coal at 115°F (Solid Line – C_{ij} = 0.0, Dashed Line – Generalized C_{ij})

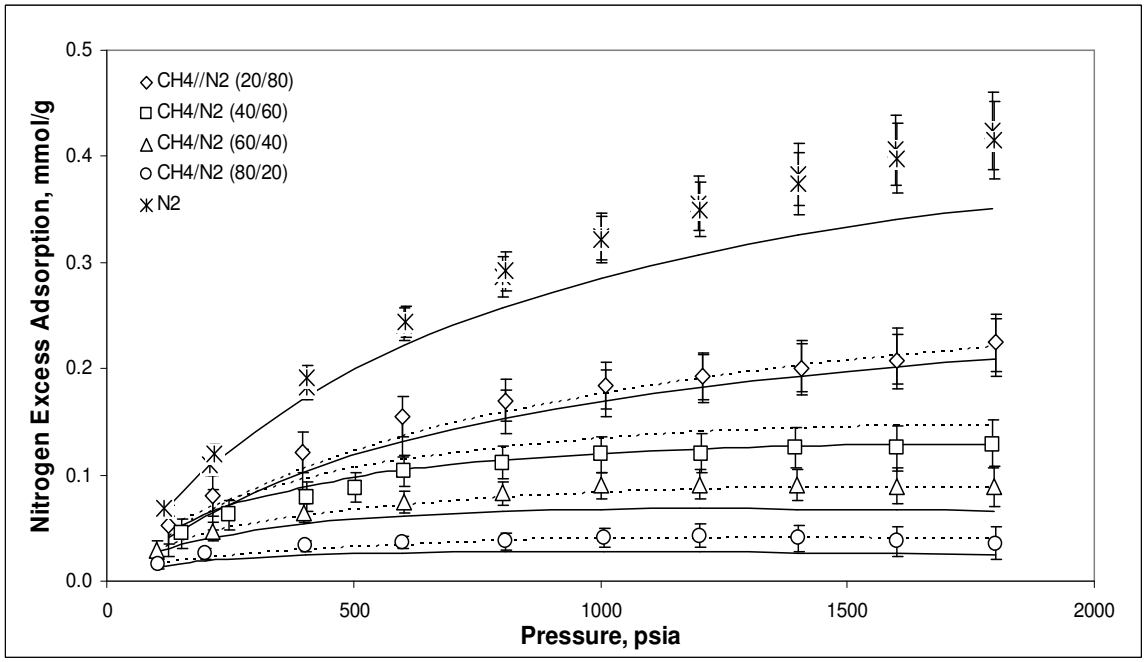

Figure C.8 – Case 2
Nitrogen Adsorption in Methane/Nitrogen Mixtures on Wet Fruitland OSU #1 Coal at 115°F (Solid Line – C_{ij} = 0.0, Dashed Line – Generalized C_{ij})

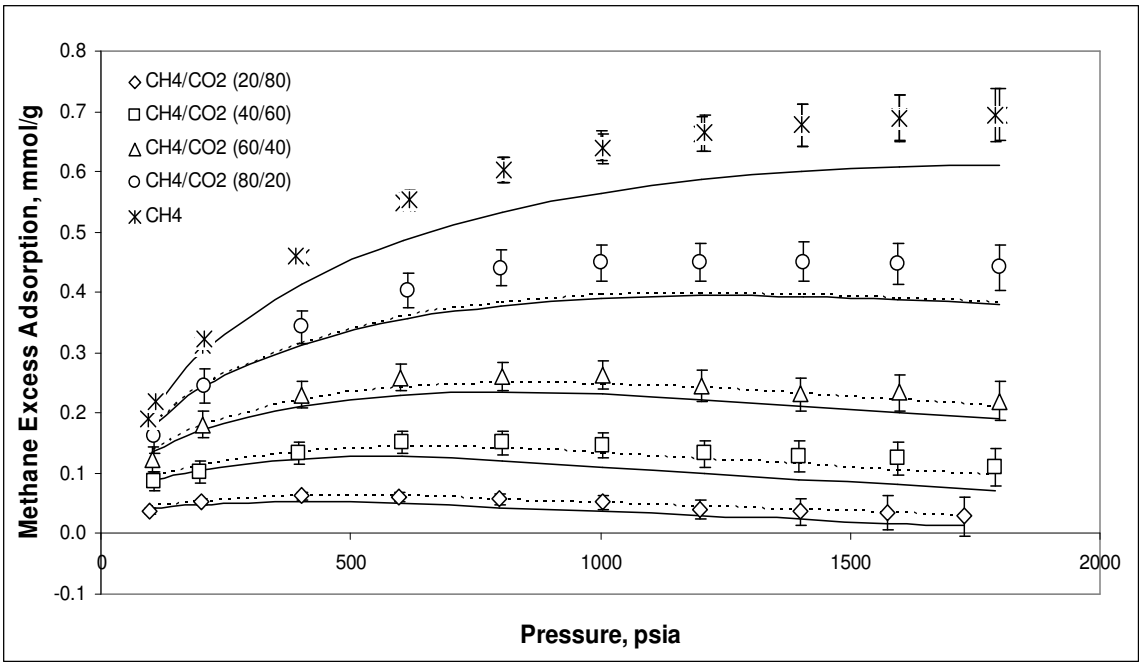

Figure C.9 – Case 2
Methane Adsorption in Methane/CO_2 Mixtures on Wet Fruitland OSU #1 Coal at 115°F (Solid Line – C_{ij} = 0.0, Dashed Line – Generalized C_{ij})

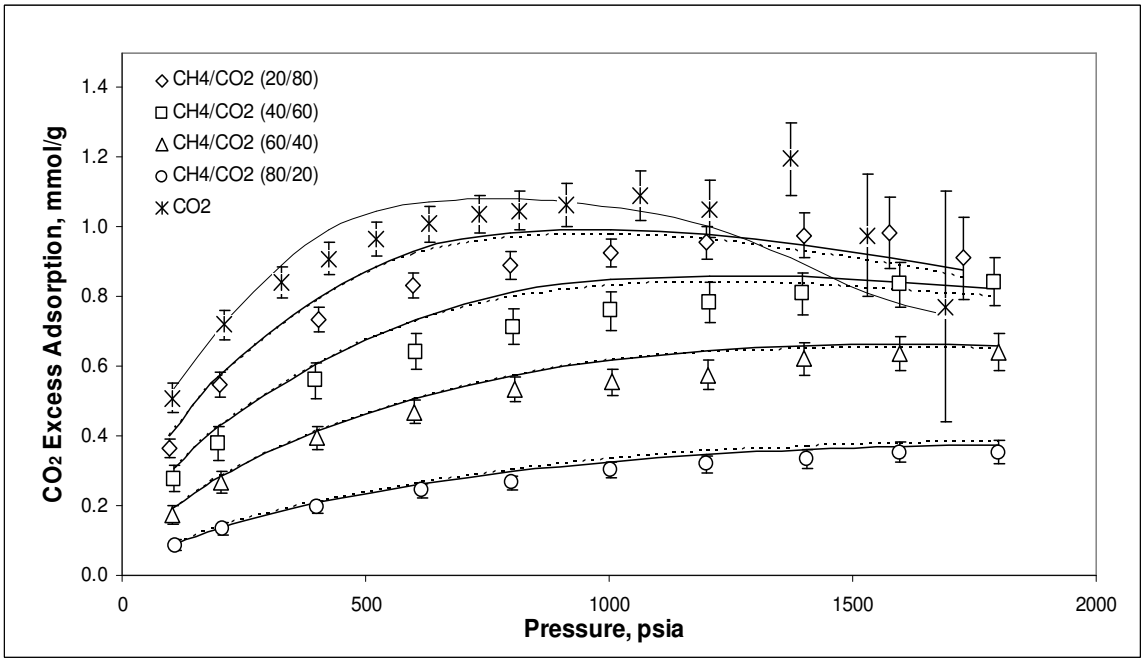

Figure C.10 – Case 2
CO_2 Adsorption in Methane/CO_2 Mixtures on Wet Fruitland OSU #1 Coal at 115°F (Solid Line – C_{ij} = 0.0, Dashed Line – Generalized C_{ij})

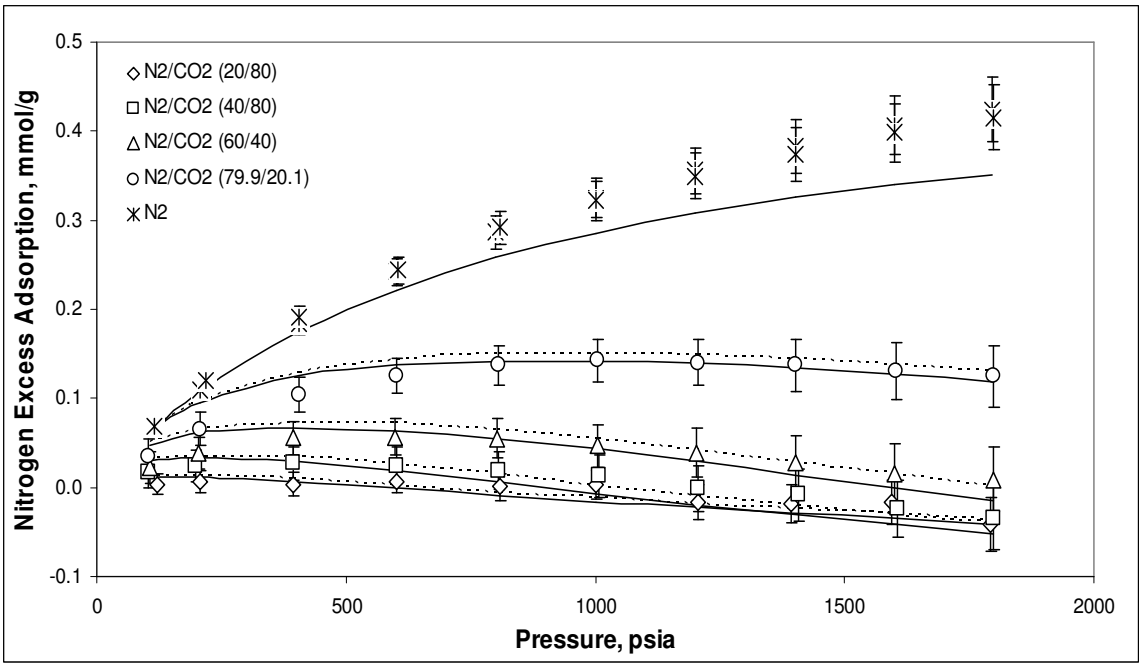

Figure C.11 – Case 2
Nitrogen Adsorption in Nitrogen/CO_2 Mixtures on Wet Fruitland OSU #1 Coal at 115°F (Solid Line – C_{ij} = 0.0, Dashed Line – Generalized C_{ij})

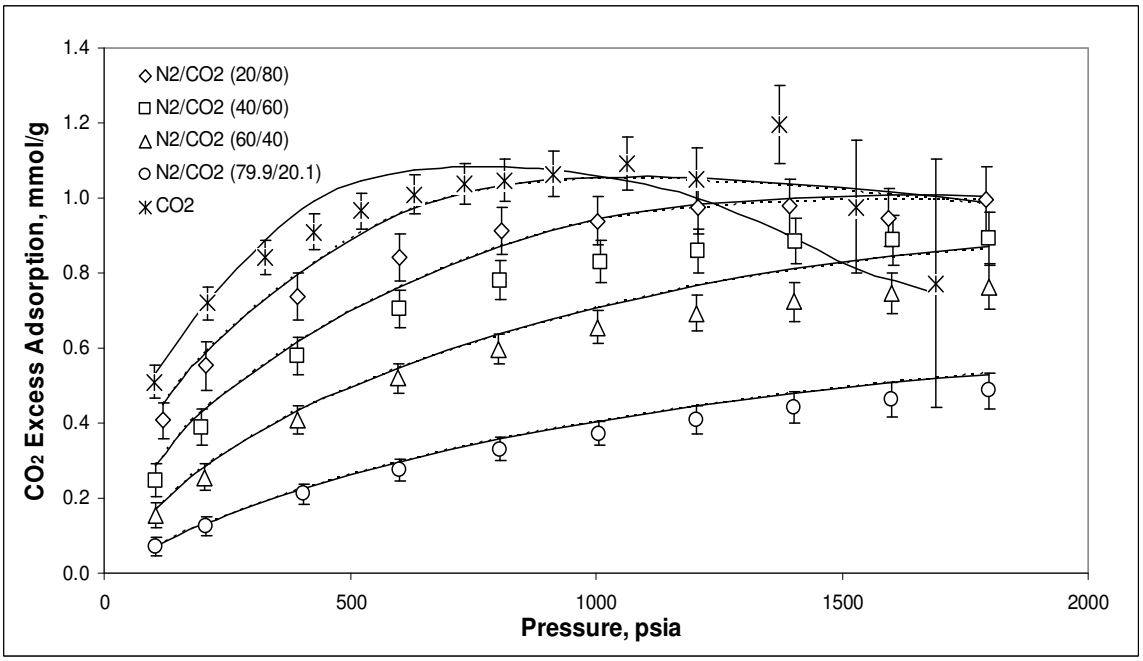

Figure C.12 – Case 2
CO_2 Adsorption in Nitrogen/CO_2 Mixtures on Wet Fruitland OSU #1 Coal at 115°F (Solid Line – C_{ij} = 0.0, Dashed Line – Generalized C_{ij})

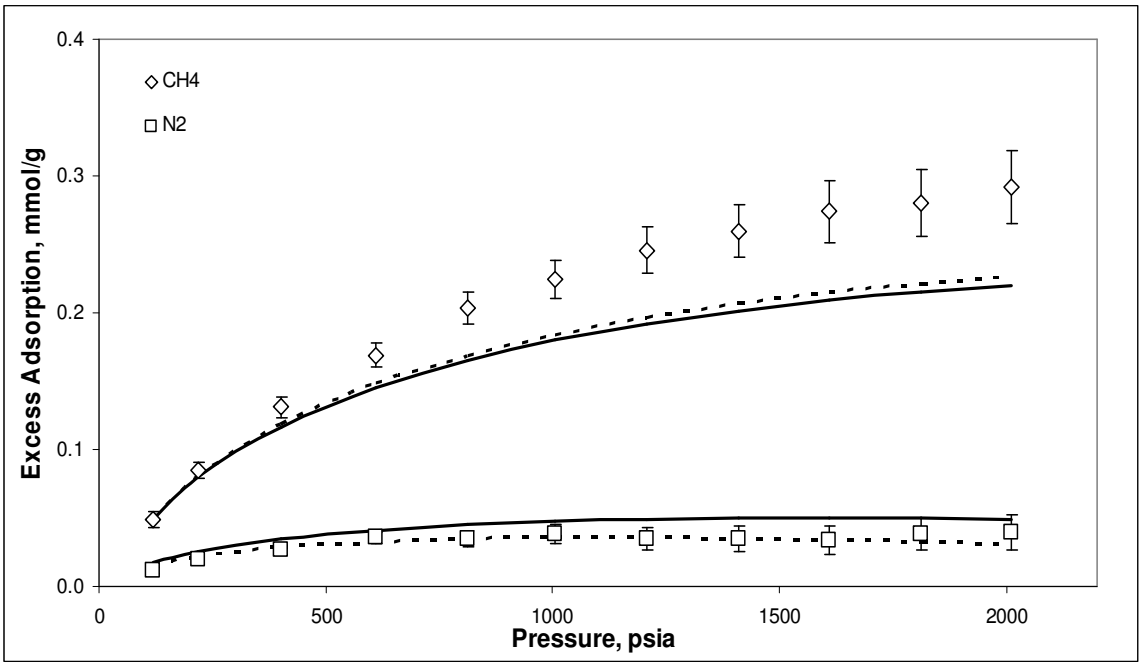

Figure C.13 – Case 2
Methane/Nitrogen 50/50 Feed Gas Adsorption on Wet Tiffany Coal at 130°F
(Solid Line – C_{ij} = 0.0, Dashed Line – Generalized C_{ij})

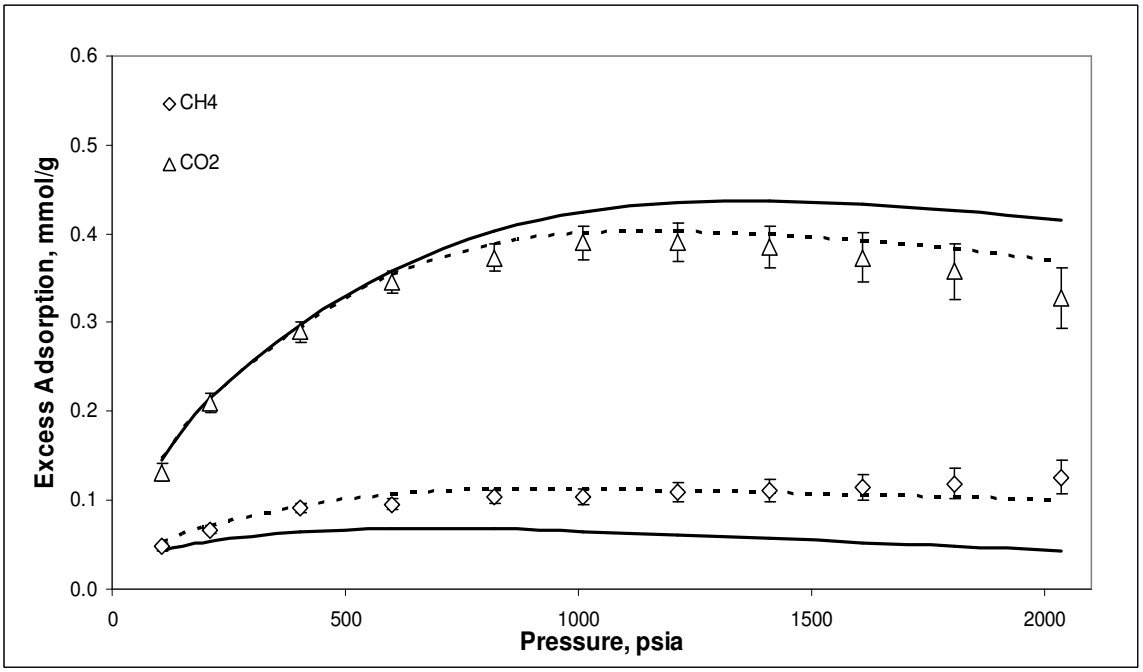

Figure C.14 – Case 2
Methane/CO_2 41/59 Feed Gas Adsorption on Wet Tiffany Coal at 130°F
(Solid Line – C_{ij} = 0.0, Dashed Line – Generalized C_{ij})

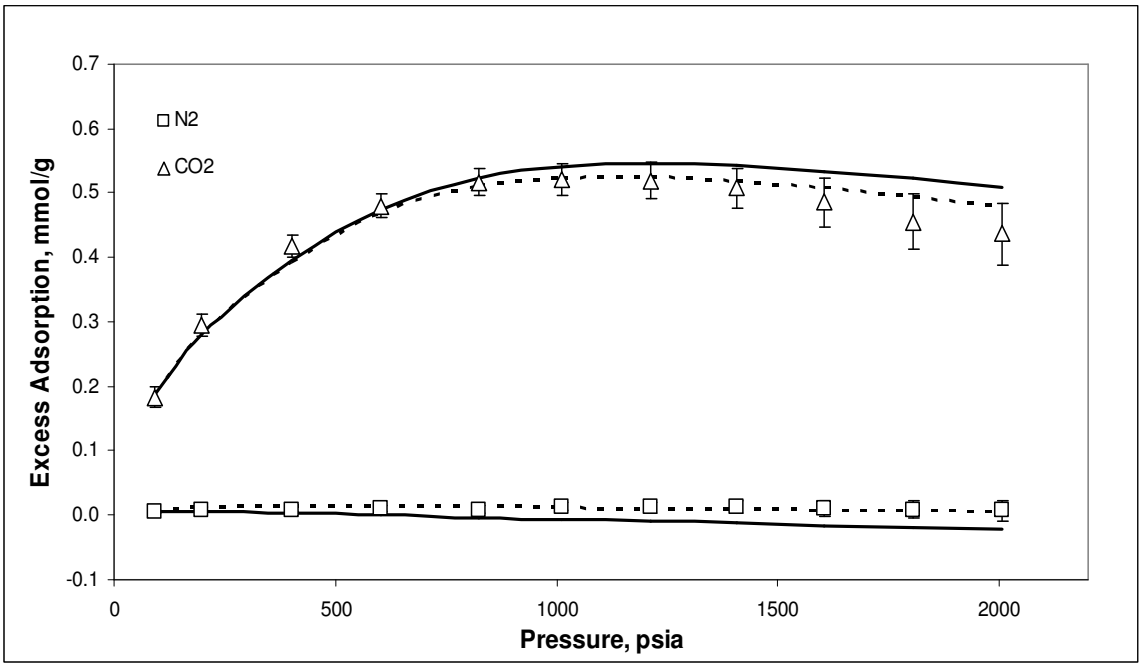

Figure C.15 – Case 2
Nitrogen/CO_2 20/80 Feed Gas Adsorption on Wet Tiffany Coal at 130°F
(Solid Line – C_{ij} = 0.0, Dashed Line – Generalized C_{ij})

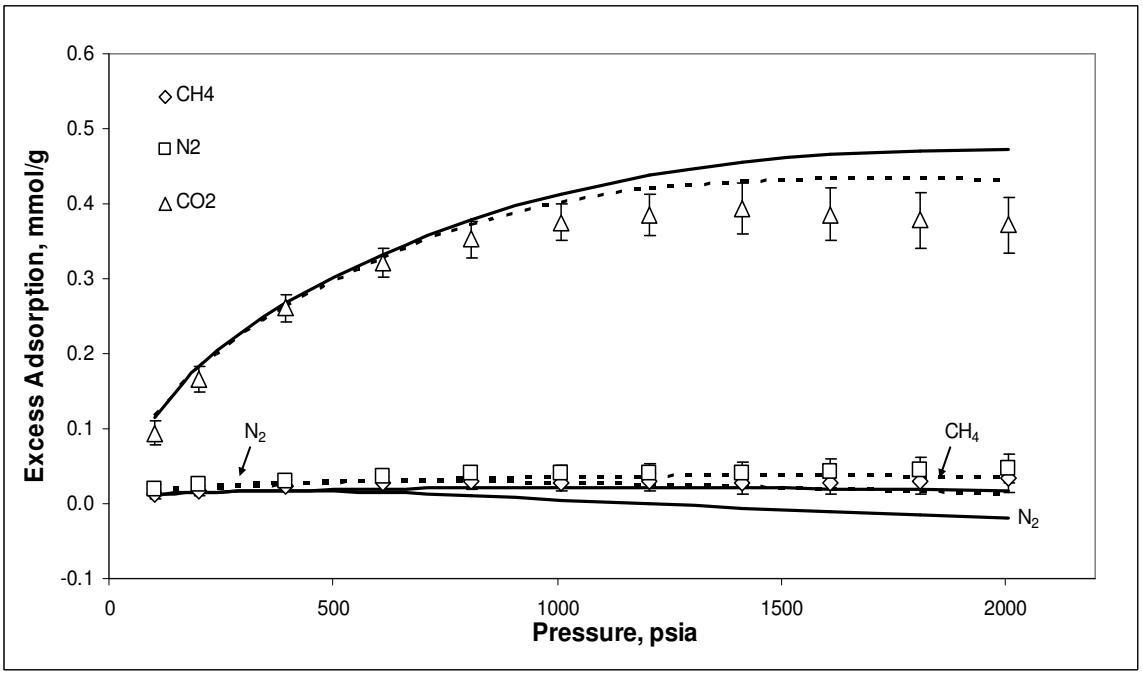

Figure C.16 – Case 2
Methane/Nitrogen/CO_2 10/40/50 Feed Gas Adsorption on Wet Tiffany Coal at 130°F
(Solid Line – C_{ij} = 0.0, Dashed Line – Generalized C_{ij})

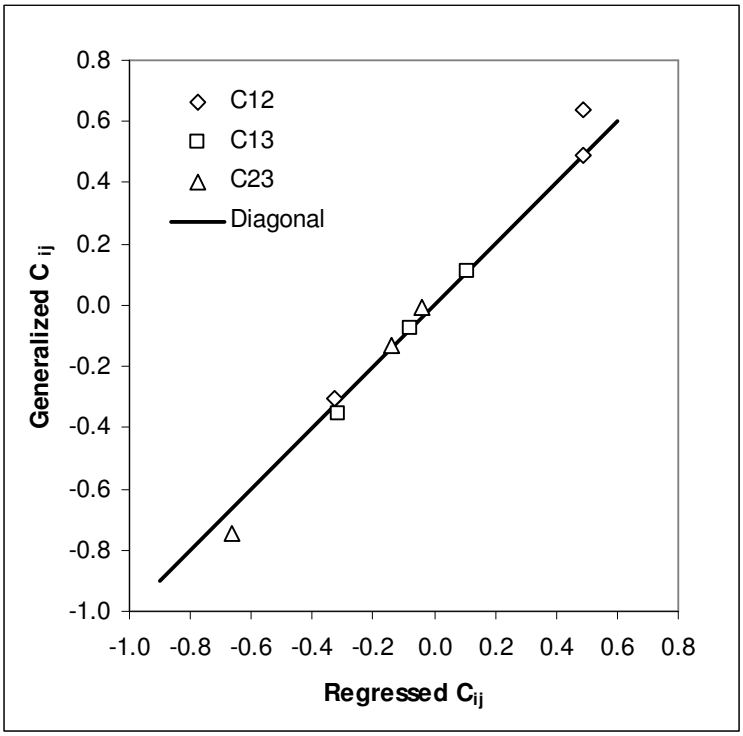

Figure C.17 – Case 2: Comparison of the Regressed and Generalized SLD-PR Binary Interaction Parameters (1 – Methane, 2 – Nitrogen, 3 – CO_2)

Appendix C.4 – Generalization of Mixed-Gas Adsorption Using CO_2 Excess Adsorption

This section presents the results of the mixture adsorption on wet coals by using the SLD-PR generalized parameters from the CO_2 correlations (Case 3). The weighted average absolute deviations (WAAD) of the pure and mixed-gas adsorption on wet coals are listed and the generalized predictions of all components adsorption in the mixed-gas adsorption are also plotted. The tables and figures are arranged as was done previously for methane.

Table C.13 – Case 3: Summary Results for SLD-PR Modeling of Pure and Binary Mixture Adsorption on Wet Illinois #6 Coal at 115°F

	Weighted Average Absolute Deviation, WAAD			
Pure Gases				
Methane	2.74			
Nitrogen	0.26			
CO_2	0.62			
Feed Mixture	*C_{ij} = 0.0*		*Generalized C_{ij}*	
Methane/Nitrogen	*Methane*	*Nitrogen*	*Methane*	*Nitrogen*
20/80	0.46	1.02	0.31	0.93
40/60	0.97	1.31	1.00	0.94
60/40	1.14	1.15	1.24	0.62
80/20	1.27	0.65	1.35	0.27
All Feed	0.96	1.03	0.97	0.69
Methane/CO_2	*Methane*	*CO_2*	*Methane*	*CO_2*
20/80	0.43	0.37	0.59	0.51
40/60	0.81	0.51	0.83	0.74
60/40	1.94	0.38	1.19	0.44
80/20	2.01	0.42	1.78	0.33
All Feed	1.30	0.42	1.10	0.50
Nitrogen/CO_2	*Nitrogen*	*CO_2*	*Nitrogen*	*CO_2*
20/80	0.72	0.30	0.72	0.30
40/60	0.98	0.26	0.98	0.25
60/40	1.00	0.49	1.00	0.49
80/20	1.39	0.33	1.41	0.33
All Feed	1.02	0.34	1.03	0.34

Table C.14 – Case 3: Summary Results for SLD-PR Modeling of Pure and Binary Mixture Adsorption on Wet Fruitland OSU #1 Coal at 115°F

	Weighted Average Absolute Deviation, WAAD			
Pure Gases				
Methane	0.63			
Nitrogen	1.65			
CO_2	0.60			
Feed Mixture	$C_{ij} = 0.0$		*Generalized* C_{ij}	
Methane/Nitrogen	*Methane*	*Nitrogen*	*Methane*	*Nitrogen*
20/80	0.82	1.02	0.80	1.04
40/60	0.33	1.26	0.33	1.31
60/40	0.19	0.34	0.18	0.27
80/20	0.57	0.53	0.56	0.45
All Feed	0.47	0.79	0.46	0.77
Methane/CO_2	*Methane*	*CO_2*	*Methane*	*CO_2*
20/80	0.77	0.69	0.31	0.71
40/60	0.88	0.65	0.19	0.63
60/40	0.46	0.61	0.30	0.61
80/20	0.57	0.84	0.51	1.20
All Feed	0.67	0.70	0.33	0.79
Nitrogen/CO_2	*Nitrogen*	*CO_2*	*Nitrogen*	*CO_2*
20/80	0.46	0.60	0.40	0.58
40/60	0.40	0.66	0.27	0.63
60/40	0.39	0.41	0.52	0.39
80/20	0.36	0.16	0.57	0.15
All Feed	0.41	0.46	0.44	0.44

Table C.15 – Case 3: Summary Results for SLD-PR Modeling of Pure and Mixture Adsorption on Wet Tiffany Coal at 130°F

	Weighted Average Absolute Deviation, WAAD					
Pure Gases						
Methane	1.01					
Nitrogen	1.17					
CO_2	0.68					
Feed Mixture	$C_{ij} = 0.0$			*Generalized* C_{ij}		
Methane/Nitrogen	*Methane*	*Nitrogen*		*Methane*	*Nitrogen*	
50/50	2.97	1.64		2.74	0.45	
Methane/CO_2	*Methane*	*CO_2*		*Methane*	*CO_2*	
41/59	4.08	1.29		0.66	0.70	
Nitrogen/CO_2	*Nitrogen*	*CO_2*		*Nitrogen*	*CO_2*	
20/80	1.73	1.26		0.60	1.08	
Methane/Nitrogen /CO_2	*Methane*	*Nitrogen*	*CO_2*	*Methane*	*Nitrogen*	*CO_2*
10/40/50	0.66	2.56	1.03	0.29	1.54	0.80

Table C.16 –- Generalized Correlations of the EOS BIPs Using CO_2 Excess Adsorption at 400 psia (Case 3)

$$C_{CH4-N2} = \frac{1.582}{\sqrt{n^{Ex}_{CO2@400}}} - 1.686$$

$$C_{CH4-CO2} = 0.074\left(\frac{Car}{\varepsilon_{ss}/k}\right)^2 - 0.695$$

$$C_{N2-CO2} = 2.153\left(\chi_C\right)^2 - 1.113$$

Table C.17 – Case 3: Regressed and Generalized EOS BIPs for CBM Gas Adsorption on Wet Illinois #6 Coal

	CH_4	**N_2**	**CO_2**
Surface Area, m^2/g	40.3	20.5	48.0
ε_{ss}/k, K	21.0		
Λ_b	-0.20		
Slit Length, nm	1.15		
	Regressed C_{ij}	**Generalized C_{ij}**	
Methane-Nitrogen	0.77	0.34	
Methane-CO_2	0.10	0.16	
Nitrogen-CO_2	0.01	-0.01	

Table C.18 – Case 3: Regressed and Generalized EOS BIPs for CBM Gas Adsorption on Wet Fruitland OSU #1 Coal

	CH_4	**N_2**	**CO_2**
Surface Area, m^2/g	62.3	42.0	67.6
ε_{ss}/k, K	23.7		
Λ_b	-0.20		
Slit Length, nm	1.15		
	Regressed C_{ij}	**Generalized C_{ij}**	
Methane-Nitrogen	-0.07	-0.02	
Methane-CO_2	-0.06	-0.07	
Nitrogen-CO_2	-0.10	-0.10	

Table C.19 – Case 3: Regressed and Generalized EOS BIPs for CBM Gas Adsorption on Wet Tiffany Coal

	CH_4	**N_2**	**CO_2**
Surface Area, m^2/g	30.1	19.8	37.2
ε_{ss}/k, K	22.3		
Λ_b	-0.20		
Slit Length, nm	1.15		
	Regressed C_{ij}	**Generalized C_{ij}**	
Methane-Nitrogen	0.66	0.62	
Methane-CO_2	-0.34	-0.30	
Nitrogen-CO_2	-0.52	-0.52	

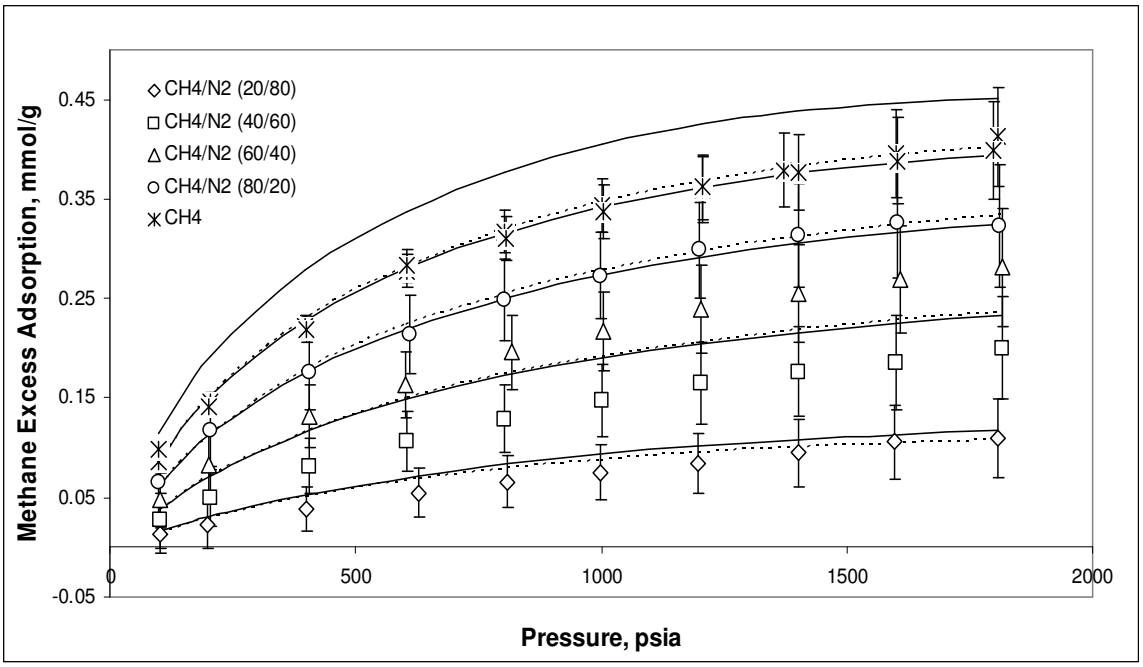

Figure C.18 – Case 3
Methane Adsorption in Methane/Nitrogen Mixtures on Wet Illinois #6 Coal at 115°F (Solid Line – C_{ij} = 0.0, Dashed Line – Generalized C_{ij})

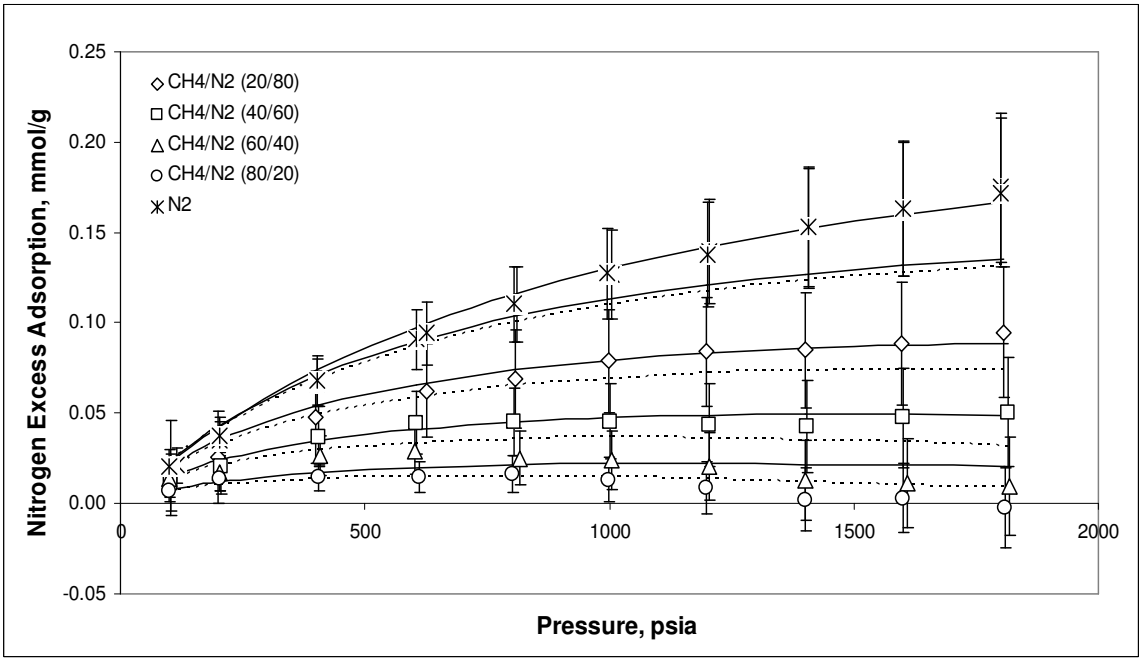

Figure C.19 – Case 3
Nitrogen Adsorption in Methane/Nitrogen Mixtures on Wet Illinois #6 Coal at 115°F (Solid Line – C_{ij} = 0.0, Dashed Line – Generalized C_{ij})

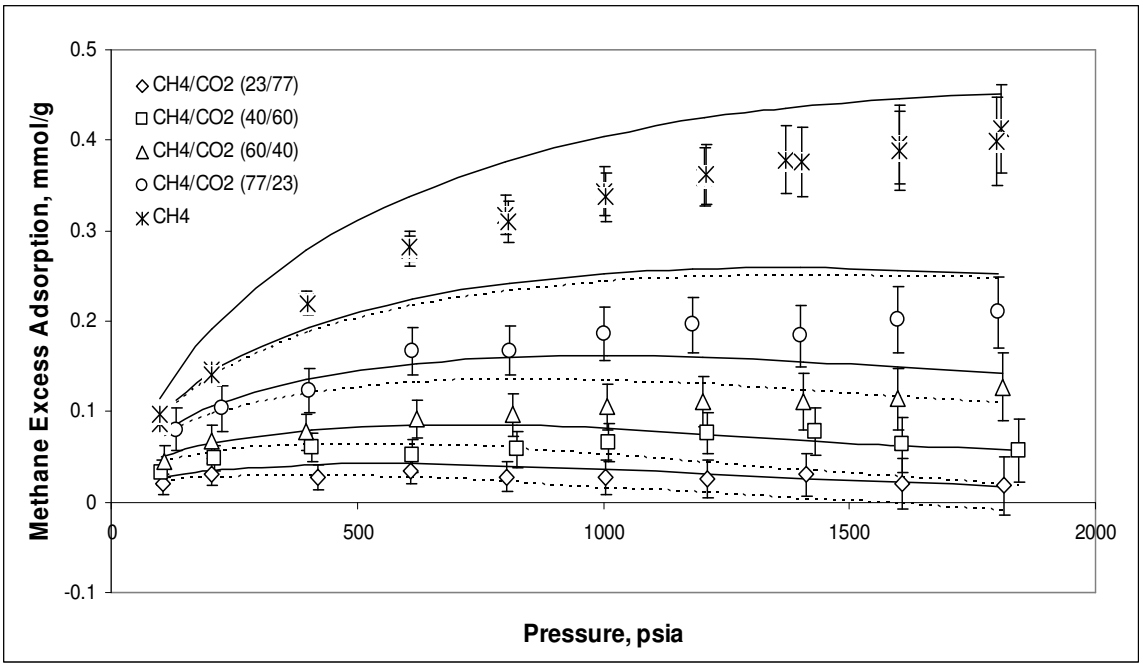

Figure C.20 – Case 3
Methane Adsorption in Methane/CO_2 Mixtures on Wet Illinois #6 Coal at 115°F
(Solid Line – C_{ij} = 0.0, Dashed Line – Generalized C_{ij})

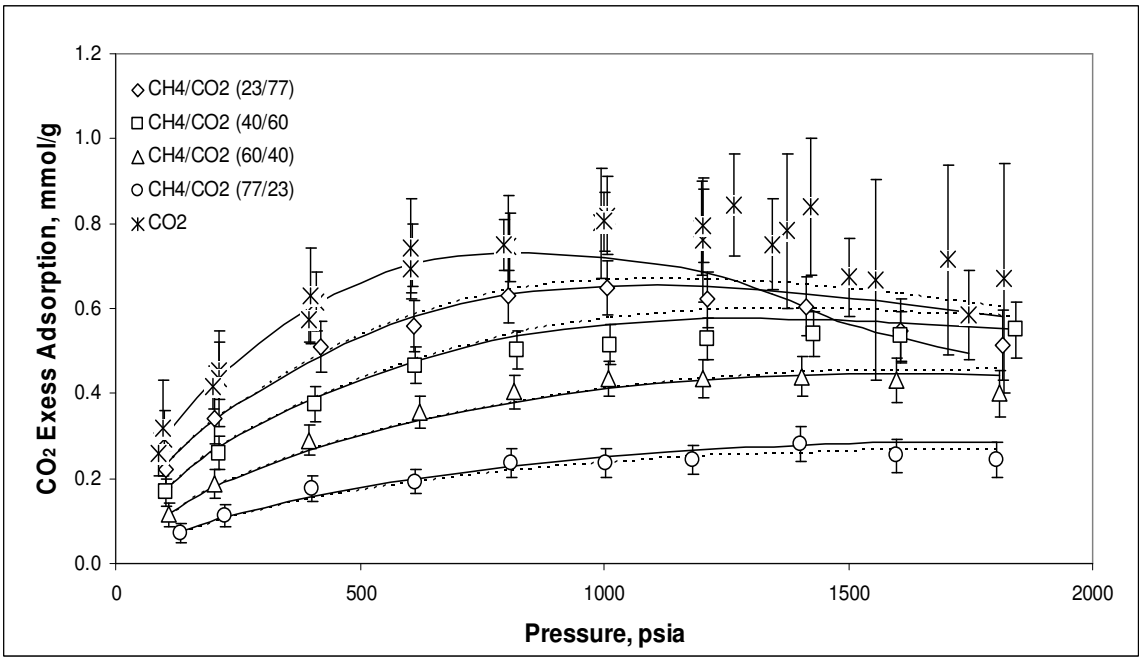

Figure C.21 – Case 3
CO_2 Adsorption in Methane/CO_2 Mixtures on Wet Illinois #6 Coal at 115°F
(Solid Line – C_{ij} = 0.0, Dashed Line – Generalized C_{ij})

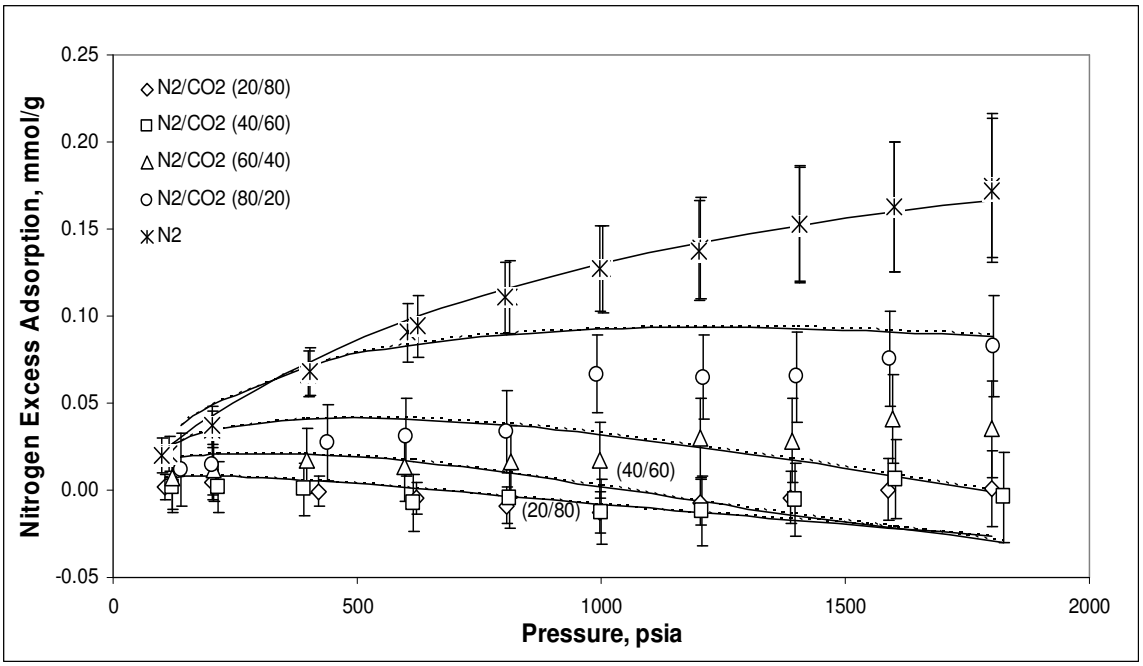

Figure C.22 – Case 3
Nitrogen Adsorption in Nitrogen/CO_2 Mixtures on Wet Illinois #6 Coal at 115°F
(Solid Line – C_{ij} = 0.0, Dashed Line – Generalized C_{ij})

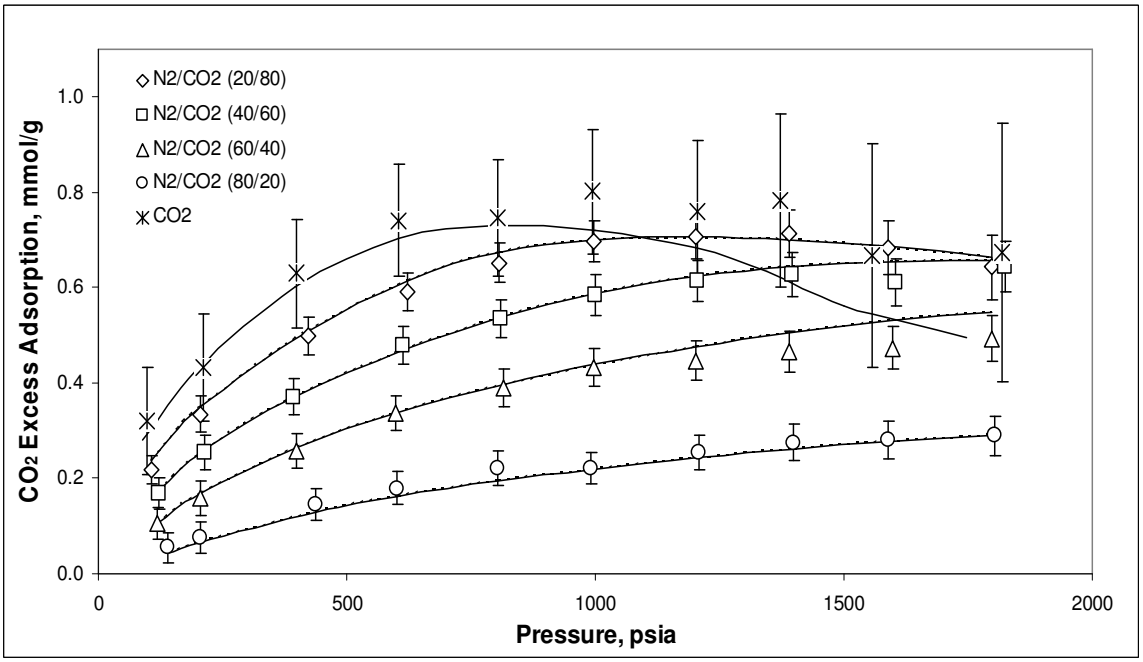

Figure C.23 – Case 3
CO_2 Adsorption in Nitrogen/CO_2 Mixtures on Wet Illinois #6 Coal at 115°F
(Solid Line – C_{ij} = 0.0, Dashed Line – Generalized C_{ij})

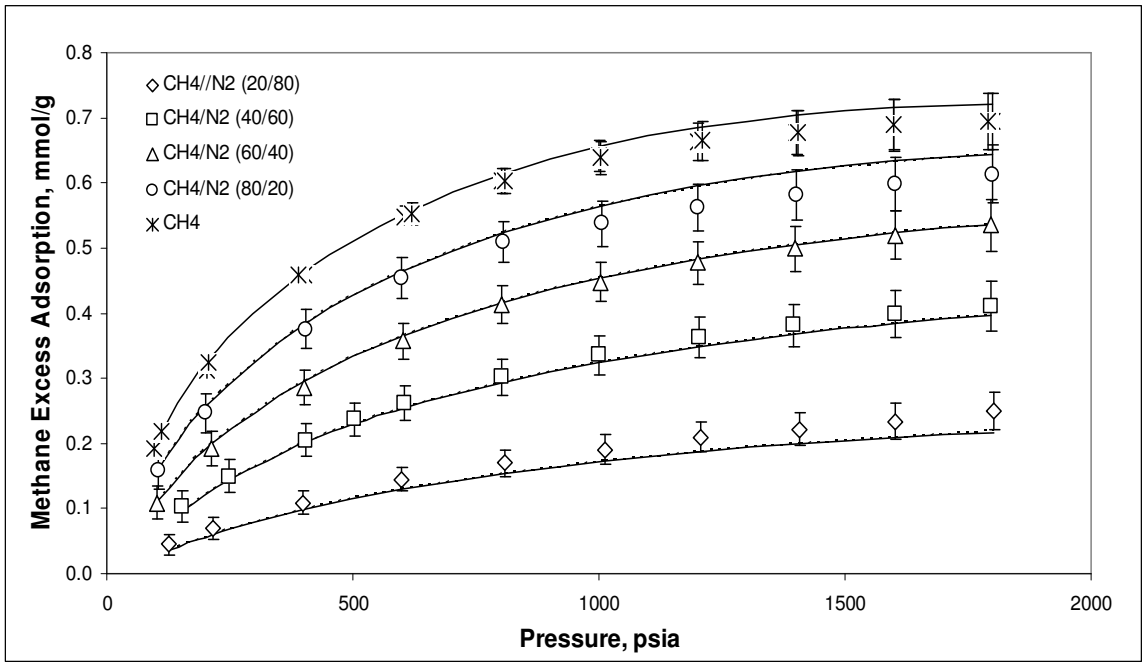

Figure C.24 – Case 3
Methane Adsorption in Methane/Nitrogen Mixtures on Wet Fruitland OSU #1 Coal at 115°F (Solid Line – C_{ij} = 0.0, Dashed Line – Generalized C_{ij})

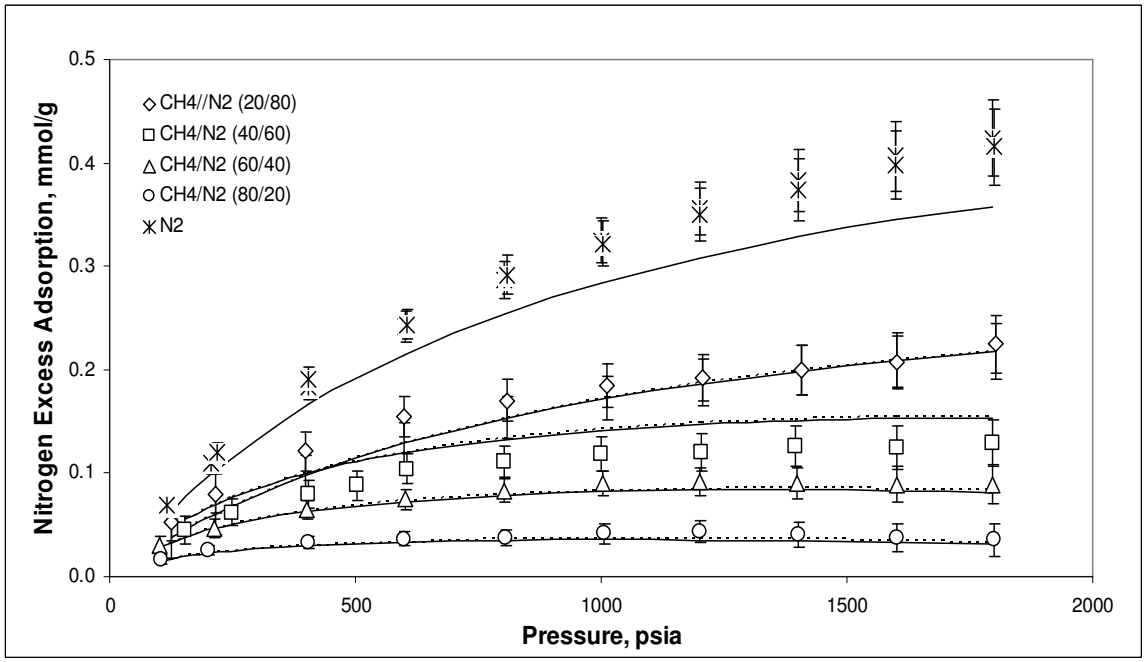

Figure C.25 – Case 3
Nitrogen Adsorption in Methane/Nitrogen Mixtures on Wet Fruitland OSU #1 Coal at 115°F (Solid Line – C_{ij} = 0.0, Dashed Line – Generalized C_{ij})

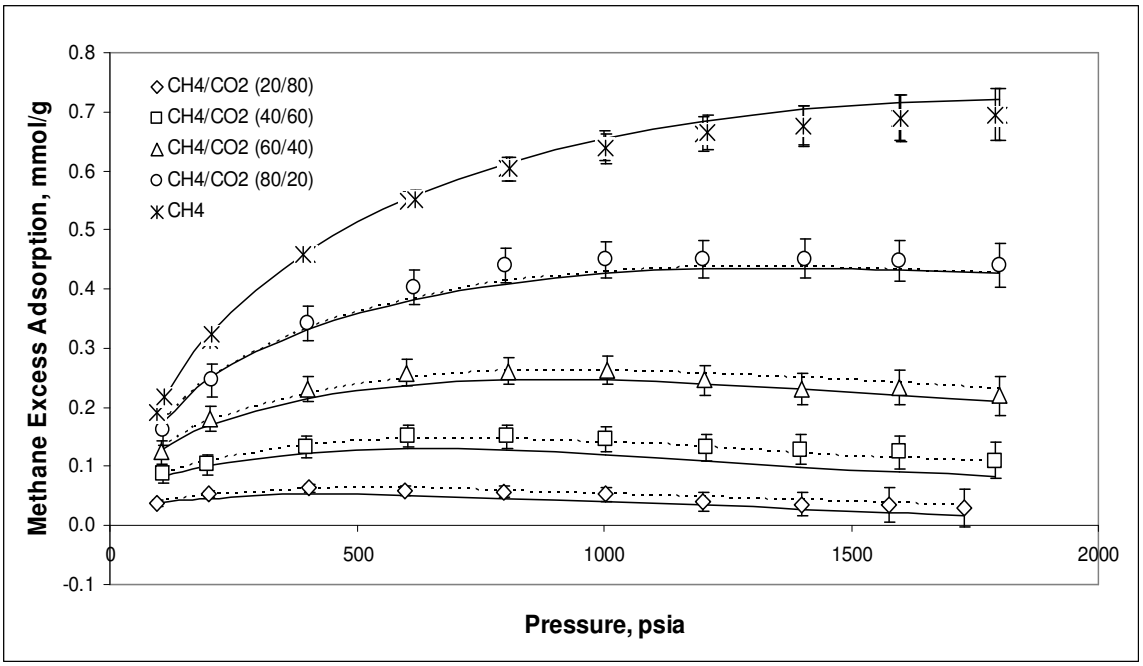

Figure C.26 – Case 3
Methane Adsorption in Methane/CO_2 Mixtures on Wet Fruitland OSU #1 Coal at 115°F (Solid Line – C_{ij} = 0.0, Dashed Line – Generalized C_{ij})

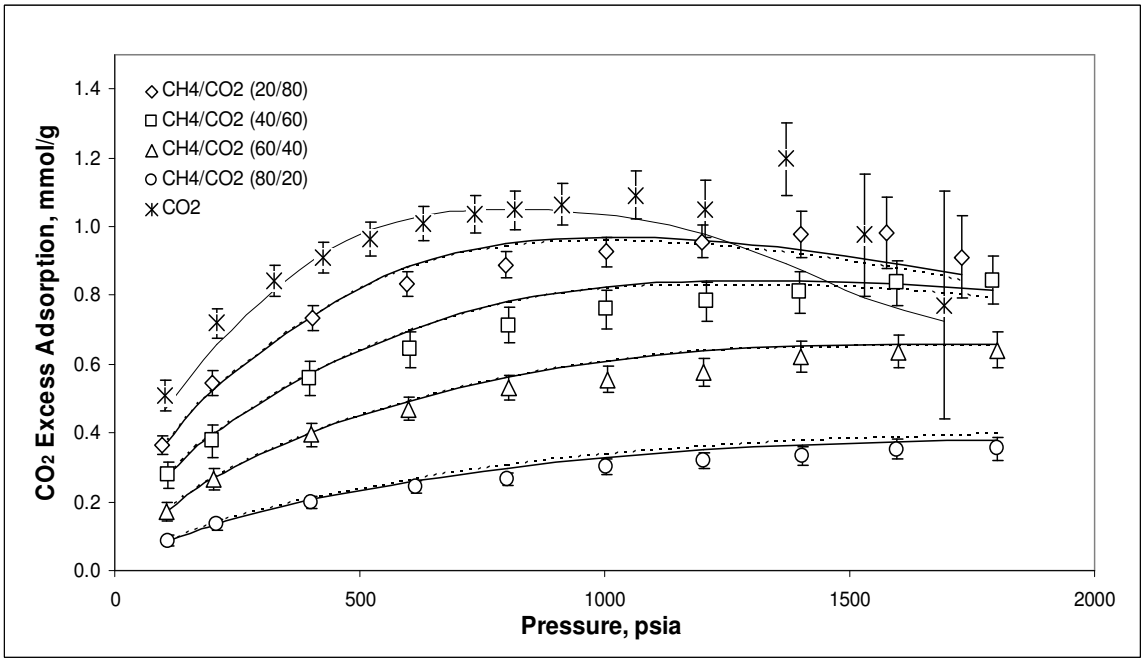

Figure C.27 – Case 3
CO_2 Adsorption in Methane/CO_2 Mixtures on Wet Fruitland OSU #1 Coal at 115°F (Solid Line – C_{ij} = 0.0, Dashed Line – Generalized C_{ij})

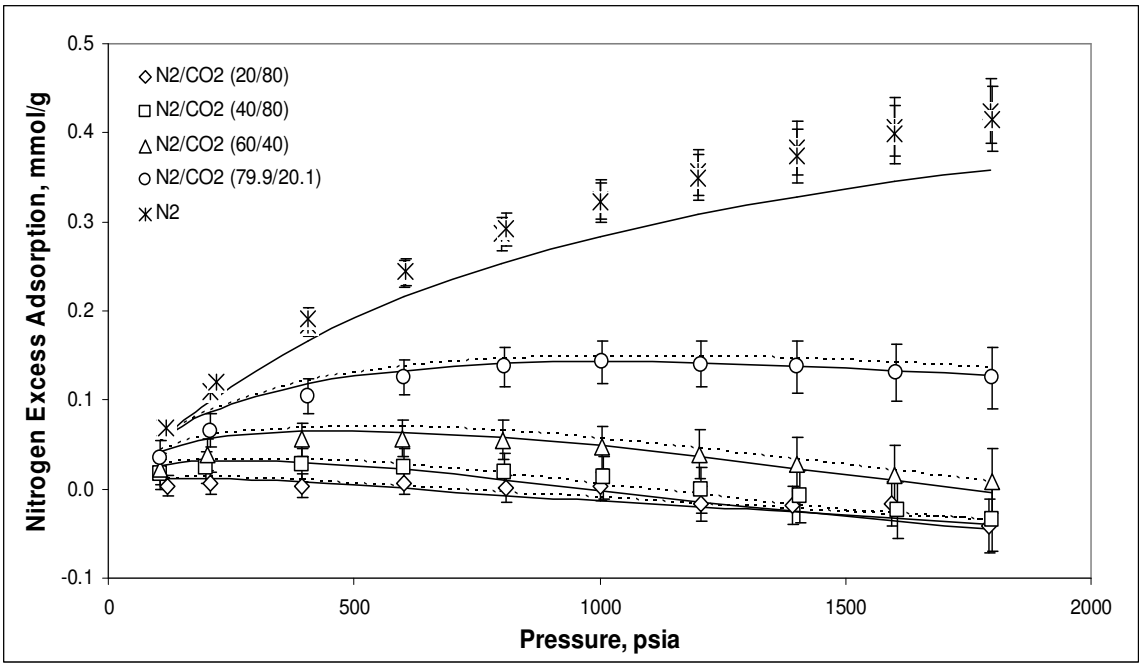

Figure C.28 – Case 3
Nitrogen Adsorption in Nitrogen/CO_2 Mixtures on Wet Fruitland OSU #1 Coal at 115°F (Solid Line – C_{ij} = 0.0, Dashed Line – Generalized C_{ij})

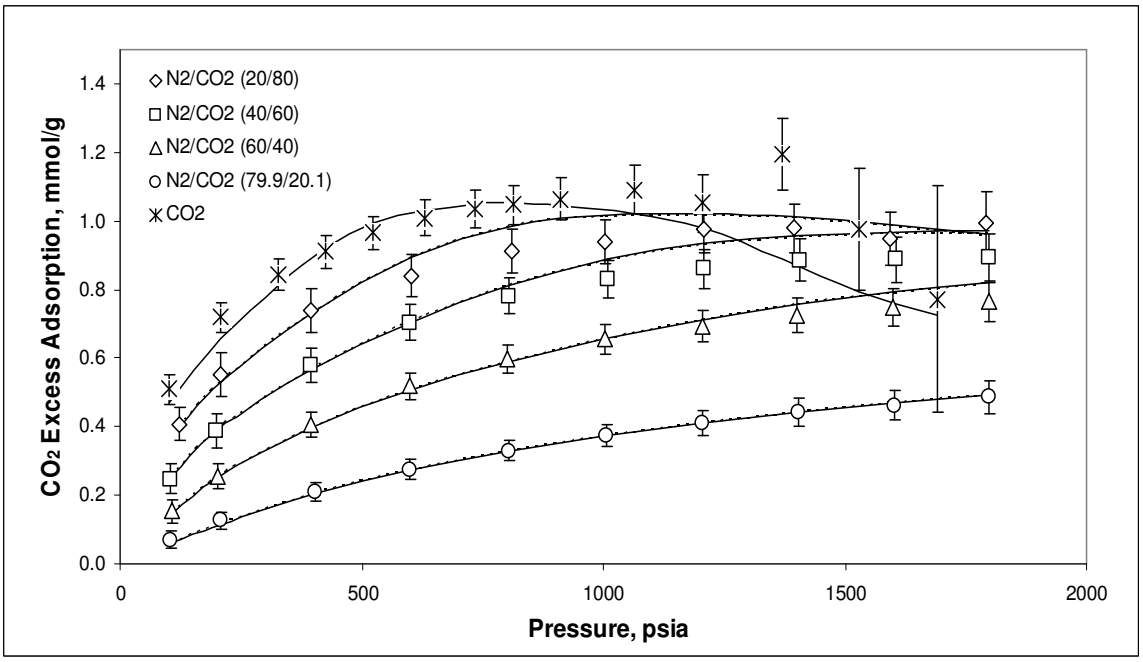

Figure C.29 – Case 3
CO_2 Adsorption in Nitrogen/CO_2 Mixtures on Wet Fruitland OSU #1 Coal at 115°F (Solid Line – C_{ij} = 0.0, Dashed Line – Generalized C_{ij})

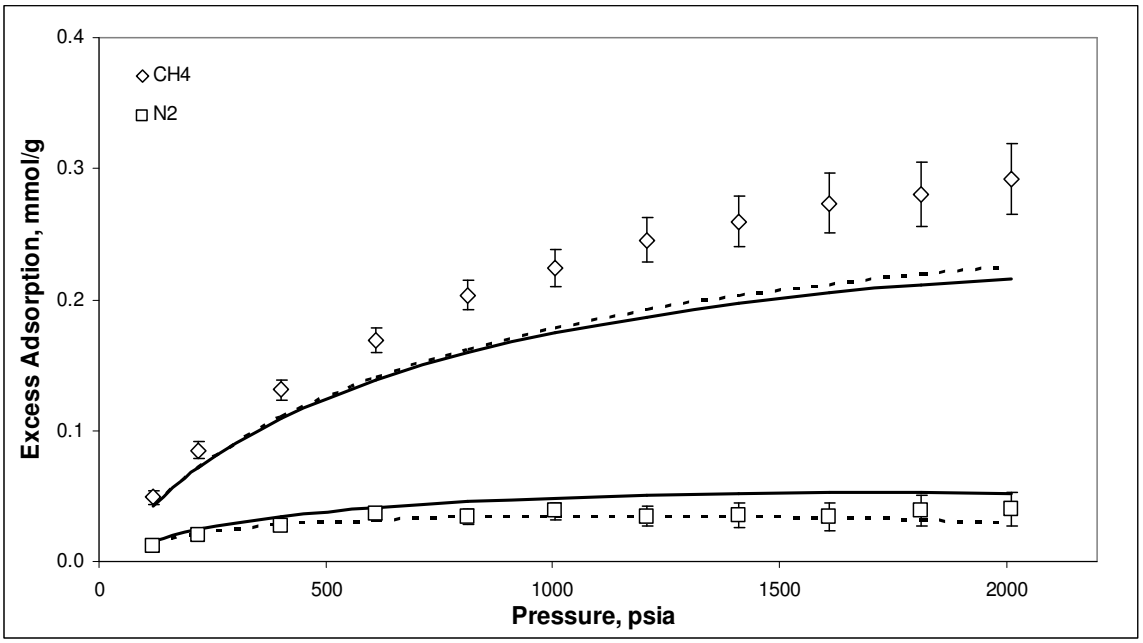

Figure C.30 – Case 3
Methane/Nitrogen 50/50 Feed Gas Adsorption on Wet Tiffany Coal at 130°F
(Solid Line – C_{ij} = 0.0, Dashed Line – Generalized C_{ij})

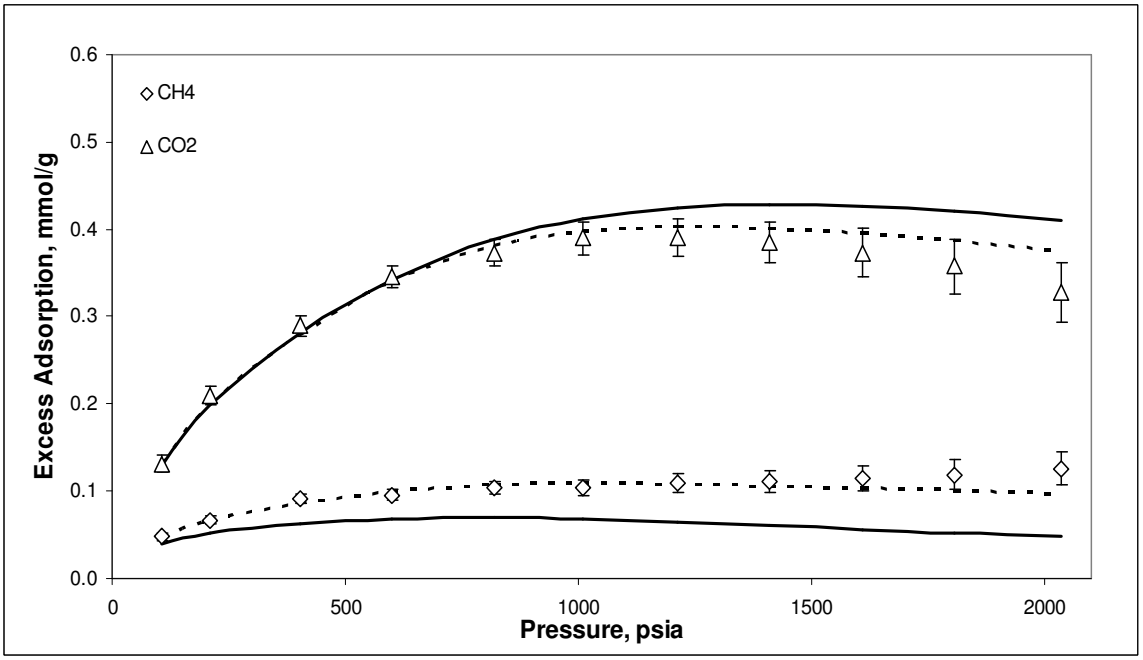

Figure C.31 – Case 3
Methane/CO_2 41/59 Feed Gas Adsorption on Wet Tiffany Coal at 130°F
(Solid Line – C_{ij} = 0.0, Dashed Line – Generalized C_{ij})

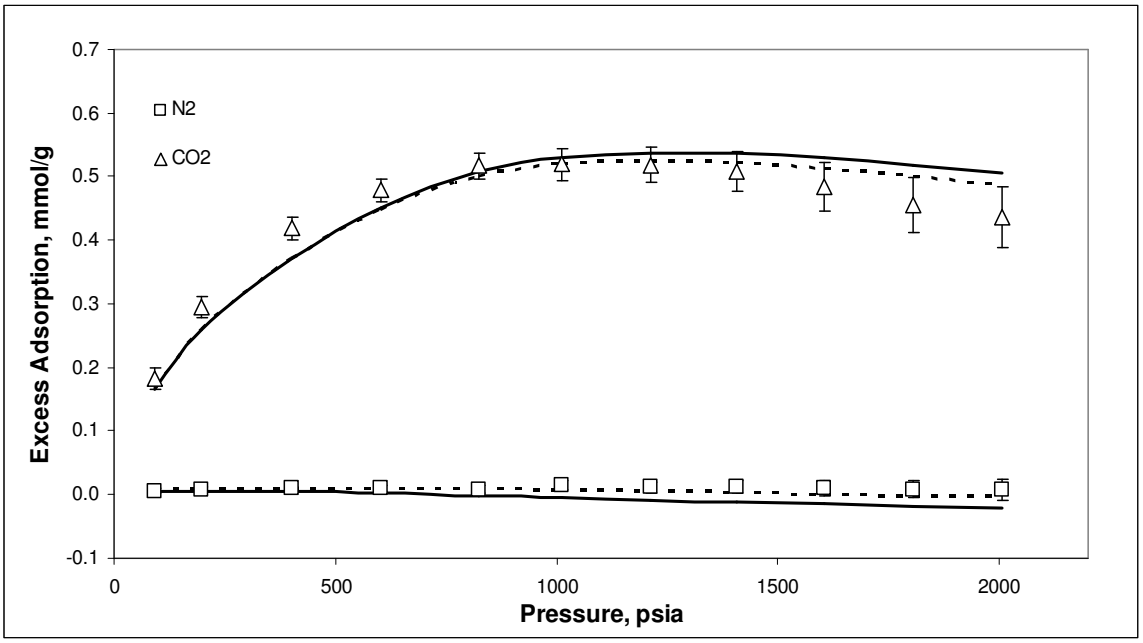

Figure C.32 – Case 3
Nitrogen/CO_2 20/80 Feed Gas Adsorption on Wet Tiffany Coal at 130°F
(Solid Line – C_{ij} = 0.0, Dashed Line – Generalized C_{ij})

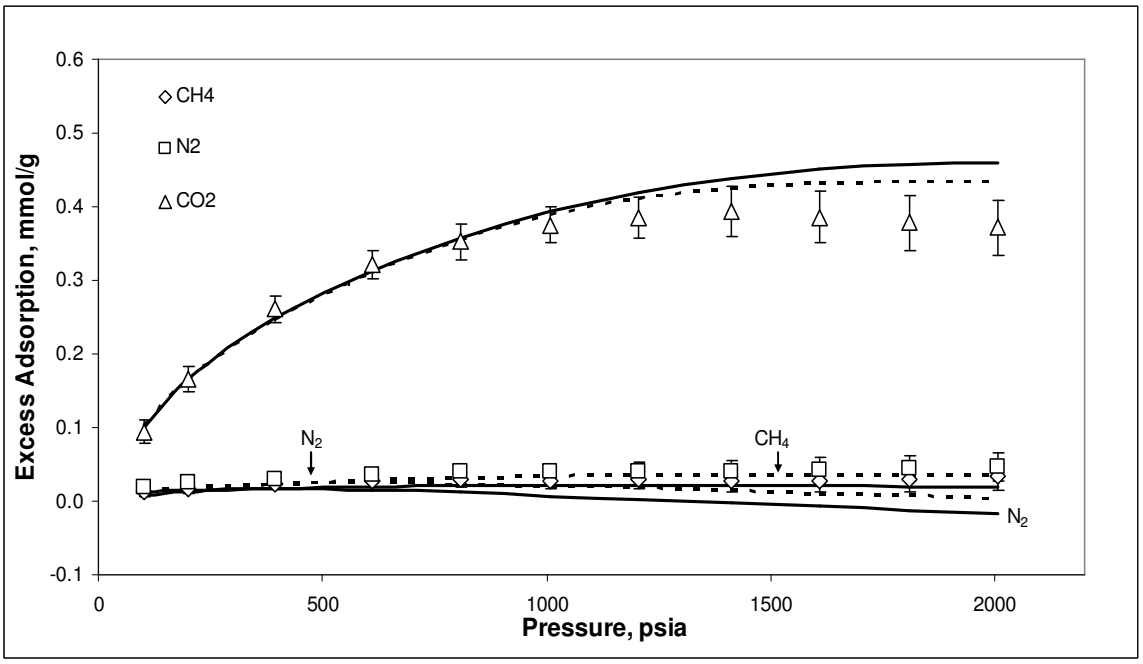

Figure C.33 – Case 3
Methane/Nitrogen/CO_2 10/40/50 Feed Gas Adsorption on Wet Tiffany Coal at 130°F
(Solid Line – C_{ij} = 0.0, Dashed Line – Generalized C_{ij})

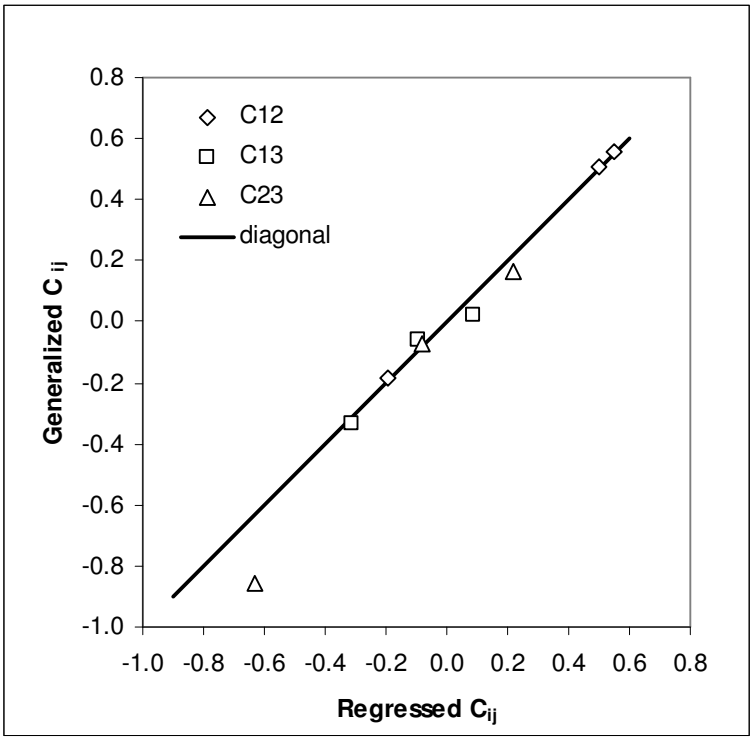

Figure C.34 – Case 3: Comparison of the Regressed and Generalized SLD-PR Binary Interaction Parameters (1 – Methane, 2 – Nitrogen, 3 – CO_2)

VITA

Jing Shyan Chen

Candidate for the Degree of

Master of Science

Thesis: SIMPLIFIED LOCAL-DENSITY MODELING OF PURE AND MULTI-COMPONENT GAS ADSORPTION ON DRY AND WET COALS

Major Field: Chemical Engineering

Biographical:

Personal Data: Born in Kluang, Johor, Malaysia, on April 01, 1981, the daughter of Chen Ah Chong and Lim Pek Yong

Education: Graduated from Chong Hwa High School, Kluang, Johor, Malaysia, in December 1999; received Bachelor of Science in Chemical Engineering from Oklahoma State University, Stillwater, Oklahoma, in May 2005
Completed the requirements for the Master of Science in Chemical Engineering at Oklahoma State University, Stillwater, Oklahoma in December, 2007

Professional Memberships: American Institute of Chemical Engineer

Name: Jing Shyan Chen Date of Degree: December, 2007

Institution: Oklahoma State University Location: Stillwater, Oklahoma

Title of Study: SIMPLIFIED LOCAL-DENSITY MODELING OF PURE AND MULTI-COMPONENT GAS ADSORPTION ON DRY AND WET COALS

Pages in Study: 173 Candidate for the Degree of Master of Science

Major Field: Chemical Engineering

Scope and Method of Study:
The Simplified Local-Density/Peng-Robinson (SLD-PR) adsorption model was utilized to generalize pure and mixed-gas adsorption predictions of methane (CH_4), nitrogen (N_2) and carbon dioxide (CO_2) on nine coal matrices. For this analysis, adsorption measurements for CH_4, N_2 and CO_2 on OSU coals and Argonne premium coals were used. These measurements consisted of essentially the complete OSU adsorption database on coals. The database contains both dry and wet coals. Further, it contains binary and ternary gas measurements on wet coals. The coals considered in this study were Illinois #6, Beulah Zap, Wyodak, Upper Freeport and Pocahontas, Fruitland OSU #1, Fruitland OSU #2, Tiffany, and Lower Basin Fruitland.

The SLD-PR model parameters were regressed to obtain representations for each coal. Then, the parameters were generalized as simple functions of adsorbent characteristics originating from the proximate and ultimate analyses of the coals.

Findings and Conclusions:
The SLD-PR model parameters (surface area, and ε_{ss}/k) were generalized in terms of the coal fixed carbon, carbon fraction, equilibrium moisture content, and methane excess adsorption at 400 psia. Using these methane-calibrated generalizations, the SLD-PR model described the adsorption of pure CH_4, N_2 and CO_2 on the coals considered with an overall weighted average absolute deviation (WAAD) of 1.1. This compares to a WAAD for individual representations of these coals of 0.6.

The SLD-PR generalized parameters generated from the pure gases were used to predict mixture adsorption of these gases on wet coals. Specifically, gas mixture adsorption on Wet Fruitland Coal, Wet Illinois #6 Coal and Wet Tiffany Coal was modeled. With few exceptions, the model can predict the mixture adoption behavior within three times the experimental uncertainties using only the pure-component parameters.

Equation-of-State binary interaction parameters (BIPs) were incorporated to further improve the mixture prediction results. Upon successful representation of the available binary data, the BIPs were generalized in terms of coal characteristics. The use of generalized BIPs resulted mixture gas adsorption predictions within twice the experimental uncertainties on average.

ADVISER'S APPROVAL: Dr. Khaled A.M. Gasem